Australian & New Zealand Orthopaedic Research Society

ANZORS 20th Annual Scientific Meeting

Flinders University
182 Victoria Square
Adelaide, South Australia

Flinders UNIVERSITY

21st – 23rd September 2014

Australian & New Zealand Orthopaedic Research Society

ANZORS 20th Annual Scientific Meeting

Contents

ANZORS 20th Annual Scientific Meeting

President's Welcome

It is a great honour for us to host the 20th annual ANZORS (The Australian and New Zealand Orthopaedic Research Society) conference in Adelaide from September 21-23, 2014. It has been very encouraging to see that we have received a record number of abstracts this year, and we would like to welcome all of you; including distinguished guest speakers, presenters and attendants.

The beauty of this conference is that we all speak the same language in the orthopaedic realm. We hope that this meeting will provide you with a very friendly environment and a great opportunity to exchange scientific information, discuss collaboration amongst researchers and clinicians, and promote orthopedic research.

We thank all the participants for their contribution to the formation of this meeting, particularly the invited speakers, chairs, and committee members. Special recognition must go to Dr Dominic Thewlis and Dr Egon Perilli for being great local hosts, and to Dr Dominic Thewlis for his hard work in assembling this fantastic program.

We express our deep gratitude and great appreciation for the generous support of the sponsors who are listed in the abstract booklet.

Finally, we wish all of you enjoy both the conference programme and your stay in Adelaide. We hope that together, we can make our contribution to orthopedic research and translation. I wish this meeting a great success.

Prof Jiake Xu
President
The Australian and New Zealand Orthopaedic Research Society

School of Pathology and Laboratory Medicine
The University of Western Australia
Jiake.Xu@uwa.edu.au

Australian & New Zealand Orthopaedic Research Society

ANZORS 20th Annual Scientific Meeting

Our Sponsors

zimmer

Personal Fit. Renewed Life.

BRUKER

Bruker microCT

ANZORS 20th Annual Scientific Meeting

Committee Members

President W/Prof Jiake Xu	Head of Molecular Laboratory, School of Pathology and Laboratory Medicine, University of Western Australia
Secretary Dr Dominic Thewlis	Senior Lecturer in Biomechanics, School of Health Sciences, University of South Australia
Treasurer A/Prof Nathan Pavlos	Head of the Cellular Orthopaedics Laboratory, Centre for Orthopaedic Research, School of Surgery, University of Western Australia.
2014 Host Organiser Dr Egon Perilli	Senior Research Fellow, Medical Device Research Institute, School of Computer Science, Engineering and Mathematics, Flinders University
Immediate Past President Prof Hala Zreiqat	NHMRC Senior Research Fellow and Head of the Tissue Engineering and Biomaterials Research Unit, Faculty of Engineering, University of Sydney

Organising Committee

Dr Egon Perilli

Dr Dominic Thewlis

Dr John Costi

Dr John Arnold

Prof Hala Zeriqat

A/ Prof Nathan Pavlos

W/Prof Jiake Xu

Scientific Committee

(alphabetical surname order)

Dr John Arnold

Dr Tania Crotti

A/Prof Colin Dunstan

Prof David Findlay

A/Prof David Haynes

Dr Pazit Levinger

Dr Zufu Lu

Dr Saulo Martelli

Dr David Musson

A/ Prof Nathan Pavlos

Dr Egon Perilli

A/Prof Peter Pivonka

A/Prof Bogdan Solomon

Dr Dominic Thewlis

W/Prof Jiake Xu

Prof Hala Zeriqat

Australian & New Zealand Orthopaedic Research Society

ANZORS 20th Annual Scientific Meeting

Travel Grant Recipients

(alphabetical surname order)

ANZORS is proud to support its early career researchers. This year we have awarded 22 travel grants. This represents a significant reinvestment of our funds to support the dissemination of quality orthopaedic research.

Zohreh Barani Lonbani	Queensland University of Technology, QLD
Michal Bartnikowski	Queensland University of Technology, QLD
Yong Chen	The University of Sydney, NSW
Stephanie Fountain	Queensland University of Technology, QLD
Ryan Gao	University of Auckland, NZ
Vaida Glatt	Queensland University of Technology, QLD
Gaurav Jadhav	University of Western Australia, WA
Chloe Lerebours	Monash University, VIC
Helen Liley	University of Auckland, NZ
Bay Sie Lim	University of Western Australia, WA
Nicole Locehel	Queensland University of Technology, QLD
ZuFu Lu	The University of Sydney, NSW
Joe Lynch	Canberra Hospital, ACT
Hossein Mokhtarzadeh	University of Melbourne, VIC
David Musson	University of Auckland, NZ
Simao Neto Brito da Luz	Griffith University, QLD
Benjamin Ng	University of Western Australia, WA
Liene Pluduma	Riga Technical University, Latvia
Seyed-Iman Roohani-Esfahani	The University of Sydney, NSW
Masha Shahi Avadi	Leeds University, UK
Jonathan Walter	University of Melbourne, VIC
Xiang Zhu	University of Western Australia, WA

ANZORS 20th Annual Scientific Meeting

Keynote Speakers

Dr Roland Steck

Dr Roland Steck is the Deputy Director of the Medical Engineering Research Facility (MERF) of the Queensland University of Technology (QUT) in Brisbane. After completing his PhD at the AO Research Institute Davos and ETH Zurich (Switzerland) in 2001 and a postdoctoral fellowship at the Cleveland Clinic Foundation in the USA, he joined QUT in 2005 to conduct research into the development and characterisation of novel fracture fixation implants for murine models of diaphyseal and metaphyseal bone fracture healing, as well as of new experimental models of soft tissue trauma.

In 2011, he was appointed as Deputy Director of MERF, a state-of-the-art research and teaching facility with surgical theatres and research laboratories for pre-clinical studies, and laboratories for anatomical and surgical skills training. In this role he works towards developing MERF into a technology rich interface between the health community and industry by providing a research and training environment that facilitates the translation of novel concepts from basic research to clinical implementation.

Dr Jacob Munro

Dr Jacob Munro is an Orthopaedic Surgeon in Auckland, New Zealand. He specialises in primary and revision arthroplasty of the hip and knee, management of hip pathology in the young patient and foot and ankle surgery. He maintains an interest in orthopaedic trauma, especially hip and lower limb fractures and periprosthetic fractures. His public practice is based at Auckland City Hospital with outpatient services at the Greenlane Clinical Centre. He consults privately at Eastwood Orthopaedic Clinic and operates at Mercy and Ascot Hospitals.

He is currently the Clinical lead for the NZ National Early Rehab After Surgery (ERAS) for THA and TKA. He sits on the Australia New Zealand Hip Fracture Registry Board. He is the New Zealand Research Officer for AO Asia Pacific Trauma Group.

Dr Munro is also a Senior Lecturer with Auckland University Medical School, Department of Surgery and closely affiliated with the Auckland Bioengineering Institute and the Bone Cartilage Group University of Auckland Medical School. He has research interests in the basic science fields of biomechanics and musculoskeletal biology as well as participating in clinical research across the

spectrum of Orthopaedics. His current basic science research projects include: development of tendon and cartilage scaffolds for MSK reconstruction, patient specific modeling of the pelvis and lower limb with application to novel solutions for paediatric and adult deformity, assessment of radiologic fusion in adult spine surgery using advanced MRI sequencing and PET CT, finite element modeling of the adult spine and biomechanical modeling of the pelvis with bone loss after THA. He completed his PhD in Biomechanics in April 2014.

Professor David Hunter

Professor Hunter is a rheumatology clinician researcher whose main research focus has been clinical and translational research in osteoarthritis (OA). He is the Florance and Cope Chair of Rheumatology and Professor of Medicine at University of Sydney, and Staff Specialist at Royal North Shore Hospital and North Sydney Orthopaedic and Sports Medicine Centre. A native of New Zealand and an Australian citizen, he earned his Bachelor of Medicine, Bachelor of Surgery, and Master of Sports Medicine at the University of New South Wales. He completed a fellowship in Rheumatology at the Royal Australian College of Physicians, a Masters of Sports Medicine from UNSW, and earned a Masters of Medical Science (Clinical Epidemiology) from the University of Newcastle. He established a full-time career in medical research in 1999, received his PhD in 2001 and then maintained an academic faculty appointment in Boston University amongst the foremost OA clinical researchers. He returned to Australia in 2010. His research is focused on a number of key elements in OA including (but not limited to) the epidemiology of osteoarthritis, the application of imaging to better understand structure and function with application to both epidemiologic research and clinical trials, novel therapies in disease management and heath service system delivery of chronic disease management. He is an editor for leading international journals in his field. He has authored books on osteoarthritis and has over 300 publications in peer-reviewed journals.

Dr Dan Barker

Dan holds a Doctor of Philosophy Degree from the Flinders University of South Australia, as well as a Master of Engineering Science and Bachelor of Engineering (Honors) from the University of Adelaide, Australia.

Following his PhD, Dan undertook a post-doctoral fellowship with Lund University, a leading orthopaedic research centre in Europe, examining methods of tibial tray loosening using the Finite Element Method. Upon returning to Australia, Dan moved into the commercial arena as a Design Engineer for Portland Orthopaedics, a start-up engineering company in Sydney. Dan subsequently managed the technology group at Portland. Dan then joined Johnson & Johnson Medical in various commercial roles including Business Development Manager for Computer Assisted Surgery and New technologies and eventually as the Business Unit Manager for Acclarent, the company's Ear, Nose and Throat medical device business. Thereafter, Dan worked as a freelance medical device design consultant before joining Zimmer as the Asia Pacific Director for Research and Development.

Dr Liza Raggatt

Dr Liza Raggatt received her PhD from the University of Adelaide in 2000. After a postdoctoral Fellowship in the USA she returned to Australia and has been working in Brisbane for the last 11 years. Since returning to Australia Dr Raggatt research career has focused on understanding the role of macrophages in bone biology. Dr Raggatt and her team have characterized a new bone cell population that is redefining our understanding of bone homeostasis and fracture repair. More recently, Dr Raggatt's research has evolved to investigate how macrophages influence the haematopoietic stem cell (HSC) niche in the bone marrow in the context of HSC stem cell transplantation.

Venue

Flinders University (Victoria Square Campus)
182 Victoria Square
Adelaide, South Australia

Program

Day 1 (Sunday 21st September)

8.00 - 8.30	*Registration & coffee/tea*		
8.30 - 8.35	**Welcome**	**ANZORS President – W/Prof Jiake Xu**	
8.35 - 9.15 **Session Chair:** **W/Prof Jiake Xu**	**Keynote**	**Dr Roland Steck** **'Biomechanics of Fracture Healing: Renewed Interest in an Old Topic'**	
9.15 – 10.55	**Bone Biology 1**	**Author**	**Title**
Session Chair: **W/Prof Jiake Xu**	**9.15-9.27**	**Daniel Reinke**	**Evidence for altered osteoclastogenesis in splenocyte cultures from cyp27b1 knockout mice**
	9.27-9.39	**Xiang Zhu**	**Alexidine dihydrochloride attenuates osteoclasts formation and bone resorption via induction of mitochondrial-activated apoptotic program**
	9.39-9.51	**Song Chen**	**Modeling and parameter identification of gene regulatory networks in human osteoblasts**
	9.51-10.03	**H. Kamitakahara**	**Modulation of autophagy and apoptosis in human osteoclasts in vitro: preliminary data**
	10.03-10.15	**Zufu Lu**	**Synergistic effect of nanomaterials and bmp-2 signalling in inducing osteogenic differentiation of adipose tissue-derived mesenchymal stem cells**
	10.15-10.27	**Sylvia Saad**	**Semaphorin-3a, neuropilin-1 and plexin-a1 are increased during osteoclast formation and further elevated by prosthetic particles in vitro**
	10.27-10.39	**Yu-Wen Su**	**Osteoblast derived-neurotrophin-3 (nt-3) as a novel cross-talk signal promotes osteoclast formation**
10.40 - 10.55	*Coffee break*		
10.55 - 12.15	**Clinical 1**	**Author**	**Title**
Session Chair: **A/Prof Bogdan Solomon**	**10.55-11.07**	**Mario Zotti**	**Early wear of 36mm and 28mm metal on highly cross-linked polyethylene articulations in total hip arthroplasty**
	11.07-11.19	**Caroline Moran**	**Osteolysis and wear of large and standard metal on highly cross-linked polyethylene articulations**
	11.19-11.31	**Jerry van de Pol**	**Can impaction bone grafting of osteoporotic tibial plateau fractures facilitate immediate unrestricted weight bearing?**
	11.31-11.43	**Fiona Zhou**	**Methotrexate chemotherapy triggers touch-evoked pain and increased bone innervation in young rats**
	11.43-11.55	**Diana Perriman**	**How reliable is computer assisted hip arthroplasty polyethylene wear measurement using current radiography practices?**
	11.55-11.59	Amy Watts	A systematic review of diagnostic methods for shoulder impingement syndrome
	11.59-12.03	Christopher Wilson	A double blinded, randomized, controlled proof of concept study to compare post-operative analgesic and mobilization outcomes of local infiltration analgesia, single shot femoral nerve block and intrathecal morphine in primary total knee arthroplasty
	12.03-12.07	T. Fisher	Methods of evaluating the volume of os coxae in vivo and ex vivo
	12.07-12.11	B. McDonald	The outcome of pedicle screw instrumentation removal for chronic low back pain: a prospective study
12.15 – 13.00	**Tissue Engineering**	**Author**	**Title**
Session Chair: **Dr David Musson**	**12.15-12.27**	**Michal Bartnikowski**	**Viscoelastic properties of hydrogel blends for cartilage tissue engineering**
	12.27-12.39	**Yongjuan Chen**	**Zirconium ions up-regulate the bmp/smad signalling pathway and promote the proliferation and differentiation of human osteoblasts.**
	12.39-12.43	Iman Roohani	Development of 3D printed ceramic scaffolds for treatment of segmental bone defects
	12.43-12.47	Ryan Gao	Rotator cuff augmentation: an in vivo study using a lactoferrin seeded biomaterial scaffold
	12.47-12.51	Mengzhen Yan	Peri-prosthetic bone structure and integrity change with implant material stiffness in the ovine model
	12.51-12.55	Young Jung No	Injectable radiopaque and bioactive polycaprolactone-ceramic composite for Orthopaedic augmentation
13.00 – 14.00	*Lunch*		
14.00 - 14.40 **Session Chair:** **A/Prof Bogdan Solomon**	**Keynote**	**Dr Jacob Munro** **'Osteolysis after hip arthroplasty: Understanding load transfer in the pelvis'**	

14.40 - 15.20	Imaging 1	Author	Title
Session Chair:	**14.40-14.52**	**Pascal Buenzli**	**Layered distribution of osteocytes within single osteons**
Dr Egon Perilli	**14.52-15.04**	**Drew Grosser**	**Early migration of the r3 uncemented acetabular component: a prospective 2 year radiostereometric analysis**
	15.04-15.08	D. Muratovic	Knee osteoarthritis bone marrow lesions detected by two different magnetic resonance sequences are characterised by different morphological and microstructural cartilage-subchondral bone changes
	15.08-15.12	J. Abrahams	RSA assessment of cup migration after cup cage reconstructions of periprosthetic acetabular fractures with pelvic discontinuity and comminuted unreconstructable both column acetabular fractures
	15.12-15.16	C. Lerebours	The relationship between porosity and specific surface in human cortical bone: three-dimensional measurements from compact to porous cortical bone tissue
	15.16-15.20	J. Abrahams	Patterns of migration of revision acetabular components using radiostereometric analysis (RSA)
	15.20-15.24	Anneka Stephens	Long-leg alignment pre and post-operatively for primary total knee arthroplasty: a comparison of computer tomographic imaging and long leg radiograph analysis
15.25 - 15.40	*Coffee/tea break*		
15.40 - 16.40	**Biomechanics 1**	**Author**	**Title**
Session Chair:	**15.40-15.52**	**Bryant Roberts**	**Relationships between proximal tibia bone microarchitecture and dynamic joint loads in end-stage knee osteoartrhitis – a preliminary study**
Dr Claire Jones	**15.52-16.04**	**Saulo Martelli**	**The repertoire of possible muscle synergies during walking**
	16.04-16.16	**Pazit Levinger**	**Balance response during induced falls in people with knee osteoarthritis**
	16.16-16.20	**G. Wei**	**Custom test rig for in vitro measurement of human knee cartilage stresses under physiological load**
	16.20-16.28	Jonathan Walter	Contact contributions to inverse dynamic knee loads during gait
	16.28-16.32	David Musson	Why are younger patients undergoing ACL reconstruction more prone to re-rupture?
	16.32-16.36	Joe Lynch	Abnormal Knee Kinematics During Step and Turn Following Multiple-Ligament Knee Reconstruction
16.40 - 17.40	**Clinical 2**	**Author**	**Title**
Session Chair:	**16.40-17.52**	**Stephanie Fountain**	**A method for monitoring animal activity in orthopaedic studies**
Dr Jacob Munro	**17.52-17.04**	**Christopher Wilson**	**A comparison between 'signature personalised patient care' to conventional total knee arthroplasty and computer-assisted navigation**
	17.04-17.16	**Laurant Kang**	**Limitations in predicting outcome following multiple-ligament knee injury and treatment: a systematic review of current literature**
	17.16-17.28	**Martin Hua**	**The quality of surgical technology assessment reports prepared for MSAC**
	17.28-17.32	Annika Theodoulou	A systematic review on the use of patient reported outcome measures (proms) in knee arthroplasty research
	17.32-17.36	Thomas Clifton	Initial outcomes of direct anterior- compared to posterior approach for total hip arthroplasty

Day 2 (Monday 22nd September)

8.00 - 8.15	*Coffee/tea break*		
8.15 - 9.15	**PhD Award**	**Author**	**Title**
Session Chair: **Dr Dan Barker**	**8.15-8.27**	**Bay Sie Lim**	**Roquin is a novel regulator of bone homeostasis**
	8.27-8.39	**Dale Robinson**	**Mechanical properties of human cartilage ranging from healthy to osteoarthritic**
	8.39-8.51	**Gaurav Jadhav**	**Morc3 is a novel regulator of bone homeostasis**
	8.51-9.03	**Benjamin Ng**	**Furin is an important regulator of osteoclastic bone resorption**
	9.03-9.15	**Zohreh Lonbani**	**The effect of cryotherapy on the vascular regeneration following closed soft tissue trauma**
9.15 - 9.55 **Session Chair:** **Prof David Findlay**	**Keynote**	**Professor David Hunter** **'Subchondral bone in osteoarthritis and therapeutic potential'**	
9.55 - 10.15	*Coffee/tea break*		
10.15 - 11.05	**ECR Award**	**Author**	**Title**
Session Chair: **Prof David Hunter**	**10.15-10.27**	**Matthew Prideaux**	**Isolation of osteocytes from human trabecular bone**
	10.27-10.39	**Stuart Callary**	**Wear of highly cross-linked polyethylene in total hip replacement**
	10.39-10.51	**Claire Jones**	**Biomechanical evaluation of a novel suture anchor for rotator cuff repair**
	10.51-11.03	**John Arnold**	**Are changes in knee biomechanics and physical activity in free living conditions after total knee arthroplasty related? A study combining 3D gait analysis and high resolution use of time recall**
11.10 - 12.30	**Annual General Meeting and Election of new Executive Committee members**		
12.30 - 16.30	**Networking afternoon in the Adelaide Hills (Barristers Block Winery)** A bus will collect delegates outside the conference venue at 12.30. Transport to and from Barristers is included in the conference registration fee. The afternoon is an opportunity for you to sample some of the food and wine the Adelaide Hills has to offer, while mixing with your colleagues in an informal environment.		
19.00 -	**Conference Dinner (only available for delegates who have purchased a ticket in advance)** T-Chow Chinese Restaurant 68 Moonta St. Adelaide 5000		

Day 3 (Tuesday 23rd September)

8.00 - 8.30	*Coffee/tea break*		
8.30 - 9.10 **Session Chair: Dr John Costi**	**Keynote**	**Dr Dan Barker** **'Is Academic Orthopaedic Research valued by Medical Device Companies?: An ex-academic commercial researcher's perspective'**	
9.10 - 10.45	**Bone Biology 2**	**Author**	**Title**
Session Chair: **A/Prof Nathan Pavlos**	**9.10-9.22**	**KWK. Yeung***	**In situ bone formation by controlled release of magnesium ions**
	9.22-9.34	**X. Zhao***	**Strontium promote the osteogenic differentiation of msc through attenuating the cell quiensent and enhancing asymmetric differentiation**
	9.34-9.46	**Masakazu Kogawa**	**Examining the response of bone cells to infection following total hip replacement**
	9.46-9.58	**Renee Ormsby**	**Evidence that metal wear particles exert a pro-osteoclastogenic effect on osteocytes**
	9.58-10.10	**Zhirui Jiang**	**Decreased number of proliferating chondrocytes and delayed hypertrophy in mucopolysaccharidosis vii growth plate**
	10.10-10.22	**Kent Algate**	**Hdac-1 is highly expressed at sites of peri-prosthetic osteolysis and its inhibition suppresses osteoclast activity in vitro**
	10.22-10.34	**M. Zawawi**	**Caffeic acid phenethyl ester abrogates bone resorption in a murine calvarial model of polyethylene particle-induced peri-prosthetic osteolysis**
	10.34-10.38	Vincent Kuek	EGFL7 is expressed in bone microenvironment and promotes angiogenesis via ERK, STAT3 and integrin signaling cascades
	10.38-10.42	Vaida Glatt	Effect of mechanical environment on the bmp-2 dose-response of large segmental defect healing
	10.42-10.48	Prem P Dwivedi	Glypican-3 (but not Glypican-1) inhibits bmp activity and osteogenesis in vitro
	* Awarded ANZORS-China travel scholarship		
10.50 – 11.00	*Coffee/tea break*		
11.00 - 12.10	**Biomechanics 2**	**Author**	**Title**
Session Chair: **Dr Roland Steck**	**11.00-11.12**	**Isaac Lawless**	**Intervertebral disc and facet joint contributions to the six axis mechanical properties of the human lumbar functional spinal unit**
	11.12-11.24	**Nicole Loechel**	**The effect of reverse dynamization on bone healing**
	11.24-11.36	**Jonathan Caldow**	**Biomechanical outcomes of a novel surgical rotator cuff tendon repair technique**
	11.36-11.40	Wen Wu	A musculoskeletal model for the evaluation of shoulder muscle and joint function
	11.40-11.44	Saulo Martelli	A new software pipeline for micro-finite-element simulations of whole-bone mechanics
	11.44-11.48	Melissa Ryan	Time-elapsed screw insertion into cancellous bone
	11.48-11.52	Lloyd Fletcher	Effects of accumulated fatigue damage on the fracture resistance of cortical bone
	11.52-11.56	Xiaoming Wang	Multiscale cortical bone remodelling: towards predicting whole bone strength
	11.56-12.00	David Ackland	A novel prosthetic total joint replacement system for the human temporomandibular joint
	12.00-12.04	Dhara Amin	Effect of potting technique on the six degree of freedom viscoelastic properties of human lumbar spine segments
	12.04-12.08	Helen Liley	The influence of the parasagittal groove angle on cartilage stress and degeneration in the equine metacarpophalangeal (fetlock) joint
12.10 - 13.15	*Lunch*		
13.15 - 13.55 **Session Chair: A/Prof Nathan Pavlos**	**Keynote**	**Dr Liza Raggatt** **'Macrophages: a viable therapeutic target to enhance endochondral fracture repair'**	

13.55 - 14.40	Imaging 2	Author	Title
Session Chair:	**13.55-14.07**	**Egon Perilli**	**Nano-CT imaging of human trabecular bone using a laboratory system**
Dr Jacob Munro	**14.07-14.19**	**Joel Fuller**	**The reliability of DEXA measurements of bone mineral density in the metatarsals**
	14.19-14.23	Guangyi Li	Impact of subchondral bone plate integrity on the homeostasis of the underlying subchondral trabecular bone in late-stage osteoarthritis
	14.23-14.27	Drew Grosser	Early migration chracteristics of the cl2 cementless femoral stem and corail femoral stem: a radiostereometric analysis (RSA) study
	14.27-14.31	Daniel Miles	Imaging femoral periprosthetic osteolysis around total hip arthroplasties using a human cadaver model
	14.31-14.35	Anneka Stephens	Radiographic alignment analysis: interobserver variability post total knee arthroplasty
14.40 - 15.00	*Coffee/tea break*		
15.00 - 16.30	**Biomechanics 3**	**Author**	**Title**
Session Chair:	**15.00-15.12**	**Samuel Grasso**	**Effect of ligament combination on menisci and cartilage loading following multiple ligament knee reconstruction**
A/Prof Peter Pivonka	**15.12-15.24**	**Simao Brito da Luz**	**Subject-specific knee kinematics using MRI informed parallel mechanism**
	15.24-15.36	**Rosidah Ab-Lazid**	**The holding strength of cancellous screws depends on insertion torque, bone microarchitecture and areal bone mineral density**
	15.36-15.48	**Mark Taylor**	**Simple measures of patient weight, bone properties and geometry are predictors of femoral neck strains**
	15.48-16.00	**Hamidreza Farhoudi**	**Three-dimensional frictional moment induced from head-cup bearings of hip joint implants**
	16.00-16.12	**Rami Al-Dirini**	**Measuring the in-vivo response of muscle and subcutaneous fat tissues under quasistatic sitting loads using high-fidelity subject-specific FE models**
	16.12-16.16	Khosro Fallahnezhad	A three dimensional finite element model of the head–neck junction of a modular total hip arthroplasty
	16.16-16.20	Mahsa Avadi	In vitro degradation of mechanical properties of porcine femoral head bone for development of an in vitro of avascular necrosis
	16.20-16.24	Hossein Mokhtarzadeh	Lower limb muscles function as we age: implication for sarcopenia
	16.28-16.32	Gino Coates	Feasibility of using Kinect 2 depth map to determine thoracic kyphosis angle
	16.32-16.36	Ruwindi Setunge	Quadricep and hamstring force ratio in the transverse plane: implications for ACL injury
	16.36-16.40	Animesh Singla	In vitro testing of 4- and 5- strand constructs for ACL reconstruction
	16.40-16.44	A. Sideris	Clinical assessment of knee kinematic parameters using the KneeKG system
16.45-17.00	**Close**	**ANZORS President – W/Prof Jiake Xu**	

Abstracts

DAY 1

KEYNOTE 1 – Dr Roland Steck

BIOMECHANICS OF FRACTURE HEALING: RENEWED INTEREST IN AN OLD TOPIC

[1]Roland Steck

[1]Medical Engineering Research Facility, Queensland University of Technology, Brisbane, QLD

The importance of the biomechanical environment for the healing of bone fractures has been acknowledged for a long time. Starting in the 1960s, ground breaking research was conducted in an effort to better understand the optimal mechanical conditions for reliable and timely fracture healing [1, 2]. However, during the 90s, the main focus in bone fracture healing research shifted significantly towards more biological topics, emphasising on finding biological agents, such as growth factors, that would improve bone healing in challenging situations. Nevertheless, soon it was realised that even with the application of growth factors and other pharmaceutical agents, the understanding of the underlying biomechanics in fracture healing remains essential, and furthermore, that the action of biological agents can be improved by an appropriate mechanical environment. This has led to a renewed interest in this area in recent years. Since then, implant and sensor technologies have experienced significant improvements, which make new research into the biomechanics of fracture healing very exciting. This presentation will highlight the state of the art in this research field and some of the recent advances in this area resulting from research conducted by the Trauma Research group at the Queensland University of Technology in Brisbane.

Two major types of fracture healing mechanisms can be distinguished. In cases of simple fractures, primary bone healing may occur if the fracture segments are perfectly repositioned and the fracture surfaces can be subjected to compression by means of purpose-designed fracture fixation implants (*i.e.* compression plates). This fixation has been termed "absolute stability" and it prevents any interfragmentary movement from occurring. Primary bone healing is essentially a process of osteonal bone remodelling that occurs across the fracture line, thereby bridging it with new osteons, until the fracture line is ultimately eliminated. For a long time, the ultimate goal of surgical fracture treatment was to achieve this type of fracture healing, and any sign of callus formation was considered a negative outcome.
However, clinically, secondary bone healing which occurs in fractures stabilised with so-called "relative" stability, is much more common than primary bone healing. The majority of fractures heal through a combination of intramembranous and endochondral bone formation, via the formation of a fracture callus. This type of "natural" fracture healing occurs through a well-orchestrated succession of the four overlapping phases: inflammation, soft callus formation, callus mineralisation and remodelling. Through a cartilaginous template, this healing mechanism is more robust, and proved to be quite successful in cases of comminuted fractures. Specifically, this mechanism relies on a certain degree of fracture fixation flexibility, and it has been shown that the callus size increases with increasing flexibility in the fracture fixation up to a point, at which the fixation is too flexible and the fracture segments can no longer bridge, thereby resulting in a non-union or delayed-union. In an attempt to establish theories around the optimum degree of flexibility for fast and robust fracture healing, terms like "interfragmentary motion" and "interfragmentary strain" have been coined and limits for these values, within which fracture healing may occur, have been defined [2, 3].

In order to be able to apply stable fracture fixation with a defined degree of flexibility, the development of locking screw implants has been instrumental. These screws form a solid, angular and stable connection with the plate, thereby changing the principle of fixation from one where the construct stability is dependent upon friction between the fixation plate and the underlying bone, to one that is inherently stable and where the construct stiffness is defined by the material and geometric properties of the fixation implants alone. This allows for the stabilisation of fractures in a more "biologic" fashion, which can often be applied in a minimally invasive manner.

The adoption of the locking screw principle to miniaturised plate implants and other advances in implant technologies has revolutionised fracture healing research in small rodents. For the first time it is now possible to study the influence of different fixation stiffnesses on the molecular processes governing fracture healing in mice and rats under standardised conditions [4, 5].

While it is tempting to apply this so-called biological fracture fixation using locking screws universally in surgical fracture treatment, clinical experience has shown that in some cases this treatment is not successful, resulting in a high incidence of non-unions. Particularly simple fractures with a single transverse fracture line appear to be difficult to treat using locking screw constructs and often only lead to a small fracture callus on the far-cortical side away from the plate, but fail to form any callus or lead to union of the fracture segments directly underneath the plate. This has been

attributed to the non-uniform and overall insufficient interfragmentary movement in these locking screw constructs. Consequently, new implants have since been designed aiming to subject the entire fracture gap to a uniform strain field. However, these so-called Dynamic Locking Screws or Far Cortical Locking Screws, require careful characterisation to determine whether these claims prove to be true and lead to the desired clinical outcome.

Most recently, attention has also shifted from attempting to provide a single optimal fracture fixation stiffness throughout the entire healing period, to a better understanding of the role of the mechanical environment during the different stages of secondary bone healing with the potential to adapt the construct stiffness over the course of fracture healing. Clinically, the dynamisation of fracture fixation implants after a period of non-responsiveness of the fracture (*i.e.* no callus being visible on x-rays) has been applied with some success for some time, although the scientific basis for this procedure is scarce. Furthermore, in attempts to establish the fundamental processes of this dynamisation procedure, animal experiments have not always been able to explain or replicate this clinical success [6, 7]. A closer examination of the different phases of secondary fracture healing reveals that it could be advantageous to have a more flexible fixation during early stages of healing, and then a stiffer fixation during consolidation and remodelling phases [8]. This concept of reverse dynamisation is currently being examined in segmental defects [9] and transverse osteotomies in rats [10].

One of the goals for better understanding the role of the mechanical environment on fracture healing is to use this knowledge to accelerate the bone fracture healing process by means of active mechanical stimulation. This idea is not new, but previous attempts to establish the efficacy of such active stimulation methods have always been hampered by the inability to separate the active loading stimulation from the loading experienced by the animal during normal locomotion and daily activity [11-13]. Nevertheless, new research is currently being conducted in sheep, based upon a novel design for an external fixator that is able to separate the active loading applied to the experimental fracture gap by an external fixator construct from that experienced during normal locomotion. This research is further enhanced by new telemetric and GPS-based activity measurements, as well as measurements of the fracture gap loading that has been enabled by advances in sensor technology.

In summary, new research that has been enabled by the development of new implants and sensor technologies allows us to further enhance our understanding of the role of biomechanics on different phases of bone healing. This knowledge should not only help to accelerate normal fracture healing in general, but it should also improve the clinical outcome of those fractures that are currently difficult to treat.

Acknowledgments
These research projects by the Trauma Research Group at QUT have been supported by the AO Research Foundation, the Australian Research Council, the National Health and Medical Research Council, and the OTC Foundation.

REFERENCES

1. Perren, S.M. and B.A. Rahn, Biomechanics of fracture healing. Can J Surg, 1980. 23: p. 228-32.
2. Claes, L.E., et al., Effects of mechanical factors on the fracture healing process. Clin Orthop Relat Res, 1998: p. S132-47.
3. Perren, S.M. and J. Cordey, The concept of interfragmentary strain, H.K. Uhthoff and E. Stahl, Editors. 1980, Springer-Verlag: Berlin, New York. p. 63-77.
4. Steck, R., et al., Influence of internal fixator flexibility on murine fracture healing as characterized by mechanical testing and microCT imaging. Journal of Orthopaedic Research, 2011. 29: p. 1245-1250.
5. Matthys, R. and S.M. Perren, Internal fixator for use in the mouse. Injury, 2009. 40: p. S103-S109.
6. Claes, L.E., et al., Early dynamization by reduced fixation stiffness does not improve fracture healing in a rat femoral osteotomy model. J Orthop Res, 2009. 27: p. 22-27.
7. Claes, L.E., et al., Late dynamization by reduced fixation stiffness enhances fracture healing in a rat femoral osteotomy model. Journal of orthopaedic trauma, 2011. 25: p. 169-74.
8. Epari, D.R., et al., A case for optimising fracture healing through inverse dynamization. Med Hypotheses, 2013. 81(2): p. 225-7.
9. Glatt, V., et al., Improved Healing of Large Segmental Defects in the Rat Femur by Reverse Dynamization. JBJS(Am), 2012: p. 2063-2073.
10. Loechel, N., et al., The Effect of Inverse Dynamization on Bone Healing, in Annual Meeting of the ANZORS. 2013: Sydney, Australia.
11. Goodship, A.E. and J. Kenwright, The influence of induced micromovement upon the healing of experimental tibial fractures. J Bone Joint Surg Br, 1985. 67: p. 650-5.
12. Augat, P., et al., Shear movement at the fracture site delays healing in a diaphyseal fracture model. J Orthop Res, 2003. 21: p. 1011-7.
13. Bishop, N.E., et al., Shear does not necessarily inhibit bone healing. Clin Orthop Relat Res, 2006. 443: p. 307-314.

SESSION 1 – BONE BIOLOGY 1

EVIDENCE FOR ALTERED OSTEOCLASTOGENESIS IN SPLENOCYTE CULTURES FROM *CYP27B1* KNOCKOUT MICE

[1]Daniel C. Reinke, [1]Masakazu Kogawa, [2]Kate Barratt, [2]Paul H. Anderson, [2]Howard A. Morris, [1]Gerald J. Atkins

[1]Bone Cell Biology Group, Centre for Orthopaedic & Trauma Research, University of Adelaide
[2]School of Pharmacy and Medical Sciences, University of South Australia, Adelaide, SA, Australia
email: daniel.reinke@adelaide.edu.au

INTRODUCTION

The metabolism of 25(OH)-vitamin-D (25D) by osteoclasts, by virtue of their expression of CYP27B1, results in osteoclastogenesis with decreased associated resorptive activity, consistent with CYP27B1 conferring amelioration of osteoclastic resorption under 25D replete conditions [1, 2]. We are examining in more detail osteoclastogenesis in mice with global deletion of the *Cyp27b1* gene (*Cyp27b1*KO). We hypothesised that osteoclasts differentiated from these mice would display enhanced resorptive capacity due to the lack of the ameliorating effect of endogenous 1α,25$(OH)_2$-vitamin D (1,25D) synthesis.

METHODS

Splenocytes isolated from four *Cyp27b1*KO mice or their wild-type (WT) littermates between 6-8 weeks of age were pooled and cultured under osteoclast-forming conditions (recombinant RANKL 100 ng/ml and M-CSF 25 ng/ml) for up to 10 days. Osteoclast formation was measured by staining for the osteoclast marker tartrate resistant acid phosphatase (TRAP). Bone resorption activity was measured by plating the cells on a bone-like substrate. TRAP staining was performed for days 6, 7 and 8 of differentiation and resorption was quantified after day 10.

RESULTS AND DISCUSSION

Results indicate significant differences between genotypes in terms of osteoclastogenesis with fewer TRAP-positive multinucleated cells formed at all time points in *Cyp27b1*KO cultures ($p < 0.05$) compared to WT. There was an apparent difference between genotypes in terms of resorption, with osteoclasts formed in *Cyp27b1*KO cultures resorbing to a greater extent on a per cell basis than their WT counterparts ($p < 0.03$). Intriguingly, the expression of osteoclast marker genes *Nfatc1, Trap, Ctsk, Oscar* and *Ca2* increased in *Cyp27b1*KO cultures earlier in response to RANKL but declined with time to a greater extent than WT cultures. Our data indicates abnormal osteoclastogenesis due to the absence of CYP27B1 expression, consistent with the notion that endogenous metabolism of 25D optimises osteoclastogenesis and ameliorates the resulting activity of mature osteoclasts.

CONCLUSIONS

The loss of *Cyp27b1* expression results in decreases in osteoclast number and size, indicating the importance of autocrine synthesis of 1,25D in osteoclast lineage cells.

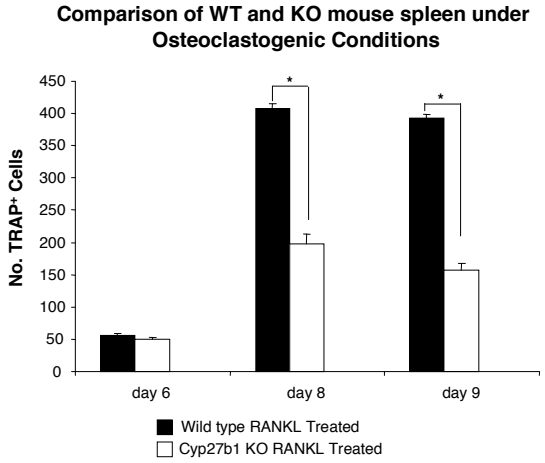

Figure 1: The relative osteoclastogenic potential of *Cyp27b1*KO splenocytes against wild-type. Data shown are mean counts ± SEM from quadruplicate wells. Significant indicated by *($p < 0.05$) using two way ANOVA.

ACKNOWLEDGEMENTS

This study was funded by NHMRC Project Grant APP1029926.

REFERENCE

1. Kogawa, M., et al. *Journal of Steroid Biochemistry and Molecular Biology*. **121**: p 277-280, 2010
2. Kogawa, M., et al. *Endocrinology*. **151**(10): p. 4613-25, 2010.

ALEXIDINE DIHYDROCHLORIDE ATTENUATES OSTEOCLASTS FORMATION AND BONE RESORPTION VIA INDUCTION OF MITOCHONDRIAL-ACTIVATED APOPTOTIC PROGRAM

[1]Xiang Zhu, [1]Pei Y Ng, [2]James H Steer, [1]Nathan J Pavlos, [1]Ming H Zheng, [1]Tak S. Cheng

[1]School of Surgery, Centre for Orthopedic Research, University of Western Australia
[2]School of Medicine and Pharmacology, University of Western Australia
email: 21012646@student.uwa.edu.au

INTRODUCTION

Excessive osteoclast (OC) formation and bone resorption are the main mechanisms that lead to severe osteolytic bone diseases, such as osteoporosis and bone metastatic tumors [1]. Thus the induction of OC death (apoptosis) represents a potential therapeutic mechanism for the treatment of such osteolytic diseases. Alexidine dihydrochloride (AD), a positively charged dibiguanide compound found in contact lens cleaning solutions and oral mouthwashes, induces lipid-phase separation and domain formation of negatively charged cellular membranes and has been shown to exhibit apoptosis-inducing properties[2,3]. The most negatively charged biological membranes known to nature and highly abundant in OC, the mitochondria is a potential candidate target for AD-induced apoptotic effects.

METHODS

MTS was used to test the cytotoxicity effect of AD on OC precursor cells. In vitro osteoclastogenesis, PCR and bone resorption assays were carried out to determine the effects of AD on OC formation and function. Western blot analyses, caspase-3 activity, flow analysis and ATP assays were conducted to investigate the role of AD in regulation of mitochondrial function and apoptosis in OC.

RESULTS AND DISCUSSION

In vitro RANKL-induced osteoclastogenesis was inhibited by AD in a dose-dependent manner (Figure 1) and correlated with suppression of OC-specific marker genes (TRAP, CTSK, CTR and DC-STAMP). Additionally, AD attenuated the bone-resorbing activity of mature OCs. Mechanistically AD disrupted mitochondrial function and induced classical mitochondrial apoptotic program involving members of the Bcl-2 family, cytochrome c release, triggering activation of caspase-3 and -9 apoptotic cascades and ultimately leading to nuclear condensation and cell death.

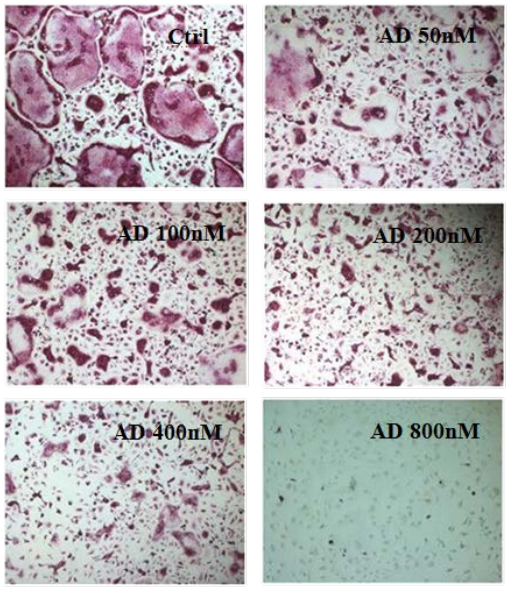

Figure 1: A figure showing AD inhibits RANKL-induced osteoclastogenesis in mouse BMM cells.

CONCLUSIONS

Our findings demonstrates that AD inhibited OC formation and function by inducing mitochondrial-activated apoptotic program. Thus, AD may represent an alternative therapeutic agent for the treatment of osteolytic bone diseases.

REFERENCES

1. Tanaka Y, et al., *Curr Drug Targets Inflamm Allergy*. **4**:325-328, 2005.
2. Yanai R, et al., *Eye Contact Lens*.**37**:57-60, 2011.
3. Yip KW, et al., *Mol Cancer Ther*. **5**:2234-2240, 2006.

MODELING AND PARAMETER IDENTIFICATION OF GENE REGULATORY NETWORKS IN HUMAN OSTEOBLASTS

[1]Song Chen, [2]Paul Smith, [1]Qinghua Qin, and [2,3]Rachel Li

[1]Materials and Manufacturing Group, College of Engineering and Computer Science, Australian National University, ACT
[2]Trauma and Orthopaedic Research Unit, Department of Surgery, Canberra Hospital, ACT
[3]Department of Immunology and Genetics, John Curtin School of Medical Research, Australian National University, ACT
email: song.chen@anu.edu.au

OBJECTIVE

A mathematical model to describe the gene regulatory network based on hysteretic function by combining the engineering hysteresis model and bone cells' response in low-frequency (LF) electromagnetic fields (EMFs).

METHODS

A general dynamical model including the modified Bouc-Wen hysteresis model as the hysteresis component was developed. The cultured OBs were exposed to the LF-EMFs for 3 days in serial doses of magnetic flux at 0, 0.05, 0.15, 0.25, 0.5, 0.7mT combined with frequency conditions of 40, 80, 160, 320, 640Hz. Proliferations of OBs were measured using Cell Counter (Vi-CellTM XR, BECKMAN) and genes related to osteogenetic pathways were studied using RT-qPCR Array (PAHS-026Z,QIAGEN).

RESULTS AND DISCUSSION

The model developed was capable of describing the gene expression in a hysteresis loop and generating transient behavior. Our results showed that the OBs' response in LF-EMFs could partially identify the parameters at frequency response. The number of parameters were reduced by the frequency response. We also observed that the proliferations of OBs were influenced by the combination of frequency and magnetic flux of LF-EMFs. The coupling effect of EMF on OBs was highly dependent on the frequency (Hz) of LF-EMFs and genes related to osteogenetic pathways were up/down-regulated after LF-EMFs intervention. These results confirmed that the influence of LF-EMFs on OBs was suitable for characterising the gene regulatory networks in OBs.

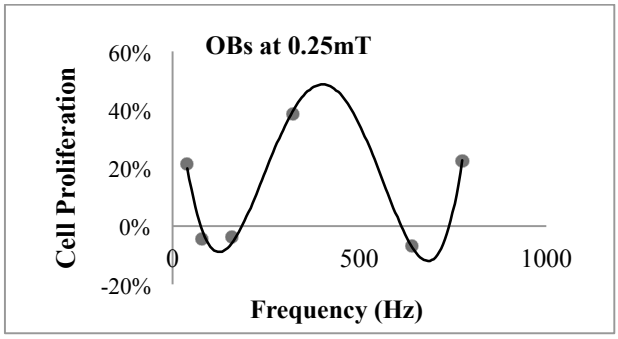

Figure 1: Frequency response of osteoblasts cell proliferation under LF-EMF.

CONCLUSION

This model was supported by biological data and has the potential to further develop as a high throughput program to identify biomarkers in osteogenesis.

ACKNOWLEDGEMENT

Great thanks to CSC and ANU scholarship.

CONFLICT OF INTEREST DECLARATION

In the interests of transparency and to help reviewers assess any potential bias, ANZORS requires authors of original research papers to declare any competing commercial interests in relation to the submitted work. Referees are also asked to indicate any potential conflict they might have reviewing a particular paper.

If you have accepted any support such as funds or materials, tangible or intangible, concerned with the research by the commercial party such as companies or investors, choose YES below, and state the relation between you and the commercial party.

If you have not accepted any support such as funds or materials, choose NO.

Do you have a conflict of interest to declare? (DELETE TEXT as appropriate)

1. **NO**

Modulation of Autophagy and Apoptosis in Human Osteoclasts *In Vitro:* Preliminary Data

[1]H Kamitakahara, [1]T Crotti, [1]D Haynes, [2]M Smith, [1] AASSK Dharmapatni

[1]Discipline of Anatomy and Pathology, School of Medical Sciences, University of Adelaide, Adelaide, SA
[2]Rheumatology Research Unit, Repatriation General Hospital, Daw Park, Adelaide, SA
Email: hannah.kamitakahara@student.adelaide.edu.au

INTRODUCTION

Rheumatoid arthritis (RA) is a chronic autoimmune disease that leads to irreversible cartilage and bone loss in synovial joints. The influx of inflammatory and immune cells triggers synovial hyperplasia and increases numbers of bone-resorbing osteoclast (OC) cells. Accumulating evidence indicate defective (reduced) apoptosis as a critical point of intervention [1, 2]. Recently, an increase in the pro-survival mechanism named autophagy has been observed in synovial tissue, and inversely correlated with levels of apoptosis [1, 3], suggesting mutual inhibition via molecular crosstalk. A major role for TNF-α in stimulating OC autophagy has been demonstrated [3]. As such, it was hypothesized that modulating autophagy in cultured OCs exposed to TNF-α, will affect apoptosis and osteoclastogenesis. The aim of this experiment was to investigate the effect of autophagy and apoptosis modulators on gene and protein expression associated with apoptosis and osteoclastogenesis *in vitro*.

METHODS

Osteoclasts were differentiated *in vitro* from human peripheral blood monocytes of 4 healthy donors, in the presence of 50ng/ml soluble RANKL and 25 ng/ml M-CSF[4]. Cells were pretreated with TNF-α 5ng/ml for 24 hrs before treatments and then treated with/out an autophagy inhibitor (Hydroxychloroquine/HCQ 50μg/ml) [5], autophagy inducer (Rapamycin 100μM) [6] or apoptotic inducer (Embelin 15μmol/lt) for 24 hours. Total RNA was extracted on day 14 to assess expression of autophagy genes (Beclin-1, LC3), apoptotic (caspase-3 and -9) and OC markers (TRAP) by quantitative real-time PCR. Cells were also fixed for immunocytochemistry of autophagy markers, Beclin-1 and LC3. Differences between treatments were analyzed using Kruskall Wallis followed by Mann Whitney tests. P-value <0.05 considered significant.

RESULTS AND DISCUSSION

Treatments modulated the expression of autophagy, apoptosis and osteoclast genes. Rapamycin significantly induced LC3 mRNA compared to HCQ and Embelin treated cells, as expected (Figure 1). Unexpectedly, Rapamycin also induced Caspase 3 and Beclin-1 mRNA increased following HCQ and Embelin treatment but the difference to control cells was not significant. There was a significant increase in caspase-3, but not caspase-9 mRNA following Embelin treatment compared to untreated cells, indicating induction of the extrinsic apoptosis pathway. TRAP mRNA was induced by Rapamycin, but not HCQ or Embelin treatment, although this was not statistically significant.

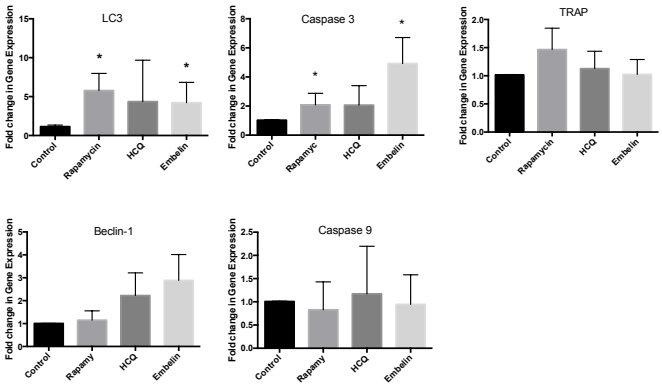

Figure 1: Change in gene expression, * p<0.05 compared to control

Dual immunoflourescent staining confirmed the presence of autophagy proteins at baseline and changes following treatments. Colocalisation of Beclin-1 and LC3 was observed in areas in the cultured osteoclasts (Figure 2).

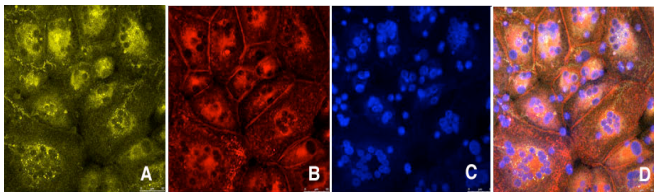

Figure 2: A, Beclin- **1 (yellow), B, LC3 (red), C, DAPI (blue) and D, overlay Beclin-1, LC3 and DAPI**

CONCLUSIONS

These results support the postulate that pharmacological modulation of autophagy is associated with changes in apoptosis and OC genes [3].

ACKNOWLEDGEMENTS

This study is supported by Grant in Aid 2014, the Arthritis Australia, State and Territory Affiliates, Arthritis SA

REFERENCES

1. Xu K, et al., *Inflammation Research*. **62**:229-237, 2013
2. Dharmapatni A, et al., *Arthritis Research & Therapy*. **11**:1-11, 2009
3. Lin N, et al., *Ann Rheum Dis*. **72**:761-768, 2013
4. Holding C, et al., *Biomaterials*. **27**:5212-5219, 2006
5. Lagneaux L, et al., *Br J Haematol*. **112**:344-352, 2001
6. Klionsky D, et al., *Autophagy*. **4**:151-175, 2008

Synergistic Effect of Nanomaterials and BMP-2 Signalling in Inducing Osteogenic Differentiation of Adipose Tissue-Derived Mesenchymal Stem Cells

Lu ZF[1], SI Roohani-Esfahani[1], JJ Li[1] and Zreiqat H[1]

[1.] *Biomaterials and Tissue Engineering Research Unit, School of AMME, the University of Sydney, Sydney, 2006, Australia*

email: zufu.lu@sydney.edu.au

INTRODUCTION

Mesenchymal stem cells (MSCs) hold a great promise for the repair and regeneration of large bone defects and non-union bone fractures, which remains a major clinical challenge for orthopaedic surgeons. A deep understanding of the signalling pathways controlling MSCs into osteogenic lineage will significantly advance the MSC-based approaches for bone tissue regeneration. Our strategy to understand these signalling pathways is to mimic the components within bone microenvironment, as they are critical in providing sufficient signals to drive the osteogenic differentiation of MSCs.

In the present study we seek to understand the interactions of three days of bone morphogenetic protein-2 treatment (BMP-2, mimicking transient induction of BMP-2 after bone injury) and bioactive glass nanoparticles (nBG) incorporated polycaprolactone (PCL) coating on hydroxyapatite/β-tricalcium phosphate(HA/TCP) scaffolds (nBG-PCL/HA/TCP scaffolds, mimicking bone nanostructure) in directing osteogenic differentiation of adipose tissue-derived mesenchymal stem cells (ASCs) and the underlying signalling pathways involved .

METHODS

We first examined the effects of short (three days) BMP-2 stimulation on osteogenic differentiation of ASCs, followed by the combinational effects of short BMP-2 stimulation and nBG-PCL/HA/TCP scaffold by setting up the following groups: (1): ASCs seeded on HA/TCP scaffolds (control group), (2): ASCs seeded on nBG-PCL/HA/TCP scaffolds, (3): ASCs preconditioned with BMP-2 and seeded on HA/TCP scaffolds, (4): ASCs preconditioned with BMP-2 and seeded on nBG-PCL/HA/TCP scaffolds. We further investigated the mechanisms underlying the synergistic effect of BMP-2 stimulation and nBG-PCL/HA/TCP scaffold in inducing the osteogenic differentiation of ASCs.

RESULTS AND DISCUSSION

First, compared to ASCs without BMP-2 pre-conditioning, ASCs treated with BMP-2 (50 ng/mL) for 3 days showed significantly higher levels of Runx-2, collagen type I, osteopontin, and bone sialoprotein gene expression and ALP enzyme activity at 4 and 14 days.

Second, we observed that the combination of BMP-2 pre-conditioning and culturing on nBG-PCL/HA/TCP scaffolds produced the most significant induction of osteogenic gene expression and ALP activity, compared to ASCs grown on HA/TCP scaffolds without BMP-2 pre-conditioning; ASCs grown on HA/TCP scaffolds with BMP-2 pre-conditioning, and to ASCs grown on nBG-PCL/HA/TCP scaffolds without BMP-2 preconditioning.

In addition, we investigated the effect of nBG-PCL/HA/TCP scaffold substrate on Wnt-3a expression in ASCs. Compared to ASCs on HA/TCP scaffolds, ASCs cultured on nBG-PCL/HA/TCP scaffolds showed significantly higher Wnt-3a protein expression (3-fold increase) as early as 5 hours after seeding, which increased up to about 5 folds at 24 hours. The role of Wnt-3a signalling in nBG-PCL/HA/TCP scaffold-mediated ASCs osteogenic induction was further investigated by adding Wnt-3a signalling inhibitor (IWR-1) into the culture medium. ASCs pre-conditioning with BMP-2 (3 days) and seeded on nBG-PCL/HA/TCP scaffolds in the presence of IWR-1 significantly decreased the levels of Runx-2, collagen type I, osteopontin and bone sialoprotein gene expression, as well as ALP activity at day 14.

Last, we found that activated β1-integrin protein expression in ASCs cultured on nBG-PCL/HA/TCP scaffolds was 4 and 7-fold higher, respectively, compared to those cultured for 5 and 24 hours on HA/TCP scaffolds, while no change was found for total β1-integrin expression between these two groups; and blocking of β1-integrin signalling in BMP-2 pre-conditioned ASCs cultured on nBG-PCL/HA/TCP scaffolds showed two major effects: (1) decreased Wnt-3a protein expression at 5 and 24 hours, and (2) inhibited Runx-2, collagen type I, osteopontin and bone sialoprotein gene expression, as well as ALP activity at day 14.

CONCLUSIONS

This study revealed that different components in the bone tissue microenvironment constitute a coordinated signalling network which controls stem cell fate into osteogenic differentiation. This highlights the importance of identifying the signals in each component of the bone tissue microenvironment that are spatially and temporally necessary for bone repair and regeneration.

ACKNOWLEDGEMENTS

The authors acknowledge the Australia National Health and Medical Research Council (NHMRC) for its funding for the research. The authors also acknowledge Rebecca Cooper Foundation.

SEMAPHORIN-3A, NEUROPILIN-1 AND PLEXIN-A1 ARE INCREASED DURING OSTEOCLAST FORMATION AND FURTHER ELEVATED BY PROSTHETIC PARTICLES *IN VITRO*

Saad S[1], Dharmapatni ASSK[1], Crotti TN[1], Cantley M[1], Algate K[1], Findlay DM[2], Atkins GA[2] and Haynes DR[1]
[1] Discipline of Anatomy and Pathology, School of Medical Sciences, the University of Adelaide, Adelaide, SA
[2] Departments of Orthopedics and Trauma, Adelaide, SA
Email: sylvia.saad@student.adelaide.edu.au

INTRODUCTION

Peri-prosthetic osteolysis (PPO) is due to an inflammatory reaction to wear particles released from prosthetic implants [1]. The associated bone loss is largely due to increased bone resorption by osteoclasts [1]. Semaphorin-3a (sem3a), neuropilin-1 (nrp1) and plexin-A1 (plexA1) are immunoregulatory and axonal guidance molecules that, as a bound complex, inhibit osteoclast differentiation via disruption of immune-receptor tyrosine-based activation motif (ITAM) co-stimulatory signalling [2]. Our preliminary data observed significantly higher expression of sem3a and nrp1 proteins at sites of PPO compared to osteoarthritic tissues ($p<0.05$) (ANZORS 2013). Here we further investigate the effect of prosthetic particles on sem3a, nrp1 and plexA1 gene and protein expression in human osteoclasts *in vitro*.

METHODS

Human peripheral blood mononuclear cells (PBMCs) were isolated from whole blood buffy coats as previously reported [3]. Cells were cultured with and without particles of prosthetic material, polyethylene (PE). Sem3a, nrp1 and plexA1 protein and gene expression were investigated using immunofluorescence and quantitative real-time (qRT)-PCR, respectively. Co-expression of sem3a, nrp1 and plexA1 with clathrin-coated vesicles *in vitro* was visualised using dual-immunofluorescent staining.

RESULTS AND DISCUSSION

Immunofluorescent staining (fig. 1) showed osteoclastic multi-nucleated cells expressing sem3a and nrp1 within the cytoplasm. Cell surface nrp-1 was seen particularly at sites of cell-cell contact. Gene expression of sem3a, nrp1 and plexA1 progressively increased over the 17-day cell culture (fig. 2). When osteoclasts were cultured with PE particles, expression of all factors increased by more than 3-fold at day 14 (table 1).

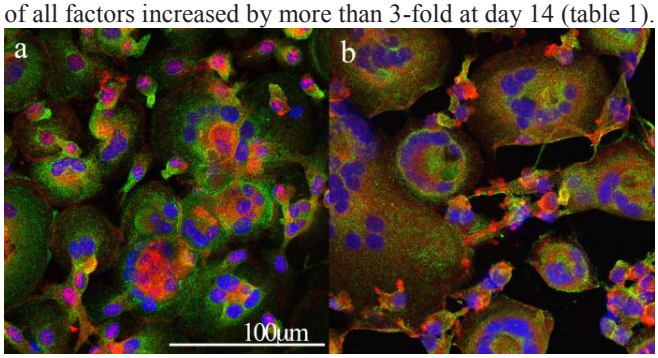

Fig. 1. Sem3a (red-a), nrp1 (red-b) and clathrin (green) expression in RANKL-stimulated osteoclasts *in vitro*

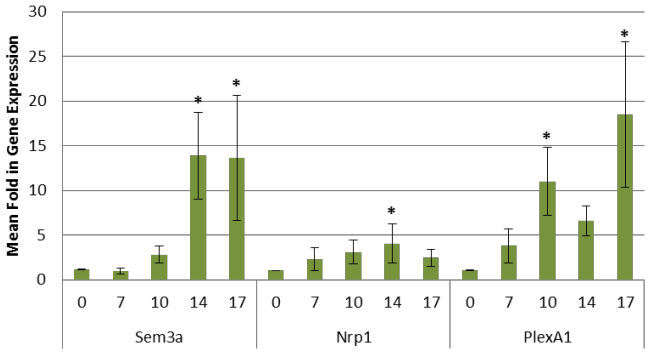

Fig. 2. Sem3a, nrp1 and plexA1 gene expression qRT-PCR. The mRNA expression over 17 days compared to day 0 (relative to hARP, mean±SEM, *$p<0.05$, n=12).

Table 1 Mean fold values of sem3a, nrp1 and plexA1 gene expression in day 14 PBMCs with or without PE (relative to hARP) assessed by qRT-PCR.

	No PE [a]	PE [a]	P values
Sem3a	1.07 ± 0.15	3.65 ± 1.01	0.0085*
Nrp1	1.70 ± 0.46	5.42 ± 1.57	0.0186*
PlexA1	2.12 ± 0.59	13.34 ± 9.30	0.1269

[a] Mean SQA ± SEM; n=6, * $P<0.05$ statistically significant

CONCLUSIONS

Sem3a produced by neuronal cells and osteoblasts have the ability to inhibit osteoclast bone resorption [2, 4]. Our findings show that sem3a, nrp1 and plexA1 expressed by the osteoclast could be involved in autocrine and paracrine signalling with the osteoblast [5]. High expression of nrp1 at sites of cell-cell interaction may indicate a cell fusion role, similar to its axonal guidance actions with neuronal cells (6). Importantly, sem3a, nrp1 and plexA1 are markedly elevated by prosthetic particles and sem3a and nrp1 are highly expressed at sites of peri-implant osteolysis.

REFERENCES

1. Shen, Z et al. *Arthritis Res Ther*. **8**(3), 2006.
2. Hayashi, M et al. *Nature*. **485**(7396):69-74, 2012.
3. Holding, CA et al. *Biomaterials*. **27**(30):5212-5219, 2006.
4. Catalano, A. *J Immunol*. **185**(10):6373-6383, 2010.
5. Sims, NA et al. *Semin Cell Dev Biol*. **19**(5):444-451, 2008.
6. Nakamura, F et al. *J Neurobiol*. **44**(2):219-29, 2000.

OSTEOBLAST DERIVED-NEUROTROPHIN-3 (NT-3) AS A NOVEL CROSS-TALK SIGNAL PROMOTES OSTEOCLAST FORMATION

[1]Yu-Wen Su, [2]Shek-Man Chim, [1]Rosa Chung, [1]Chiaming Fan, [1]Tristan J King, [2]Jiake Xu, [1]Xin-Fu Zhou, [1]Cory J Xian

[1] School of Pharmacy and Medical Sciences, Sansom Institute for Health Research, University of South Australia, Adelaide, SA
[2]School of Pathology and Laboratory Medicine, University of Western Australia, WA
email: Yu-Wen.Su@unisa.edu.au

INTRODUCTION

Studying modulators of osteoclast formation/activity is important due to their critical roles in physiological bone remodeling and in bone loss disorders. Recently, brain-derived neurotrophic factor or BDNF has been shown to be an important factor promoting osteoclast formation and bone loss in multiple myeloma patients [1]. Whether other members of the neurotrophic factor family (nerve growth factor or NGF, neurotrophin-3 or NT-3, and NT-4) also can regulate osteoclast formation and function is unknown.

Recently, we observed the most prominent induction of NT-3 among all NTs (NT-3 by 60 folds vs other NTs < 20 folds) during osteogenic differentiation of bone marrow stromal cells in vitro [2]. The current study investigated potential roles and action mechanisms of osteoblast-derived NT-3 in modulating osteoclast formation in vitro.

METHODS

Normal rat bone marrow stromal cells were induced for osteogenesis and mineralization in vitro, and conditioned medium was collected at day 0 or day 14 of osteogenic induction. Recombinant NT-3 protein (rhNT-3) or osteogenic conditioned medium were investigated for their abilities in promoting osteoclast formation in the presence or absence of M-CSF, RANKL, anti-NT-3 neutralising antibody or normal IgG in normal rat bone marrow cells or in mouse osteoclast precursor RAW264.7 cells The treatment effects were examined by numbers of TRAP positively-stained multinuclear osteoclasts formed and levels of mRNA expression of osteoclastogenesis-regulatory genes (receptors RANK and OSCAR, and osteoclast proteinase cathepsin-K).

To examine potential action mechanisms of NT-3 in promoting osteoclastogenesis, mRNA expression of NT-3 and receptor TrkC was examined during osteoclastogenesis in rat bone marrow cells. In addition, potential direct effect of rhNT-3 in promoting activation of NF-kB, in the presence or absence of RNAKL, was investigated in osteoclast precursor RAW264.7 cells stably transfected with NF-kB luciferase reporter construct. Furthermore, as an indication of potential indirect effect of NT-3 in osteoclastogenesis, effects of treatments with 100ng/ml rhNT-3 or anti-NT-3 or normal IgG (7.5μg/ml) on mRNA expression of osteoclastogenesis-regulatory molecules (TNF-α, IL-1β, IL-6 and RANKL/OPG ratio) were examined by qRT-PCR during osteogenesis of bone marrow stromal cells.

RESULTS AND DISCUSSION

rhNT-3 or osteogenic conditioned medium collected during mineralizing stage (at day 14 of culture, but not at day 0) promoted osteoclastogenesis in rat bone marrow cells, as shown by the numbers of osteoclasts formed or by the mRNA expression levels of RANK, OSCAR and cathepsin-K. The osteoclastogenic effect of the osteogenic conditioned medium was blocked by the presence of anti-NT-3 antibody, suggesting ability of osteoblast-derived NT-3 in supporting osteoclast formation. In addition, rhNT-3 protein (or the osteogenic conditioned medium) and RNAKL together were found to synergistically promote osteoclastogenesis.

During osteoclastogenesis in rat bone marrow cells, up-regulated expression of NT-3 and receptor TrkC was observed, suggesting potential direct autocrine/paracrine regulatory roles of NTs in regulating osteoclast formation. However, rhNT-3 protein was not able to promote NF-κB activation in osteoclast precursor cells, suggesting NT-3 action on osteoclast formation may not directly involve NF-κB activation. On the other hand, rhNT-3 protein was found to up-regulate mRNA expression of pro-osteoclastogenic cytokines TNF-α, IL-1β, and IL-6 and enhanced RANKL/ OPG ratio during osteogenesis of rat bone marrow stromal cells in vitro, suggesting potentially an indirect role of NT-3 in promoting osteoblast-mediated supportive effect for osteoclast formation (by inducing osteoclastogenic cytokines).

CONCLUSIONS

Expression of NT-3 and receptor TrkC during osteoclast-ogenesis, suggesting a potential direct autocrine/paracrine role of NT-3 in regulating osteoclast formation. Osteoblast-derived NT-3 can promote osteoclastogenesis, suggesting a possible role of NT-3 as a novel crosstalk signal between osteoblasts and osteoclasts. While effect of NT-3 on osteoclast formation does not appear to directly involve NF-κB activation, NT-3 can also indirectly promote osteoclastogenesis by inducing osteoclastogenic cytokines TNF-α, IL-1β, IL-6 and enhancing RANKL/OPG expression ratio in osteoblasts.

ACKNOWLEDGEMENTS

This work was supported by University of South Australia.

REFERENCES

1. Sun C-Y et al, *Int J Cancer*. **130**, 827–836, 2012.
2. Su Y-W et al, *ANZBMS Conference* 2013, Melbourne.

SESSION 2 – CLINICAL 1

EARLY WEAR OF 36MM AND 28MM METAL ON HIGHLY CROSS-LINKED POLYETHYLENE ARTICULATIONS IN TOTAL HIP ARTHROPLASTY

Mario Zotti[1,2], Oksana Holubowycz[1,2], Stuart Callary[1,2] and Donald Howie[1,2]

[1]Centre for Orthopaedic and Trauma Research, The University of Adelaide &
[2]Department of Orthopaedics and Trauma, Royal Adelaide Hospital
email: mario.zotti@health.sa.gov.au

INTRODUCTION

Laboratory and *in vivo* studies have shown low early wear rates of highly cross-linked polyethylene (HXLPE), compared to that of conventional polyethylene [1]. Consequently, HXLPE has been widely adopted as the polyethylene of choice in metal-on-polyethylene articulations in total hip arthroplasty (THA). Concurrently, the use of larger articulations has increased [2] and 36 mm articulations have been shown to reduce the incidence of dislocation one year following THA, compared to 28 mm articulations [3]. However, large articulations were associated with increased wear compared to standard articulations using conventional PE [4]. Therefore, the aim of this study was to compare early polyethylene wear of 36 mm and 28 mm metal on HXLPE articulations in primary THA.

METHODS

326 hips in 326 patients (164 – 28 mm and 162 – 36 mm articulations) underwent radiographic analysis of wear, measured as 2D femoral head penetration (FHP) using PolyWare™ (Rev 5, Draftware, IN, USA).

These patients were previously enrolled into a RCT which examined the effect of articulation size on the incidence of dislocation one year following THA. Patients had been randomized intra-operatively to receive either a 28 mm or 36 mm cobalt chrome head with a 10 Megarad electron beam irradiated, subsequently melted, gas plasma sterilized HXLPE liner (Longevity™).At the time of operation, all patients in the current study were ≥60 years old and underwent primary THA with a cemented femoral and uncemented acetabular component through a posterior approach.

Analysis used combinations of available AP and lateral radiographs taken at 4-6 days, 6 weeks, 3 months, 1, 2 (Australia), 3 (UK) and 5 years post-operatively. Bedding-in/creep was assumed to be complete by the end of the first post-operative year.Mean steady-state 2D wear rates (mm/yr) were calculated using all available radiographs from one year., The effect of time and articulation size on FHP was further analysed using statistical modelling.

RESULTS AND DISCUSSION

There were no significant differences between the 36 mm and 28 mm cohorts in age, gender, BMI, component orientation and outer diameter of the acetabular component.

The 2D and volumetric wear rates, as well as proportion of the cohorts exceeding ≥0.1 mm/year (associated with the prevalence of osteolysis in conventional PE [5]) are presented in Table 1.Statistical modelling showed no effect of time on 2D femoral head penetration irrespective of head size after 3 months (p=0.65).

CONCLUSION

There were no significant differences between 36mm and 28mm articulations regarding early 2D- and volumetric wear rates. Up to five years following primary metal on HXLPE THAs, the mean 2D wear rates and proportion of patients with 2D wear rates ≥0.1 mm/yr did not differ significantly between the 36 mm and 28 mm articulation cohorts.

ACKNOWLEDGEMENTS

Dr Stuart Howell, Statistician, Data Management and Analysis Centre, The University of Adelaide;
The Large Articulation Study Group [3]

REFERENCES

[1] Kurtz S, et al. History and systematic review of wear and osteolysis outcomes for first-generation highly crosslinked polyethylene. *Clinical Orthopaedics and Related Research*, 2011;469: 2262-77.
[2]Australian Orthopaedic Association, National Joint Replacement Registry Annual Report, 2013, Adelaide, Australia
[3] Howie D, et al. Large femoral heads decrease the incidence of dislocation after total hip arthroplasty. A randomized controlled trial. *JBJS-A* 2012;94:1095-102.
[4] Livermore J, et al. Effect of femoral head size on wear of the PE acetabular component. *JBJS-A* 1990;72:518-28.
[5] Dumbleton J,et al. A literature review of the association between wear rate and osteolysis in total hip arthroplasty, *J Arthroplasty* 2002; 17:649-661.

Table 1. Wear of 36mm compared to 28mm articulations

Outcome	36mm (n=162)	28mm (n=164)	p value
2D mean wear rate (median, range) [mm/year]	-0.01 (0.00, 1.0-0,88)	0.00 (0.01. -1.4-0.62)	0.34
Proportion of cohort ≥0.1mm/yr	23 of 162 (14.2%)	23 of 164 (14.0%)	-
Volumetric wear rate [mm^3/year]	28 (0, 0-222)	24 (2, 0-292)	0.67

CONFLICT OF INTEREST DECLARATION

In the interests of transparency and to help reviewers assess any potential bias, ANZORS requires authors of original research papers to declare any competing commercial interests in relation to the submitted work. Referees are also asked to indicate any potential conflict they might have reviewing a particular paper.

If you have accepted any support such as funds or materials, tangible or intangible, concerned with the research by the commercial party such as companies or investors, choose YES below, and state the relation between you and the commercial party.

If you have not accepted any support such as funds or materials, choose NO.

Do you have a conflict of interest to declare?

YES

If YES, please complete as appropriate:

1. The author(s) did receive payments or other benefits or a commitment or agreement to provide such benefits from a commercial entity.
   State the relation between you and the commercial entity:

2. A commercial entity paid or directed, or agreed to pay or direct, any benefits to any research fund, foundation, educational institution, or other charitable or nonprofit organization with which the authors are affiliated or associated.

Research support from Zimmer

OSTEOLYSIS AND WEAR OF LARGE AND STANDARD METAL ON HIGHLY CROSS-LINKED POLYETHYLENE ARTICULATIONS

Caroline Moran, Oksana Holubowycz, Donald Howie, Bogdan Solomon

Centre for Orthopaedic and Trauma Research, University of Adelaide, Department of Orthopaedics and Trauma, Royal Adelaide Hospital and the, Adelaide, South Australia
email: Caroline.Moran@adelaide.edu.au

INTRODUCTION

Laboratory and subsequent clinical studies have shown low rates of early wear of highly cross-linked polyethylene, compared to that of conventional polyethylene. As a result, there has been almost universal adoption of highly cross-linked polyethylene as the polyethylene of choice in metal-on-polyethylene articulations in total hip arthroplasty (THA), as well as increasing use of larger articulations. Although wear of conventional polyethylene has been shown to be related to periprosthetic osteolysis, the relationship between wear of highly cross-linked polyethylene (HXLPE) and osteolysis remains uncertain. Our aim was to determine the incidence and volume of periacetabular osteolysis at a minimum of seven years following primary THA in patients receiving standard and large metal on HXLPE articulations.

METHODS

122 patients (69 patients - 28 mm articulation, 53 patients - 36 mm articulation; median age 72 yrs, range 65-86; 51M, 71F) have undergone a quantitative computed tomography (CT) scan, with metal artefact reduction protocol, to detect and measure osteolysis at a minimum of seven years following THA. These patients were previously enrolled into a randomized controlled trial which examined the effect of articulation size on the incidence of dislocation one year following THA. Patients were randomized intra-operatively to receive either a 28 mm or 36 mm cobalt chrome head articulating with a 10mRad electron beam irradiated, melt annealed, gas plasma sterilized HXLPE liner. Osteolysis was defined as a localized area of bone loss of at least 1 cm^3, with a well-defined sclerotic border, clear communication between the defect and the joint space, and absence of pre-existing acetabular cysts, determined from pre-operative or early post-operative plain radiographs. Polyethylene wear from one to seven years following THA was also measured, using a computerized edge detection technique (PolyWare Rev 5, Draftware) of analyzing standard radiographs.

RESULTS AND DISCUSSION

Ten of the one hundred and twenty two patients were excluded because possible osteolytic lesions identified on CT could not be definitively classified due to inadequate or missing early plain radiographs; a further 11 patients were identified as having pre-existing acetabular cysts. Eight of the remaining one hundred and one patients (4 – 36 mm articulation) were found to have osteolytic lesions adjacent to the acetabular component; all were located in the ilium adjacent to either fixation screws or empty screw holes. The median lesion volume was 1.7 cm^3 (range 1.1 – 5.4 cm^3). No femoral osteolysis was detected in any of the patients. The median linear wear rate in the patients with osteolysis was 0.04 mm/yr (range 0.02 – 0.1 mm/yr).

This study is one of the largest to use CT to identify osteolysis. Although the incidence and volume of osteolysis adjacent to metal on HXLPE articulations at seven years was low, it is of some concern that osteolytic lesions were detected, particularly in the absence of clinically significant wear. Further monitoring of these lesions will determine whether they develop into larger, clinically relevant osteolytic lesions.

CONCLUSIONS

Seven years after THA with a metal on HXLPE articulation, 8 of 101 patients with no pre-existing acetabular cysts had periacetabular osteolytic lesions >1cm^3 in the absence of significant HXLPE wear.

ACKNOWLEDGEMENTS

Funding support received from the National Health and Medical Research Council and Zimmer.

CONFLICT OF INTEREST DECLARATION

In the interests of transparency and to help reviewers assess any potential bias, ANZORS requires authors of original research papers to declare any competing commercial interests in relation to the submitted work. Referees are also asked to indicate any potential conflict they might have reviewing a particular paper.

If you have accepted any support such as funds or materials, tangible or intangible, concerned with the research by the commercial party such as companies or investors, choose YES below, and state the relation between you and the commercial party.

If you have not accepted any support such as funds or materials, choose NO.

Do you have a conflict of interest to declare?

YES

If YES, please complete as appropriate:

1. The author(s) did receive payments or other benefits or a commitment or agreement to provide such benefits from a commercial entity.
   State the relation between you and the commercial entity:

2. A commercial entity paid or directed, or agreed to pay or direct, any benefits to any research fund, foundation, educational institution, or other charitable or nonprofit organization with which the authors are affiliated or associated.

   A portion of research funding support for the study was received from Zimmer.

CAN IMPACTION BONE GRAFTING OF OSTEOPOROTIC TIBIAL PLATEAU FRACTURES FACILITATE IMMEDIATE UNRESTRICTED WEIGHT BEARING?

G.J. van de Pol[1], S.A. Callary[1,2], G.J. Atkins[2], D. Thewlis[3], L.B. Solomon[1,2]

1 - Department of Orthopaedics and Trauma, Royal Adelaide Hospital, Adelaide, SA 5000, Australia
2 - Centre for Orthopaedic and Trauma Research, The University of Adelaide, Adelaide, SA 5005, Australia
3 - University of South Australia, Adelaide, SA 5000, Australia
email: bogdansolomon@mac.com

INTRODUCTION

Osteoporotic tibial plateau fractures (TPFs) are difficult to treat with either open reduction internal fixation (ORIF) or acute total knee arthroplasty (TKA) and have high complication rates, poor outcomes and often fail at short to mid-term follow-up. We propose that the use of impaction bone grafting (IBG) as an adjuvant to ORIF will improve the outcomes of osteoporotic TPFs.

METHODS

Ten consecutive osteoporotic TPFs, median T score -2.9 (-2 to -4.5), were treated with IBG alone (one Schatzker III fracture) or with ORIF augmented with IBG, using on average allograft from 2.1 femoral heads/case (range 1-4 heads or 25-100cm^3). Postoperative, all patients were mobilized unrestricted and had their gait analyzed throughout follow-up. Fracture reduction was assessed on plain radiographs and CT-scans; maintenance of fracture reduction was monitored using plain radiographs, CT and RSA. Graft integration was assessed by comparison of immediate post-operative CT scans with scans at a minimum of one year (Figure 1). In case plates or screws were removed at a minimum of one year after fixation, histology samples were taken from the grafting site.

RESULTS AND DISCUSSION

All surgeries were uneventful. Postoperatively, one patient developed a transient peroneal nerve palsy. All remaining patients progressed to full weight bearing within six weeks and regained a normal gait by three months. One fracture failed catastrophically at six months and underwent revision to a TKA. Seven fractures healed with a cranio-caudal migration of less than 3 mm (range 0-2.6 mm using RSA and 0-2 mm using CT) (Table 1). The remaining two fractures had an isolated posterolateral fragment depression of 13.5 mm and 9 mm respectively. This did not affect the overall joint alignment or clinical outcomes. At latest CT follow-up, on average 51% of the graft area (range 36% to 70%) had remodelled into new host bone. Histological analysis showed rich cellularity with trabecular bone, signs of endochondral ossification and areas of mineralized and unmineralized cartilage.

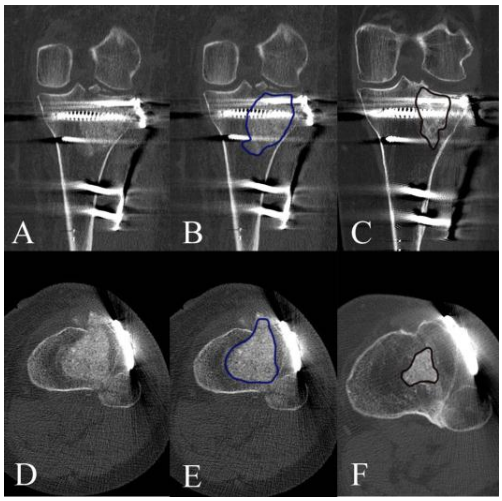

Figure 1: Incorporation measurements of the graft area on coronal (A-C) and axial (D-F) CT slices of Patient 1. Day 2 post ORIF and IBG (B and E) images were compared with slices at the same level 19 months after surgery (C and F).

CONCLUSIONS

Impaction bone grafting shows promising results as an adjuvant treatment to ORIF of tibial plateau fractures involving osteoporotic bone, with 70% of cases healing with minimal displacement despite immediate unrestricted weight bearing.

Table 1: Cranio (+ive) - caudal (-ive) migration of fracture fragment measured with CT scan and RSA in millimeters.

	Case 1	Case 2	Case 3	Case 4	Case 5	Case 6	Case 7	Case 8	Case 9	Case 10
CT	-2	0	-1	n/a	n/a	-9	0	-13.5	-1	n/a
RSA	-2.8	0.2	-1.8	0.8	-2.6	n/a	-0.6	-13.5	n/a	n/a

Methotrexate chemotherapy triggers touch-evoked pain and increased bone innervation in young rats

Fiona H. Zhou, Yingnan Yu, Xin-Fu Zhou, Cory J. Xian

Sansom Institute of Health Research, School of Pharmacy and Medical Sciences, University of South Australia, Adelaide, SA 5001
email: fiona.zhou@unisa.edu.au

INTRODUCTION

Although bone pain caused by cancer chemotherapy is a well-recognized significant problem, with approximately 1 in 10 childhood cancer patients being reported to experience isolated bone pain along with other skeletal complications [1], the underlying mechanisms are poorly understood and there is no specific treatment. In this study, effects of methotrexate (MTX) treatment on pain in the hind legs and on the extent of sensory innervation of the tibial bone were examined in young rats.

METHODS

Rats were weighed and received once daily subcutaneous injections of MTX at 0.75 mg/kg or saline for 5 days (n = 8/treatment group), mimicking the intensive induction phase of MTX treatment for childhood leukaemia as previously described [2]. Based on the animal behavioural tests used to examine skeletal pain induced by bone cancer or fractures [3,4], we modified these tests, as outlined in figure 1, to examine whether MTX treatment induced pain and immobility in a 20-day time course following the first dosing. To examine effects of MTX treatment on bone innervation, we processed frozen tibial sections for immunohistochemistry for nociceptive substance calctonin gene related peptide (CGRP), a marker for sensory nerve.

RESULTS AND DISCUSSION

MTX treatment increased von-Frey filament stimulation-induced mechanical allodynia and palpation nocifensive score in the tibia, and it also reduced mobility of the rats after tibial palpation. MTX-treated rats showed reduced loading (numbers of stands) on hind limbs, commencing early during treatment and being most obvious 2 weeks after the end of treatment, despite the lack of any ongoing pain during normal locomotion. These coincided with the increase in innervation of CGRP-positive sensory nerve fibres in tibial periosteum peaking on day 14 following the first MTX injection. These data suggest that methotrexate chemotherapy triggers touch-evoked pain involving enhanced sensory nerve innervation of the bone.

CONCLUSIONS

This acute MTX treatment model of touch-evoked pain may provide an excellent tool to understand the biological mechanism of chemotherapy induced pain and immobility.

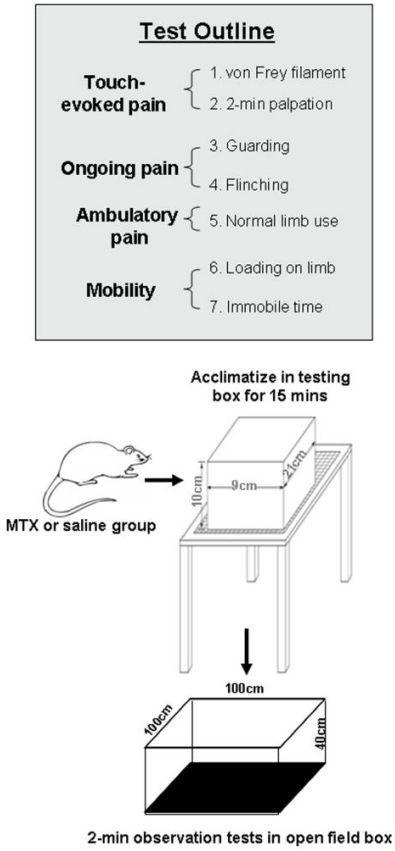

Figure 1: Diagram outlining the animal behavioural tests for bone pain and immobility.

ACKNOWLEDGEMENTS

This work was funded in parts by project grants from Channel-7 Children's Research Foundation of South Australia and National Health and Medical Research Council (NHMRC) of Australia.

REFERENCES

1. Hogler W, et al., *Pediatr Blood Cancer*. **48**: 21-27, 2007.
2. Xian CJ, et al., *Bone*. **41**: 842-850, 2007.
3. Honore P et al., *Nat Med*. **6**: 521-528, 2000.
4. Koewler NJ et al., *J Bone Miner Res*. 22: 1732-1742, 2007

HOW RELIABLE IS COMPUTER ASSISTED HIP ARTHROPLASTY POLYETHYLENE WEAR MEASUREMENT USING CURRENT RADIOGRAPHY PRACTICES?

[1,2]Diana Perriman, [1]Shyam Rajagopalan, [3]Teresa Neeman and [1,2]Paul Smith

[1]Trauma and Orthopaedic Research Unit, Canberra Hospital, ACT.
[2]College of Medicine, Biology and the Environment, The Australian National University, ACT.
[3]The Statistical Consulting Unit, The Australian National University, ACT.

Email: diana.perriman@act.gov.au

INTRODUCTION

Clinical studies of polyethylene wear use plain x-rays taken at different time points throughout the life of the prosthesis. The necessity for these images to be obtained using identical x-ray acquisition parameters has not been tested. We compared wear-measurement values using identical and non-identical images from the same patients in order to evaluate the degree of error associated with non-identical x-ray parameters when measuring polyethylene wear.

METHODS

Polyethylene wear measurements (Polyware Pro) were made from x-rays from 34 patients (38 hips) postoperatively and at final follow-up (mean 9-years) where multiple AP and lateral images of the same patient were available. Two sets of measurements made one week apart were compared. One set (non-identical) were randomly selected from the post-op and follow-up x-rays. This simulated 'usual practice' where wear calculations are made using x-rays which may or may not be identically acquired. In the other method (identical) the same x-rays were used on both occasions. Intra-class correlation coefficients ($ICC_{2,1}$), Bland-Altman limits of agreement and the degree of bias between the measurements for each method were calculated.

RESULTS AND DISCUSSION The $ICC_{2,1}$ for identical and non-identical 2D wear were 0.98 vs 0.71; for 2D linear wear/year were 0.99 vs 0.84; for 3D wear 0.98 vs 0.46; volumetric wear 0.99 vs 0.48; and volumetric wear/year 0.99 vs 0.3. The limits of agreement (LOA's) for identical and non-identical wear measurements were ± 0.14mm vs ± 1.12mm for 2D linear wear; ± 0.21mm vs ±1.3mm for 3D wear; and ± 34.5mm^3 vs ± 777.35mm^3 for volumetric wear. There was minimal bias in the time one minus time 2 measurements.

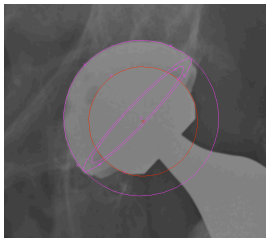

Figure. AP Hip x-ray with digital edge detection using Polyware Pro software.

CONCLUSIONS

Intra-observer reliability of x-ray re-measurement was excellent but non-identical x-rays markedly reduced the $ICC_{2,1}$ values. The LOA were wider for all non-identical measurements but particularly for volumetric wear. The results suggest that extraordinary rigour needs to be applied to standardizing radiographic parameters for wear measurement to be sufficiently accurate for use in research.

Table 1. Repeatability of radiographic wear measurements with identical selection of x-rays within patient at 6 weeks post-op and final follow-up compared to non-identical x-ray selection at both time points

Measurement	X-ray selection	Median (range)	$SD_{diff\text{-}intra}$ [a]	Bias [b] ±LOA [c]	95%CI [d]
2D Linear (mm)	Identical	0.00 (-0.30 – 0.18)	0.07	-0.01 (± 0.14)	-0.03 to 0.18
	Non-identical	0.00 (-1.10 – 1.94)	0.57	0.05 (± 1.12)	-0.13 to 0.24
3D Linear (mm)	Identical	-0.02 (-0.40 – 0.28)	0.12	-0.03 (± 0.21)	-0.07 to 0.01
	Non-identical	0.01 (-1.40 – 1.66)	0.66	0.01 (± 1.3)	-.21 to 0.22
Volumetric (mm3)	Identical	-2.00 (-76.0 – 28.0)	17.58	-2.92 (± 34.5)	-8.7 to 2.86
	Non-identical	-4.50 (-864.0 -1461.0)	392.61	-39.00 (± 777.35)	-168.05 to 90.05

A SYSTEMATIC REVIEW OF DIAGNOSTIC METHODS FOR SHOULDER IMPINGEMENT SYNDROME

[1]Amy Watts, [2]Ben Williams and [3]Jegan Krishnan

[1]The International Musculoskeletal Research Institute, Flinders University, Adelaide, SA
[2]Flinders Medical Centre, Adelaide, SA
[3]Department of Orthopaedic Surgery, Flinders Medical Centre, Adelaide, SA
email: amy.watts@imri.org.au

INTRODUCTION

Shoulder impingement syndrome (SIS) is a common debilitating condition, treated across multiple health disciplines including Orthopaedics, Physiotherapy, and Rheumatology. There is little consistency in diagnostic criteria with 'Shoulder impingement syndrome' being used for a broad spectrum of complex pathologies. We assessed patterns in diagnostic procedures for SIS across multiple disciplines.

METHODS

This is a systematic review of electronic databases MEDLINE, PubMed, The Cochrane Library, Embase, Scopus and CINAHL five years of publications, January 2009 - January 2014. Search terms for SIS included subacromial impingement syndrome, subacromial bursitis. Searches were delimited to articles written in English. The PRISMA guidelines were followed. Two reviewers independently screened all articles, data was then extracted by one reviewer and twenty percent of the extraction was independently assessed by the co-reviewer. Studies included were intervention studies examining individuals diagnosed with SIS and we were interested in the process and method used for the diagnosis.

RESULTS AND DISCUSSION

The search strategy yielded 3339 articles of which 1931 were duplicates. A further 1297 were excluded based on relevance obtained from title/abstract. A total of 111 articles were identified investigating SIS across fifty-three different journals internationally. Twelve different medical and allied health disciplines have investigated twenty-five different surgical and conservative treatments. Studies document their diagnostic approach, reporting on duration of symptoms, medical history, physical examination tests and radiological investigations. Duration of symptoms for inclusion ranged from a minimum of 1 week to 18 months where the median duration of symptoms is 3 months observed in 46 percent of the studies. Commonly used physical tests were Neer's test, Hawkins-Kennedy test, Jobe and Yocum, and a further eight tests identified. Neer's test or Hawkins-Kennedy tests were individually used in 74 percent of studies. Forty-five of the studies used more than one and up to six physical tests per study to determine the presence of impingement. Radiological investigations were reported in fifty-one studies, twenty-seven of these required more than one radiological investigation to confirm the diagnosis of SIS. Comparisons between disciplines identify important differences in diagnostic criteria used by different health professionals.

CONCLUSIONS

This study highlights the variety of diagnostic methods which are currently used between health disciplines and will be a useful comparative tool for clinicians. Diagnostic transparency is pertinent for shoulder impingement syndrome to ensure all disciplines are treating the same pathology and importantly to contribute to our understanding of the common pathology.

ACKNOWLEDGEMENTS

The authors would like to acknowledge Raechel Damarell, Senior Medical Librarian at Flinders University for her contribution and ongoing assistance with the search strategy.

A DOUBLE BLINDED, RANDOMIZED, CONTROLLED PROOF OF CONCEPT STUDY TO COMPARE POST-OPERATIVE ANALGESIC AND MOBILIZATION OUTCOMES OF LOCAL INFILTRATION ANALGESIA, SINGLE SHOT FEMORAL NERVE BLOCK AND INTRATHECAL MORPHINE IN PRIMARY TOTAL KNEE ARTHROPLASTY.

[1]Christopher Wilson, [2]Jason Koerber and [3]Jegan Krishnan

[1]Department of Orthopaedics, Repatriation General Hospital, Adelaide, SA
[2]Department of Anaesthesia, Flinders Medical Centre and Repatriation General Hospital, Adelaide, SA
[3]Department of Orthopaedics, Flinders Medical Centre, Adelaide, SA
email: amy.watts@imri.org.au

INTRODUCTION

Total knee arthroplasty is associated with early postoperative pain. Appropriate pain management is important to facilitate postoperative rehabilitation and positive functional outcomes. This study compares outcomes in TKA with three techniques; local infiltration analgesia, single shot femoral nerve block and intrathecal morphine.

METHODS

Forty-five patients undergoing elective primary Total Knee Arthroplasty (TKA) with were randomized into one of three groups in a double blind proof of concept study. Study arm 1 received local infiltration analgesia ropivacaine intra-operatively, an elastomeric device of ropivacaine for 24 hours post-op. Study arm 2 received a femoral nerve block of ropivacaine with placebo local infiltration analgesia and placebo intrathecal morphine. Study arm 3 received intrathecal morphine, placebo femoral nerve block and placebo local infiltration analgesia. All patients received standardized pre-operative, intraoperative and Post-operative analgesic medication.

Participants were mobilized at 4 hrs, 24hrs and 48 hrs post operation. Range of Motion, Visual Analogue Scale (VAS) pain intensity scores and two minute walk test and Timed Up and Go test were performed. Postoperative use of analgesic drugs was recorded. Knee Society Score (KSS), Oxford Knee Score and Knee Injury and Osteoarthritis Outcome Score (KOOS) were completed at preoperative and 6 weeks post op.

RESULTS AND DISCUSSION

Assessment of the efficacy of analgesia will be conducted using VAS pain scores collected preoperatively, 0-24hrs and 24-48 hours postoperatively between the three randomized groups. Frequency of use of other analgesia and need for PCA will be compared between groups at 0-24hr and 24-48hrs post operatively. The assessment of functional outcomes will be measured between the three groups by comparing the ability to mobilize the first 4 hrs after surgery, maximal flexion and extension, two minute walk test and timed up-and-go preoperatively, on postoperative day 1 and 2 and 6 weeks. Patient reported outcome measures KSS, Oxford Knee score and KOOS will be compared for the three study arms.

CONCLUSIONS

Results from the study will provide important information for the management of TKA in the hospital setting. The comparison of the three commonly used analgesic techniques and mobilization outcomes are pertinent for physiotherapy and rehabilitation management, anaesthetic specialists, nursing staff, orthopaedic surgeons and patients.

ACKNOWLEDGEMENTS

The authors would like to acknowledge the assistance of the International Musculoskeletal Research Institute data collection and management and for financial in-kind support.

METHODS OF EVALUATING THE VOLUME OF OS COXAE IN VIVO AND EX VIVO

Fisher TJ, Abrahams J, Solomon LB, Stamenkov R, Callary SA, Howie DW

Department of Orthopaedics and Trauma, Royal Adelaide Hospital, Adelaide
Centre for Orthopaedic and Trauma Research, University of Adelaide, Adelaide
email: Bogdan.Solomon@Health.sa.gov.au

INTRODUCTION

Significant variation exists in the volume of the pelvis [1]. This variation has significant implications in the planning of revision and primary total hip arthroplasty, which are often complicated by osteolysis.

Ex vivo measurement of bone volume may be accomplished by a number of direct methods, including a 3D light scanning stroboscope and a water displacement method. In vivo measurement poses a greater challenge and is of more clinical relevance. Computed tomography is a non-invasive technique for the measurement of bone volume using the area of sequential axial slices to approximate the volume of an object. Given the unique geometry of a hemi-pelvis, this study compared the results of volume measurements of the hemi-pelvis using the above-mentioned techniques with a view to validating CT obtained measurements for use in a clinical setting.

METHODS

The volume of the hemi-pelvis was measured in twenty cadaver specimens. Volumes were measured using a water displacement method, an accuracy validated 3D light scanning stroboscope (ArtecEva™), and on CT imaging.

The bones were made impervious to water prior to immersion, and the total volume of water displacement was measured. Using a 3D scanning stroboscope, each hemi-pelvis was scanned and computer analysed. The ArtecEva™ has a known accuracy of 100 microns [2].

CT images were taken and imported into the radiology software suite Vitrea™, which facilitated measuring the cross-sectional area of each CT slice with a thickness of 3 mm. Measurements were undertaken in a blinded fashion on two occasions and with separate observers.

Metal acetabular components were also placed in the bones, which were reimaged with high resolution spiral CT and remeasured using Vitrea™. This process was undertaken in order to determine the precision and accuracy of the CT measurement technique in the presence of metal artefact.

RESULTS AND DISCUSSION

Across all three techniques, concordance was demonstrated. The mean bias and standard deviation of the difference in measurement between stroboscope and CT was 1% and 4% respectively, that between stroboscope and water displacement was 3% and 6% respectively. The mean bias and standard deviation of the difference between CT measurements of specimens with metal components and stroboscopic measurements was 6%.

CONCLUSIONS

Measurement of the volume of the hemi-pelvis using CT slices is accurate and comparable to stroboscopic and water displacement methods, and is useful as a clinical tool in planning revision total hip arthroplasty. The variation in measured volumes between native bones and those with metal prostheses was within acceptable limits.

REFERENCES

1. Solomon LB, et al. The variability of the volume of os coxae and linear pelvic morphometry. Considerations for total hip arthroplasty. *J Arthroplasty*. 2014 Apr;**29(4)**:769-76.
2. http://www.artec3d.com/hardware/artec-eva/specifications/

THE OUTCOME OF PEDICLE SCREW INSTRUMENTATION REMOVAL FOR CHRONIC LOW BACK PAIN: A PROSPECTIVE STUDY

B McDonald, M Zotti, C Tsimiklis, T Fisher, W Yoon, O Osti

Aims: There have been a limited number of small case series reporting improvement in patients' function and pain scores following removal of pedicle screw metalwork for non-traumatic lumbar fusion surgery. The investigators' aim was to determine from a patient cohort the degree of satisfaction and improvement in pain status after removal of pedicle screw instrumentation and factors that may influence the outcome.

Methods: Patients who had removal of pedicle screw instrumentation for posterolateral lumbar fusion in the preceding 2 years were identified from the database of a single spinal surgeon's case series. All patients completed pre- and post-operative Oswestry Low Back Pain Distability Questionnaire (ODI).

Patient inclusion criteria were persistent axial low back pain imaging confirmed solid fusion, non-radicular symptoms and no other cause found for pain e.g. infection. Exclusion criteria included exchange of metalwork, revision fusion or other additional therapeutic procedures.

Results: 21 patients were identified from the database with a mean follow-up of 14 months (range 3-24 months).

There were 2 postoperative hematomas requiring aspiration but no additional complications such infections, re-operations or deteriation of neurological deficits.

Treatment success as assessed from the ODI analysis was rated as excellent in 6/21, good in 7/21, fair in 5/21 and poor in 2/21.

Reduced class II opioids, benzodiazepines or neuromodulator use was reduced in 7/21, no different in 11/21 and increased in 3/21.

The proportion of patients with an improvement in VAS was 13/21 (62%) with an improvement of at least 2 or more being (43%) 9/21 of patients surveyed.

14 of the 21 patients (67%) of patients indicated that they would undergo the same treatment again given their experience and outcome.

Conclusion:
In this series, removal of pedicle screw implants in individuals with ongoing low back pain following solid fusion lead to good or excellent results in 2/3 of patients and did not lead to any adverse effects and/or complications.

SESSION 3 – TISSUE ENGINEERING

VISCOELASTIC PROPERTIES OF HYDROGEL BLENDS FOR CARTILAGE TISSUE ENGINEERING

[1]Michal Bartnikowski, [1]Maria Woodruff and [1]Travis Klein

[1]Institute of Health and Biomedical Innovation, Queensland University of Technology
Email: m.bartnikowski@qut.edu.au

INTRODUCTION

Poroviscoelasticity of native tissues is widely recognized and has implications in terms of load response and cell-matrix interactions [1, 2]. In the context of articular cartilage tissue engineering (TE), hydrogels are frequently used as scaffolds to substitute and induce the target tissue. As cartilage is highly complex and ordered, it may be proposed that approximation of its viscoelastic features may positively influence the stimulation of its regrowth. Quantification and comparison of hydrogel and cartilage explant standard elastic modulus (E), equilibrium modulus (E_{EQ}), elastic storage and loss moduli (E' and E" respectively) and damping ratio (ζ) may provide insight into which material characteristics positively influence chondrogenesis. Whilst E gives a general overview of stiffness and E_{EQ} illustrates the stiffness of a stress-relaxed material, the E' and E" are indicative of the stiffness, and presence of, the elastic (E') and viscous (E") components of the tested materials under variable strain rates, and ζ describes the energy loss fraction due to hysteresis in loading. In this study we explored the relationships between hydrogel crosslinking modality, constituents and concentrations, and their effects on the above parameters in comparison with cartilage tissue.

METHODS

Hydrogel groups comprised of methacrylate-functionalized gelatin (gelatin methacrylamide; gelMA) and gellan gum (gellan gum methacrylate; GGMA), plain gellan gum (GG) and methyl cellulose (MC) in various blends (Table 1). Hydrogels were mixed with photoinitiator (Irgacure 2959), cast into molds and crosslinked with UV light. Articular cartilage explants were from femoral condyles of two donors undergoing total knee replacement. Mechanical testing consisted of a 0.5% strain/sec elastic modulus measurement (10-15% strain), sinusoidal compression over a range of frequencies (E' and E"; 0.01-10.24 Hz, 2% amplitude, from 10% strain), and stress relaxation (at 10 and 15% strain; E_{EQ}). ζ was calculated from force-displacement data.

RESULTS AND DISCUSSION

GelMA formed covalent networks that exhibited primarily elastic properties, with very low E" and ζ. Combination of gelMA with the thermo-ionic polysaccharide GG increased viscous characteristics whilst slightly improving overall stiffness. Alternately, combination with the covalent-thermo-ionic GGMA dramatically increased stiffness beyond an additive effect whilst also promoting viscous behavior. MC decreased stiffness and negligibly affected viscous properties; however, all MC blends remained in solution at lower temperatures. Whilst all groups featured significantly lower moduli than human cartilage explants, viscous characteristics of some groups were comparable with the native tissue.

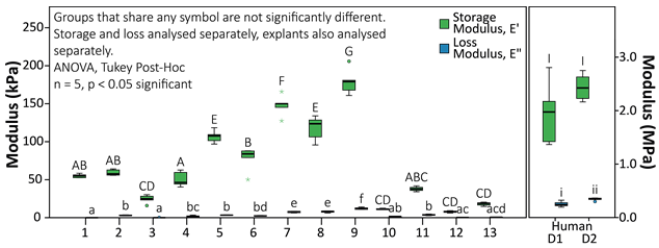

Figure 1: Storage and loss moduli of all groups at 1.28 Hz

CONCLUSIONS

Mechanical characterization of hydrogel viscoelasticity provides a valuable avenue through which to compare native cartilage and replacement tissues, aiding materials innovation.

ACKNOWLEDGEMENTS

MB acknowledges the Australian Postgraduate Award and the Queensland Government Smart Future's PhD Scholarship. MW and TK acknowledge the Australian Research Council (FT110100166, LP100200084 and LP110200082).

REFERENCES

1. Meyers M & Chawla, K, *Mechanical Behavior of Materials.* **2nd Edition**:97-161, 2009.
2. Schinagl et al., *Depth-Dependent Confined Compression Modulus of Full-Thickness Bovine Articular Cartilage.* **JOR**:15, 4, 1997

Table 1: Hydrogel test groups; components present in concentration indicated multiplied by number of '+', or absent when blank

Components	Hydrogel Groups												
	1	2	3	4	5	6	7	8	9	10	11	12	13
GelMA (10%)	+	+	+	+	+	+	+	+	+				
GG (0.25%)		+		+						+	++		
MC (0.25%)			+	+		+		+					
GGMA (0.25%)					+	+	++	++	++++			++	++++

ZIRCONIUM IONS UP-REGULATE THE BMP/SMAD SIGNALING PATHWAY AND PROMOTE THE PROLIFERATION AND DIFFERENTIATION OF HUMAN OSTEOBLASTS

Yongjuan Chen, Seyed-Iman Roohani-Esfahani, Zufu Lu, Hala Zreiqat, Colin R Dunstan

Biomaterials and Tissue Engineering Research Unit, School of AMME
The University of Sydney, Sydney, NSW 2006
Email: yong.chen@sydney.edu.au

INTRODUCTION

Zirconium (Zr) containing materials have been widely used in dental applications and as coatings for orthopaedic implants due to their contributions to biocompatibility, increased mechanical strength, and high corrosion resistance. Recently we have developed a novel baghdadite ceramic ($Ca_3Zr[O_2Si_2O_7]$) by incorporating zirconium (IV) oxynitrate ($ZrO(NO_3)_2$) in a calcium silicate-based ceramic. It has been shown this ceramic scaffold has excellent osteogenic bio-activity in vitro and in vivo when compared to calcium silicate ceramics. Zr ions from baghdadite ceramics can be released into aqueous media. However, the mechanism for this enhanced bioactivity has not been identified, and, in particular, the in vitro effects of Zr ions on human osteoblasts (HOBs) have not previously been studied.

METHODS

Primary HOBs were treated with media containing $ZrO(NO_3)_2$ and $ZrCl_4$ at concentrations of 5, 50 and 500 μM respectively, and media alone or containing 50 μM $NaNO_3$ were used as controls. These HOB cultures were analysed as follows. MTT assay was carried out to evaluate HOB cell viability after 1, 3 and 7 days. Mineralised matrix formation was detected in HOBs after 21 and 28 days. qRT-PCR of RNA extracted from HOBs after 3 and 7 days was conducted to analyse the gene expression of osteogenic genes, BMP2 and BMP receptor genes. Protein expression of BMP2, SMAD1, p-SMAD1/5 and β-actin in HOBs at D3 and D7 was assessed by Western Blot. Immunostaining for Ki67, BMP2, and p-SMAD1/5 was carried out in HOBs at D7.

RESULTS AND DISCUSSION

Zr ions increase HOB cell proliferation and induce mineralisation in HOB cultures Compared to the controls, at D1, D3 and D7, $ZrO(NO_3)_2$ and $ZrCl_4$ at all concentrations greater than 5 μM significantly stimulated HOB proliferation. Immunostaining showed, compared to the controls, Ki67-positive cells in Zr-treated HOBs at D7 were significantly increased in all treatment groups, by 20-50%. The bone nodule formation in the HOB cells treated with Zr solutions was increased in a dose-dependent manner at both D21 and D28, indicating Zr ions stimulated matrix mineralisation by HOBs. Therefore, Zr ions were found to both increase the proliferation of HOB precursors and to enhance their differentiation into osteoblasts.

Zr ions up-regulate osteoblast genetic markers and BMP2 gene expression in HOBs Both Zr solutions strongly increased OPN, BSP, Runx2 and OC osteogenic gene expression in the HOBs cultured for 3 and 7 days. The upregulation of osteogenic genes indicates that Zr induces osteogenesis in primary HOBs. At D3 and D7, BMP2, BMPR1a and BMPR1b gene expression was significantly up-regulated in HOBs treated with both Zr solutions at 500 μM as well as $ZrCl_4$ at 50 μM but BMPR2 expression was not changed.

Zr ions activate the BMP/SMAD1/5 signaling pathway As the BMP2 and its receptor gene expression was up-regulated by Zr chemicals, we further investigated the expression of BMP2 protein levels and its downstream effectors of SMAD1 and p-SMAD1/5. BMP2 protein, by normalising to β-actin, was found to be increased 20% in HOBs after treatment with $ZrO(NO_3)_2$ at 500 μM and from 40% to 60% with $ZrCl_4$ treatment at 5 and 50 μM. Zr ions significantly activated the protein levels of SMAD1 as well as p-SMAD1/5 in HOBs with dose-responsive effects. To confirm the activation of BMP2 and p-SMAD1/5 protein in HOBs by Zr ions, immunostaining was carried out to detect the protein localisation in HOBs. BMP2 was localised strongly in the HOB nuclei and weakly in the cytoplasm in the control; whereas, in HOBs treated with Zr at 50 and 500 μM, BMP2 reactivity was significantly elevated with accumulation strongly in the nuclei and cytoplasm. Similarly, p-SMAD1/5 was localised in the HOB nuclei and not cytoplasm in controls. However, in HOBs treated with Zr solutions, p-SMAD1/5 was observed to appear strongly in the nuclei and weakly in the cytoplasm. These results indicate that Zr ions significantly stimulate BMP2 protein expression and subsequently stimulate SMAD1/5 phosphorylation and pathway activation.

BMP2 is a potent stimulator of osteoblast differentiation and its increased expression and the marked increase in phosphorylated SMAD1/5 provide evidence that BMP2 is a mediator of the osteogenic effects of Zr ions.

CONCLUSIONS

Zr ions appear able to induce both the proliferation and the differentiation of primary HOBs. This is associated with up-regulation of BMP2 expression and activation of BMP signaling suggesting this action is at least in part mediated by BMP signaling.

Development of 3D printed Ceramic scaffolds for Treatment of Segmental Bone Defects

[1]Iman Roohani, [2]Peter Newman and [3]Hala Zreiqat

[1]Biomaterials and Tissue Engineering Research Lab Unit, School of AMME, University of Sydney, NSW 2006.
Email: iman.roohani@sydney.edu.au

INTRODUCTION

There is an unmet need for a suitable scaffold that can be used to heal load-bearing segmental bone defects (SBDs). SBDs are defined as injuries in which a section of bone is completely shattered and/or absent. The size of the missing bone is large enough that bone cannot regenerate on its own (critical sized defects) or results in the formation of nonunions, malunions, and loss of function [1]. SBDs can be brought on by trauma, disease, and age. Trauma can be related to fractures, sport, and blast injuries. Autologous bone grafting has long been considered the gold standard for treating SBDs however limited availability of secondary graft sites and associated donor site morbidity are major drawbacks of this treatment [1]. During past 30 years, various ceramic, polymer and composite scaffolds have been investigated to overcome the problems. However the translation of these scaffolds from lab to clinics has been limited due to their low mechanical stability. Although, synthetic alternatives are being increasingly investigated to overcome these problems, a suitable SBD scaffold is yet to be made [2].

METHODS

3D models of scaffolds with different patterns were designed and converted to printer instruction language. Sr-HT-Gahnite ($Sr\text{-}Ca_2ZnSi_2O_7$(HT)-$ZnAl_2O_4$(Gahnite))[3] ink was obtained by mixing appropriate amount of precursor, powder, surfactants, gelation agent and thickener at a proper sequential order. The 3D printer (Hyrel 3D, USA) equipped with a robotic arm and a high precision dispenser (Ultimus V) was used to construct the scaffolds layer by layer via direct assembly of the ink. The samples were dried and finally sintered at 1250˚C for 3h. Mechanical properties of the scaffolds with different patterns were investigated by an Instron machine.

RESULTS AND DISCUSSION

A suitable SBD scaffold should have combined mechanical strength, high porosity (ideal pore size for SBD scaffolds ranges from 300 to 900 µm in diameter and overall porosity ranges from 60 to 90%) and bioactivity. A wide range of scaffolds with different properties can be found in the literature. Some implants exhibited very low compressive strength properties, 2–12MPa, which correlates with the natural compressive strength of trabecular bone. These scaffolds should be considered for non-load-bearing applications because they also exhibited lower modulus values (up to 25MPa), which are well below the natural range of trabecular bone (50–500MPa). Cortical bone strength ranges between 100 and 230 MPa. Scaffolds that do not match this strength will require surgical fixation to prevent crushing /failure of the implant. Mechanical testing results indicated that our 3D printed highly porous Sr-HT-Gahnite scaffolds have a compressive strength and modulus values close to that of cortical bone

.

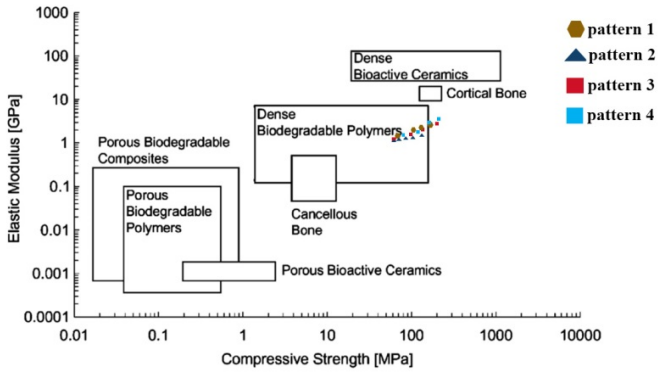

Figure 1- Compressive strength and modulus of 3D printed scaffolds with different patterns in compare with that for biocompatible ceramic, polymer and composite materials at porous and cancellous and cortical bone.

CONCLUSIONS

This study provides evidence that 3D printed Sr-HT-Gahnite scaffolds allow the generation of a unique design that is suitable for the regeneration of SBDs.

ACKNOWLEDGEMENTS

The authors acknowledge the Australia National Health and Medical Research Council (NHMRC), and the Australian Research Council (ARC) for funding this research. The authors also acknowledge Rebecca Cooper Foundation.

REFERENCES

1. Buma S, et al., *Biomaterials.* **25**:1487-1495, 2004.
2. Rezwan K, et al., *Biomaterials*, **27:** 3413-3431, 2006.
3. Roohani-Esfahani, et al., *ActaBiomaterialia*, 9: 7014-7024, 2013.

CONFLICT OF INTEREST DECLARATION

In the interests of transparency and to help reviewers assess any potential bias, ANZORS requires authors of original research papers to declare any competing commercial interests in relation to the submitted work. Referees are also asked to indicate any potential conflict they might have reviewing a particular paper.

If you have accepted any support such as funds or materials, tangible or intangible, concerned with the research by the commercial party such as companies or investors, choose YES below, and state the relation between you and the commercial party.

If you have not accepted any support such as funds or materials, choose NO.

Do you have a conflict of interest to declare? (DELETE TEXT as appropriate)

YES

NO (DELETE all text below)

If YES, please complete as appropriate:

1. The author(s) did receive payments or other benefits or a commitment or agreement to provide such benefits from a commercial entity.

Disclosure: Advanced Surgical Design and Manufacture Limited (ASDM) (ASX: AMT) announced the execution of a global Licence Agreement with The University of Sydney relating to the Sr-HT-Gahnite

2. A commercial entity paid or directed, or agreed to pay or direct, any benefits to any research fund, foundation, educational institution, or other charitable or nonprofit organization with which the authors are affiliated or associated.

ROTATOR CUFF AUGMENTATION: AN IN VIVO STUDY USING A LACTOFERRIN SEEDED BIOMATERIAL SCAFFOLD

[1]Ryan Gao, [1]Matthew WJ Street, [1]Karen E Callon, [1]Donna Tuari, [1]Ashvin Thambyah
[2]Brendon Coleman, [1]Jillian Cornish, [1]David S Musson

[1]University of Auckland, Auckland, New Zealand
[2]Middlemore Hospital, Auckland, New Zealand
Email: r.gao@auckland.ac.nz

INTRODUCTION

Tendon injuries, particularly those of the rotator cuff, can cause significant pain and functional impairment. Our aging population has led to an almost four fold increase in surgical rotator cuff repairs over the past 10 years.[1] However, repairs of large rotator cuff tears have variable success rates, with re-tear rates post arthroscopic repair reported to be as high as 69%[2,3].

The aim of this study was to assess the efficacy of Lactoferrin (a potent bone anabolic factor[4]) and a decellularised ovine forestomach extracellular matrix (ECM) scaffold in augmenting tendon repair and improving surgical outcomes.

METHODS

Forty-six Sprague-Dawley rats underwent unilateral supraspinatus repair, after receiving complete surgical supraspinatus tears (Figure 1). The animals were divided into 3 groups 1: un-augmented control, receiving single row repair; 2: an augmented repair using a decellularised ECM scaffold alone; and 3: an augmented repair with the decellularised ECM scaffold in combination with Lactoferrin. The repairs were assessed at 6 and 12 weeks post operatively. Primary endpoints assessed include biomechanical testing for load to failure, elasticity and stiffness and histological scoring of bone–tendon interdigitation, collagen fibre density and alignment; as well as inflammatory response and vascularity of the tendon.

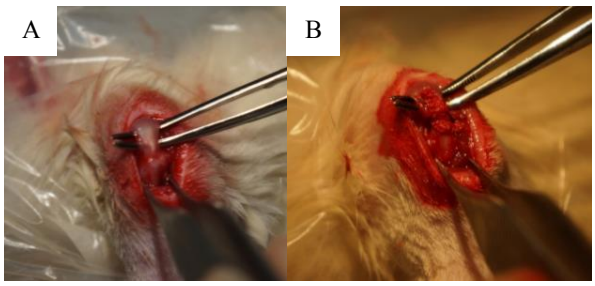

Figure 1. Supraspinatus repair. A) un-augmented repair. B) Augmented repair with ECM scaffold.

RESULTS AND DISCUSSION

At 6 weeks the ECM scaffolds had completely degraded in all animals. Group 3 scored highest in the overall histological evaluation of healing. Both groups 2 and 3 scored significantly higher than group 1, with improved collagen fibre orientation and bone and tendon interdigitation at 6 and 12 weeks. Both stiffness and modulus were increased in group 2, compared to groups 1 and 3 at both time points, although this did not reach significance (11.8N/mm stiffness in group 2 vs. 9.1N/mm and 9.5N/mm in groups 1 and 3, respectively, at 12 weeks).

CONCLUSIONS

This study demonstrated the positive effects of augmenting rotator cuff tendon repairs in a rat model, and provides a method for evaluating the potential of novel biomaterials to improve clinical outcomes.
However, we feel that further research is required to identify the ideal augment for delivering Lactoferrin and improving tendon-bone healing.

ACKNOWLEDGEMENTS

Auckland Medical Research Foundation - Postdoctoral Fellowship of Dr. Musson
Dr. Satya Amirapu, University of Auckland
Mr. Jacob Munro, University of Auckland

REFERENCES

1. Mall NA, Lee AS, Chahal J, et al. An evidence-based examination of the epidemiology and outcomes of traumatic rotator cuff tears. Arthroscopy. 2013;29:366-76.
2. Duquin TR, Buyea C, Bisson LJ. Which method of rotator cuff repair leads to the highest rate of structural healing? A systematic review. Am J Sports Med. 2010;38:835-41.
3. Gallatz LM, Ball CM, Teefey SA, et al. The outcome and repair integrity of completely arthroscopically repaired large and massive rotator cuff tears. J Bone Joint Surg Am. 2004;86-A:219-24.
4. Cornish J. Lactoferrin promotes bone growth. Biometals. 2004;17:331-5.

PERI-PROSTHETIC BONE STRUCTURE AND INTEGRITY CHANGE WITH IMPLANT MATERIAL STIFFNESS IN THE OVINE MODEL

[1,2]Mengzhen Yan, [1]Dr. Nicky Bertollo, [2]Professor Mark Hoffman and [1]Professor William Walsh

[1] Surgical and Orthopaedic Research Laboratory, Prince of Wales Clinical School, UNSW Australia, NSW
[2] School of Materials Science and Engineering, UNSW Australia, NSW
Email: w.walsh@unsw.edu.au

INTRODUCTION

Osteopenia and osteoporosis are significant health issues in today's society, particularly for an ageing population where bone and joint degeneration leads to replacement surgery involving the implantation of materials. Post-operative osteopenia is a clinical problem seen to depend upon implant materials as a result of stress shielding. Peri-prosthetic bone becomes more porous though good fixation was achieved [1-3]. The aim was to determine the time dependent healing of peri-prosthetic bone in response to titanium alloy (Ti), polymethylmethacrylate (PMMA) and a control empty defect by changes in structure and mechanical properties.

METHODS

PMMA implants were custom generated and implant topographies were investigated prior to surgical procedure. Ti and PMMA dowels of 6mm diameter were inserted in line-to-line fashion into the tibiae of 4 crossbred merino wethers (18 months, 55-65 kgs). Empty defects of same diameter were also created. Animals were euthanized at 4 and 12 weeks post-operative then tibiae were harvested. Radiography, micro-CT and push-out testing were conducted to investigate bone structure and implant fixation respectively; nanoindentation was carried out in axial, coronal and sagittal planes in medial samples at incrementing distances from the implant edge to investigate intrinsic mechanical properties. The General linear model of univariate analysis was applied with pair-wise least significant difference post-hoc comparison.

RESULTS AND DISCUSSION

Push-out shear strength decreased for PMMA and increased for Ti with time (**Table *1***). All peri-prosthetic sites, including empty defects, saw increased porosity at cull time points. Through nanoindentation, the axial orientation was confirmed to be stiffer compared to sagittal and coronal, which were similar in stiffness to one another. No significant changes in peri-prosthetic bone surrounding the Ti or PMMA implants were found as compared to intact bone. Stiffnesses in all orientations of bone adjacent to the empty defect were lower by 12 weeks (**Figure *1***).

	4 week	**12 week**
PMMA	5.1 ± 1.8 MPa	2.6 ± 2.3 MPa
Ti	17.6 ± 3.8 MPa	20.3 ± 7.9 MPa

Table 1: Push-out shear strength (MPa) of bone adjacent to PMMA and Ti implants at 4 and 12 weeks post-operative.

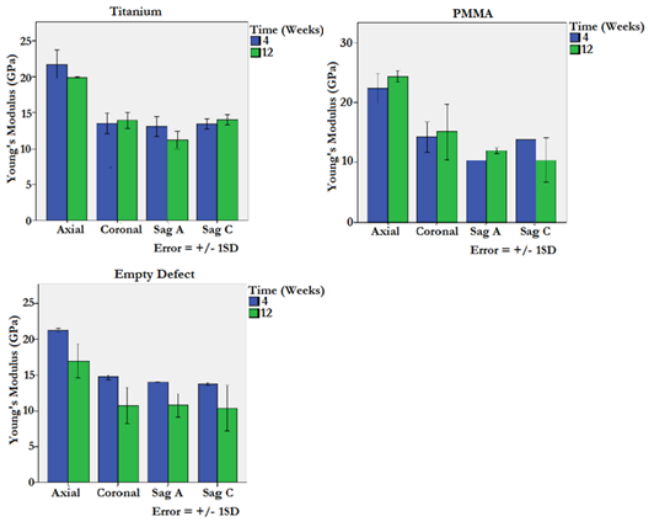

Figure 1: Graphs indicating changes to bone stiffness in different orientations with respect to time and implant material.

CONCLUSIONS

Intrinsic mechanical properties of peri-prosthetic bone without an implant is compromised but structurally, all peri-prosthetic bone showed signs of increased porosity.

ACKNOWLEDGEMENTS

The authors would like to thank Dr. Chris Christou for his surgical expertise, Mr. John Rawlinson and Mr. Gregory Mitchell for their animal care and husbandry and Mr. Bill Joe for his help with the nanoindenter. We also thank all staff and students from the School of Materials Science and Engineering and Surgical and Orthopaedic Research Laboratory.

REFERENCES

1. Svehla, M., et al., *The Journal of Arthroplasty*, **17**(3): p. 304-311, 2002.
2. Chen, D., et al., *Journal of Orthopaedic Surgery and Research*, **6**(1): p. 56, 2011.
3. Bertollo, N., et al., *The Journal of Arthroplasty*, **26**(7): p. 1000-1007, 2011.

INJECTABLE RADIOPAQUE AND BIOACTIVE POLYCAPROLACTONE-CERAMIC COMPOSITE FOR ORTHOPAEDIC AUGMENTATION

[1,#]Young Jung No, [1]Seyed-iman Roohani, [1]Zufu Lu, [2]Thomas Schaer and [1,*]Hala Zreiqat

[1]Biomaterials and Tissue Engineering Unit, School of AMME, The University of Sydney, Sydney 2006, NSW, Australia
[2]Comparative Orthopedic Research Laboratory, Department of Clinical Studies, School of Veterinary Medicine, New Bolton Centre, University of Pennsylvania, Kennett Square, PA, USA.
[#]Presenting author – email: yono7153@uni.sydney.edu.au; [*]Corresponding author – email: hala.zreiqat@sydney.edu.au

INTRODUCTION

Injectable bone cements (IBCs) such as polymethylmethacrylate (PMMA) and calcium phosphate cement can be used to provide mechanical stability in weakened osteoporotic bone for hardware augmentation during fracture healing. Currently available IBCs do not have the required simultaneous combination of high flexural strength, high radiopacity, and high bioactivity. To address the shortcomings of currently available IBCs, composites based on biodegradable **polycaprolactone** (PCL) and with incorporation of various vol.% of bioactive ceramic **baghdadite** (Bag, $Ca_3ZrSi_2O_9$) microparticles have been developed. The composite becomes injectable when heated above its melting temperature.

METHODS

PCL (M_w: ~80,000) was cryogenically grinded and mixed with baghdadite particles (mean diameter: 1.7µm), then melt extruded to form homogeneous PCL-Bag composites with varied vol.% baghdadite (PCL, PCL-1%Bag, PCL-5%Bag, PCL-10%Bag). Force of injection at injection rate of 0.75cm^3/min, and temperature of material at the nozzle exit (length: 9mm, diameter 2.2mm) was measured after melting 2.0g of the composite at 75°C. Flexural stress vs. strain graphs were obtained from 3-point bending tests on rectangular samples (6x12x50mm, 5mm/min ramp rate). Radiopacity of the composites in Hounsfield units (HU) were obtained by using cone beam computed tomography (CBCT) at 70keV. Primary human osteoblast (HOB) proliferation on PCL-Bag composites was measured via colorimetric method through detecting the absorbance of formazan (λ=492nm). Relative gene expressions of Runx2, osteocalcin (OC) and osteopontin (OPN) were obtained by a sequence of RNA isolation, cDNA synthesis, and real-time polymerase chain reaction.

RESULTS AND DISCUSSION

PCL, PCL-1%Bag, and PCL-5%Bag required 600-700N, and PCL-10%Bag required ~900N of compressive force for injection. All formulations exited the nozzle between 55-60°C, and cooled to below 50°C after 1min. When compared to PMMA, which can have prolonged exothermic polymerization temperatures in excess of 70°C, PCL, PCL-1%Bag, PCL-5%Bag and PCL-10%Bag possess lower risk of thermal necrosis of surrounding tissue. PCL-10%Bag showed significant increase ($p<0.05$) in flexural strength (29.7±2.0 MPa) compared to PCL (23.8±0.7 MPa). All groups remained intact at 0.3 flexural strain (Figure 1a). Increased loading of baghdadite particles increased the radiopacity of PCL (Figure 1b). PCL, PCL-1%Bag, PCL-5%Bag and PCL-10%Bag showed -108±25 HU, 389±104 HU, 1669±48 HU and 2971±195 HU at 70keV respectively. There was significant increase in HOB proliferation on PCL-5%Bag compared to PCL at day 3, and on PCL-10%Bag compared to PCL at day 7 (Figure 2a). PCL-1%Bag, PCL-5%Bag and PCL-10%Bag showed significantly increased Runx2 expression in day 3 compared to PCL. PCL-10%Bag showed significantly increased OPN and OC gene expression in day 7 compared to all other formulations. (Figure 2b-d)

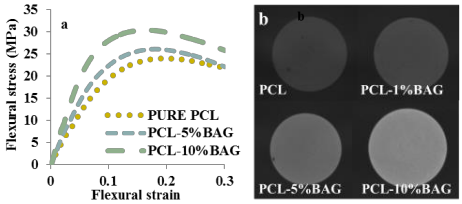

Figure 1: a) Flexural stress strain curves; b) CBCT images of PCL-Bag composites

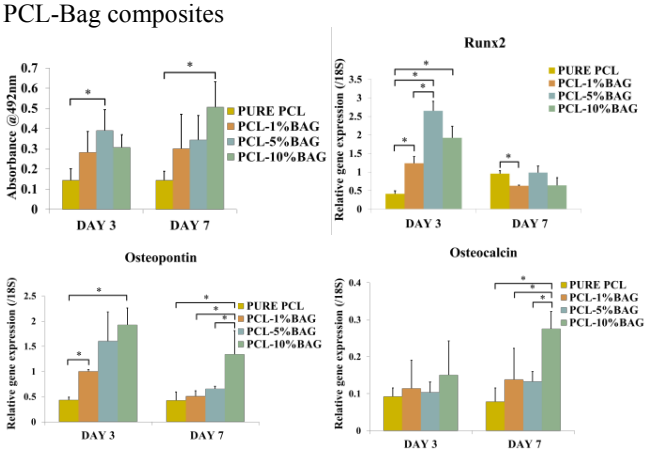

Figure 2: a) HOB proliferation; HOB gene expression of b) Runx2, c) OPN and d) OC. *: $p<0.05$

CONCLUSIONS

PCL composites with variable baghdadite microparticle loading were extensively characterized *in vitro*. In particular, PCL-10%Bag possesses high flexural strength, high radiopacity and good bioactivity for new bone formation. PCL-10%Bag formulation could be a putative candidate for a bone void filler or hardware augmentation where immediate mechanical loading could improve in patient outcome.

KEYNOTE 2 – Dr Jacob Munro

OSTEOLYSIS AFTER HIP ARTHROPLASTY: UNDERSTANDING LOAD TRANSFER IN THE PELVIS

Jacob Munro

Department of Orthopaedic Surgery Auckland City Hospital

Total hip arthroplasty (THA) is one of the most successful interventions in any form of surgery. In the 21st century patients with degenerative hip disease can expect to return to a very high level of pain free function when their joint is replaced. Despite technologic advances in materials we have not yet created the perfect implant, that is, one that does not alter the biomechanics of the skeleton or suffer mechanical failure during the patients lifetime. Bone loss, or osteolysis, secondary to local and systemic physiologic effects will continue to present management challenges to the arthroplasty surgeon. While osteolytic defects are commonly observed in long-term follow-up, how such lesions alter stress distribution is less clear. Many patients with osteolysis are asymptomatic with medical comorbidity that makes surgical intervention risky. Can we safely observe these lesions or do we place patients at an increased risk of fracture? Finite element (FE) models of skeletal tissue are useful in allowing us to predict the effect of changes in bone architecture and material properties. The specific focus of our research is the analysis of load distribution in the pelvis when defects arise in the retro-acetabular region using validated FE models. Computational evaluation has been applied to a population of patients with variable volume cancellous, and in some cases cortical defects, in the retro-acetabular region. Initially, loads occurring during walking and a fall onto the side were assessed. A fracture algorithm was applied to determine differences in load and site of failure in the presence of defects. Cancellous and cortical defects caused increases in cortical stress during loads consistent with routine activity but these were consistently well below theoretical yield stress. During a fall onto the side, defects were observed to cause lower load to failure in the smaller females pelvis and those with larger volume defects (>20cm^3).

SESSION 4 – IMAGING 1

LAYERED DISTRIBUTION OF OSTEOCYTES WITHIN SINGLE OSTEONS

[1]Pascal R Buenzli, [2]C David L Thomas and [2]John G Clement

[1]School of Mathematical Sciences, Monash University, Clayton, VIC 3800
[2]Melbourne Dental School, The University of Melbourne, VIC 3010
email: pascal.buenzli@monash.edu

INTRODUCTION

Osteocytes have been suggested to control both matrix deposition and the generation of new osteocytes during bone formation, by prompting the burial of osteoblasts in the synthesising matrix [1]. A detailed analysis of this suggestion requires a knowledge of the 3D distribution of osteocytes in new bone with respect to the moving deposition front. In this contribution, we investigate the distribution of osteocytes in single osteons from 3D micro-CT scans. A method of analysis of osteocyte distribution is developed, which does not rely upon realigning osteon and/or Haversian canal boundaries as done previously [2]. This avoids tedious post-processing and enables the systematic study of osteocyte distribution in their undeformed, irregular osteonal environment.

METHODS

Synchrotron x-ray micro-CT scans of a femoral cortical bone sample from a 20-year old male collected previously [2] were re-analysed. These scans of voxel size 1.47 µm enabled the clear visualisation of osteocyte lacunae (Lc) and Haversian canals (HCs) in 3D, and occasionally, of newly formed osteons seen as lower density regions around HCs. The osteon boundary (cement line CL), central HC, and lacunae were segmented (Fig. 1A) to provide the position, size, and orientation of lacunae within the newly deposited bone. The 3D distance of the lacunae to the CL and to the HC were calculated and the lacuna volumetric density (#/mm^3) was determined as a function of these distances. Because the separation between the CL and HC is naturally irregular, a normalised wall width w ($0 \leq w \leq 1$) was defined through the construction of a family of 3D mathematical surfaces parameterised by w. These surfaces morph the CL (w=0) into the HC boundary (w=1) gradually and smoothly, enabling the definition of pseudo-lamellae (Fig. 1A). Lacuna density in the whole new bone region could then be estimated as a function of this normalised wall width.

RESULTS AND DISCUSSION

Close to the CL and HC boundaries, the density of lacunae exibits well-defined large-amplitude oscillations with distance from the boundaries. The period of the oscillations is about 8–10 µm, and is of the order of the width of two successive human bone lamellae [1]. With increasing distance from the CL and HC boundaries, the osteon's irregular geometry disrupts this oscillating pattern and artificially decreases lacuna density. The definition of the normalised wall width in such irregular geometry (a measure of 'radial' distance normal to the mathematically constructed pseudo-lamellae of Fig. 1A) prevents this artificial decrease and shows that oscillations in lacuna density persist away from the boundaries (Fig. 1B). These oscillations are consistent with Marotti's suggestion that secondary osteons are composed of an alternative sequence of lamellae containing osteocytes, and acellular lamellae [1]. A mismatch between the real lamellae and our pseudo-lamellae could result in density oscillations not decreasing to zero. However, Marotti's suggestion remains debated to date [3] and our results may also indicate an alternative sequence of lamellae with high density and low density of lacunae.

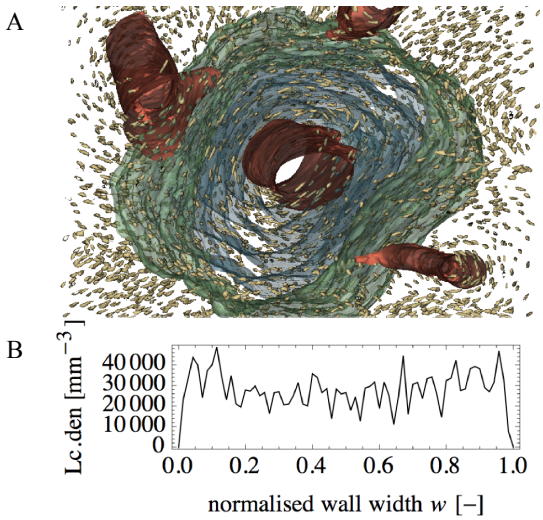

Figure 1: **A** Osteon segmentation, showing CL (green, w=0), HC (red, w=1), lacunae (yellow), and pseudo-lamellae (blue, w=0.2, 0.4, 0.6, 0.8); **B** Lacuna density vs w.

CONCLUSIONS

The lamellar structure of secondary osteons provides much information on the successive positions of the bone surface during formation, but this structure is not visible in 3D micro-CT scans. Mathematical constructions of pseudo-lamellae provide a method of analysis of the layered distribution of osteocytes in irregular geometries.

ACKNOWLEDGEMENTS

PRB is the recipient of an ARC Discovery Early Career Research Award (DE130101191).

REFERENCES

1. Marotti G, *Ital J Anat Embryol* **101**:25–79, 1996
2. Hannah K et al., *Bone* **47**:866–871, 2010
3. Pazzaglia et al., *Anat Rec* **295**:1421–1429, 2012

EARLY MIGRATION OF THE R3 UNCEMENTED ACETABULAR COMPONENT: A PROSPECTIVE 2 YEAR RADIOSTEREOMETRIC ANALYSIS

[1]Drew Grosser, [2]Sam H. Benveniste, [3]Donald Bramwell and [3]Jegan Krishnan

[1]The International Musculoskeletal Research Institute Inc., Repatriation General Hospital, Daw Park, SA, Flinders University, Bedford Park, SA, Australia
[2]Department of Orthopaedics, Repatriation General Hospital, Daw Park, SA, Australia
[3]The International Musculoskeletal Research Institute Inc., Department of Orthopaedic Surgery, Flinders Medical Centre, Bedford Park, SA, Australia
email: drew.grosser@imri.org.au

INTRODUCTION

Radiostereometric Analysis (RSA) is an accurate measure of implant migration following total joint replacement surgery. Early implant migration predicts later loosening and implant failure, with RSA a proven short-term predictor of long-term survivorship. The proximal migration of an acetabular cup has been demonstrated to be a surrogate measure of component loosening and the associated risk of revision [1]. RSA was used to assess migration of the R3 acetabular component which utilises an enhanced porous ingrowth surface. Migration of the R3 acetabular component was also assessed when comparing the fixation technique of the femoral stems implanted.

METHODS

Twenty patients undergoing primary total hip arthroplasty were implanted with the R3 acetabular cup. The median age was 70 years (range, 53-87 years). During surgery tantalum markers were inserted into the acetabulum and the outer rim of the polyliner. RSA examinations were performed postoperatively at 4 to 5 days, 6, 12 and 24 months. Data was analysed for fourteen patients to determine the migration of the acetabular cup relative to the acetabulum. Of these fourteen patients, six were implanted with a cementless femoral stem and eight with a cemented femoral stem. Patients were clinically assessed using the Harris Hip Score (HHS) and Hip Disability and Osteoarthritis Outcome Score (HOOS) preoperatively and at 6, 12 and 24 months postoperatively.

RESULTS AND DISCUSSION

RSA revealed no significant acetabular cup migration in all planes of translation and rotation with mean translations below 0.40 mm and mean rotations below 1 deg at 24 months. The data suggests that acetabular migration occurred primarily in the first 6 months postoperatively. We observed mean translations at 24 months of 0.36 mm (x-axis), 0.39 mm (y-axis) and 0.35 mm (z-axis). Mean rotations of 0.68 deg (x-axis), 0.99 deg (y-axis) and 0.77 deg (z-axis) were also observed at 24 months. Micromotion along the proximal-distal translation (y-axis) plane represented proximal migration of the acetabular component (Figure 1). On investigation of the femoral stems (cementless and cemented) implanted with the R3 acetabular cup, the mean proximal migration of the acetabular cup for both was 0.39 mm (CI 0.19-0.58). For cementless femoral stems a mean proximal migration of 0.45 mm (CI 0.09-0.98) and for cemented femoral stems a mean proximal migration of 0.35 mm (CI 0.24-0.45) were observed (Figure 1). A significant difference in the clinical assessment of patients when comparing pre-operative with 6, 12 and 24 months were also observed ($p < 0.0001$). All clinical assessments demonstrated equivalent results when comparing the post-operative follow-up time points and the R3 acetabular cup and stem combinations.

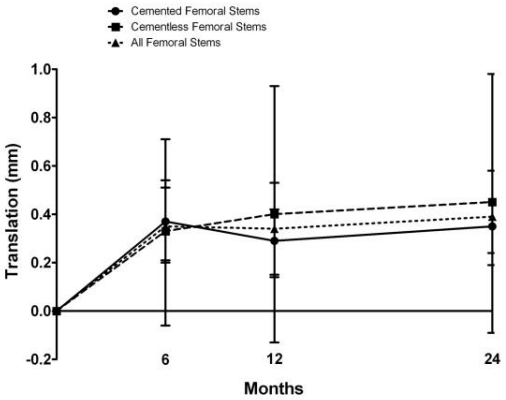

Figure 1: Proximal-distal translation (y-axis) of the acetabular cup for cemented, cementless and all femoral stems at 6, 12 and 24 months postoperatively.

CONCLUSIONS

Mean translations and rotations were higher than previously reported for acetabular components with the enhanced porous ingrowth surface [2]. The magnitude of proximal migration 24 months postoperatively was within published 'acceptable' levels, albeit within the 'at risk' range of 0.2-1.0 mm [1]. Comparison of the proximal migration for cementless and cemented femoral stems expressed similar outcomes, a trend also observed with the clinical assessments. These findings support further investigation and analysis of the R3 acetabular component.

REFERENCES

1. Pijls BG, et al., *Acta Orthopaedica*. **83:**583-591, 2012.
2. Bourne RB et al., *Orthopedics*. **31(12 Suppl 2):**818-826, 2008.

CONFLICT OF INTEREST DECLARATION

In the interests of transparency and to help reviewers assess any potential bias, ANZORS requires authors of original research papers to declare any competing commercial interests in relation to the submitted work. Referees are also asked to indicate any potential conflict they might have reviewing a particular paper.

If you have accepted any support such as funds or materials, tangible or intangible, concerned with the research by the commercial party such as companies or investors, choose YES below, and state the relation between you and the commercial party.

If you have not accepted any support such as funds or materials, choose NO.

Do you have a conflict of interest to declare? (DELETE TEXT as appropriate)

YES

If YES, please complete as appropriate:

1. The author(s) did receive payments or other benefits or a commitment or agreement to provide such benefits from a commercial entity.
   State the relation between you and the commercial entity:

   N/A

2. A commercial entity paid or directed, or agreed to pay or direct, any benefits to any research fund, foundation, educational institution, or other charitable or nonprofit organization with which the authors are affiliated or associated.

   The Department of Orthopaedics, Repatriation General Hospital (through its research arm, the International Musculoskeletal Research Institute Inc.) received payment from Smith & Nephew to cover the costs of undertaking this research project.

   No member of the research team received a personal financial benefit from their involvement in this research project.

KNEE OSTEOARTHRITIS BONE MARROW LESIONS DETECTED BY TWO DIFFERENT MAGNETIC RESONANCE SEQUENCES ARE CHARACTERISED BY DIFFERENT MORPHOLOGICAL AND MICROSTRUCTURAL CARTILAGE-SUBCHONDRAL BONE CHANGES

[1,2]Muratovic D., [3]Cicuttini F.M., [3]Wluka A.E., [3]Wang Y., [2]Findlay D.M., [4]Otto S., [5]Taylor D., [5]Collings S., [1]Humphries J.M., [1]Lee Y-R., [6]Mercer G., [1,2]Kuliwaba J.S.
[1]Bone and Joint Research Laboratory, Anatomical Pathology, SA Pathology, Adelaide, SA
[2]School of Medicine, The University of Adelaide, Adelaide, SA
[3]School of Public Health & Preventive Medicine, Monash University, Melbourne, VIC
[4]Anatomical Pathology, SA Pathology, Adelaide, SA
[5]Department of Radiology, MRI Unit, Royal Adelaide Hospital, Adelaide, SA
[6]Department of Orthopaedics, Repatriation General Hospital, Adelaide, SA
e-mail: dzenita.muratovic@health.sa.gov.au

INTRODUCTION

Bone Marrow Lesions (BMLs) are of predictive and prognostic value in knee osteoarthritis (OA). Visualized only by magnetic resonance imaging (MRI) they are defined as bright area of subchondral bone on fluid-sensitive sequences and dull gray area on fat-sensitive sequences. Choice of appropriate MR sequence is of vital importance when assessing BMLs. However, presence or absence in different sequences is not yet well understood. The aim of this study was to investigate the relationship between presence and absence of BMLs for two different MR sequences and to characterise changes in the morphology and microstructure within cartilage, subchondral bone and bone marrow in OA knees.

METHODS

Tibial plateaus were obtained from 46 patients (24 male and 22 female) aged 51-86 years undergoing total knee replacement surgery for OA. To identify the BMLs, MRI scans were performed *ex vivo* using specific T1 and PDFS weighted sequences. MR images were used for cartilage volume quantification. Three groups were defined based on presence or absence of BML characteristic signal: **No BML** (No BML is detected by MRI); **PDFS-BML** (BML is detected only by PDFS weighted sequence); **T1/PDFS-BML** (BML is detected by T1 and PDFS weighted sequences). Micro-computed tomography (Micro-CT) was used to analyze microstructure of the subchondral bone. Three volume of interest (VOI) were selected: 1) Ovoid (40x25mm diameter) to cover whole medial compartment; 2) Cylinder (10x5mm diameter) to contain BML; 3) Cylinder (10x5mm diameter) contralateral to BML as No-BML. Degenerative changes within cartilage and subchondral bone were assessed microscopically by OARSI grading system and routine histopathology. Bone turnover indices (osteoid and erosion surfaces) were also quantitated.

RESULTS AND DISCUSSION

20% of all tibial plateaus did not have any subchondral bone pathology detected by MRI. BMLs were detected in 78% of specimens. BMLs seen by PDFS sequences represented 64%, BMLs seen by both sequences T1/PDFS represented 36% of all BMLs. There was an increase in microscopic cartilage-subchondral bone degeneration (p=0.05) and significantly reduced cartilage volume between OA knees with T1/PDFS-BML compared to knees with No-BML detected (p=0.007), or with PDFS-BML (p=0.03). Subchondral bone of the medial compartment in knees with T1/PDFS-BML detected had higher BV/TV (p=0.003), thicker trabeculae (p=0.002) and predominately more plate-like trabeculae (p=0.0004) compared to knees with No BML detected. Analysis of BMLs and matched No-BML regions provided valuable information regarding the microstructural differences within the same medial compartment, showing that PDFS-BML have similar microstructure compared with matched PDFS-No-BML. On the other hand, PDFS-BML and PDFS-No-BML have less BV/TV, less separated and plate-like trabeculae compared to both T1/PDFS-BML (p=0.03) and T1/PDFS-No-BML (p=0.001). Complementary to bone microstructure there was an increase in bone turnover parameters (OV/TV, OV/BV, OS/TV) in knees with T1/PDFS BML compared to knees where No BML was detected (p=0.003). Histological assessment of bone marrow indicated presence of several abnormalities in both BMLs and No BMLs. There was significantly more necrosis presented than edema in all groups (p=0.01) and it was predominantly exhibiting in knees with T1/PDFS-BML.

CONCLUSIONS

This study has demonstrated a relationship between loss of cartilage volume and degree of cartilage degeneration for presence and absence of knee BMLs on specific MR sequences. BMLs detected by different MR sequences are characterised by a different degree of change in microstructure of the subchondral bone and it appears that these changes are more systemic rather than localized. Therefore we suggest that it is possible that these two MR sequences provide complementary information and detect BMLs with different tissue-level characteristics rather than one being superior to the other. Furthermore, our results suggest that BMLs seen only in PDFS sequences might represent a change in subchondral bone at an earlier stage of OA disease, whereas BMLs seen in both sequences may represent a later stage of disease with less possibility to resolve. Therefore, BMLs detected with specific sequences could act as a valid biomarker for identification of individuals at risk of progressive OA or monitoring therapy. We recommend the use of two MR sequences to identify BMLs and further propose the labeling of BMLs as follows: **BML Type 1** seen only by fluid sensitive sequences with less severe microstructural and morphological changes and **BML Type 2** seen by fluid and fat sensitive sequences with more severe microstructural and morphological changes.

RSA ASSESSMENT OF CUP MIGRATION AFTER CUP CAGE RECONSTRUCTIONS OF PERIPROSTHETIC ACETABULAR FRACTURES WITH PELVIC DISCONTINUITY AND COMMINUTED UNRECONSTRUCTABLE BOTH COLUMN ACETABULAR FRACTURES

Abrahams JM, Solomon LB, Callary SA, Howie DW

Department of Orthopaedics and Trauma, Royal Adelaide Hospital, Adelaide
Centre for Orthopaedic and Trauma Research, University of Adelaide, Adelaide
email: Bogdan.Solomon@Health.sa.gov.au

INTRODUCTION

Cementless cup fixation relies on initial press-fit followed by bony ingrowth. Initial cup press-fit is not achievable in the presence of pelvic discontinuity with severe bone loss or multi-comminuted both column fractures. Radiostereometric analysis (RSA) of primary acetabular component migration has defined cups that migrate < 1.3mm at 24 months as stable [1]. To-date the migration patterns and outcomes of cup-cage reconstructions is unknown. This study investigated the initial cup stability using a cup-cage reconstruction of such cases using the precise technique of (RSA).

METHODS

Two groups of patients were considered for this study. Patients in group one had periprosthetic acetabular fractures and pelvic discontinuity in the presence of osteolysis, preventing effective fracture fixation. Patients in group two were elderly patients that had multicomminuted acetabular fractures involving both the anterior and posterior columns. These fractures were not amendable to internal fixation. All reconstructions were treated with fracture distraction and a cup-cage acetabular construct, utilizing large porous tantalum acetabular components.

A consecutive cohort of 19 patients was investigated. There were eight patients in group one and eleven patients in group two. All patients had 0.8mm tantulum markers inserted in the bony pelvis introperatively to facilitate RSA analysis, and had RSA radiographs taken post-operatively at 6 weeks, 3 months, 6 months, 12 months and at subsequent follow-up thereafter. All patients had a minimum 12-month follow-up.

RESULTS AND DISCUSSION

There were 8 males (3 in group one and 5 in group two), and there were 11 females (5 in group one and 6 in group two). The median age was 80 in group one (65 – 89) and 81 in group two (71 – 88).

One patient that died four days after surgery and one patient that could not undertake RSA radiographs beyond the 6 week follow-up were excluded. Both patients were in group two.

For the remaining patients the median follow-up was 12 months (6 to 36). One patient in group one suffered a post-operative infection that was treated with a staged revision. All patients group one exceeded their pre-operative level of activity within the first three months of the post-operative period. All patients in group two, excluding the deceased patient, regained their pre-injury level of activity and function within 3 months of the post-operative period.

All acetabular reconstructions were assessed as stable over time on plain radiographs. In contrast RSA demonstrated cup migration in excess of 6mm. Depsite this, all but one cup stabilized or had a decrease in the rate of migration by 6 months. Patients in group one, which had less iliac bone fragmentation, stablised earlier than patients in cohort two. Across both groups, only nine cups had less than 1.3mm of migration at 12 months.

CONCLUSIONS

Hip bone fracture distraction and stabilization with a cup-cage construct shows prominisng early results in the reconstruction of pelvic discontinuity not amenable to anatomic reduction and plate fixation. Short term cup stabilization can be achieved, but may have to be redefined for this reconstruction technique.

REFERENCES

1. Nieuwenhuijse MJ, et al. Good diagnostic performance of early migration as a predictor of late aseptic loosening of acetabular cups: results from ten years of follow-up with Roentgen stereophotogrammetric analysis (RSA). *J Bone Joint Surg Am*. 2012 May 16; **94**(10):874-80.

The relationship between porosity and specific surface in human cortical bone: three-dimensional measurements from compact to porous cortical bone tissue.

[1,2]C. Lerebours, [3,4]C. D. L. Thomas, [3,4]J. G. Clement, [1]P. R. Buenzli, [2,4]P. Pivonka

[1]School of Mathematical Sciences, Monash University, VIC 3800, Australia.
[2]Northwest Academic Centre, University of Melbourne, VIC 3021, Australia.
[3]Melbourne Dental School, University of Melbourne, VIC 3010, Australia.
[4]Australian Inst. Musculoskeletal Science, VIC 3021, Australia.
Email: chloe.lerebours@monash.edu

INTRODUCTION

Bone cells are well known to be regulated biochemically and biomechanically. The notion that the microscopic availability of bone surface affects bone remodeling is, however, less established. Bone-resorbing and bone-forming cells require a bone surface to attach to and initiate the matrix renewal. For bone a characteristic relationship between bone volume fraction (BV/TV) and specific surface (BS/TV), (surface available per unit of total volume) has previously been proposed based on 2D histological measurements [1]. This relationship has been proposed to be bone intrinsic: a unique continuous relation from trabecular to cortical bone and to not depend on the skeletal site. In this paper, we investigate the relationship between porosity and specific surface with human cortical bone using high-resolution micro-CT imaging.

METHODS

Images from femoral cortical bone samples of the Melbourne Femur Collection were obtained using synchrotron radiation micro-CT (SPring8, Japan). Sixteen individuals were analyzed to find bone volume fraction values between 0.2 and 1. In an attempt to understand the behavior of the specific surface as bone volume fraction decreases a series of computational morphological models were developed with increasingly complex assumptions about the manner in which pores were distributed and merged in a cortical cross section (Figure 1).

RESULTS AND DISCUSSION

Our experimental findings (Figure 2) indicate that the BV/TV vs BS/TV relationship is subject-specific rather than intrinsic. While interpolating with the same polynomial, it leads to a correlation of $r^2 = 0.88$; when using the whole data set, subject specific interpolation leads to excellent correlations ranging from $0.91 \leq r^2 \leq 0.99$. Trabecular-like microstructures with BV/TV lower than 0.4 were rarely found even in severely osteoporotic patients, indicating that such structures may be resorbed quickly.

The morphological models show that the BV/TV and BS/TV of cortical bone from compact to porous are well represented by microstructures emerging from the coalescence of cylindrical pores. The changes of BS/TV can be modeled by increase in pore area rather than pore density, consistently with previous findings [2]. The cortical data points from our experiments deviate significantly from the analytical BV/TV-BS/TV relation provided by Martin [1]. This discrepancy can be attributed to the fact that Martin's relationship was interpolated largely from trabecular.

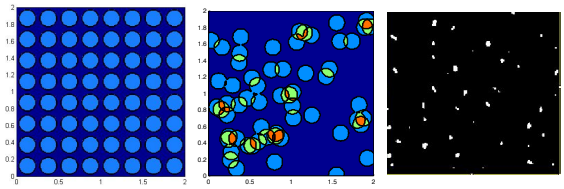

Figure 1: Theoretical models describing the growing and merging of pores.

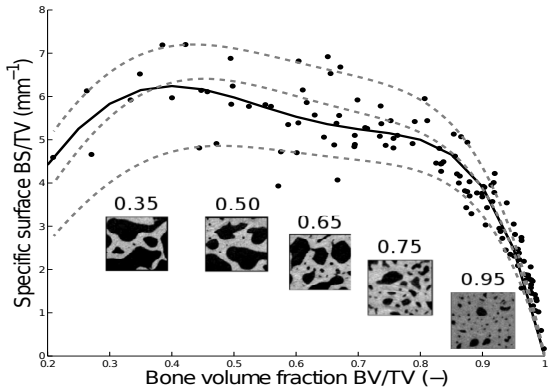

Figure 2: Bone volume fraction BV/TV (-) vs specific surface BS/TV (mm^{-1}) relationship. Our results are presented in black dots with a global curve fitting (black curve) as well as three subject-specific curve fittings. Images of the VOI with their BV/TV values are shown.

CONCLUSIONS

Our results suggest that the BV/TV vs BS/TV relationship follows a dome-shaped curve, but that data points from different patients define patient-specific curves. Furthermore, the specific surface of porous cortical bone may be significantly higher than that of trabecular bone with matched porosities. This will be investigated more systematically in future studies.

REFERENCES

1. Martin R. B., *Critical Reviews in biomedical Engineering,* **10**(3), 179-222, 1984.
2. Thomas C. D. T. et al., *Journal of anatomy*, **209**(2):219-230, 2006.

PATTERNS OF MIGRATION OF REVISION ACETABULAR COMPONENTS USING RADIOSTEREOMETRIC ANALYSIS (RSA)

Abrahams JM, Howie DW, Callary SA, Solomon LB

Department of Orthopaedics and Trauma, Royal Adelaide Hospital, Adelaide
Centre for Orthopaedic and Trauma Research, University of Adelaide, Adelaide
email: Bogdan.Solomon@Health.sa.gov.au

INTRODUCTION

Radiostereometric analysis (RSA) of primary acetabular component migration has defined cups that migrate < 1.3mm at 24 months as stable [1]. To date no study has used RSA to investigate the stability of revision acetabular components, which are likely to be different. This study investigated the stability of revision aceatabular components using RSA.

METHODS

55 acetabular (50 patients) revisions for severe bone loss performed in our institution between 2003 and 2012 that had tantalum beads inserted at the time of surgery were included in this study. There were cup alone, cup plus augment, cup-cage or cup-cage plus augment reconstructions. Postoperatively, baseline RSA radiographs were taken in the first four postoperative days and then at three, six and 12 months, and at each follow up thereafter. Two dimensional migration of the acetabular component was calculated as the vectorial sum of medial and superior migration. Minimum follow up was one year (range 1 - 10 years).

RESULTS AND DISCUSSION

Four patients (4 hips) died from conditions not related to the procedure in the first six months post-surgery. Two hips (2 patients) had inadequate RSA follow-up due to one hip being revised for recurrent hip dislocation at three months; one hip being revised for infection at three months. The median migration of all acetabular components was 0.9 mm (0.1 to 5.6mm) at six months, and 0.9mm (0.2 to 7.0mm) at 12months.

Thirty-four components migrated less than 1.3mm at 12months and did not migrate any further afterwards – these components were classified as stable.

Eight components migrated more than 1.3mm but less than 3mm at 3 and 12 months and did not migrate further after 24 months – these components were classified as probably stable.

Three components migrated less than 3mm in the first three months but greater than 3mm in the first 12 months and did not migrate further after 24 months. These components were classified as possibly stable. None of these patients were symptomatic at last follow-up.

Four components migrated more than 3mm at 3 months and continued to migrate and were classified as unstable. These patients were symptomatic and subsequently revised.

CONCLUSIONS

Using the precise technique of RSA, this study has shown that majority of revision acetabular components are stable at mid-term follow-up and behave similarly to primary components. The different patterns of migration were related to the extent of bone deficiency and type of reconstruction.

REFERENCES

1. Nieuwenhuijse MJ, et al. Good diagnostic performance of early migration as a predictor of late aseptic loosening of acetabular cups: results from ten years of follow-up with Roentgen stereophotogrammetric analysis (RSA). *J Bone Joint Surg Am*. 2012 May 16; **94**(10):874-80.

CONFLICT OF INTEREST DECLARATION

In the interests of transparency and to help reviewers assess any potential bias, ANZORS requires authors of original research papers to declare any competing commercial interests in relation to the submitted work. Referees are also asked to indicate any potential conflict they might have reviewing a particular paper.

If you have accepted any support such as funds or materials, tangible or intangible, concerned with the research by the commercial party such as companies or investors, choose YES below, and state the relation between you and the commercial party.

If you have not accepted any support such as funds or materials, choose NO.

Do you have a conflict of interest to declare? (DELETE TEXT as appropriate)

YES

If YES, please complete as appropriate:

1. The author(s) did receive payments or other benefits or a commitment or agreement to provide such benefits from a commercial entity.
   State the relation between you and the commercial entity:

Zimmer PTY LTD research grant.

Long-leg alignment pre and post operatively for primary total knee arthroplasty, a comparison of computer tomographic imaging and Long Leg Radioagraph analysis.

[1]Anneka Stephens, [2]Meenu Shunmugam and [3]Christopher Wilson and [1]Jegan Krishnan

[1]International Musculoskeletal Research Institute, Adelaide SA
[2]Flinders Medical Centre, Adelaide SA
[3]Repatriation General Hospital, Adelaide SA
Flinders University, Adelaide SA
email: anneka.stephens@imri.org.au

INTRODUCTION

There are conflicting views when assessing the best imaging modality by which to assess long leg alignment pre and post operatively for patients' receiving primary total hip replacements. It has been a long standing standard that long-leg radiographs are used for measuring and interpreting alignment of the lower limb, but recently it has been suggested that CT imaging may be a better option for this assessment.

METHODS

Patients awaiting total knee replacement surgeries were invited to participate in this clinical trial. 120 participants' consented and completed both pre and post-operative long-leg radiographs, and lower limb CT scans. Long leg radiographs were analysed and measured by senior orthopaedic surgeons pre and post-operatively, while CT scans were analysed using the perth protocol method by trained radiologists. Mechanical alignment of the lower limb was calculated using both imaging modalities, the CT "scout" scan was used for the measurement of the mechanical alignment.

Pre-operatively the patients had their imaging performed between 1 year and 1 week pre-operatively, and following surgery their imaging was standardised to 6 months post-operatively. For long leg radiographs, patients were asked to stand with their feet shoulder width apart and toes forward facing (on occasion deformities would not allow for this stance, and they were asked to adopt this stance to the best of their ability).

RESULTS AND DISCUSSION

The results were analysed using pearsons correlation tests, correlation was shown to be good between the mechanical alignment measurements taken from long leg radiographs, and also from CT scout scans. Preliminary results have shown that correlation between the two modalities is 0.7, displaying a good level of correlation. Interobserver and intra observer analysis of the mechanical alignment taken from long leg radiographs is shown to be excellent with preliminary correlation being 0.9. Bland Altman plots of the data have shown that the trend line associated with difference in measurement is linear. Please see figure 1 (pre-op only). This trend demonstrated that the greater the varus deformity of the knee then the increase in discrepancy between the alignment measurements taken from differing modalities.

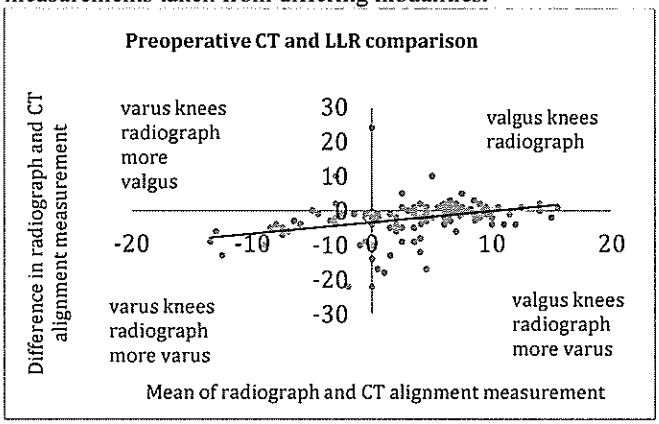

Figure 1: Bland-Altman plot of average alignment measurements and the difference between the measurement taken from CT of lower limb, and long leg radiograph.

CONCLUSIONS

The correlation results show that CT scans could be using in place of long leg radiographs, and this could assist in measuring the alignment of patients with deformities rendering them unable to stand. Radiation dose has been a main focus of many papers reviewing this correlation previously, but as the mechanical alignment does not require an investigational CT scan to be performed, but only a scout CT scan, the radiation dose is quite comparable to that of a long leg radiograph. CT scans have the additional ability of being able to place the whole image of the leg onto one screen, whereas x-ray of the entire leg required the merging of three different cassettes. This leads to additional human error with the aligning of these cassettes by the radiographer prior to taking the image, and following exposure.

CT scans could be considered for measuring the alignment of the lower limb prior to and after total knee replacement.

ACKNOWLEDGEMENTS

Biomet Australia Pty Ltd – contributed funding in support of the research conducted for this paper.

CONFLICT OF INTEREST DECLARATION

Do you have a conflict of interest to declare?

YES

1. A commercial entity (Biomet) paid or directed, or agreed to pay or direct, any benefits to nonprofit organization (IMRI) with which some of the authors are employed.

SESSION 5 – BIOMECHANICS 1

RELATIONSHIPS BETWEEN PROXIMAL TIBIA BONE MICROARCHITECTURE AND DYNAMIC JOINT LOADS IN END-STAGE KNEE OSTEOARTRHITIS – A PRELIMINARY STUDY

[1]Bryant C Roberts, [2]Dominic Thewlis, [3]Bogdan Solomon, [4]Graham Mercer, [5]Daryl Teague, [1]Karen J Reynolds and [1]Egon Perilli

[1]Medical Device Research Institute, School of Computer Science, Engineering and Mathematics, Flinders University, SA [2]School of Health Sciences, University of South Australia, Adelaide, SA [3]Department of Orthopaedics and Trauma, Royal Adelaide Hospital and Discipline of Orthopaedics and Trauma, The University of Adelaide, SA [4]Department of Orthopaedic Surgery, Repatriation General Hospital, Adelaide, SA, [5]Burnside War Memorial Hospital, Adelaide, SA Australia
email: bryant.roberts@flinders.edu.au

INTRODUCTION

In knee osteoarthritis (OA), local changes in areal bone mineral density in the tibia, as measured by dual X-ray absorptiometry, are suggested to be related to abnormal *in vivo* joint loading [1]. The relationship between *in vivo* measures of knee joint loading and changes in subchondral bone 3D microarchitecture, however, has not yet been explored.

The aim of this study is to examine, on end-stage OA patients undergoing total knee replacement (TKR), the relationships between knee joint loads measured *in vivo* using gait analysis prior to surgery, and variations in bone microarchitecture of their excised knees quantified with 3D micro-computed tomography (micro-CT). Preliminary results are presented.

METHODS

Patients: Six knee OA patients scheduled for TKR surgery (mean (SD) age 66 (6) years, body mass 86 (20) kg).

Gait Analysis: Patients underwent pre-operative gait analysis at self-selected walking speed. Kinematic and kinetic data were collected with 12 Vicon cameras (MX-F20) and four force platforms, and analysed with Visual3D v5.0 (C-motion Inc., MD, USA). Kinetic variables included the external moments at the knee: the peak external (ERM) and internal rotation moments (IRM), and peak knee adduction moment (KAM), all normalized by bodyweight. The peak tibio-femoral joint contact force (JCF) was calculated, with a musculoskeletal model based on Delp et al. [2] using Matlab.

Micro-CT analysis: After surgery, tibial plateaus were retrieved and scanned with micro-CT (model 1076, Skyscan, Belgium). Subchondral bone microarchitecture was analysed (CTAnalyser, Skyscan) in 4 regions of interest (ROIs, 10 mm diameter, 3 mm length), selected via software in the antero-medial (AM), antero-lateral (AL), postero-medial (PM) and postero-lateral (PL) condyle. Calculated 3D morphometric parameters: bone volume fraction (BV/TV), trabecular thickness, trabecular number, structure model index (SMI).

Statistics: Differences in microarchitecture among the four knee subregions were tested by using repeated measures ANOVA followed by a Bonferroni *post hoc* test. Associations between measurements from gait analysis and bone microarchitecture were investigated using Pearson's correlations. Significance level was set to p=0.05.

RESULTS AND DISCUSSION

Statistically significant differences in subchondral bone microarchitecture were found among subregions, with the AM ROI exhibiting increased BV/TV (+119%, Fig.1a), trabecular thickness (+32%), trabecular number (+68%), and decreases in SMI (-81%) compared to the AL region. BV/TV in the AM region was negatively correlated with peak ERM ($r = -0.88$, $p < 0.05$) (Fig.1b). Positive trends were observed in the correlations "BV/TV AM vs. peak KAM" ($r = 0.73$, $p = 0.10$), and "BV/TV AM vs. peak JCF" ($r = 0.75$, $p = 0.09$).

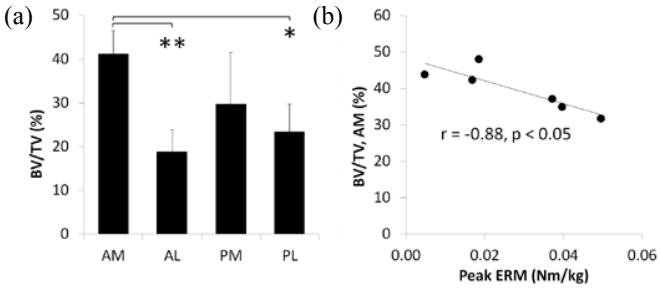

Figure 1: (a) average BV/TV and standard deviation (error bars) in the four anatomical ROIs within the tibial plateaus of six subjects (* p<0.05, ** p<0.01). (b) scatter plot with best fit line of "BV/TV AM vs. peak external rotation moment (ERM)".

CONCLUSIONS

Our preliminary results suggest that a decrease in peak external rotation moment during stance is significantly associated to increases in BV/TV in the AM tibial subchondral bone region. The increase in bone volume in this region could be linked to an adaptation of the bone due to altered loading patterns that generate increased stresses in this condyle [3]. Further analysis is required to elucidate the role of rotation moments on proximal tibia subchondral microarchitecture. Recruitment of further patients is ongoing, for enabling an appropriately powered statistical analysis.

ACKNOWLEDGEMENTS

Study supported by Arthritis Australia-Zimmer Australia (Grant in Aid 2013, Perilli E.), and Catalyst Grant DFEEST, Premier's Research Industry Fund, SA (2013, Perilli E.).

REFERENCES

1. Thorp, LE, et al., *Bone*. **39**:1116-1122, 2006
2. Delp, SL, et al., *IEEE Trans Biomed Eng*. **37**:757-67, 1990
3. Adouni, M, et al., *J Orthop Res*. **32**:69-78, 2014

THE REPERTOIRE OF POSSIBLE MUSCLE SYNERGIES DURING WALKING

[1,2]Saulo Martelli, Daniela Calvetti[3], Erkki Somersalo[3], Marco Viceconti[4]

[1]School of Computer Science, Engineering and Math., Medical Device Research Institute, Flinders University, Adelaide, SA
[2]North West Academic Centre, The University of Melbourne, St Albans, Australia
[3]Department of Mathematics, Case Western Reserve University, Cleveland, USA
[4]Department of Mechanical Engineering and INSIGNEO Institute for in silico Medicine, University of Sheffield, Sheffield, UK
email: saulo.martelli@flinders.edu.au

INTRODUCTION

Our central nervous system (CNS) recruits muscles targeting multiple and competing goals, relative importance of which is itself learned, task dependent, healthy condition dependent, and noise plague the sensory inputs and muscles output in determining the appropriate motor command [1]. However, current methods used for calculating muscle forces assume that the CNS adheres to a known optimal behavior and calculates a single representative muscle force pattern. Statistical methods can provide information about the repertoire of muscle synergies by inputting qualitative observations of muscle forces, errors on the model and motion parameters, and physiological constraints [2]. We demonstrate the use of a Bayesian statistical framework for calculating the repertoire of muscle forces during walking.

METHODS

Skin-mounted marker trajectories, ground reaction forces and electromyography (EMG) signals from the principal muscle groups were taken from a 25 year old woman while walking, and used in conjunction with a musculoskeletal model from a body-matched donor. Both the model and the data have been presented earlier [3]. It has been shown that calculated joint angles, joint moments, muscle lever arms, muscle and joint forces are in good agreement with corresponding published patterns. The balance equation at the joints was defined using the muscle lever arms and joint moments extracted from the model. The spectrum of possible muscle synergies, solutions of the equilibrium problem at the joints, was calculated using METABOLICA [3], software that combines Bayesian statistics and Markov Chain Monte Carlo for studying indeterminate inverse linear problems. A spectrum of muscle synergies of 200,000 samples was generated for each of the 102 walking frames by constraining muscle forces between the peak isometric forces and zero. The raw EMG signal for the gluteus maximus, rectus femori, vastus lateralis, tibialis anterior, gastrocnemius medialis and the biceps femoris long head was band-pass filtered (8th order, Butterworth filter, 10-400 Hz) to minimize noise due to motion artefacts and the surface EMG amplifier; rectified and low-pass filtered (2nd order, Butterworth filter, 6 Hz). The EMG envelope was scaled to match the peak of the optimal-control muscle force normalized by the muscles' peak isometric force. The muscle synergy that best matched the EMG envelope was identified from the calculated spectrum using a least-squared algorithm. The optimal-control solution and the best-match statistical solution were compared with the EMG envelope in terms of peak and mean error. A repertoire (200,000 samples) of possible muscle synergies was calculated by assuming a possible variation of muscle forces equal to the 5% of the muscles' peak isometric force.

RESULTS AND DISCUSSION

The best-match statistical solution most closely followed the EMG envelope, particularly during late stance for gluteus maximus and tibialis anterior, and during early stance for rectus femoris. Though, no solutions of the joint balance problem exactly matched the EMG envelope (Figure 1).The optimal-control solution showed a peak error of < 492 N and a mean error of < 149 N both for the gastrocnemius medialis. The best-fit statistical solution showed a peak error of < 122 N and a mean error < 36 N both for the gluteus maximus.

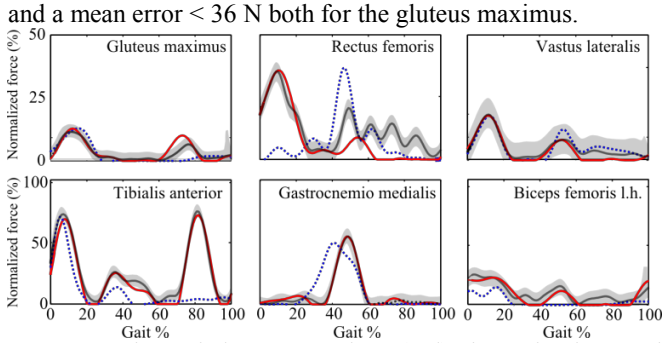

Figure 1: The scaled EMG envelope (red), the optimal-control solution (blue), the best-match statistical solution (black), and the repertoire of muscle synergies (gray band).

CONCLUSIONS

The statistical approach most closely followed the EMG envelope without assuming a pre-defined CNS behavior. Therefore, the statistical method is well suited to calculate the repertoire of muscle synergies for every possible CNS behavior. Residual discrepancies can be further reduced by improving the quality of recording of muscle signals and improving the model.

ACKNOWLEDGEMENTS

Australian Research Council (DE140101530).

REFERENCES

1. Loeb GE. *Biol. Cybern.* **106**:757–65, 2012.
2. Heino J et al. *Comp Meth Pro Bio*. **97**:151–67, 2010.
3. Martelli S et al. *J Biomech*. **47**:1784-91, 2014.

BALANCE RESPONSE DURING INDUCED FALLS IN PEOPLE WITH KNEE OSTEOARTHRITIS

[1]Pazit Levinger, [1]Calum Downie, [1]Hanatsu Nagano, [1]Aaron Petersen[1], [1]Alan Hayes, [2]Kerrie M Sanders, [3]Flavia Cicuttini, [1]Rezaul Begg

[1]Institute of Sport, Exercise and Active Living, Victoria University, Melbourne, VIC

[2] NorthWest Academic Centre, Department of Medicine, University of Melbourne, Western Health, VIC

[3] Faculty of Medicine, Nursing & Health Sciences, Monash University , VIC

email: pazit.levinger@vu.edu.au

INTRODUCTION

Knee osteoarthritis (OA) is a painful, debilitating and life-altering joint disease and a major risk factor for falls. The prevalence of falls in people with OA is substantially higher with approximately 50% of people with knee OA over the age of 60 reporting one or more falls each year. The mechanism causing people with knee OA to fall is also poorly understood. The capacity to respond and react against an imbalance episode, such as in tripping, is markedly reduced in older people. However, in people with knee OA, the mechanism responsible for dynamic postural control may be further impaired due to pain and poor muscle strength. Therefore, the aim of this study was to investigate balance recovery responses during an induced fall in people with knee OA compared to asymptomatic healthy controls.

METHODS

Twenty four participants with clinical symptoms of knee OA (50% males, mean ± SD age 68.6 ± 6.2 years, height 169.3 ± 10 cm, mass 80.7 ± 14.5 kg and body mass index (BMI) of 27.7 ± 4.1 kg/m^2) and fifteen asymptomatic healthy controls (73% males, age 72.4 ± 4.8 years, height 170.1 ± 8.8 cm, mass 76 ± 12.2 kg and BMI of 26.1 ± 3 kg/m^2) were recruited. Reflective markers were attached to the participants' upper and lower body according to the full body Plug-In-Gait model (Oxford Metrics Group, Oxford, England). Three dimensional (3D) motion analysis system (VICON, Oxford Metrics) with 10 Cameras (MX-T 40S, 100Hz) and three force plates (AMTI model BP600900TT, Watertown, MA, USA; 1000Hz) were used to capture and analyse step cycle parameters and knee joint biomechanics (e.g., angles, and moments) as well as the body Centre of Mass (COM) during the balance recovery tasks. Participants were positioned in a static forward leaning position such that approximately 20% of their body weight was recorded on a force transducer placed in series with a horizontal restraining cable. Participants were then released from the induced unbalanced position and were instructed to recover their balance using a single forward step. The following parameters were extracted for the first step response between initial reaction (as recorded by force plates) and the first foot contact: step length, step velocity, Centre of Mass (COM) velocity in the horizontal direction, knee angle at foot contact, maximum knee angle, external knee sagittal plane moment, knee power absorption and knee negative work (between foot contact and knee maximum flexion). The number of steps required to regain balance (step response) was also recorded and classified as single step, double (2 steps) and multiple steps (more than 2 steps). Multivariate analysis with Bonferroni adjustment was used to detect differences between the groups and between step response (single, double, multi steps).

RESULTS AND DISCUSSION

Forty two and 40% from the OA and control groups respectively responded with a single step; 25% and 20% responded with a double step and 33% and 40% responded with multiple steps respectively. Significant slower COM velocity ($p = 0.04$) was found for the OA group (0.9 ± 0.2m/s) compared to the control (1.1 ± 0.1m/s). Smaller maximum knee flexion angle ($p=0.02$) was also detected in the OA group (41.5± 12.8°vs. 46.3 ± 7.7°). Irrespective of groups, significant differences between single step and multistep responses were found for step length, ($p=0.04$), knee negative work ($p=0.004$), sagittal plane knee moment ($p=0.01$) and knee peak power ($p=0.001$) were found between single step response and multiple step response whereas multi steppers demonstrated reduced step length (0.72 ± 0.18 vs 0.89 ± 0.14m), knee absorption power (-1.40 ± 1.42 vs -4.47 ±2.75 W/kg), knee flexion moment (0.79 ± 0.70 vs 1.21 ± 0.56 Nm/kg) and knee negative work (-0.03 ± 0.05 vs -0.20 ± 0.15 J/kg).

CONCLUSIONS

To recover balance from an induced falling position, older adults often require multiple steps to arrest their forward momentum and maintain their COM within the base of support. Multiple steppers responded with a shorter step and a reduction in knee joint loading and power absorption despite their similar COM velocity to the single steppers. Multiple step response has been reported to be predictor of a future fall [1]. A slower COM forward velocity was exhibited in the knee OA group despite no differences in step length or step velocity. Moreover, a reduced peak knee flexion angle at recovery limb foot contact was also demonstrated in the OA group which might be an attempt to reduce joint load due to knee joint pathology and any associated impairment in quadriceps muscle strength. These results suggest different adaptive strategies being used by the knee OA participants to recover balance.

ACKNOWLEDGEMENTS

This study was funded through the Australian Government's Collaborative Research Network (CRN).

REFERENCES

1. Mille ML, et al., *J Gerontol A Biol Sci Med Sci*. **68**:1540-1548, 2013.

Custom Test Rig for *In Vitro* Measurement of Human Knee Cartilage Stresses Under Physiological Load

[1]GU Wei, [1]Jonathan Walter, [1]Marcus Pandy

[1]Department of Mechanical Engineering, University of Melbourne, VIC
email: w.gu12@student.unimelb.edu.au

INTRODUCTION

Abnormal cartilage deformation is a primary factor contributing to the development of knee osteoarthritis (OA) [1, 2]. Because of the inability to measure cartilage biomechanics non-invasively, finite element (FE) analysis has been implemented to simulate *in vivo* cartilage mechanical behavior. Many knee joint FE models have been reported in the literature, but these models typically oversimplify cartilage mechanical behavior and lack vigorous validation.

The aim of this study was to build and evaluate novel subject-specific FE knee models with nonlinear cartilage properties measured from human cartilage tissue. In order to validate the FE models, a testing device was built for in vitro compression of cadaveric knee joints with simultaneous measurement of dynamic pressure, load and displacement.

METHODS

The test rig (Figure 1) was constructed using Item America Profile 8 aluminum extrusions and custom-made aluminum fixtures. The device affords the flexibility of adjusting five degrees of freedom at the knee: flexion-extension, varus-valgus, internal-external rotation, anterior-posterior translation and medial-lateral translation. Superior-inferior translations were controlled by a NOOK screw jack.

A JR3 load cell was attached beneath the screw jack to measure the axial force exerted on the specimen knee during testing. The load cell had a maximum force range of 2000 N and accuracy of 2.5%. A linear displacement variable transducer (LVDT) (maximum range: 10 mm) was used to accurately ($\pm$0.025 mm) measure relative movements between the femur and tibia. Pressure distribution in the medial and lateral compartments of the tibiofemoral joint were measured dynamically using a Tekscan I-scan sensor system with #5076 sensor, which has a resolution of 27.6 sensing units per cm^2 and a maximum capacity of 13.7 Mpa. A custom LabView program was used to record load cell and LVDT data synchronized with the I-scan pressure measurements. Two webcams were used to acquire images of the knee joint from two different angles. The 3D orientations of the tibia and femur were reconstructed from the webcam images using custom Matlab programs.

RESULTS AND DISCUSSION

The webcam system measured bone position to an accuracy of 0.4 mm.

The rig axial deformation was 0.25 mm under compressive load of 1700 N. The deformation of the test rig in translational direction was approximately 2 mm under 2000 N when 45° knee flexion was simulated. A porcine knee pilot loading study was conducted with the test rig to ensure the feasibility of experimental protocol.

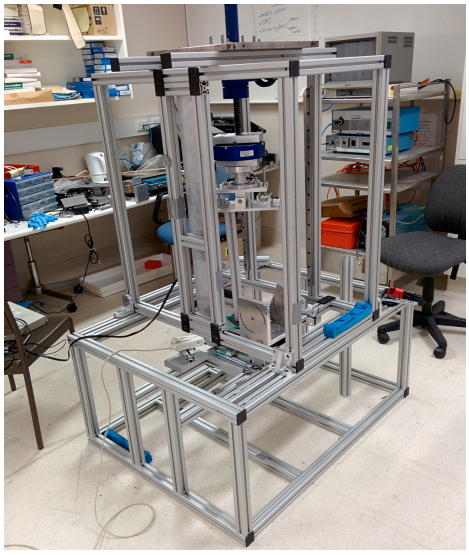

Figure 1: Custom test rig for in vitro measurement of articular cartilage stresses at the knee.

CONCLUSIONS

Our preliminary experiments suggest that it is feasible to perform in vitro knee joint loading tests using the custom test rig. Our future work involves collecting data from healthy cadaver human knee specimens. These data will be used to validate our subject-specific FE modelling protocol aimed at calculating cartilage stresses and strains under physiological load.

ACKNOWLEDGMENTS

This work was funded by an ARC Discovery grant and a VESKI Innovation Fellowship to MGP. We thank Dr John Costi of Flinders University for donating the pressure transducer used in this study.

REFERENCES

1. Bachrach, N.M., et al., *J Biomech*. **28**(12): p. 1561-9, 1995.
2. Miyazaki, T., et al., *Annals of the Rheumatic Diseases*.**61**(7): p. 617-622, 2002.

CONTACT CONTRIBUTIONS TO INVERSE DYNAMIC KNEE LOADS DURING GAIT

[1]Jonathan Walter, [2]Nuray Korkmaz, [3]Benjamin Fregly and [1]Marcus Pandy

[1]Department of Mechanical Engineering, University of Melbourne, Melbourne, VIC
[2]Department of Mechanical Engineering, Istanbul University, Avcilar/Istanbul, Turkey
[3]Department of Mechanical and Aerospace Engineering, University of Florida, FL, USA
email: walterj@unimelb.edu.au

INTRODUCTION

Accurate modelling of contact and muscle forces could help diagnose and treat patients with common biomechanical knee disorders such as osteoarthritis (OA) [1]. Knowledge of how measured tibio-femoral contact loads relate to external loads calculated from inverse dynamics during normal and modified gait could be used to improve musculoskeletal models as well as treatments[2]. This study aimed to quantify the relationship between measured contact loads and the external loads at the knee calculated by inverse dynamics for multiple subjects and a variety of gait patterns.

METHODS

Experimental data from five "Grand Challenge Competitions to Predict In Vivo Knee Loads" were used for this study [3]. Four patients with load-measuring knee replacements performed over-ground gait (Normal, Trunk Sway, Medial-Thrust, and Walking Pole) with simultaneous collection of knee contact loads, marker positions, and ground reaction forces (GRF). Institutional review board approval and informed consent were obtained. Inverse dynamic loads were calculated using a scaled musculo-skeletal model about the knee joint center location in the tibia reference frame. Implant contact measurements were processed for comparison to the external loads in the superior-inferior force (Fy), adduction-abduction moment (Mx) and flexion-extension moment (Mz) directions. Corresponding contact and inverse dynamics loads were compared by calculating mean ratios and Spearman correlation coefficients during stance phase.

RESULTS AND DISCUSSION

The contribution of contact to the external adduction moment varied considerably between subjects and gait patterns with a mean ± SD ratio of 59±40% and a moderate correlation coefficient of 0.61 for normal gait, indicating that a simple relationship may not exist between contact and external adduction moments (Table 1). A larger than expected contribution of contact to the external flexion moment occurred, (22±16%). The contribution of contact to the external superior-inferior force remained more consistent than the other loads with higher correlations, ($0.72<\rho<0.76$). While all gait patterns showed reduced ratios of contact to external adduction moments from normal gait, trunk sway and medial thrust gait also increased the ratio of contact to external superior-inferior force.

CONCLUSIONS

This study quantified the contribution from measured contact loads to the external loads obtained from inverse dynamics analysis for multiple subjects and various gait patterns. The flexion moment from contact contributed larger than expected in all gait patterns and subjects (i.e. >10%), suggesting that the common modelling assumption of zero contact contribution to the external flexion moment is not valid, and thus contact must be modelled for accurate calculation of lower-limb muscle forces. The contribution of the contact adduction moment was variable between subjects, which further necessitates the need for musculoskeletal models to incorporate the effects of both contact and muscle forces. The results of this study are relevant to those interested in developing computational simulations of the knee during gait and to those studying the effects of gait pattern modifications on knee-joint loading in patients with knee OA.

ACKNOWLEDGMENTS

This work was funded by an Australian Council Discovery Projects Grant #DP120101973.

REFERENCES

1. Pandy M, et al., *Ann Rev Biomed Eng*. **12**:401-433, 2010.
2. Walter J, *J Orthop Res*. **28**:1348-1354, 2010
3. Fregly B, *J Orthop Res*. **30**:503-513, 2012

Table 1: Ratio and correlation coefficients of contact to inverse dynamic loads at the knee during stance phase. Red text indicates a mean greater than normal gait and blue text indicates a mean lower than normal gait.

Load	Measure	Normal	Medial Thrust	Walking Pole	Trunk Sway
Mx	**Correlation ρ**	0.61	0.55	0.50	0.44
	Ratio % Mean(STD)	59(40)	52(44)	50(36)	31(44)
Mz	**Correlation ρ**	0.44	0.46	0.66	0.22
	Ratio % Mean(STD)	22(16)	10(20)	8(12)	17(18)
Fy	**Correlation ρ**	0.73	0.72	0.76	0.73
	Ratio % Mean(STD)	230(39)	268(63)	227(37)	261(57)

Why are younger patients undergoing ACL reconstruction more prone to re-rupture?

[1]David S Musson, [1]Ryan Gao, [1]Matthew WJ Street, [1]Dorit Naot, [1]Karen E Callon, [1]Satya Amirapu, [2]Brendon Coleman, [1]Jillian Cornish

[1]University of Auckland, Auckland, New Zealand
[2]Middlemore Hospital, Auckland, New Zealand
email: d.musson@auckland.ac.nz

INTRODUCTION

Anterior cruciate ligament (ACL) tears are the most common ligamentous knee injuries, often occurring in otherwise healthy, active, young individuals. A recent study using New Zealand ACC claim data suggests that total ACL surgeries cost in the region of $18,250,000 NZD per year in New Zealand, with global re-rupture rates estimated at 3.6%. This suggests that the annual cost of surgically repairing re-ruptured ACLs would be in the region of $650,000 NZD, although this is likely an underestimation.

Interestingly, recent local data from the UniSports Sports Medicine clinic in Auckland, NZ showed a higher failure rate in younger patients for hamstring reconstruction. Here, a retrospective review of 694 ACL reconstructions carried out between January 2009 and December 2012 showed overall re-rupture rates were 4.4% for hamstring and 1.9% for bone-patellar tendon-bone grafts. In patients younger than 20 years however, the re-rupture rate was 10.4% for hamstrings and 0% for bone-patella tendon-bone grafts.

In this study we aim to determine the biological reasons which may contribute to the high re-rupture rates of younger patients.

METHODS

During harvesting of the hamstring tendon for ACL reconstruction, either end of the tendon will be trimmed to allow for the ideal graft diameter and length. The sections of hamstring tendon not used as a graft have been collected and analysed in our study. The distal portion of the tendon has been stained for histological assessment of tendon fibre thickness, the most proximal 5mm of the tendon used for gene expression analysis and the final approximate 4cm of tendon used for biomechanical analysis of stiffness, modulus and ultimate load to failure. Hamstring tendons harvested from patients under the age of 20 will be compared to those 20 and over.

RESULTS AND DISCUSSION

No statistical differences were found in the mean stiffness of either age group - 18.9 N/mm in those under 20, compared to 14.6 N/mm in those 20 and over. However, there appears to be a distinct group of younger patients with a stiffness of over 20 N/mm, compared to the majority of all aged patients who appear to have a stiffness of under 15 N/mm (Figure 1). Further analysis is in progress to determine if this corresponds with differences in collagen fibre thickness and/or expression of genes important in tendon biology.

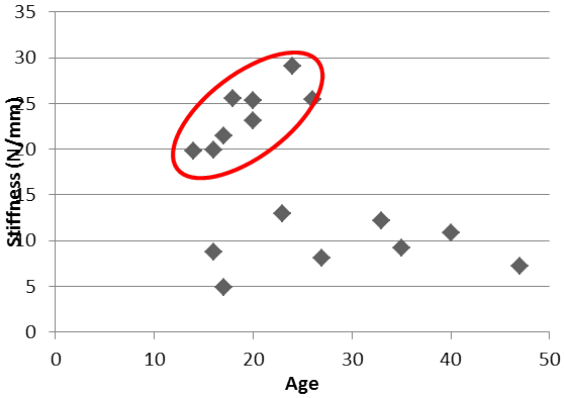

FIGURE 1. Hamstring biopsy stiffness correlated to age in patients undergoing ACL reconstruction

CONCLUSIONS

Here we have identified a distinct group of outlier, younger patients whose hamstring tendons appear to be stiffer than normal. Further sample collection and analysis is ongoing to determine the biological reasons for these differences. Determining the biological reasons which may contribute to the high re-rupture rates of younger patients undergoing ACL reconstruction could significantly impact current clinical practices.

ACKNOWLEDGEMENTS

Auckland Medical Research Foundation

ABNORMAL KNEE KINEMATICS DURING STEP AND TURN FOLLOWING MULTIPLE-LIGAMENT KNEE RECONSTRUCTION

Joe Lynch[1,2], Corey Scholes[1], Brett Fristch[1], Milad Ebrahimi[1], Myles RJ Coolican[1], Paul N Smith[2], Richard Smith[3], David A Parker[1]

[1]Sydney Orthopaedic Research Institute, Chatswood NSW
[2]Trauma and Orthopaedic Research Unit, Canberra ACT
[3]The University Sydney, Lidcombe NSW
email: joe.lynch@act.gov.au

INTRODUCTION

There is a lack of knowledge regarding the biomechanical outcomes of surgical reconstruction following multiple-ligament knee injury (MLKI). Specifically, activities that require a change of direction could produce altered knee kinematics in this group due to the increased rotational loads applied to the knee joint. The purpose of this study was to compare the kinematic differences in the MLKI reconstructed knee with normal knees during a step and turn task.

METHODS

Three-dimensional gait analysis was conducted on 16 patients who had undergone ligament reconstruction with one of three consultant orthopaedic surgeons and 16 matched healthy controls. Patients were asked to descend two steps onto their injured leg and pivot 90° before initiating level walking. A set of skin-mounted markers on anatomical landmarks and segment clusters was used to track motion and three-dimensional knee angles were calculated during the motion. Angles at initial foot strike and end of weight acceptance were extracted, as well as range of knee motion during weight acceptance and over the total pivot. Group-level and single-subject statistical analysis was used to detect differences between reconstructed and healthy knee kinematics.

RESULTS AND DISCUSSION

At initial foot contact during step descent, the reconstructed group displayed significantly ($p<0.05$) more externally rotated tibiae than healthy controls (Fig 1). In addition, significantly increased internal rotation of the tibia was observed during weight acceptance onto the reconstructed limb. Single subject analysis revealed considerable variability in responses between reconstructed knees and controls with up to 63% of the cohort displaying significant differences in flexion and varus-valgus motion during the step-turn task (Table 1). Additional analysis revealed that differences in foot progression angle may confound the differences in tibial rotation identified.

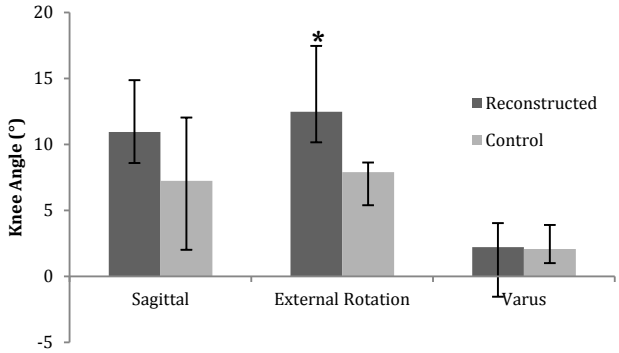

Figure 1: Group flexion, axial rotation and adduction (varus) angles in reconstructed and control knees at initial foot contact in step descent.

CONCLUSIONS

The present study reveals that the effect of injury and reconstruction may not be systematic in all patients. Importantly, the majority of reconstructed patients appear to pre-empt pivoting by rotating their foot prior to contact with the ground thereby potentially reducing the load on the joint. The reasons for this compensation strategy could have important implications for rehabilitation.

Table 1: Total percentage (%) of patients (n=16) with significant ($p<0.05$) differences at heel strike and Range of Motion (RoM) compared to their matched healthy controls

Movement	Proportion of patients different to control for Initial Contact Angle		Proportion of patients different to control for Weight Acceptance RoM	
	% with an increased angle	% with a decreased angle	% with an increased RoM	% with a decreased RoM
- Flexion	63	25	25	56
- Valgus/Adduction	31	19	38	38
- Varus/Abduction	38	6	0	13
- Internal Rotation	0	0	63	19
- External Rotation	75	6	0	0

SESSION 6 – CLINICAL 2

A METHOD FOR MONITORING ANIMAL ACTIVITY IN ORTHOPAEDIC STUDIES

[1]Stephanie Fountain and [1]Devakar Epari

[1]Institute of Health and Biomedical Innovation, Queensland University of Technology, Brisbane, QLD
email: stephanie.fountain@uqut.edu.au; d.epari@qut.edu.au

INTRODUCTION

Mechanical stimuli have been shown to influence fracture healing [1], yet the loading histories of animals used in orthopaedic studies are rarely monitored. This is because there are no standard methods for doing so. However, recent developments in micro-electro-mechanical systems (MEMS) technology have made it feasible to a develop practical, affordable and user friendly monitoring device for long-term animal studies. Three potential technologies for monitoring activity including pedometers, GPS and inertial sensors (comprised of accelerometers and gyroscopes), were explored, from which a final activity monitoring system was developed.

METHODS

Four pedometers were secured via a body harness to a sheep which was left to roam the animal yard (for 3 sessions). Pedometer step counts were then compared with those recorded from observation using a hand held counter (validated from review of video footage). Seven GPS devices were walked around the perimeter of the animal yard (for 5 laps) and the distance logged was compared with the manually measured distance (taken using a measuring wheel).

Inertial sensors were secured to the body harness during two, 20 minute, filmed activity sessions. From aligning the data set with the video footage, samples of walking, running and standing data were extracted from the data set. Of the extracted data, 75 % was used to establish a pattern recognition algorithm using the neural network toolbox of matlab, 25 % was used to test the accuracy of the algorithm.

RESULTS AND DISCUSSION

Each of the tested devices was able to monitor activity with reasonable accuracy. The inertial sensor approach had the highest accuracy, with the pattern recognition algorithm accurately distinguishing between both standing and moving (99.9 % accuracy) and walking and running (94 ± 2 % accuracy) (Figure 1). The pedometers however, appeared to slightly overestimate the step count while the GPS devices appeared to underestimate distance travelled (Table 1).

Both pedometers and GPS provide basic activity counts, but the GPS is far more expensive and has a shorter battery life. Furthermore, subsequent tests revealed that the GPS was unable to capture small bursts of movement over short distances. The inertial sensors produce a more comprehensive loading history, which justify the higher cost (compared with pedometers) and required processing time.

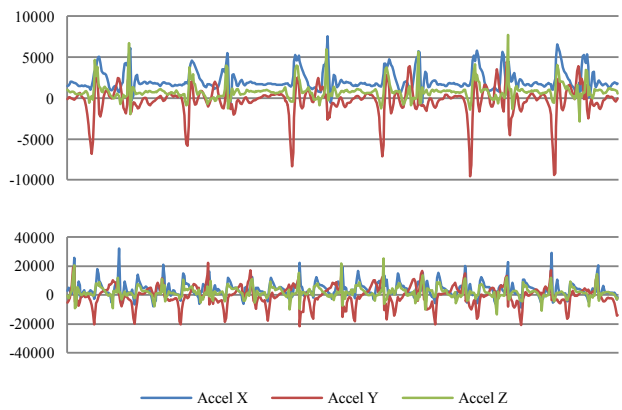

Figure 1: Acceleration (m/s^2) data from inertial sensors during walking (top) and running (bottom) over 5 seconds.

CONCLUSIONS

Inertial sensors are recommended for obtaining detailed animal loading histories in orthopaedic studies. Future studies are underway to investigate the correlation between activity and fracture healing.

ACKNOWLEDGEMENTS

The authors acknowledge Sabel Labs of Griffith University for use of their inertial sensors.

REFERENCES

1. Epari D, et al., *Journal of Engineering in Medicine*. **224**:1543-1553, 2010.

Table 1: Accuracy of tested device measurements compared with manual measurements.

Device	Measurement	Accuracy
Pedometer	Step count	112 ± 8 %
GPS	Distance travelled	78 ± 7 %
Inertial Sensor	Activity recognition (walking versus running)	94 ± 2 %

A COMPARISON BETWEEN 'SIGNATURE PERSONALISED PATIENT CARE' TO CONVENTIONAL TOTAL KNEE ARTHROPLASTY AND COMPUTER-ASSISTED NAVIGATION

[1,2]Christopher Wilson, [2,3]Anneka Stephens, [1]Graham Mercer, [2,4]Jegan Krishnan

[1]Department of Orthopaedics, Repatriation General Hospital, SA
[2]Flinders University, Bedford Park, SA
[3]International Musculoskeletal Research Institute Inc, Repatriation General Hospital, SA
[4]Department of Orthopaedics, Flinders Medical Centre, SA
anneka.stephens@imri.org.au

INTRODUCTION

Alignment and soft tissue balance are two of the most important factors that influence early and long term outcomes for total knee arthroplasty (TKR). The current practice involves the use of plain radiographs for pre-operative planning and conventional instrumentation for intra-operative alignment. Plain radiographs have limited accuracy and conventional instrumentation has been reported to have significant variations that can affect the ultimate accuracy and reproducibility of surgery.

The aim of this study was to assess the Biomet Signature patient specific instrumentation (PSI) system which uses patient specific guides developed from pre-operative MRI and to compare this TKR system with conventional instrumentation and computer-assisted navigation (CAS).

METHODS

Patients were invited to participate from the routine elective TKR waiting list at the Repatriation General Hospital, South Australia. Participants were then randomised into groups of 50 patients in each arm of the study. All participants received Biomet Vanguard implants. Patients were assessed pre-operatively by weight bearing long leg x-rays, standard views and Perth Protocol CT scans as well as clinical assessment by Knee Society Score (KSS).

Surgical plans for patients randomised to receive the Signature instrumentation were developed pre-operatively by the surgeon based on the patient's MRI, performed between 6 months and 6 weeks pre-operatively.

Participants underwent TKR and were followed up for a period of one year post-operatively with radiographic review at 6 months and KSS at 1 year follow-up.

RESULTS AND DISCUSSION

Six month post-operative mean alignment was comparable between all three groups in the study as measured by long leg x-ray. No statistically significant differences in terms of mean mechanical alignment could be detected between the three arms of the study.

No significant difference was observed between the three arms of the study for femoral tibial axis measurements determined by CT Perth Protocol; however the Signature group had the smallest standard deviation suggesting that the spread of outliers was smallest in this group.

The results seen in mechanical alignment were reflected in the KSS outcomes; mean scores for KSS were 138.4 (Signature), 144.2 (Conventional) and 142.6 (CAS). These values were not significantly different between study arms.

CONCLUSIONS

The results of this study suggest that the Biomet Signature personalized care plan compares well to both conventional and computer assisted total knee replacement surgery with respect to alignment and clinical scores. The Signature system was easily incorporated into our routine arthroplasty practice. One significant downside to the system is the requirement for a pre-operative MRI which can be difficult for patients of high BMI or with claustrophobia. The Signature system also requires less invasive surgical dissection than CAS.

In summary the Signature system performs well compared to other TKR techniques and is a safe, reliable and reproducible method for performing TKR.

ACKNOWLEDGEMENTS

We acknowledge the support of Biomet in funding this study.

CONFLICT OF INTEREST DECLARATION

In the interests of transparency and to help reviewers assess any potential bias, ANZORS requires authors of original research papers to declare any competing commercial interests in relation to the submitted work. Referees are also asked to indicate any potential conflict they might have reviewing a particular paper.

If you have accepted any support such as funds or materials, tangible or intangible, concerned with the research by the commercial party such as companies or investors, choose YES below, and state the relation between you and the commercial party.

If you have not accepted any support such as funds or materials, choose NO.

Do you have a conflict of interest to declare?

YES

A commercial entity paid or directed, or agreed to pay or direct, any benefits to any research fund, foundation, educational institution, or other charitable or nonprofit organization with which the authors are affiliated or associated.

The Biomet Signature™ Study was a commercially sponsored, phase IV post-marketing study sponsored by Biomet Australia Ltd. No authors of the study received direct personal financial considerations from the commercial sponsor and payments were for the purposes of conducting the study and supporting the ongoing research activities of the department of orthopaedics.

Limitations in predicting outcome following multiple-ligament knee injury and treatment: A systematic review of current literature

[1,2]Laurant Kang, [1]Corey Scholes, [1]Brett Fritsch, [3]David Hunter, [1]Myles Coolican and [1]David Parker

[1]Sydney Orthopaedic Research Institute, Chatswood, NSW
[2]Sydney Medical School, The University of Sydney, Sydney, NSW
[3]Institute of Bone and Joint Research, Kolling Institute, University of Sydney and Rheumatology Department, Royal North Shore Hospital
email: lkang@sori.com.au

INTRODUCTION

Clinicians currently lack an ability to predict the outcomes of a patient following multiple-ligament knee injury (MLKI), despite past research efforts. The purpose of this systematic review was to describe the current state of literature on the outcomes of patients with MLKI and examine demographic, injury and intervention characteristics predictors of patient self-reported outcomes.

METHODS

Searches were performed in MEDLINE, PUBMED, SCIRUS, SCIENCEDIRECT and the Cochrane Central Register for studies in English which examine factors associated with patient outcomes following MLKI and treatment. The selection criteria for article inclusion were: (1) MLKI defined as injury with injury of at least 2 major knee ligaments, (2) patients outcome quantified with standardised, validated patient self-reported questionnaires (3) with statistical analysis to assess the influence of factors on patient-reported outcomes. Article quality was assessed using Level of Evidence, the Cochrane Library Risk of Bias and the Downs and Black methodology score and review findings grouped into patient demographics, injury characteristics and intervention characteristics.

RESULTS AND DISCUSSION

A total of 42 studies were included that were relevant to patient demographics (N = 7), injury characteristics (N = 25) and intervention characteristics (N = 28). All but 9.5% of the articles were classified as Level III or IV evidence and the majority of articles were limited by a high risk of selection bias, largely due to a dearth of randomised controlled trials. Overall, the average Downs-Black score was 16.69 out of 28 and this was similar across sub-categories. Analysis of higher-quality papers (Downs-Black ≥18, 3rd quartile score) revealed that the Lysholm, IKDC and Tegner score were most commonly used as the self-reported outcome and that higher education level, transosseous fixation technique and reconstruction for cruciate ligaments, presence of posteromedial corner injuries and early functional rehabilitation were positively associated with the 3 scores, while being female, age>40, increasing number of ligaments injured, the presence of fracture, nerve damage, smoking history, ultra-low velocity injuries attributed to obese BMI were identified as negative predictors.

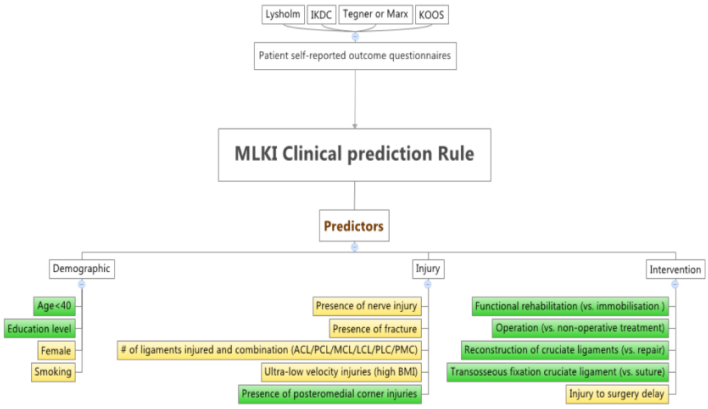

Figure 1: Conceptual prediction model for MLKI patient outcome

CONCLUSIONS

The overall low quality of the existing literature forms a considerable barrier in conceptualising a predictive model for MLKI outcomes, particularly after surgical intervention. The systematic review has analysed the top-quality papers and develop a conceptual prediction model required for further validation. While the difficulty of conducting randomised controlled trials in this population is well recognised, future observational studies should be supported by rigorous statistical methodology to control for confounding effects between potential predictive factors.

THE QUALITY OF SURGICAL TECHNOLOGY ASSESSMENT REPORTS PREPARED FOR MSAC

[1]Martin Hua, [2]Tristan Boonstra, [1]Patrick J Kelly, [1]Andrew Wilson, [1]Jonathan Craig, [1]Angela Webster

[1]Sydney School of Public Health, University of Sydney, NSW
[2]Royal Melbourne Hospital, Parkville, VIC
email: mhua8891@uni.sydney.edu.au

INTRODUCTION

In Australia, surgical technologies require a formal health technology assessment (HTA) as part of the consideration for Medicare Benefits Schedule (MBS) funding. The Medical Services Advisory Committee (MSAC) commissions HTA and advises the Minister for Health in this regard. As 70% of total Australian health expenditure is government funded, the MBS status of a surgical technology is imperative to its diffusion into Australia. For surgical technologies, MSAC may thus be conceived as the gatekeeper and HTA as the key to the Australian healthcare system [1]. However, stakeholders remain concerned over perceived inconsistencies between evidence, expert opinion and MBS funding decisions [2]. Whilst reports are published after MSAC makes its recommendation, the perceived inconsistencies may hinder their implementation, delay MBS funding and/or diffusion of the technology. This emphasises the need for transparency in funding decisions. We aimed to assess the quality of reporting of surgical HTA reports underpinning MBS funding decisions.

METHODS

We performed a cohort study of surgical HTA reports published by MSAC from 1998 to 2013. We used a checklist proposed by the European Collaboration for Assessment of Health Interventions [4] to assess the quality of reports across eleven domains. We used linear regression analysis to investigate any differences in quality over time or among surgical and other non-pharmaceutical health technologies.

RESULTS AND DISCUSSION

We included 41 surgical HTA – 16 resulted in a MSAC recommendation for full MBS funding. Figure 1 shows the quality of domain reporting. Evaluations of safety (93%), effectiveness (84%), economic (75%) and organisational implications (100%) were better reported than psychological, social and ethical considerations (40%). The basic (74%), methodological (58%), background (82%), contextual (48%), status quo (52%) and technical information (68%) framing HTA were inconsistently reported. Differences in domain by technology type were minor, but safety was noticeably better in surgical HTA. On average, overall quality increased by almost 2% ($P<0.001$) each year, with no significant difference between surgical and other technological types ($P=0.22$) (See Figure 2).

HTA play a central role in the diffusion of surgical technologies in Australia. Their implementation may be hindered if contextual and methodological aspects are unclear and at risk of bias [3]. Strong qualitative themes within a standard template for HTA reports in particular provides reassurance that stakeholder perspectives have been considered, thus minimising perceptions of bias [4]. Whilst overall quality increased over time, continued improvements are required for domains such as the methodological aspects of HTA and psychological, social and ethical considerations.

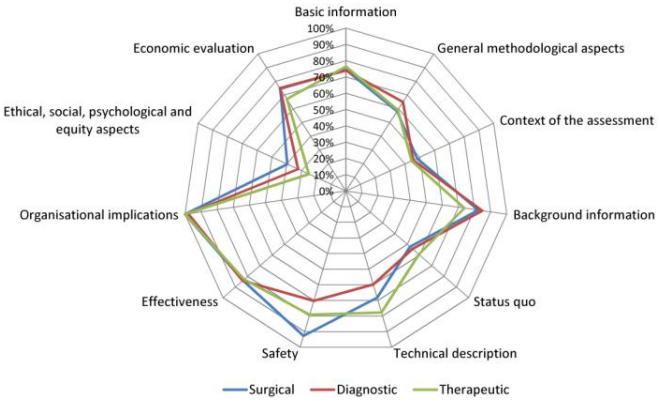

Figure 1: Quality of HTA reports by domain, stratified by surgical, diagnostic and non-surgical therapeutic technologies

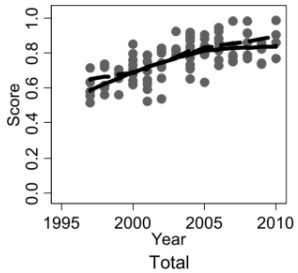

Figure 2: Overall quality scores of HTA reports over time.

CONCLUSIONS

Overall quality of surgical HTA reporting increased over time, but continued improvement across certain domains will strengthen the transparency of MBS funding decisions.

REFERENCES

1. Hailey D. International Journal of Technology Assessment in Health Care. **25**(Supp 1): 61-67, 2009
2. Johri M, et al., International Journal of Technology Assessment in Health Care. **19**(1):179-193, 2003.
3. Department of Health, Canberra, Australia, 2009.
4. Busse R, et al., International Journal of Technology Assessment in Health Care. **18**(2): 361-422, 2002.

A SYSTEMATIC REVIEW ON THE USE OF PATIENT REPORTED OUTCOME MEASURES (PROMS) IN KNEE ARTHROPLASTY RESEARCH

[1]Annika Theodoulou, [2]Andrew Spiteri and [3]Jegan Krishnan

[1]The International Musculoskeletal Research Institute Inc., Repatriation General Hospital, Daw Park SA, Flinders University, Bedford Park, SA, Australia
[2] Department of Orthopaedic Surgery, Flinders Medical Centre, Bedford Park, SA, Australia
[3]The International Musculoskeletal Research Institute Inc., Department of Orthopaedic Surgery, Flinders Medical Centre, Bedford Park, SA, Australia
email: Annika.Theodoulou@imri.org.au

INTRODUCTION

A growing number of valid and reliable instruments exist to assess patient outcomes following knee arthroplasty. This review aims to quantify the use of widely accepted PROMs within knee arthroplasty literature and explores potential discrepancies in the choice of PROMs utilised in publications of particular journals, study designs and from researchers of various countries.

METHODS

A systematic search of 8 electronic databases (OvidSP Medline, Pubmed, CINAHL, Embase, Cochrane Library, Scopus, PEDro and Web of Knowledge) was performed to identify studies published from January 2013 to 20th December 2013. Search terms included both controlled vocabulary and free-text terms. Two authors independently selected the studies to be included in the review. Eligibility for inclusion was published clinical trials concerning knee arthroplasty of which had used one or more patient reported outcome measures. Included studies were limited to English publications while review, validation and non-human studies were excluded from this review.

RESULTS AND DISCUSSION

Of the 1,996 publications retrieved, 568 met the inclusion criteria and were included in this systematic review (Figure 1). To date, publications considered revealed outcome measures consistently reported included the following; Knee Injury and Osteoarthritis Outcome Score (KOOS), Oxford Knee Score (OKS), Western Ontario and McMaster Universities Osteoarthritis Index (WOMAC), the Knee Society Score (KKS), the American Knee Society Score (AKSS), Short Form 36 Health Survey, Hospital for Special Surgery Score and EuroQOL-5D (EQ-5D).

On presentation, the results of the systematic review will highlight the percentage of patient reported outcome measures used in particular study designs, sample sizes and study topics of interest. Trends in follow-up time points and in measures employed in various countries will be identified. Discrepancies between measures published in high and low impact journals will also be discussed.

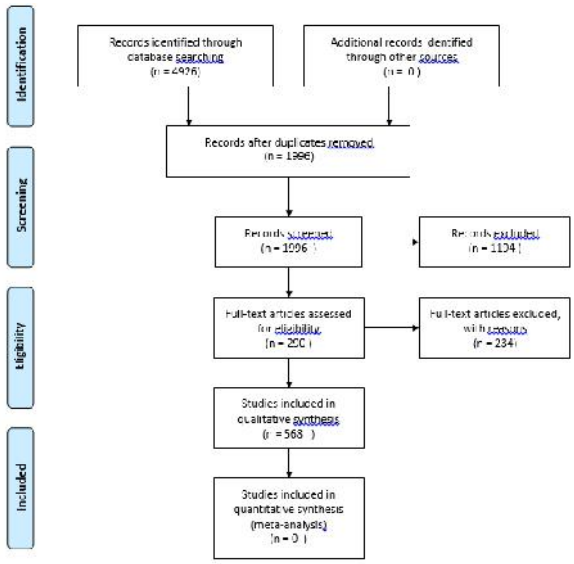

Figure 1: PRISMA[1] flow chart of literature search and selection process.

CONCLUSIONS

Patient reported outcome measures are key tools for investigating results of knee arthroplasty. Clarity on the use of PROMs across various study designs, sample sizes and journals can assist investigators in choosing the most suitable PROMs to employ in future research.

ACKNOWLEDGEMENTS

The authors gratefully acknowledge and thank Raechel Damarell, Senior Librarian for Medicine, for assistance and advice towards the conduct of the search strategy.

REFERENCES

[1] Moher D, Liberati A, Tetzlaff J, Altman DG, The PRISMA Group (2009). *P*referred *R*eporting *I*tems for *S*ystematic Reviews and *M*eta-*A*nalyses: The PRISMA Statement. PLoS Med 6(6): e1000097. doi:10.1371/journal.pmed1000097

CRITICAL REVIEW: EFFECT OF OBESITY AND MORBID OBESITY ON HIP AND KNEE ARTHROPLASTY OUTCOMES

[1,2]Robyn Kievit, [1,2]Donald Bramwell and [2]Jegan Krishnan

[1]International Musculoskeletal Research Institute, Repatriation General Hospital, Daw Park, SA
[2]School of Medicine, Flinders University, SA
email: Robyn.kievit@imri.org.au

INTRODUCTION

Much is known of the effects of high Body Mass Index (BMI) on arthroplasty (1-5); however there is high heterogeneity in the data and surgeons are hesitant to operate on high BMI patients, despite their significant improvements in pain and patient satisfaction (5). This critical review of obesity (BMI>30) and morbid obesity (MO) (BMI>40) in hip and knee arthroplasty literature analyses the major systematic reviews and meta-analyses published in the last 5 years, as well as relevant reviews, prospective and retrospective studies that would otherwise not have been included in the more restrictive systematic review process. This review aims to determine whether a definitive conclusion can be drawn in terms of whether there is a cut-off for operating on patients of particular BMI and whether the role of comorbidities, rather than obesity itself, play a role in the poorer functional outcomes seen with patients of high BMI; taking into account complications, infection, functional outcomes, pain and comorbidities.

METHODS

A search of 8 electronic databases (OvidSP Medline, Pubmed, CINAHL, Embase, Cochrane Library, Scopus, PEDro and Web of Knowledge) was performed to identify studies published from January 2009 - June 2014. Search terms included both controlled vocabulary and free-text terms, including "arthroplasty", "joint replacement", "hip", "knee ","weight "," BMI", "comorbidities "," morbidity "," pain" and "obesity". Eligibility for inclusion included published clinical trials concerning arthroplasty and review articles. Searches were restricted to articles written in English.

RESULTS AND DISCUSSION

Although the association between high levels of obesity and rates of infection and revision are well documented, there is a range of opinion on the value and clinical outcome for arthroplasty on patients at the middle to upper range of obesity. Systematic reviews have been conducted in both hip and knee arthroplasty; some addressing obesity (1,2,5) and some addressing MO (3,4). Authors continuously recommend not denying surgery to any patient on the basis of BMI (1,2,3,5). Infection rate is significantly higher for both obese and MO patients and sometimes there is a significant difference between MO and obese patients (4). The cost of treating the infection is a deciding factor for surgeons (4). Complications are higher for both MO and obese patients and sometimes MO patients have significantly higher complication rates than obese (4). Wound healing is not widely discussed in the literature (3,4). Revision rate is significantly higher for MO and obese patients compared to non-obese, but this depends on the reasons for revision included in the systematic review (2). Weight loss is recommended, however evidence is lacking for its need and effectiveness both pre and post-operatively (1,2,4,5). Clinical KSS outcomes in MO are significantly worse compared to obese patients (3), but not necessarily significantly different between obese and non-obese patients in hip and knee functional scores (1,2). Change in pre and post-operative values appears to me more indicative of a successful outcome for MO patients than post-operative measures alone. There are limitations to the current knee and hip clinical/functional scores in terms of their relevance for MO patients (4). There is little consistency in the ways authors measure or account for comorbidities in determining outcomes.

CONCLUSIONS

Although debate exists as to whether to operate on obese and MO patients, these patients demonstrate significant improvement between their pre- and post-operative scores and pain scores are similar to non-obese patients. Consistency is needed in the reporting of comorbidities in these studies. Infection risk and corresponding costs should be weighed against the outcomes gained for MO patients. Modified high BMI surgical protocols need to be developed to minimize infection risk and assist surgeons in these procedures.

ACKNOWLEDGEMENTS

None

REFERENCES

1. Haverkamp et al., *Acta Orthopaedica*. **82**(4),417–22, 2011.
2. Kerkhoffs et al., *The Journal of Arthroplasty*,**94**, 1839–1844, 2012.
3. McElroy et al., *The Journal of Knee Surgery*, **26**(2),83–8, 2013.
4. Samson et al., *ANZ Journal of Surgery*, **80**(9), 595–9, 2010.
5. Vincent et al., *Journal of Orthopaedic Surgery and Research*, **7**(1), 16, 2012.

INITIAL OUTCOMES OF DIRECT ANTERIOR- COMPARED TO POSTERIOR APPROACH FOR TOTAL HIP ARTHROPLASTY

[1]Mario Zotti, [2]Thomas Clifton, [3]Alexander Dodds, [4]Anthony Spriggins

[1,3,4] Sportsmed SA, Stepney
[1,2] Royal Adelaide Hospital
email: tclifton85@gmail.com

INTRODUCTION

The direct anterior approach (DAA) for total hip arthroplasty (THA) has been shown to decrease time to ambulation through minimally invasive and muscle sparing techniques, when compared to the traditional posterior method [1,2]. This paper aims to compare early outcomes and component position between approaches.

METHODS

A retrospective cohort study was conducted comparing posterior (N=34) and direct anterior (N=34) approaches to THA performed by a single arthroplasty surgeon. Perioperative complications such as blood loss, operative time and hospital stay were assessed using case notes.
Offset and component abduction angle were measured with digitalised callipers on radiographs. Functional outcomes were assessed using the Oxford Hip Scoring (OHS) system at the patients follow up appointments.

RESULTS AND DISCUSSION

All 68 patients completed their initial postoperative review and radiographs. There were no significant differences between the cohort demographics with respect to age or BMI.

The median follow-up time to assessment using OHS was 3 months for DAA and 4 months for posterior.

The DAA group had a reduced mean and median length of stay of 4.5 and 4 days (range 3-6) respectively compared to 5.7 and 5 days (range 5-11) for the posterior approach ($p<0.05$).

There was a significant reduction in the acetabular abduction angle in the DAA cohort with a mean of 39.1 and median 39.5 (range 24-50) compared to 44.1 and 44.2 (range 29-55) in the posterior cohort respectively ($p<0.05$). There was no significant difference in radiographically measured offset.

Transfusion rates were 34% compared with 41% for the DAA compared to Posterior approach with a mean of 0.97 units compared to 1.4 units of blood per patient in the cohort overall.

There was an 11 minute mean operative time difference (longer) for DAA compared posterior calculated from an aggregate of the last 5 patients of each cohort. Compared to the first 5 cases (127 minutes), the surgical time in the last 5 DAA cases was reduced by a mean of 20 minutes (107 minutes).

There was no significant difference in functional outcomes, though a trend to improved scores at early follow-up in DAA.

	DAA	POSTERIOR
MEDIAN	44	39.5
MEAN	41.4	35.7
Range	25-48	17-48
Mean follow up (years)	0.25	0.41
P	0.14	

Figure 1. Oxford scoring system

CONCLUSION

There was a significant reduction in length of hospital stay in the DAA cohort. There was a trend to reduced transfusion requirements as well as comparable offset in the DAA compared to posterior approach cohort. Comparable early functional scores were attained (see figure 1). Longer-term follow up of cup migration, polyethylene wear, and revision rates are required to assess component stability.

REFERENCES

1. Martin et al., *The Journal of Arthroplasty* **28** (2013) 849–854
2. Nakata et al., The Journal of Arthroplasty **Vol. 24** No. 5 2009

DAY 2

SESSION 1 – PhD AWARD

ROQUIN IS A NOVEL REGULATOR OF BONE HOMEOSTASIS

[1]Bay Sie LIM, [1]Jennifer TICKNER, [1]Shek Man (Jacky) CHIM, [2]Euphemie LANDAO, [2]Nathan PAVLOS, [1]Jiake XU
[1]School of Pathology and Laboratory Medicine, the University of Western Australia, WA
[2]School of Surgery, the University of Western Australia, WA
Email: 20594496@student.uwa.edu.au

INTRODUCTION

With the emerging field of osteoimmunology, many inflammatory diseases such as rheumatoid arthritis, periodontal disease, and spondyloarthritis, have highlighted the intimate relationship between the immune and skeletal system. This is inevitable as the bone organ system houses stem cells and is the major site of haematopoiesis. However, the underlying mechanism by which the immune system regulates bone homeostasis and vice versa remains to be elucidated.

To gain insights into the molecular genetics and mechanisms of osteoimmunology, we have employed a chemical (ENU) mutagenesis screen to identify novel regulators of bone homeostasis that interplay with the immune system. We identified the San Roque (san/san) mutant mouse line, which carries a M199R mutation in the Roquin (*Rc3h1*) gene. The mutation results in the dysregulation of follicular helper T cells (T_{FH}) and san/san mice display an autoimmune disease consistent to Systematic Lupus Erythematosus (SLE) [1].

METHODS

The bone phenotype of San Roque mutant mice and wild type littermate was assessed using X-ray, microCT and histomorphometry. *In vivo* calcein labelling was conducted to analyse the bone apposition rate. Flow cytometry analysis was performed to assess the population of osteoclast progenitors in bone marrow and T_{FH} in spleen. *In vitro* osteoclastogenesis, osteoblastogenesis and osteoclast-osteoblast co-culture were performed to assess the differentiation and functionality of bone cells. Cell signalling pathways and gene expressions of bone cells were analysed using Western Blotting and real-time Q-PCR respectively.

RESULTS AND DISCUSSION

Preliminary X-ray analysis revealed that san/san mice exhibit a lower bone density in comparison to WT littermates. MicroCT and histological analyses confirmed a low bone mass phenotype in san/san mice with a significantly reduced bone volume (BV/TV) as compared to WT littermates. Real-time PCR showed elevated expression of RANKL in whole bone isolated from san/san mice relative to WT mice. Flow cytometry analysis revealed that the increased RANKL expression was accompanied by a significant expansion of putative osteoclast progenitor populations in the san/san mice relative to WT mice. Consistent with the observed increase in progenitors, we also observed enhanced osteoclastogenesis and osteoclast activity from bone marrow macrophages (BMMs) derived from san/san mice, accompanied by enhanced RANKL-mediated MAPK signalling. *In vivo* bone calcein labelling showed a reduction in bone mineral apposition rate in the san/san mice indicating that osteoblast activity was also affected. In keeping with this phenotype, san/san calvarial-derived osteoblast cultures showed a reduction in bone nodule formation. Furthermore, co-culture experiments revealed that calvarial osteoblasts of san/san mice have a reduced ability to support osteoclastogenesis, suggesting an extrinsic contribution to the pre-priming effect of osteoclast progenitors within the bone marrow niche in san/san mice.

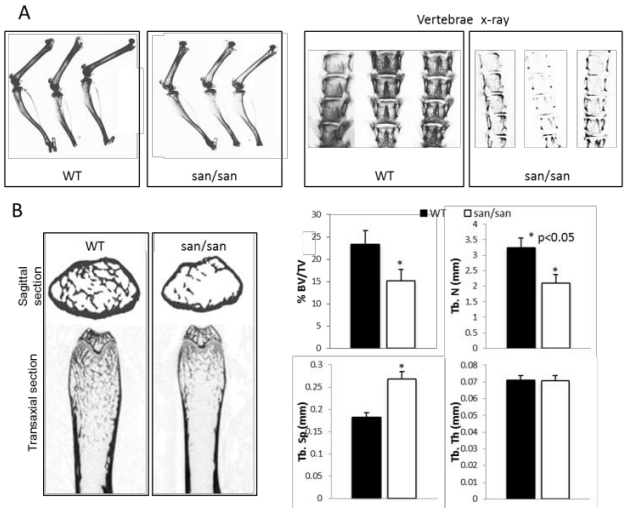

Figure 1: (A) X-ray and (B) microCT images of wild type (WT) and San Roque (san/san) mutant mice. San Roque mutant mice exhibit an osteoporotic phenotype in comparison to wild type littermates.

CONCLUSIONS

Taken together, our data documents that the Roquin gene is an important regulator of bone homeostasis. San Roque mouse emerges as a useful model to investigate the molecular genetics and mechanisms of bone loss, and osteoimmunology.

ACKNOWLEDGEMENTS

This project is supported by funds from the NHMRC. We are grateful for the technical assistance of the Centre for Microscopy, Characterization, and Analysis, UWA.

REFERENCES

1. Vinuesa, C.G., et al., A RING-type ubiquitin ligase family member required to repress follicular helper T cells and autoimmunity. *Nature*, 2005. **435**(7041): p. 452-8.

MECHANICAL PROPERTIES OF HUMAN CARTILAGE RANGING FROM HEALTHY TO OSTEOARTHRITIC

[1]Dale L. Robinson, [2]Mariana E. Kersh, [1,3]Nicole C. Walsh, [1]David C. Ackland, [4]Richard N. de Steiger R, [1]Marcus G. Pandy
[1]University of Melbourne, VIC, Australia, [2]University of Illinois at Urbana-Champaign, Illinois, USA,
[3]St Vincent's Institute of Medical Research, VIC, Australia, [4]Epworth Healthcare, VIC, Australia
email: d.robinson1@student.unimelb.edu.au

INTRODUCTION

A better understanding of how the mechanical properties of human articular cartilage are affected by osteoarthritis (OA) is essential for improving OA treatment. The microstructure of cartilage is comprised of a complex arrangement of macromolecules and solid/liquid phases. Consequently, its stiffness exhibits hyperelastic (strain dependent) behaviour and its volumetric properties, described by Poisson's ratio, vary spatially in all three directions [1]. How these material properties are altered by OA is not well understood. Therefore, the aims of this study were firstly, to measure the hyperelastic stiffness and Poisson's ratios of human articular cartilage under unconfined compression; and secondly, to describe how these parameters vary with the degree of OA pathology.

METHODS

Specimen preparation: Seventy-four osteochondral (cartilage+bone) cylindrical plugs (diam. ~5 mm) were harvested from the femoral condyles and tibial plateau of nine patients undergoing total knee arthroplasty (age 68.0±8.2 years) and from one cadaver specimen (63 year-old donor). From these plugs, an inner core (diam. 3.0 mm) was extracted for mechanical testing. Histological measurements were performed on the remaining outer ring to determine the severity of OA based on the OARSI scale [2].

Mechanical loading experiments: The cartilage-bone specimens were tested in unconfined compression using a custom-built electro-mechanical loading apparatus. The bone end of the plug was fixed to a loading platen and the articular surface was pressed against a glass plate lubricated with saline. Applied axial force and displacement were measured with a load cell and linear variable differential transformer, respectively. Axial loading was applied at a rate of 20% s^{-1} up to a compressive strain of 30% to simulate the strain rates incurred during normal walking [3]. An inverted microscope was positioned under the glass plate to record cartilage contact area as a function of time. A rotation table and camera positioned transverse to the cartilage were used to acquire cartilage geometry prior to testing.

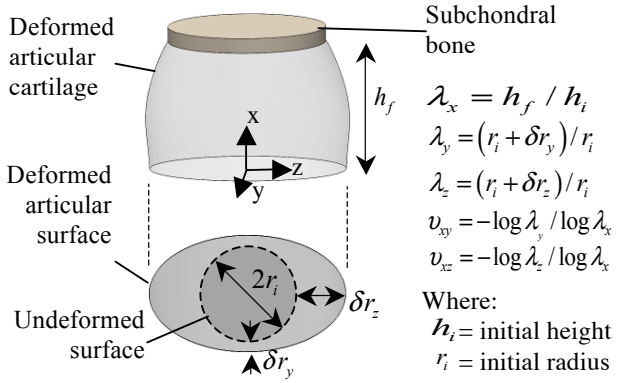

Figure 1: Deformed cartilage specimen and the equations used to calculate the Poisson's ratios, ν_{xy} and ν_{xz}.

Modelling and data analysis: The radial stretches on the articular surface (λ_y and λ_z) were calculated at 30% axial strain (λ_x = 0.7). From these data, the two orthogonal Poisson's ratios (ν_{xy}, and ν_{xz}) were calculated (Figure 1). Using the measured specimen geometry, specimen-specific finite element models were created. Cartilage was represented as a neo-Hookean incompressible, hyperelastic material [4]. In this model, the infinitesimal shear modulus (μ), which is a measure of stiffness, was determined iteratively to minimise the root mean square error between the measured and calculated axial force. A univariate linear correlation analysis was performed ($p<0.05$) to compare μ, ν_{xy} and ν_{xz} against OA grading.

RESULTS AND DISCUSSION

μ calculated across all samples was 5.42±2.65 MPa. This magnitude and range compared well with that measured for the hip joint (5.32±2.32 MPa, [4]). The Poisson's ratios calculated from the strains measured at the articular surface were ν_{xy} = 0.23±0.19 and ν_{xz} = 0.56±0.28. The ratio of these variables was 2.4, which is comparable to the value reported by Demarteau et al. [5]. All three variables correlated with OARSI grading (Table 1), indicating that cartilage mechanical properties were progressively altered by the presence of OA.

CONCLUSIONS

The results in this study indicate that the stiffness and volumetric properties of articular cartilage are altered by OA. We found that as the disease progressed, stiffness decreased, an effect that was also observed by Kleeman et al. [6]. This change would significantly affect the stress distribution through the tissue and underlying bone. The Poisson's ratios increased with the degree of OA, which increased the radial stretch at the articular surface, further altering the stress distribution. How these changes affect the functionality of the tissue remains unclear. However, they do suggest specific characteristics that ought to be restored (viz. the shear modulus and Poisson's ratios) when developing OA treatment methods.

Table 1: Correlation of μ, ν_{xy} and ν_{xz} with OARSI grading

	R (p-value)		
	μ (MPa)	ν_{xy}	ν_{xz}
OARSI Grading	-0.44 (<0.01)	0.40 (<0.01)	0.47 (<0.01)

REFERENCES

1. Wang, CC et al. *J Biomech*, **36**(3):339-53, 2003
2. Pritzker, KP et al. *Osteoarthr. Cartil* .**14**(1):13-29, 2006.
3. Bingham, J et al. *Rheumatology*, **47**(11):1622-27, 2008.
4. Henak, CR et al. *J Biomech Model Mechanobiol*, **13**(2):387-400, 2014
5. Demarteau, O et al. *Osteoarthr. Cartil* .**14**(6):589-96,2006
6. Kleeman, R et al. *Osteoarthr. Cartil* .**13**(11):958-63, 2005

MORC3 IS A NOVEL REGULATOR OF BONE HOMEOSTASIS

Gaurav Jadhav, Jennifer Tickner and Jiake Xu
School of Pathology and Laboratory Medicine, The University of Western Australia, WA
email: gaurav.jadhav@research.uwa.edu.au

INTRODUCTION

Osteoporosis contributes to the risk of bone fragility and fractures associated with long term disability and increased mortality rates. Identification of novel molecules that regulate bone homeostasis may lead us to a better treatment for osteoporosis. In the present study, a phenotype-driven N-ethyl-N-nitrosourea (ENU) mutant mouse screening approach was employed to identify an aberrant bone phenotype in a strain of (heterozygous) mutant mice. The mutation was uncovered as being within a splice donor site of intron 12 in *microorchidia 3* gene (Morc3). Morc3 is an epigenetic regulator of transcription and DNA damage response with previously unknown function in bone homeostasis [1].

METHODS

ENU-induced mutant mice were generated at the Australian Phenomics Facility at ANU. *In vivo* bone parameters were assessed by X-ray-based mammogram and microCT analysis using Skyscan 1176 instrument at 9um resolution. Bone histomorphometry analysis was performed using BioQUANT software according to standard methods. Osteoclastogenesis assays were performed using bone marrow precursors by the treatment of MCSF and Receptor Activator of NFκB Ligand (RANKL). Osteoblasts for *in vitro* analysis were generated from outgrowth cultures following enzymatic digestion of tibia and femora, and induced to differentiate and form mineralized nodules by addition of dexamethasone, beta-glycerophosphate and ascorbate.

RESULTS AND DISCUSSION

MicroCT analysis of 3 month old mutant mice femurs revealed significant thinning of the cortical bone, with significantly reduced cortical area and volume and cortical BMD (WT = 1.76 g/cm3 vs Mutant = 1.71 g/cm3, $p<0.05$). Histomorphometry analysis of WT and Morc3 mutant femurs indicated significantly reduced numbers and surface area of TRACP positive osteoclasts in the mutant. Subsequent analysis of osteoclasts derived from bone marrow monocytes *in vitro* revealed significant reductions in osteoclast formation and bone resorption. There was no detectable change in osteoblast bone nodule formation *in vitro*. Heterozygous mutant cells express Morc3 mRNA and 2 additional spliced variants which might lead to reduced levels of functional protein in mutant osteoclasts. Western Blot revealed upregulated Morc3 protein expression during osteoclast differentiation in WT but reduced Morc3 protein levels were observed in mutant osteoclasts. No difference in Morc3 protein levels were observed during osteoblast differentiation in osteoblasts from both WT and Morc3 mice. Analysis of short term signaling pathways induced by RANKL in mutant osteoclast progenitors showed discordance of MAPK signaling with significant reduction of phospho-p38, but an increase in ERK1/2 phosphorylation. Alkaline phosphatase levels were increased in mutant osteoblasts in vitro. Gene expression of osteoprotegerin (OPG) and RANKL were differentially upregulated during osteoblast differentiation such that the ratio of RANKL/OPG was reduced in Morc3 mutant total bone (flushed bone marrow) as compared to WT in accordance with observed reductions in osteoclast number. Of particular note, a remarkable increase in Stat1 protein was detected in mutant osteoclasts. Further experiments will assist in identifying whether Morc3 directly interacts with STAT1 or its upstream activator IFN β. Increased STAT1 at mRNA and protein levels in mutant osteoclasts, during differentiation, indicates a critical role of RANKL induced type I interferon-beta (IFN β) in osteoclast regulation [2].

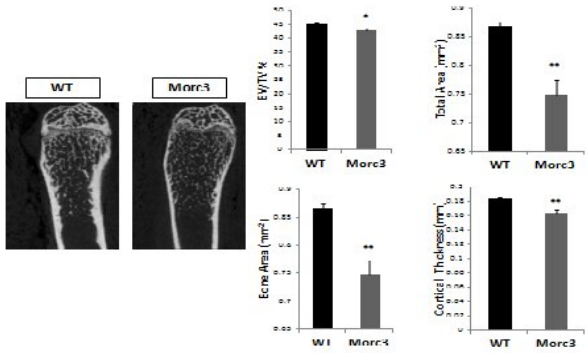

Figure 1: MicroCT analysis showing changes of cortical bone in Morc3 mutant mice femurs compared to WT mice.

CONCLUSIONS

Morc3 mutant mouse has reduced cortical bone, with reduced osteoclast formation and altered RANKL-induced signaling pathways. A significant reduction of phospho-p38 but an increase in ERK1/2 phosphorylation in RANKL induced signalling pathways in mutant osteoclast progenitors indicates differential roles of ERK and p38 MAP kinases in association with other transcription regulators like Morc3. Altogether our data suggest that Morc3 is a novel regulator of bone homeostasis.

REFERENCES

1. Li, D.Q., Nair, S.S., et al., *Epigenetics*.2013.
2. Takayanagi, H., et al., *Nature*. 2002.

FURIN IS AN IMPORTANT REGULATOR OF OSTEOCLASTIC BONE RESORPTION

[1]Benjamin Ng, [1]Dian Teguh, [2]John Creemers, [3]Nathan Pavlos, [1]Jennifer Tickner and [1]Jiake Xu

[1]School of Pathology and Laboratory Medicine, The University of Western Australia, WA
[2]Laboratory of Biochemical Neuroendocrinology, Centre for Human Genetics, KU Leuven, Belgium
[3]School of Surgery, The University of Western Australia, WA
email: ngw05@student.uwa.edu.au

INTRODUCTION

Furin, a member of the Proprotein Convertase family, processes multiple precursor proteins at basic residues and is vital for the maintenance of cellular homeostasis. The global deletion of furin leads to embryonic lethality precluding investigations of its role in postnatal bone. To address the physiological role of furin in osteoclast biology, we have investigated the role of conditional genetic ablation of furin in osteoclasts-mediated bone resorption.

METHODS

Mice with conditional genetic ablation of furin (cKO) were generated by crossing Cathepsin K-Cre knock-in mice with floxed furin transgenic mice. MicroCT scans were used to examine trabecular and cortical bone volume of femora bones. Decalcified femora were processed for histology assessment of osteoclast parameters. Furthermore, bone marrow cells were differentiated to osteoclasts and subjected to bone resorption and intracellular acidification assays.

RESULTS AND DISCUSSION

MicroCT analysis of 12 week old female mice revealed a significant increase in trabecular bone volume of cKO mice compared to floxed littermate controls (By 62%; $p<0.01$). Histomorphometric analysis revealed a trend of decrease in the number and surface area of osteoclasts in cKO mice *in vivo*. However, osteoclast formation and fusion was not significantly affected by furin deletion *in vitro*. In comparison, osteoclast bone resorptive function was significantly impaired from the lack of furin by reduced CTX (By 32%; $p<0.05$) and reduced bone resorption pit depth (By 51%; $p<0.01$). Consistent with the role of furin as the primary processing enzyme of the proton pump v-ATPase accessory subunit Ac45, the expression level of mature Ac45 protein was reduced in osteoclasts lacking furin. In line with the altered Ac45 maturation, intracellular acidification was also significantly impaired in furin deficient osteoclasts.

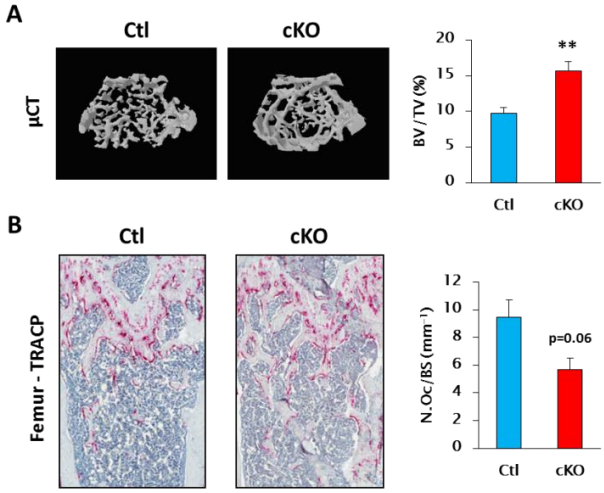

Figure 1: Conditional deletion of furin in osteoclasts results in increased trabecular bone volume (A), and a trend of decrease in osteoclast number *in vivo* (B).

CONCLUSIONS

Collectively, these data imply that furin functions as a positive regulator of osteoclastic bone resorption during bone homeostasis, in part through the proteolytic processing of the v-ATPase accessory subunit Ac45.

THE EFFECT OF CRYOTHERAPY ON THE VASCULAR REGENERATION FOLLOWING CLOSED SOFT TISSUE TRAUMA

[1]Zohreh Barani Lonbani, [1]Daniel Singh, [1]Tony Parker, [1,2]Michael Schuetz, [1]Mia Woodruff, [1]Jonathan Peake and [1]Roland Steck

[1] Institute of Health and Biomedical Innovation (IHBI), Queensland University of Technology (QUT), Brisbane, QLD
[2] Trauma Service, Princess Alexandra Hospital, Woolloongabba, Brisbane, QLD
Email: z.baranilonbani@qut.edu.au

INTRODUCTION

Icing (cryotherapy) is being widely used for the treatment of closed soft tissue trauma (CSTT), such as those resulting from sport injuries. It is believed that cryotherapy induces vasoconstriction and through this mechanism reduces inflammation [1]. However, the impact of this technique on the healing of impaired vasculature and muscle injuries following trauma remains controversial. Recent evidence suggests that the muscle regeneration is delayed after cryotherapy [2]. Consequently, we aimed to investigate the effect of cryotherapy on the vascular morphology following CSTT using an experimental model in rats by contrast-enhanced micro-CT imaging.

METHODS

Fifty four rats were divided into three main groups: control (no injury, n=6), sham (CSTT but no icing treatment, n=24) and icing (CSTT, treated with one session of ice block massaged directly on the injured muscle for 20 minutes, n=24). The CSTT was induced to the left thigh (Biceps Femoris) of anaesthetised rats (Male, Wistar) to create a standardized and reproducible vascular and muscle injury using an impact device [3]. Following trauma, animals were euthanized after 1, 3, 7, and 28 days healing time (n=6 for each time point). For a three-dimensional vascular morphological assessment, the blood vessels of euthanised rats were flushed with heparinised saline and then perfused with a radio-opaque contrast agent (Microfil, MV 122, Flowtech, USA) using an infusion pump. Both hind-limbs were dissected, and then the injured and non-injured limbs were imaged using a micro-CT scanner (µCT 40, Scanco Medical, Switzerland) and total volume of the perfused blood vessels (TVV) was calculated. More detailed morphological parameters such as vessel volume (VV), diameter (VD), spacing (VSp), number (VN) and connectivity (VConn) were quantified through high resolution (6 µm), micro-CT-scanned biopsy samples (diameter: 8mm) taken directly from the region of the injured muscles. The biopsies were then analysed histologically to confirm the results derived from contrast-enhanced micro-CT imaging.

RESULTS AND DISCUSSION

The TVV was significantly higher in the injured legs compared to the non-injured legs at day 1 and 7 in the sham group and at day 28 in both sham and icing groups. The biopsies from the injured legs of the icing group showed a significant reduction in VV, VN, VD, VConn and an increase in VSp compared to those in the sham and control groups at days 1, 3 and 7, post injury. While the injured legs of the sham group exhibited a decrease in VN and VConn 28 days post trauma, indicating a return to the original values prior to trauma, these parameters had increased in the icing group (Figure 1). Also, at day 1 post injury, VV and VD of the injured legs were significantly higher in the sham group compared to the icing group, which may be attributed to the effect of vasoconstriction induced by icing. Further histomorphological evaluation of day 1 post injury, indicated that although cryotherapy significantly reduced the injury size and influx of inflammatory cells, including macrophages and neutrophils, a delay in vascular and muscle fiber regeneration was found at later time points confirming other reports from the literature [2].

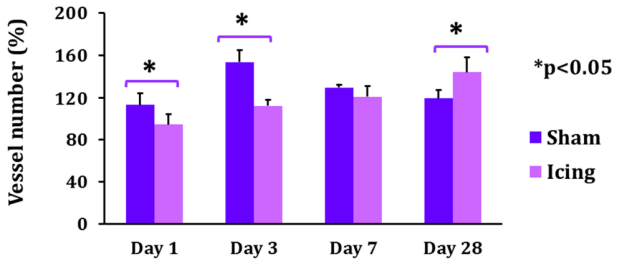

Figure 1: The average number of vessels per volume of the biopsies from the injured legs normalized to the contralateral non-injured legs (Mean±SD), indicating higher values for the sham group at early time points, and higher values for the icing group at the latest time point.

CONCLUSIONS

We have demonstrated using micro-CT imaging that the vascular morphology changes after CSTT, and that its recovery is affected by therapeutic modalities such as icing. This may be useful for the development of future clinical monitoring, diagnosis and treatment of CSTT. While icing reduces the swelling after trauma, our results suggest that it may delay the recovery of the vasculature in the injured tissue.

REFERENCES

1. Smith, *et al*. (1994), Pathophysiol., 1(4): 229-233
2. Takagi et al 2011 J Appl Physiol., 110: 382-8
3. Claes, L., *et al* (2006), J. Orthop. Res., 1178-1185

KEYNOTE 3 – Prof David Hunter

SUBCHONDRAL BONE IN OSTEOARTHRITIS AND THERAPEUTIC POTENTIAL

David Hunter

The University of Sydney

Osteoarthritis (OA) is at the forefront of an exploding epidemic of non-communicable chronic diseases. It is a condition of the whole joint – not just the cartilage – and it prominently affects the ligaments, tendons, synovium, muscle, fat and bone. As bone adapts to loads by remodelling to meet its mechanical demands, bone alterations likely play an important role in OA development. Changes in the periarticular bone in patients with OA include subchondral sclerosis, marginal osteophytosis, subchondral bone cysts, alterations in subchondral trabecular architecture, advancement of the tidemark and changes in the material properties of the subchondral bone.

Bone remodeling in the OA joint occurs preferentially in subchondral bone. A number of studies have demonstrated that bone volume fraction is increased in the subchondral bone of persons with osteoarthritis and tissue modulus decreased, which leads to reduced stiffness in the subchondral bone and, as a result, increased susceptibility to fatigue failure of the bone. Pathologically these local areas of increased remodelling have been termed bone marrow lesions which play a prominent role in symptom and disease genesis.

Understanding the pathophysiologic sequences and consequences of OA pathology will guide rational therapeutic targeting. Bone plays an incredibly important role in the etiopathogenesis of OA and its symptoms, and should be a more prominent target with regard to therapeutic developments. The above mechanisms provide a variety of potential therapeutic targets for and approaches to inhibiting subchondral bone alterations in OA.

Beyond the pharmacological and surgical advances, there are population-based interventions that are already proven effective for preventing the development of OA. These measures include lifestyle management, maintaining a healthy weight, remaining active, and avoiding joint injury. Modern health care systems are typically reactive and focused upon acute care whereas the management of OA is ideally efficient, coordinated and patient centred to support integration of evidence into practice. Inflation in the cost of health care is driving changes to health systems that will not only enhance the organizational costs of OA delivery but also health outcomes. Clinicians should pay greater heed to the benefits of weight management and exercise in the management of disease, which we are not currently doing very well.

SESSION 2 – ECR AWARD

ISOLATION OF OSTEOCYTES FROM HUMAN TRABECULAR BONE

[1]Matthew Prideaux, [1,2]Christine Schutz, [1]L. Bogdan Solomon, [2]David G. Campbell, [1]David M. Findlay and [1]Gerald J. Atkins
[1]Centre for Orthopaedic and Trauma Research, The University of Adelaide, Adelaide, SA, 5005
[2]Wakefield Orthopaedic Clinic, Adelaide, SA, 5000
email: matt.prideaux@adelaide.edu.au

INTRODUCTION

The importance of osteocytes in the regulation of bone homeostasis is becoming ever more apparent [1,2]. However, studying osteocytes is difficult due to their location deep within the mineralised bone matrix. Several murine osteocyte-like cell lines are available and techniques for isolating osteocytes from mouse bone have been described [3] but as of yet no such techniques have been documented for studying human derived osteocytes *in vitro*.

METHODS

We have developed a method for isolating osteocytes from trabecular bone taken from patients undergoing knee arthroplasty. Trabecular bone pieces were washed several times to remove marrow and subjected to sequential digestions in collagenase/EDTA. Cells were harvested after each digest and plated on collagen coated wells and cultured over a 5 day time course. Osteocyte marker gene expression was analysed by RT-PCR and cell morphology was demonstrated by phalloidin staining.

RESULTS AND DISCUSSION

Cells harvested from digests 1 and 2 expressed low levels of the osteocyte markers *SOST* and *DMP1*, with increased levels observed in digests 3 and 4. The highest levels of these markers were observed in digests 5 and 6, with a 20-fold increase in *DMP1* and a 9-fold increase in *SOST* mRNA compared to digest 1. *FGF23* mRNA expression was absent in the early digests but was observed from digest 3 onwards, increasing up to 150-fold in expression in digest 6. The osteocyte markers *PHEX* and *MEPE* were also expressed in the isolated cells and were increased in the later digests.

The cells isolated in digests 1 and 2 displayed a mixed morphology, with osteoblast-like cells and some dendritic osteocyte-like cells after 5 days of culture. Digests 3-6 contained many stellate, highly-dendritic cells, which were initially observed after 2 days of culture and increased in number and dendricity after 5 days (Figure 1).

Treatment of isolated cells from digests 3-6 with 50nM PTH or 10nM $1,25(OH)_2D_3$ for 24 hours resulted in the downregulation of *SOST* and upregulation of *FGF23* mRNA levels, respectively.

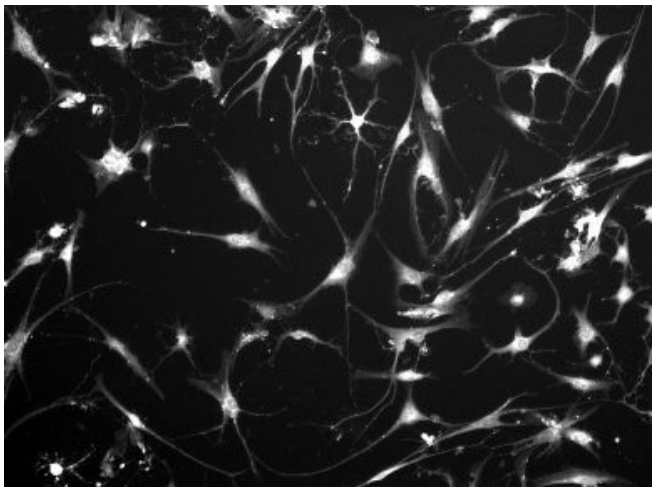

Figure 1: Typical morphology of isolated cells from digests 3-6 of human trabecular bone.

CONCLUSIONS

In conclusion, we have developed for the first time a reproducible method of isolating osteocytes from human bone. The isolated cells express osteocyte marker genes and display a dendritic osteocyte morphology. The cells also respond to anabolic hormones in similar manner to osteocytes *in vivo*. Such cells will be invaluable for furthering osteocyte research.

ACKNOWLEDGEMENTS

This study was funded by NHMRC Project Grant APP1047796.

REFERENCES

1. Atkins GJ and Findlay DM. *Osteoporosis Int*.**23(8)**:2067-2079, 2012.
2. Dallas SL, et al., *Endocrine Rev*.**34(5)**:658-690, 2013.
3. Stern AR, et al., *Biotechniques*.**52(6)**:361-373, 2012.

WEAR OF HIGHLY CROSS-LINKED POLYETHYLENE IN TOTAL HIP REPLACEMENT

Stuart Callary, Oksana Holubowycz, David Campbell, Lucian Bogdan Solomon, Donald Howie

Centre for Orthopaedic and Trauma Research, University of Adelaide,
Department of Orthopaedics and Trauma, Royal Adelaide Hospital and the, Adelaide, South Australia
email: stuart.callary@health.sa.gov.au

INTRODUCTION

Highly cross-linked polyethylene (XLPE) acetabular components were introduced to reduce wear in the late 1990's. XLPE liners are manufactured using a variety of methods that result in different amounts of cross-linking which may influence in vivo wear properties.

The improved wear properties of XLPE has encouraged the use of larger diameter articulations to address the most common cause of early revision surgery, dislocation.

Hence, the aim of this study was to measure the wear rate of XLPE liners using radiostereometric analysis (RSA) and investigate the influence of:

1. implant design/manufacturing method;
2. articulation size; and
3. patient variables including age

RSA is the most accurate method to measure wear in vivo. However, its use is limited due to the specialised knowledge, expensive equipment and prospective radiographic protocol required.

METHODS

Patient Cohorts

Six patient cohorts were prospectively enrolled into clinical wear studies at the Royal Adelaide Hospital, Wakefield Hospital and Repatriation Hospital in Adelaide, South Australia (Table 1). Each patient cohort used either a different design of XLPE liner, articulation size or patients with different age. Cohorts B and C were two arms of a randomised controlled trial investigating the effect of articulation size on wear.

Table 1: Patient Cohorts

#	XLPE TYPE	HEAD SIZE	AGE RANGE	FOLLOWUP (years)	PATIENT NUMBER
A	Marathon	28	55-80	0,0.5,1,2,6	26
B	Longevity	28	65-75	0,0.25,1,2,3,5	24
C	Longevity	36	65-75	0,0.25,1,2,3,5	21
D	Longevity	28	40-64	0,0.25,1,2,3,5	15
E	X3	32	47-76	0,0.5,1,2,5	19
F	X3	36+	55-76	0,0.5,1,2	15

Radiostereometric Analysis

All patients had tantalum markers (1.0mm diameter) inserted within the XLPE liner at the time of surgery. The total femoral head penetration was calculated using the 1 week radiograph as the reference examination. Wear rates were calculated after one year.

RESULTS AND DISCUSSION

The mean proximal bedding-in within the first year was higher for cohort A (Figure 1). The mean proximal wear rate was low for each cohort [1,2] and indicated XLPE manufacturing method did not influence the wear rate at two years (Figure 2). There was no difference in the wear rate of 28 and 36mm articulations in cohorts B and C.

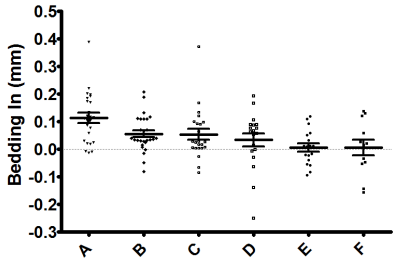

Figure 1: The mean proximal bedding-in (95%CI) within the first year for each cohort

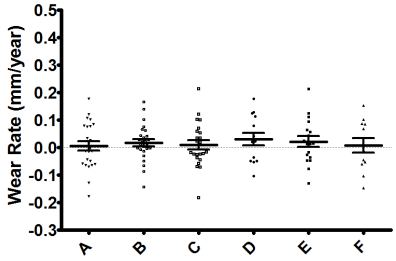

Figure 2: The mean proximal wear rate (95%CI) between one and two years for each cohort

CONCLUSIONS

This project used RSA to measure the wear of XLPE liners in 120 patients in six different cohorts. This is a significant contribution to the published literature in which only 207 patients have been reported to date, despite the widespread international use of these implants. The results to date suggest that the wear of XLPE is low. Manufacturing method and design may influence bedding-in within the first year but does not appear to influence wear between one and two years. This study indicated that articulation sized did not affect XLPE wear between one and two years.

ACKNOWLEDGEMENTS

Thank you to the Radiology Department, Royal Adelaide Hospital for supporting the RSA imaging service. Research funding was received to conduct this study from NHMRC, Zimmer, Stryker and DePuy.

REFERENCES

1. Callary et al., *Clin Orthop Rel Res* **471**:2238-44, 2013.
2. Callary et al., *Clin Orthop Rel Res* **471**:3596-00, 2013.

Conflict of Interest Declaration

In the interests of transparency and to help reviewers assess any potential bias, ANZORS requires authors of original research papers to declare any competing commercial interests in relation to the submitted work. Referees are also asked to indicate any potential conflict they might have reviewing a particular paper.

If you have accepted any support such as funds or materials, tangible or intangible, concerned with the research by the commercial party such as companies or investors, choose YES below, and state the relation between you and the commercial party.

If you have not accepted any support such as funds or materials, choose NO.

Do you have a conflict of interest to declare? (DELETE TEXT as appropriate)

YES

If YES, please complete as appropriate:

1. The author(s) did receive payments or other benefits or a commitment or agreement to provide such benefits from a commercial entity.
   State the relation between you and the commercial entity: **N/A**

2. A commercial entity paid or directed, or agreed to pay or direct, any benefits to any research fund, foundation, educational institution, or other charitable or nonprofit organization with which the authors are affiliated or associated.

   Research funding was received to conduct this study from the NHMRC, Zimmer, Stryker and DePuy.

BIOMECHANICAL EVALUATION OF A NOVEL SUTURE ANCHOR FOR ROTATOR CUFF REPAIR

[1,2,3]Claire Jones, [1,4]Andrew Morris, [2]William Robertson, [1]Stuart Callary and [1,4]Michael Sandow
[1]Centre for Orthopaedic & Trauma Research, School of Medicine, University of Adelaide, Adelaide, SA
[2]School of Mechanical Engineering, University of Adelaide, Adelaide, SA
[3]Adelaide Centre for Spinal Research, SA Pathology, Adelaide, SA
[4]Department of Orthopaedics & Trauma, Royal Adelaide Hospital, Adelaide, SA
email: claire.jones2@health.sa.gov.au

INTRODUCTION

Rotator cuff repair in the osteoporotic patient presents challenges [1]. Suture fixation using anchors or transosseous tunnels can fail due to poor bone quality. This study assessed the biomechanical performance of a novel suture anchor designed to achieve knotless transosseous fixation of rotator cuff repairs. The experimental anchor comprised a tapered plug and tapered shouldered hub made from medical-grade polyether ether ketone (PEEK), combined with Size 2 suture. Tests were performed on Prototype 1 (two plug types), leading to design changes instituted in Prototype 2 (Figure 1).

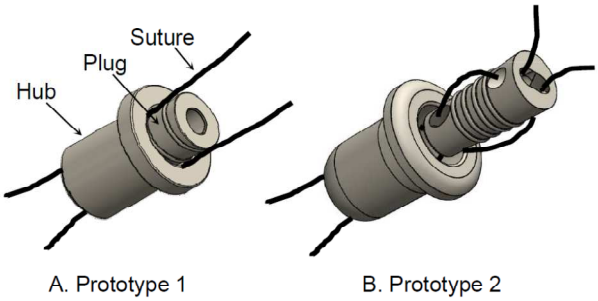

Figure 1: Diagrams of anchor hub and plug, with suture path.

METHODS

Custom fixtures and a materials testing machine (8874, Instron, Norwood, MA) were used to assess the biomechanical performance of anchor designs, suture types and dry/wet conditions. Anchor-suture constructs were tested to failure in two modes. *Suture pull-through*: the anchor-suture construct was assembled with a standardized plug locking force, beads were glued to the suture to track motion, the construct mounted in a custom fixture (Figure 2a) and a tensile load applied (1mm/s) to the suture loop. *Plug push-through*: the anchor-suture construct was mounted in the fixture (Figure 2b), and a compression load applied (1mm/s) to the plug with a custom pin. Peak load, mode of failure and suture stretch and slip was assessed.

RESULTS AND DISCUSSION

Suture pull-through: The mean ultimate load for Prototype 1 (across both plug types and three suture types, n=12) was 158.1 N (SD 48.0) and the predominant mode of failure was suture pulling through the hub-plug interface. Suture-guide fenestrations were added to the Prototype 2 plug to eliminate suture drift around the plug circumference and reduce ultimate load variability. Prototype 2 results are shown in Table 1.

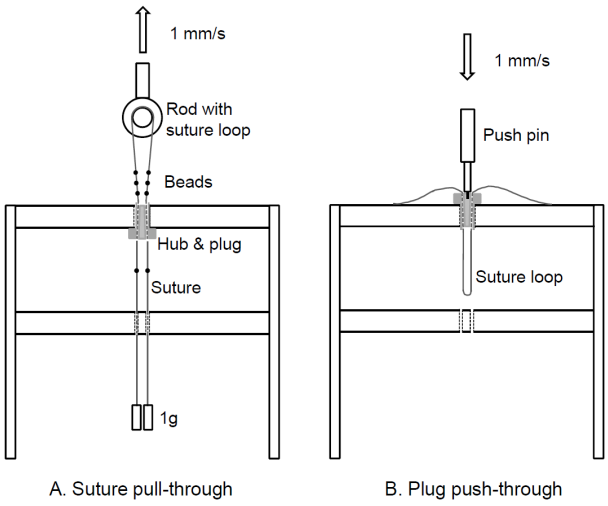

Figure 2: Anchor test configuration schematics (not to scale).

Table 1: Suture pull-through results, Prototype 2. Sutures: Maxbraid, Ethibond; Sawbones model ≈ osteoporotic bone.

Construct	n	Peak load (N) (mean±SD)
MaxBraid Dry	5	168.4±6.5
MaxBraid Wet	5	168.2±7.4
Ethibond Dry	5	137.9±2.5
MaxBraid Dry Sawbones	4	164.0±7.0

Plug push-through: The mean peak load (n=8) for Prototype 1 was 380.6 N (SD 53.1). The plug exited the hub without either component splitting. Tests are pending for Prototype 2.

CONCLUSIONS

Early results indicate the tapered hub and plug provide reproducible suture hold in wet/dry conditions, with different suture types and simulated osteoporotic bone, and peak loads similar to rotator cuff repair anchors in osteopenic bone [2].

ACKNOWLEDGEMENTS

Anchors provided by BiotechOrtho-Wright. Funding from Department of Orthopaedics & Trauma, RAH.

REFERENCES

1. Djahangiri A et al., *J Shoul Elbow Sur*. **22(1)**:45-51, 2012.
2. Pietschmann M et al., *Arch Ortho Tr Sur*. **129**:373-9, 2009.

CONFLICT OF INTEREST DECLARATION

In the interests of transparency and to help reviewers assess any potential bias, ANZORS requires authors of original research papers to declare any competing commercial interests in relation to the submitted work. Referees are also asked to indicate any potential conflict they might have reviewing a particular paper.

If you have accepted any support such as funds or materials, tangible or intangible, concerned with the research by the commercial party such as companies or investors, choose YES below, and state the relation between you and the commercial party.

If you have not accepted any support such as funds or materials, choose NO.

Do you have a conflict of interest to declare? (DELETE TEXT as appropriate)

YES

~~NO(DELETE all text below)~~

If YES, please complete as appropriate:

1. The author(s) did receive payments or other benefits or a commitment or agreement to provide such benefits from a commercial entity.

   State the relation between you and the commercial entity:

- CF Jones, A Morris and SA Callary have no conflicts to declare
- MJ Sandow (through a related entity) has a commercial interest in the experimental anchors (royalties)
- Experimental anchors were provided by BiotechOrtho-Wright. The company had no role in the design and execution of experiments, or the analysis and interpretation of data.

2. A commercial entity paid or directed, or agreed to pay or direct, any benefits to any research fund, foundation, educational institution, or other charitable or nonprofit organization with which the authors are affiliated or associated.
   N/A

ARE CHANGES IN KNEE BIOMECHANICS AND PHYSICAL ACTIVITY IN FREE LIVING CONDITIONS AFTER TOTAL KNEE ARTHROPLASTY RELATED? A STUDY COMBINING 3D GAIT ANALYSIS AND A HIGH RESOLUTION USE OF TIME RECALL INSTRUMENT

[1]John Arnold, Shylie Mackintosh[2], Timothy Olds[3], Sara Jones[2] and Dominic Thewlis[1,4]

[1]Biomechanics and Neuromotor Lab, Exercise for Health and Human Performance, University of South Australia, Adelaide, SA
[2]International Centre for Allied Health Evidence (iCAHE), School of Health Sciences, University of South Australia, Adelaide, SA
[3]Health and Use of Time (HUT) Group, Sansom Institute for Health Research, University of South Australia, Adelaide, SA
[4]Centre for Orthopaedic and Trauma Research, University of Adelaide, Adelaide, SA
email: john.arnold@mymail.unisa.edu.au

INTRODUCTION

Total knee arthroplasty (TKA) is an effective procedure for improving knee-specific and general physical function [1]. However, there is little information on whether changes in knee biomechanics after surgery measured in the laboratory are related to changes in use of time and physical activity in free-living conditions. The aim of this study was to explore the associations between changes in knee biomechanics during walking, use of time in free-living conditions and symptoms after TKA.

METHODS

Fifteen participants with knee osteoarthritis who underwent TKA were tested before and six months after surgery (6M:9F, mean age 67.8 years SD 10.4, height 1.64 m SD 0.1, body mass 85.4 kg SD 15.1, BMI 31.8 SD 5.5). Walking gait kinematics and kinetics were collected at self-selected speed with 12 cameras (VICON MX-F20, Vicon, UK) and two Kistler force platforms (9281B) at 100 Hz and 400 Hz respectively. Data were exported to Visual3D for processing (v 4.0, C-motion Inc., USA) (Figure 1). Joint angles were computed using the joint coordinate system method and external joint moments were computed using inverse dynamics (resolved in distal segment coordinate system).

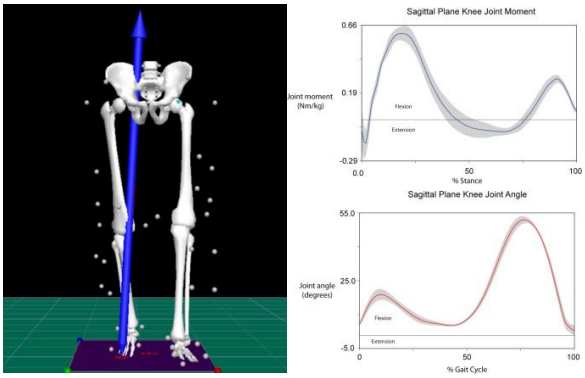

Figure 1. Knee joint kinematics and kinetics computed in Visual3D from gait data collected pre and postoperatively

Use of time data were collected for each participant using the Multimedia Activity Recall for Children and Adults (MARCA) [2]. The MARCA was administered by telephone interview to record each participant's activities over a 24 hour period on 4 days pre and postoperatively. Each activity in the MARCA is associated with an energy expenditure, so that an overall estimate of daily energy expenditure can be determined, as well as the time spent doing specific activities. Knee symptoms were documented with the Western Ontario & McMaster Universities Osteoarthritis Index (WOMAC). Relationships between changes in sagittal plane knee kinematics and external joint moments, use of time data from the MARCA and the WOMAC subscales were evaluated with Pearson's correlation coefficients.

RESULTS AND DISCUSSION

The change in sagittal plane knee range of motion (ROM) during walking was positively correlated with changes in time spent doing moderate to vigorous physical activity (MVPA) (r = 0.68, p = 0.005), inside chores (r = 0.59, p = 0.022), total daily energy expenditure (r = 0.66, p = 0.008) and time using passive transport (r = 0.66, p = 0.007). The change in peak knee flexion during swing phase was also positively correlated with change in time spent doing MVPA (r = 0.52, p = 0.047), inside chores (r = 0.52, p = 0.025) and time using passive transport (r = 0.53, p = 0.042). Changes in peak knee flexion and sagittal plane knee range of motion during loading response were positively correlated with the changes in the activities of daily living subscale (r = 0.62, p = 0.013 and r = 0.59, p = 0.021) and total WOMAC score (r = 0.61, p = 0.016 and r = 0.58, p = 0.024).

CONCLUSIONS

By combining gait analysis with a high resolution use of time instrument, this study demonstrated that improvements in knee ROM during walking measured in the laboratory are related to increases in physical activity and time spent travelling outside the home environment. Improvements in knee ROM were also related to improvements in symptoms. This underscores the importance of achieving a good functional knee ROM after TKA and provides objective evidence to support this common goal of surgery and rehabilitation for increasing post-operative physical activity.

REFERENCES

1.Ethgen, O., et al., JBJS (Am), 2004. **86**
2.Ridley, K et al. Int J Behav Nutr Phys Act, 2006. **3**(1)

DAY 3

KEYNOTE 4 – Dr Dan Barker

IS ACADEMIC ORTHOPAEDIC RESEARCH VALUED BY MEDICAL DEVICE COMPANIES?: AN EX-ACADEMIC COMMERCIAL RESEARCHER'S PERSPECTIVE

Dan Barker

Zimmer Asia-Pacific

The pressure for orthopaedic research departments to find alternative sources of funding and to commercialise research is increasing. This has led University researchers to further examine the relevance and value of their research to medical device companies. Many of the goals of orthopaedic research departments and medical device companies are aligned: advancing patient outcomes; assisting surgeons in providing better care; enhancing the performance and lifespan of implants; and solving clinically relevant problems. However, Universities have traditionally placed great importance on independence of research and the pursuit of solving problems in "pure science", whereas medical device companies have a commercial imperative and must be pragmatic in regards to research. This presentation will discuss key areas of interest for medical device companies with an emphasis on hip and knee arthroplasty. The relevance and value of current research activities in orthopaedic departments to industry will be discussed with a particular focus on predictive modelling related to implant design, longevity and clinical function

SESSION 1 – BONE BIOLOGY 2

IN SITU BONE FORMATION BY CONTROLLED RELEASE OF MAGNESIUM IONS

Yeung KWK[1,4], Wong HM[1,4], Zhao Y[1,3], Chu PK[2], Wu SL[5], Leung FKL[1,4], Luk KDK[1], Cheung KMC[1]

[1]*Department of Orthopaedics and Traumatology, The University of Hong Kong, Pokfulam, Hong Kong*
[2]*Department of Physics and Materials Science, City University of Hong Kong, Tat Chee Avenue, Kowloon, Hong Kong, China*
[3]*Center for Human Tissues and Organs Degeneration, Shenzhen Institutes of Advanced Technology, Chinese Academy of Sciences, Shenzhen 518055, China*
[4]*Shenzhen Key Laboratory for Innovative Technology in Orthopaedic Trauma, The University of Hong Kong Shenzhen Hospital, 1 Haiyuan 1st Road, Futian District, Shenzhen 518053, China*
[5]*Hubei Collaborative Innovation Center for Advanced Organic Chemical Materials, Ministry-of-Education Key Laboratory for the Green Preparation and Application of Functional Materials, Hubei Province Key Laboratory of Industrial Biotechnology, Faculty of Materials Science & Engineering, Hubei University, Wuhan, China*
email: wkkyeung@hku.hk

INTRODUCTION

Magnesium ions can affect many cellular functions including the transport of potassium and calcium ions, whilst it also modulates signal transduction, energy metabolism and cell proliferation [1]. It was recently reported that the presence of magnesium in the bone system is beneficial to bone growth and play a key role in bone remodeling and skeletal development [1-3]. In the present study, new bone substitutes containing surface treated magnesium micro-particles have been specifically designed in order to deliver proper amount of magnesium ions for stimulating *in vivo* bone formation.

METHODS

The bone substitutes were prepared by incorporating 9% TMSPM-treated Mg granules (i.e. 45μm & 150μm) into biodegradable polymer, polycaprolactone (PCL). The TMSPM silane-coupling agent treatment was used to protect the Mg particles from rapid degradation. Compression test was performed to study the mechanical properties of the bone substitute by using the MTS machine. A 7-day stimulated body fluid (SBF) immersion test was conducted to test their bioactivity. The surface composition was checked by energy dispersive x-ray spectroscopy (EDS) after immersion. The cytocompatibility and osteogenic differentiation properties of the bone substitutes were studied by MTT, ALP assays and qRT-PCR with the use of MC3T3-E1 pre-osteoblasts and human mesenchymal stem cells. Finally, the in vivo response of the bone substitutes was evaluated by using rat model of 2 months. Micro-CT was used to monitor the volume change of bone formation. Pure PCL was used as the control.

RESULTS AND DISCUSSION

The results of *in vitro* experiments demonstrated that the release of magnesium ions at 50-100 ppm/day could enhance the expression of early bone markers including alkaline phosphatase (ALP), osteopontin (OPN), runt-related transcription factor 2 (Runx2), collagen type I (Col1A1) and also the late bone marker, osteocalcin (OCN) as compared to the control (without additional Mg ions). Furthermore, magnesium ions were also able to induce ERK1/2 activation at post-culture 48 hours. With the use of the ERK1/2 inhibitor, the effect of magnesium ions on osteogenesis was attenuated. All these results suggested that specific amount of magnesium ions is participating in the bone formation process. Additionally, the effect of magnesium ions to osteoclastogenesis was studied as well. Our results proposed that same amount of magnesium ions could down-regulate the osteoclastogenic markers including macrophage colony-stimulating factor (c-fms), dendritic cell-specific transmembrane protein (DC-STAMP), interleukin 1, beta (IL-1) and receptor activator of nuclear factor-kappa B (RANK), indicating that the released magnesium ions was able to suppress osteoclasts differentiation. The volume of newly formed bone in the Mg-contained sample was found to be 80% higher than the control in rat animal model. However, bone resorption was found in the sample with high concentration of magnesium ions. Hopefully, hydrogen gas accumulation was not found in both treated and untreated samples. The compressive modulus of new bone substitutes generally maintained during the test. Although the literatures have proposed the growth and healing of bone with the presence of magnesium ions [4, 5], our results can successfully identify the particular concentration of Mg ions applied to stimulate bone formation and its mechanism.

CONCLUSIONS

The present results demonstrate that the concept of the use of magnesium ions to stimulate bone formation *in vivo* is promising.

ACKNOWLEDGEMENTS

This project is financially supported by RGC GRF (#718913), NSFC (#31370957) and the funding from Shenzhen Key Laboratory of Innovative Technology for Orthopaedic Trauma.

REFERENCES

1. Saris N, et al. Clinica Chimica Acta 2000;294(1-2):1-26.
2. Vormann J. Molecular Aspects of Med 2003;24:27-37.
3. Yoshizawa S, et al. Acta Biomater 2014 10(6):2834-2842.
4. Precival M. Applied Science and Nutrition 1999;5:1-5.
5.Bigi A et al. Acta Biomater 2010;6(6):1882-1894.

STRONTIUM PROMOTE THE OSTEOGENIC DIFFERENTIATION OF MSC THROUGH ATTENUATING THE CELL QUIENSENT AND ENHANCING ASYMMETRIC DIFFERENTIATION

[1]Xiaoli Zhao, [1]Jianhui Yue, [1,2]Di Liu, [1]Haobo Pan and [3]William W. Lu

[1]Institute of Biomedicine and Biotechnology, Shenzhen Institute of Advanced Technology, Chinese Academy of Science, Shenzhen, China
[2]Department of Pharmacology, Harbin Medical University, Harbin, China
[3]Department of Orthopaedic and Traumatology, The University of Hong Kong, HongKong, China
Email: zhaoxltju@gmail.com, wwlu@hku.hk

INTRODUCTION

Strontium ranelate has been shown to reduce the risk of vertebral fracture in postmenopausal women [1]. The beneficial effects of strontium on promoting bone formation are closely related to its capability to increase the osteogenic differentiation of mesenchymal stem cells [2,3]. However, the molecular mechanisms of strontium underlying such beneficial effects are still not fully understood. The aim of this study is to investigate the mechanism underlying the promoted effect of strontium in inducing osteogenic differentiation of mesenchymal stem cells in early stage.

METHODS

Human fetal BMSC is provided by Saiye Biotechnology Company Limited and characterized by multi-differentiation. Cells were cultured in control group (control), osteogenic group (Osteo) and strontium promoted osteogenic group (Osteo+Sr). The stemness, osteogenic and asymmetric differentiation related genes were analyzed by real-time quantitative PCR. The cell proliferation and cell cycle were analyzed through EdU and propidium iodide staining. The colony-forming unit osteoblasts (CFU-OB) was performed after 21 days by ARS staining.

RESULTS AND DISCUSSION

In the first week of hfBMSC culture, the genes related to stemness including *Oct4, Sox2, Nanog* and *Nestin* were continually expressed in control group. To the contrary, these stemness characters were gradually lost in the groups of performing osteogenic differentiation, especially for the strontium treated cells. Besides, the related osteoblastic genes such as *Osterix*, *OPN* and *BSP* were significantly enhanced in osteogenic induced group from day3. With the addition of Strontium, these genes were expressed in even higher level.

With the differentiation of MSC, the cell proliferation was reduced and more cells went into quiescent preparing for differentiation. With the addition of strontium, this effect was attenuated as showed in Figure 1. The genes of *Numb* and *Prospero* associated with asymmetric differentiation were observed promoted in strontium groups (Figure 2). In CFU-OB test, with the addition of strontium there was more osteoblast clones indicating the stronger osteogenic differentiation ability.

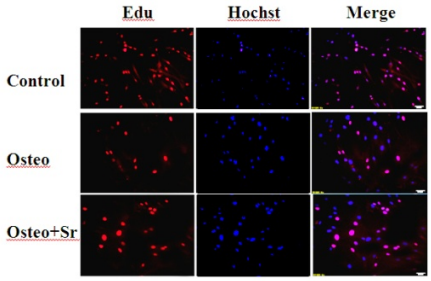

Figure 1: EdU staining for analyzing the proliferation of MSC the first day of osteogenic induction. Strontium attenuated the reduced effect on proliferation of osteogenic induction.

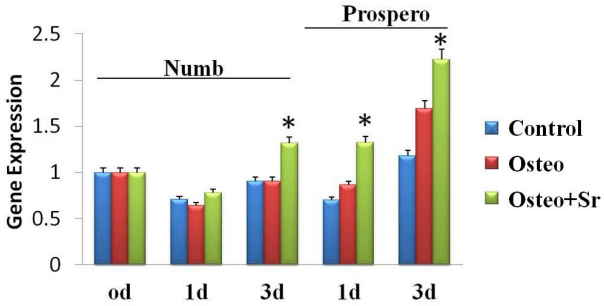

Figure 2: The genes of Numb and Prospero related to the asymmetric differentiation were enhanced by strontium.

CONCLUSIONS

During the osteogenic differentiation of hfBMSC, the promoting effect of strontium is related to its attenuate effect in quiescent of stem cell and the enhanced effect in asymmetric differentiation of stem cell in the early stage.

ACKNOWLEDGEMENTS

This study is supported by NSFC(No.81301567 and No.81270967), NSFGD (S2013040014820), the Shenzhen Peacock Program and Shenzhen Key Laboratory of Marine Biomaterials

REFERENCES

1. Seeman E, et al., *Bone*. **46**:1038-42, 2010.
2. Yang F, et al., *Stem Cells*.**29**:981-91, 2011.
3. Peng S, et al., *J Bone Miner Res*. **26**:1272-82,2011.

Examining the response of bone cells to infection following total hip replacement

Masakazu Kogawa, L. Bogdan Solomon, Caroline Moran, Renee T. Ormsby, David M. Findlay, Gerald J. Atkins
Centre for Orthopaedic and Trauma Research, University of Adelaide, Adelaide, SA
email: masa.kogawa@adelaide.edu.au

INTRODUCTION

Total hip replacement (THR) is a principal surgical procedure for patients with advanced osteoarthritis (OA). However, bacterial infection following surgery can result in prosthesis loosening and the need for revision surgery. Bacterial infections quickly activate innate immune responses, leading to local migration of polymorphonuclear and mononuclear leukocytes and the release of pro-inflammatory cytokines, some of which are known to stimulate osteoclast formation and activity. In addition, osteoblasts are known to be a significant line of defense against colonisation by bacteria and bacterial formation of biofilms. However, the effect of these infections on the osteocyte, which plays key roles in the regulation of physiological bone remodelling by controlling other cell types in bone,[1] and which are likely also to be involved in pathological bone loss, remains unclear. In this study, we have begun to address this.

METHODS

Bone samples were collected from age-matched patients undergoing either revision THR for infection-related prosthesis loosening (n = 7) or THR for primary OA (n = 18), with informed written patient consent. Small samples of bone were collected with a trephine needle from the acetabulum prior to reaming and from the iliac wing as a control. Bone samples were rinsed in PBS and homogenised in TRIzol reagent for the extraction of total RNA and the analysis of gene expression by real-time RT-PCR.

RESULTS AND DISCUSSION

Our preliminary analysis of these samples has revealed the acetabular bone of the infected group has significantly increased expression of the osteocyte-related gene *SOST* mRNA in comparison to the Primary OA group. This is consistent with our previous finding that pro-inflammatory cytokines TNF and TWEAK induced the expression of SOST/sclerostin in human osteoblasts, osteocyte-like cells and human bone samples cultured *ex vivo*.[2] We have also reported the sclerostin induces downstream catabolic effects on bone by actions on osteocyte-driven osteoclastogenesis[3] and osteocytic osteolysis.[4] The expression of sclerostin in bone is also known to reflect local strain perceived by osteocytes. Consistent with this, in the primary OA group, the expression of *SOST mRNA* from the acetublum was significantly lower than that of the iliac wing, but this relationship did not exist in the infected group. These results suggest that in the situation of infection, sclerostin may play a role in implant loosening.

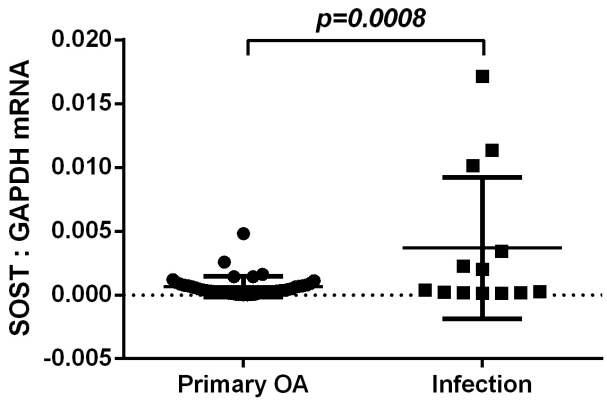

Figure 1: *SOST* mRNA expression in acetabular bone biopsies from patients undergoing THR for either primary OA or revision THR for infection-related implant loosening.

ACKNOWLEDGEMENTS

This study was funded by NHMRC Project Grant APP1004871.

REFERENCES

[1] G.J. Atkins, D.M. Findlay, Osteocyte regulation of bone mineral: a little give and take, Osteoporosis International 23(8) (2012) 2067-2079.

[2] C. Vincent, et al., Pro-inflammatory cytokines TNF-related weak inducer of apoptosis (TWEAK) and TNFalpha induce the mitogen-activated protein kinase (MAPK)-dependent expression of sclerostin in human osteoblasts, Journal of Bone and Mineral Research 24(8) (2009) 1434-1449.

[3] A.R. Wijenayaka, et al., Sclerostin Stimulates Osteocyte Support of Osteoclast Activity by a RANKL-Dependent Pathway, PloS One 6(10) (2011) e25900.

[4] M. Kogawa and A.R. Wijenayaka, et al., Sclerostin Regulates Release of Bone Mineral by Osteocytes by Induction of Carbonic Anhydrase 2, Journal of Bone and Mineral Research 28(12) (2013) 2436-2448.

EVIDENCE THAT METAL WEAR PARTICLES EXERT A PRO-OSTEOCLASTOGENIC EFFECT ON OSTEOCYTES.

[1]Renee T Ormsby, [2]Tania N Crotti, [2]David R Haynes, [1]David M Findlay and [1]Gerald J Atkins

[1]Bone Cell Biology Group, Centre for Orthopaedic & Trauma Research, and [2]Discipline of Anatomy and Pathology, The University of Adelaide, North Terrace, Adelaide, South Australia 5005, Australia
email: renee.ormsby@adelaide.edu.au

INTRODUCTION

Aseptic loosening of orthopaedic implants following total hip replacement (THR) has been associated with the induction of osteoclastogenesis. The production of metal ions caused by metal on metal wear causes stimulation of specific genes associated with osteoclastogenesis inducing resorption around implants causing loosening. Osteocytes have been shown to have a central role in mediating osteoclastogenesis.[1, 2] It is therefore likely they play a role in the response to metal particle wear. Our aim was to analyse the short-term response of mouse and human osteocyte-like cells exposed to metal wear particles *in vitro*.

METHODS

Mouse and human osteocyte like cell lines were treated with varying concentrations of Titanium Aluminium wear particles and Cobalt Chrome wear particles for 48 hours. Human trabecular bone derived osteoblasts (NHBC) were cultured for 28 days prior to treatment, which we have shown induces a mature osteocyte-like phenotype. The mouse osteoblastic cell line IDG-SW3, which differentiates to a mature osteocyte stage cells was also cultured for 28 days under mineralising conditions. RNA was extracted and used for the analysis of gene expression using real time RT-PCR.

RESULTS AND DISCUSSION

Similar to our previous findings with polyethylene wear particles[3], metal particles showed evidence of promoting a pro-osteoclastogenic phenotype in osteocytes, evidenced by the induction of a high *RANKL*:*OPG* mRNA expression ratio in human primary osteocyte-like cells and differentiated mouse IDG-SW3 cells. Furthermore, the mRNA expression of genes associated with osteocytic osteolysis (*CA2*, *CTSK*, *MMP13*)[4] increased in both cell types. *SOST* mRNA expression was also increased. We have reported that the protein product of *SOST*, sclerostin promotes osteoclastogenesis by induces the expression of *RANKL* in mature human osteocyte-like cells *in vitro*.[2]

CONCLUSION

Osteocytes exposed to metal particles showed increased expression of genes associated with osteoclastogenesis and osteocytic osteolysis, identifying osteocytes as potentially important regulators of bone turnover in peri-prosthetic loosening.

ACKNOWLEDGEMENTS

This study was funded by NHMRC Project Grant APP1041456.

REFERENCES

[1] G.J. Atkins, D.M. Findlay, Osteocyte regulation of bone mineral: a little give and take, Osteoporosis International 23(8) (2012) 2067-2079.

[2] A.R. Wijenayaka, M. Kogawa, H.P. Lim, L.F. Bonewald, D.M. Findlay, G.J. Atkins, Sclerostin Stimulates Osteocyte Support of Osteoclast Activity by a RANKL-Dependent Pathway, PloS one 6(10) (2011) e25900.

[3] G.J. Atkins, K.J. Welldon, C.A. Holding, D.R. Haynes, D.W. Howie, D.M. Findlay, The induction of a catabolic phenotype in human primary osteoblasts and osteocytes by polyethylene particles, Biomaterials 30(22) (2009) 3672-3681.

[4] M. Kogawa, A.R. Wijenayaka, R.T. Ormsby, G.P. Thomas, P.H. Anderson, L.F. Bonewald, D.M. Findlay, G.J. Atkins, Sclerostin Regulates Release of Bone Mineral by Osteocytes by Induction of Carbonic Anhydrase 2, Journal of Bone and Mineral Research 28(12) (2013) 2436-2448.

Decreased number of proliferating chondrocytes and delayed hypertrophy in Mucopolysaccharidosis VII growth plate

[1]Zhirui Jiang, [2]Clare Reichstein, [2,3]Ainslie L.K. Derrick-Roberts, [1,2,3]Sharon Byers
[1]Department of Genetics, School of molecular and Biomedical Science, The University of Adelaide, Adelaide, SA
[2]Department of Paediatrics, The University of Adelaide, Adelaide, SA
[3]Genetics and Molecular Pathology, SA Pathology (CYWHS Site), Adelaide, SA
Email: zhirui.jiang@student.adelaide.edu.au

INTRODUCTION

Short stature is a common feature in 6 of 11 types of mucopolysaccharidosis (MPS), a group of inherited lysosomal storage disorders [1]. The impaired bone growth may be attributed to accumulation of glycosaminoglycans (GAGs) that disrupts growth plate function and endochondral ossification (EO), which are regulated by complex signalling pathways. The key transition steps in EO are (i) the initiation of proliferation (ii) cessation of proliferation accompanied by cell hypertrophy and (iii) blood vessel invasion preceding bone deposition. Athough EO in normal growth plate is well characterized; the mechanism behind the dysfunction of growth plate in MPS is not fully understood. In the current study, we aim to understand the time course and pathogenesis of bone shortening and growth plate dysfunction using the naturally occurring $GUS^{mps/mps}$ (MPS VII) mouse model.

METHODS

Normal and MPS VII femurs harvested from 14 days to 7 months mice were X-rayed and the femur lengths were measured. Growth plate heights of resting, proliferative and hypertrophic zones were assessed and cell numbers in those three zones were counted using stained sections of proximal tibia growth plates of both normal and affected MPS VII mice. Chondrocyte sizes in the resting and hypertrophic zones were also evaluated. Quantitative real-time RT-PCR of apoptosis genes was performed using cDNA reverse transcribed from RNA isolated from total growth plate.

RESULTS AND DISCUSSION

Results showed that MPS VII mice have remarkably shortened bones, reaching only 70% of the normal femur length at maturity. The height of the resting zone was increased in MPS VII compared to normal while cell number and size increased. The height of the proliferative zone was unchanged from normal but the number of proliferating chondrocytes declined in MPS VII. Similar to the observations in the resting zone, the hypertrophic zone height increased in MPS VII compared to normal while cell number decreased. Elevation of the apoptosis inducer gene (caspase3) expression was observed in whole MPS VII growth plate, suggesting apoptosis may play a role in determining cell numbers in the different zones of the MPS growth plate.

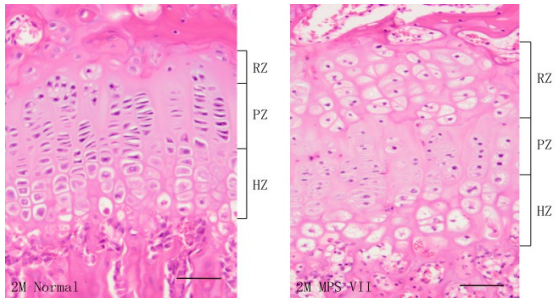

Figure 1: A haematoxylin and eosin stained normal and MPS VII growth plate isolated from 2 months mouse. RZ =resting zone; PZ=proliferating zone; and HZ= hypertrophic zone. 10x magnification, scale bar= 50µm.

CONCLUSIONS

Together the findings indicate a delay in the transition of chondrocytes to the proliferative state as well as a delay in the onset of hypertrophy, which could ultimately lead to shortened bones.

REFERENCES

1. Neufeld EF & Muenzer, *The metabolic and molecular bases of inherited disease*, McGraw hill, New York, 2001

Table 1: Comparison of growth plate histomorphometry in 2 month MPS VII mice to normal mice.

Growth plate	Zone height (µm)		Cell number (cells/mm^2)		Cell size (µm)		Cell density (% of total zone area)	
Phenotype	Normal	MPS VII	Normal	MPS VII	Normal	MPS VII	Normal	MPS VII
RZ	29.4 ± 3.6	90.1±9.2*	1893 ± 187	2471±118*	7.6 ± 0.4	15.3 ±1.2*	18.2 ±1.5	37.0±1.8*
PZ	72.7 ± 3.9	83.6±4.8	4727 ± 228	3213±138*	6.6±0.5	8.2±0.6	29.0±1.6	28.0±1.5
HZ	72.9 ± 4.1	141.3±12.5*	2933 ± 139	2152±85*	14.8 ± 1.1	20.8 ±2.0*	56.2 ±2.1	58.9±1.9

RZ= resting zone; PZ= proliferating zone; and HZ= hypertrophic zone
* represents significant difference ($p<0.05$) of MPS VII from normal, Student's t-test

HDAC-1 IS HIGHLY EXPRESSED AT SITES OF PERI-PROSTHETIC OSTEOLYSIS AND ITS INHIBITION SUPPRESSES OSTEOCLAST ACTIVITY *IN VITRO*

[1]Kent Algate, [1]Emma Murison, [1]Melissa Cantley, [2]David Fairlie, and [1]David Haynes

[1]School of Medical Sciences, University of Adelaide, Adelaide, SA, Australia
[2]Institute of Molecular Bioscience, University of Queensland, Brisbane, Qld, Australia

INTRODUCTION

Joint replacement is a successful procedure that keeps patients in a pain-free mobile state. However, many implants fail prematurely, often due to particle induced osteolysis causing loosening of the prosthesis [1]. The aggressive inflammatory reaction to particles of prosthetic material activate bone resorbing osteoclasts. As a result patients require costly revision surgery.

Recent studies investigating the epigenetic control of bone metabolism have identified Histone Deacetylases (HDACs) as potential targets to reduce excessive OC resorption. HDAC inhibitors (HDACi) have been previously shown to suppress osteoclast mediated bone resorption *in vitro* and *in vivo* [2, 3]. Research is progressing to identify and target specific HDACs involved in disease.

Unpublished observations from our laboratory have identified an increase in HDAC-1 in several bone loss pathologies. In addition, we have shown that TNFα is elevated near sites of osteolysis [4]. Therefore, the aim of this study was to investigate HDAC-1 expression in human peri-prosthetic osteolytic tissue and to determine the effect of a HDAC-1 inhibitor *in vitro* osteoclast assay stimulated with TNFα.

METHODS

Immunohistochemistry and semi-quantitative assessment (SQA) of peri-implant and osteoarthritis (OA) tissues was carried out as previously described [4] using HDAC-1 antibody (ab53091; Abcam Inc). *In vitro* assays of osteoclasts derived from human blood obtained from the Australian Red Cross were used to investigate the effects of a novel HDAC-1 inhibitor, NW-21 (20nM; University of Queensland), on TNFα stimulated OC cells. Effects of NW-21 on formation, activity, and OC related mRNA gene expression (TRAF-6) was assessed by TRAP staining, formation of resorption pits formed on dentine, and RNA extraction and qPCR.

RESULTS AND DISCUSSION

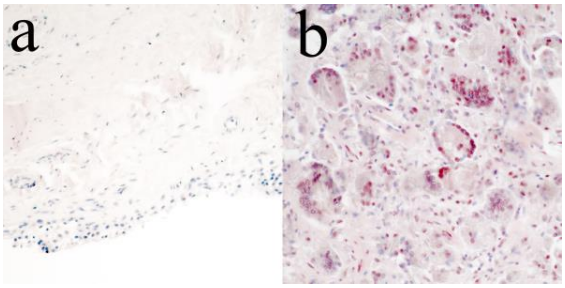

Figure 1: Immunostaining for HDAC-1 (20µg/ml) (red) of (A) control osteoarthritis and (B) revision tissue.

HDAC-1 protein expression was significantly up regulated in revision tissue (SQA = 2.9±0.2, n=12) compared to OA controls (SQA = 0.1±0.1, n=10) ($p<0.0001$) (Figure 1). Staining was particularly evident in the nuclei of the large multinucleated OC-like cells.

Suppression of HDAC-1 *in vitro* inhibited OC formation and resorption ($p<0.005$; Figure 2). Interestingly cells grown in the presence of TNFα were more susceptible to NW-21, as commencing treatment from day 7 and/or 10 effectively inhibited OC as opposed to only day 7 treatment being effective in OC (-TNFα).

qPCR analysis revealed an increase in HDAC-1 mRNA ($p<0.05$) after 4 days of culture with TNFα and a decrease in key OC signalling gene TRAF-6 ($p<0.05$). No Further reduction of these were identified post NW-21 treatment.

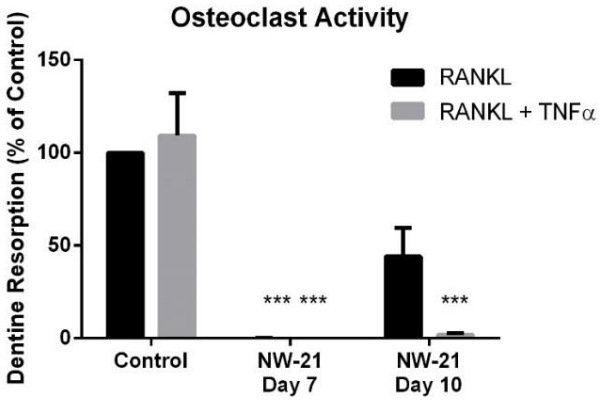

Figure 2: The effects of inhibiting HDAC-1 (NW-21; 20nM) on osteoclast bone resorption commencing treatment from day 7 or day 10 (+/- TNFα; 10ng/ml) (Mean + SEM) ***$p<0.001$.

CONCLUSIONS

These results show that HDAC-1 has an important role in the formation and activity of human OC exposed to TNFα. In addition, the data indicates that inflammatory stimulated osteolysis, such as that seen in peri-implant osteolysis, may be particularly sensitive to HDAC-1 inhibition.

REFERENCES

1. Graves SE. *Med J. Aust*. **180**: 31-34.
2. Cantley M. *J. of Cell Physiology*. **226**: 3233-3241, 2011
3. Cantley M. *J of Periodontal Res*. **46**: 697-703.
4. Holding C. *Biomaterials*. **27**: 5212-5219, 2006.

CAFFEIC ACID PHENETHYL ESTER ABROGATES BONE RESORPTION IN A MURINE CALVARIAL MODEL OF POLYETHYLENE PARTICLE-INDUCED PERI-PROSTHETIC OSTEOLYSIS

[1,2]M Zawawi,[3]E Perilli, [4]V Marino, [1]M Cantley,[5]J Xu, [1]A Dharmapatni, [1]D Haynes and [1]T Crotti

[1]School of Medical Sciences, The University of Adelaide, SA. [2]School of Medical Sciences, Universiti Sains Malaysia (USM).[3]School ofComputer Science, Engineering and Mathematics, Flinders University, SA.[4]School of Dentistry, The University of Adelaide, SA. [5]School of Pathology and Laboratory Medicine, The University of Western Australia, WA.
Email: muhamad.zawawi@adelaide.edu.au

INTRODUCTION

Prosthetic wear particle-induced bone loss by osteoclasts is a common cause of aseptic loosening around implants. Caffeic acid phenethyl ester (CAPE) has been shown as a potent and specific inhibitor of NFATc1 and NF-κβ [1,2]. CAPE inhibits osteoclastogenesis and induces apoptosis *in vitro*[3]. The current study aims to determine whether CAPE reduces bone resorption in a murine calvarial model of polyethylene (PE) particle-induced osteolysis.

METHODS

22 mice were randomly divided into 3 groups; Control (no disease and no CAPE treatment, n=7), 'PE only' (disease, n=7) and 'PE+CAPE' (disease and treated with CAPE, n=8). Six to seven days prior to administration of particles mice were scanned using the live-animal micro-computed tomography (μCT) scanner (Skyscan 1076 High Resolution *in vivo* Scanner; Skyscan, Kontich, Belgium) as a baseline measurement. At day 0, the periosteum of the mice calvariae was lightly scratched and implanted with either PBS with 1% normal mouse serum (NMS) (Control) or PE particles at concentration of 2.82×10^9 particles/mL in PBS with 1% NMS (PE only, and PE+CAPE). Mice were treated with 1mg/kg/day CAPE at days 0, 4, 7 and 10 by subcutaneous injection adjacent to the implant location (PE+CAPE). Following sacrifice at day 14, bone resorption was assessed by *ex vivo*μCT and ELISA of CTX-1 serum (RatLaps, Nordic). Serum levels of Osteoclast Associated Receptor (OSCAR) were measured by commercial ELISA (Cusabio). A rectangular region of interest (ROI) was generated for all scans to determine percentage area of bone surface resorption, and bone volume (BV) change. Statistical significance ($p<0.05$) between all groups was determined by a Kruskal-Wallis test followed by a Mann-Whitney test comparing between two particular groups.

RESULTS AND DISCUSSION

The μCT analysis showed all groups of mice had increased BV overtime as expected with normal growth. PE particles significantly induced bone loss compared to the control. The three-dimensional image at day 14 (data not shown) showed the presence of pits on the calvariae adjacent to the implanted PE consistent with a significant increase of the percentage resorbed area (Fig. 1A), a significant reduction of BV (Fig. 1B) and a significant increase of the serum CTX-1 level (Fig. 1C). Serum OSCAR levels were also significantly increased in animals given PE particles. The mice in 'PE+CAPE' group were treated with CAPE to determine its effectiveness as a treatment for peri-prosthetic osteolysis. When compared to the non-treated animals given PE particles, CAPE significantly inhibited bone loss as evident by a significant reduction of surface bone resorption (Fig. 1A) and a significant increase in BV (Fig. 1B). Serum CTX-1 and serum OSCAR levels in the PE groups were not significantly affected by the CAPE treatment (Fig. 1C and 1D).

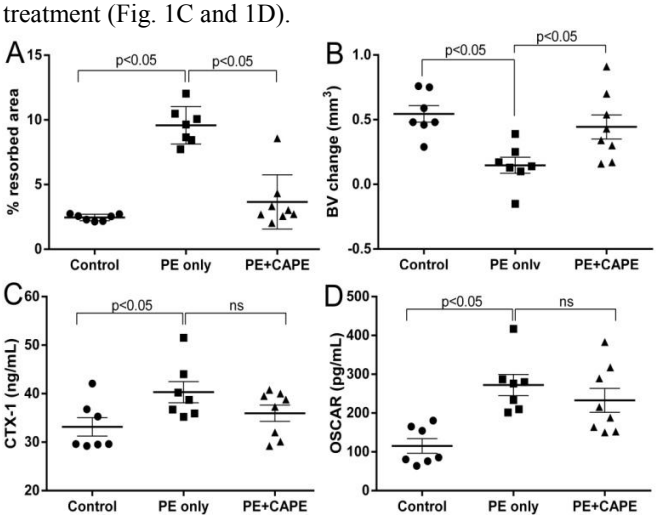

Figure 1:μCT analyses of A) Percentage resorbed area on the combined outer and inner surfaces of calvariae and B) Bone volume change. ELISA analyses of C) Serum CTX-1 and D) Serum soluble OSCAR. Data was presented as mean±standard error of the mean.

CONCLUSIONS

PE particles significantly induced localized bone loss.CAPE at 1mg/kg/day significantly inhibited bone loss in the murine calvarial model of PE particle-induced osteolysis as evident by the bone surface resorption and local bone volume change.

ACKNOWLEDGEMENTS

The work has been supported by a New Appointment Grant, Faculty of Health Sciences, University of Adelaide. Malaysian government (USM) provided support for MZ.

REFERENCES

1. Natarajan K, et al., *Immunology*. 1996.
2. Marquez N, et al., *J Pharm & Exp Therapeutics*.2003.
3. Ang E, et al., *J Cellular Physiology*. 2009.

EGFL7 IS EXPRESSED IN BONE MICROENVIRONMENT AND PROMOTES ANGIOGENESIS VIA ERK, STAT3 AND INTEGRIN SIGNALING CASCADES

[1]Vincent Kuek, [1]Shek Man Chim, [1]Siu To Chow, [1]Bay Sie Lim, [1]Jennifer Tickner, [2]Jinmin Zhao, [3]Rosa Chung, [3]Yu-Wen Su, [4]Ge Zhang, [1]Wendy Erber, [3]Cory J Xian, [5]Vicki Rosen, [1]Jiake Xu

[1]School of Pathology and Laboratory Medicine, University of Western Australia, WA
[2]Research Centre for Regenerative Medicine, Department of Orthopaedic Surgery, The first Affiliated Hospital of Guangxi Medical University, Guangxi
[3]Sansom Institute for Health Research, School of Pharmacy and Medical Sciences, University of South Australia, Adelaide
[4]Institute for Advancing Translational Medicine in Bone & Joint Diseases, School of Chinese Medicine, Hong Kong Baptist University, Hong Kong
[5]Developmental Biology, Harvard School of Dental Medicine, Boston, MA
email: jiake.xu@uwa.edu.au

INTRODUCTION

Angiogenesis plays a pivotal role in bone formation, remodeling and fracture healing. The regulation of angiogenesis in bone microenvironment is highly complex and orchestrated by intercellular communication between bone cells and endothelial cells via production of angiogenic factors. Here, we identified several EGF-like family members are differentially expressed in osteoclasts and osteoblasts which could potentially regulate bone angiogenesis. In particular, we are interested in EGFL7, which has been implicated in regulating tubulogenesis [1] during embryogenesis and hepatocellular carcinoma cell motility [2]. However, the role of EGFL7 in bone microenvironment is unknown. In this study, we aimed to establish the role of EGFL7 in regulating endothelial cell activities, angiogenesis and the signaling pathways involved in EGFL7-induced endothelial cell activities.

METHODS

In this study, we performed RT-PCR analysis to investigate the EGFL7 expression in both osteoclasts and osteoblasts during differentiation. We then produced conditioned medium containing EGFL7 and performed scratch-wound healing assay and tube formation assay to examine the effect of EGFL7 on SVEC (SV40-immortalised murine endothelial cells). In addition, we performed Western blot to investigate the potential signaling pathways of EGFL7-induced endothelial cell activities. Furthermore, we examined the angiogenic activities of EGFL7 using mouse fetal metatarsal angiogenesis assay. Finally, we used qPCR to examine the expression of EGFL7 during growth plate injury repair in rats.

RESULTS AND DISCUSSION

RT-PCR revealed that EGFL7 is expressed in osteoclasts and osteoblasts during differentiation. Addition of exogenous recombinant EGFL7 potentiates SVEC cell migration and tube-like structure formation *in vitro*. Moreover, recombinant EGFL7 promotes angiogenesis by inducing blood vessel growth featuring web-like structure in an *ex vivo* fetal mouse metatarsal angiogenesis assay. EGFL7 induced phosphorylation of extracellular signal-regulated kinase 1/2 (ERK1/2), signal transducer and activator of transcription 3 (STAT3), and integrin-specific focal adhesion kinase (FAK) in SVEC cells. Inhibition of ERK1/2 and STAT3 signaling impairs EGFL7-induced endothelial cell migration, and angiogenesis in fetal mouse metatarsal explants (Figure 1). Furthermore, inhibition of integrins using RGD peptides also impairs endothelial cell migration. Finally, EGFL7 gene expression is significantly upregulated during growth plate injury repair.

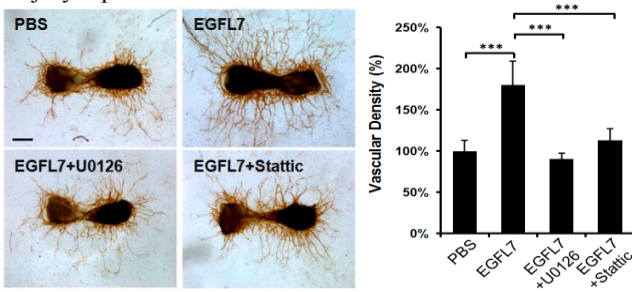

Figure 1: EGFL7-induced angiogenesis is blocked by U0126 (ERK1/2 inhibitor) and Stattic (STAT3 inhibitor).

CONCLUSIONS

We have shown that EGFL7 is expressed in the bone microenvironment and has a role in promoting endothelial cell migration, tube-like structure formation and angiogenesis through integrin-mediated pathways. This study highlights the important role that EGFL7 plays in the regulation of endothelial cell activities in bone microenvironment and might help to develop novel therapeutic approaches for bone fracture and bone disorders.

ACKNOWLEDGEMENTS

This work was funded in part by NHMRC of Australia and Western Australia Medical & Health Research Infrastructure Fund.

REFERENCES

1. De Maziere A, et al., *Dev Dyn*. **237**(3):580-591, 2008.
2. Wu F, et al., *Hepatology*. **50**(6):1839-1850, 2009.

EFFECT OF MECHANICAL ENVIRONMENT ON THE BMP-2 DOSE-RESPONSE OF LARGE SEGMENTAL DEFECT HEALING

[1]Vaida Glatt, [1]Nicole Loechel, [1]Michael Schuetz and [2]Chris Evans

[1] Institute of Health and Biomedical Innovation, QUT, Brisbane, Queensland, Australia
[2] Rehabilitation Medicine Research Center, Mayo Clinic, Rochester, USA
email:vaida.glatt@qut.edu.au

INTRODUCTION

Large segmental defects in bone do not heal well and present clinical challenges. Several treatments exist to aid the healing of large osseous defects, including recombinant human bone morphogenetic protein-2 (BMP-2). Although BMP-2 has shown preclinical efficacy in animal models, the clinical effectiveness in healing long bone defects has been disappointing. In our previous studies we demonstrated that the local mechanical environment influenced the healing of large bone defects in response to a standard dose of BMP-2[1]. The main goal of the present study is to determine if the mechanical environment can reduce the dose of BMP-2 needed for boney union. In preparation for this, it is necessary to establish a dose-response curve for BMP-2 using fixators of different stiffnesses. The preliminary data from this study are presented in this abstract.

METHODS

A rat, femoral, 5 mm defect was stabilized with different degrees of stiffness[2]. Defects were treated with 5.5 or 1.1 µg BMP-2 delivered on an absorbable collagen sponge in the same way as the INFUSE® product used clinically to enhance bone healing and compared to the 11 µg (standard dose). The rat groups healed under conditions of low, medium and high stiffness with various doses of BMP-2. Healing was monitored by weekly X-ray. At 8 weeks, the rats were euthanized. At the end of treatment all femurs were assessed with µCT. Mechanical testing and histology are still in progress.

RESULTS AND DISCUSSION

Under conditions of constant stiffness, the lowest dose of BMP-2 caused the deposition of only small amounts of bone, which failed to fill the defect no matter which stiffness external fixator was used (data not shown). In contrast, defects treated with the two higher doses of BMP-2 showed clear evidence of intra-lesional mineralization by 3 weeks (Fig.1). However, defects treated with a dose of 5.5 mg appeared to be less uniform, and at 8 weeks there was still presence of radiopaque line in all groups (Fig.1). Likewise, evidence of healing in these defects seem to be delayed by one week occurring at 3 weeks instead of 2 weeks post-op when compared to the standard dose, except in the group with highest stiffness fixator (Fig.1). Furthermore, the callus size appeared to be smaller during healing with all stiffness fixators when 5.5µg dose was used. Additionally, this data did confirm our previous findings that lower stiffness fixators had bigger callus formation as compared to the more rigid fixators[1].

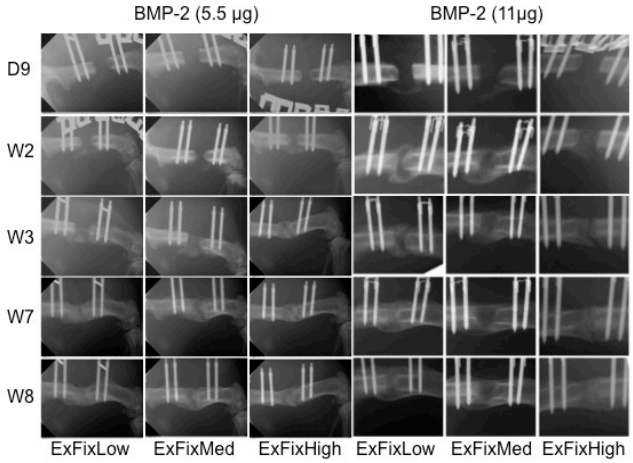

Figure 1: Representative X-ray images with different stiffness fixators and 5.5 and 11µg doses of BMP-2.

CONCLUSIONS

Defect healing was influenced by the dose of BMP-2. Although the full study is still in progress, the initial results suggest that a dose of 5.5 mg BMP-2 has the ability to drive the healing of segmental defects, but healing was delayed and the quality of healed bone was inferior when compared to 11mg of BMP-2. Although at this point it is not clear if the mechanical environment plays a role using 5.5 mg dose of BMP-2, but the presence of the radiopaque line at the end of treatment might be a consequence of prolonged movements in the defect during early stages of healing. A dose of 5.5 mg BMP-2 is thus appropriate for studying the effects of different mechanical regimens, such as reverse dynamization [1], on the healing of large bone defects. The results of this study will have significant consequences on the fixation stability used in order to maximise the regenerative capacity of bone healing while minimising the dose of BMP-2 required clinically.

ACKNOWLEDGEMENTS

U.S DoD-W81XWH-10-1-0888), Vice-Chancellor's Research Fellowship, QUT, AU.

REFERENCES

1. Glatt et al. *JBJS Am.* 2012 Nov 21;94(22):2063-73.
2. Glatt et al. *Eur Cells Mater* 23: 289-98, 2012

GLYPICAN-3 (BUT NOT GLYPICAN-1) INHIBITS BMP ACTIVITY AND OSTEOGENESIS IN VITRO

Prem P Dwivedi, Yu-Wen Su and Cory J Xian

Sansom Institute for Health Research, School of Pharmacy and Medical Sciences, University of South Australia, Adelaide, SA
email: cory.xian@unisa.edu.au

INTRODUCTION

Due to the critical role of bone morphogenic protein (BMP) signalling in bone growth, maintenance, and fracture healing, understanding the regulation of BMP activity is important. It is now known that apart from some specific regulators, activities of BMPs can also be modulated by proteoglycans (PGs). The glypican (GPC) family of heparan sulphate PGs, GPC1-6, are located on cell surface tethered by a glycosyl-phosphatidylinositol anchor or found in extracellular matrix, thus they are in a prime position to interact with extracellular signalling molecules and their receptors [1].

While previous studies (mostly in Drosophila) have suggested that GPCs may regulate signaling of Wnts, Hedgehogs, FGFs, and TGF-β, and we have recently demonstrated that glypicans (GPC1 and GPC3) are important regulators of BMP2 activity in human cranial suture mesenchymal cells [2], it is largely unclear how GPCs regulate BMP activities involved in bone formation. The current study investigated potential functions of GPCs in regulating BMP activity and osteogenesis in vitro.

METHODS

Firstly, levels of mRNA expression of the major glypicans (GPC1 & GPC3) and major osteogenic BMPs (BMP-2, 4, 7) were examined by qRT-PCR during osteogenesis of rat bone marrow stromal cells. To examine effect of glypicans on BMP activity, 100ng/ml BMP-2, 4, or 7-mediated BMP-smad activation assays were carried out in osteogenic cells (C3H10T1/2 MSCs, MC3T3E1 osteoblastic cells, and MLO-Y4 osteocytic cells) transfected with pID183-luc reporter and mouse GPC-1 or GPC-3 transgene.

To examine whether BMP2-smad activity can be modulated at the protein level, treatment effects with GPC1 or GPC3 protein (100 or 200ng/ml) or anti-GPC3 neutralising antibody or normal IgG (25 or 50μg/ml) were also investigated in MC3T3E1 cells using the pID183-luciferase reporter assay. Finally, effects of GPC3 protein in modulating osteogenesis in vitro (Alizarin red staining and expression of Runx2, osterix, and osteocalcin) were examined in MC3T3E1 osteoblastic cells treated with or without BMP-2.

RESULTS AND DISCUSSION

During osteogenesis of rat bone marrow stromal cells (BMSCs), GPC1, GPC3 and osteogenic BMPs (BMP2, BMP4 and BMP7) were found to be differentially expressed. While expression of BMP2 and BMP4 rose, BMP7 decreased during osteogenic differentiation. Interestingly, GPC3 expression was high in undifferentiated cells but declined during osteogenesis, suggesting an inverse relationship of GPC3 and the osteogenic BMPs (BMP2 and BMP4). Conversely, the expression of GPC1 was found to increase during the early phase of the osteogenesis.

When examining whether GPCs can regulate the activities of BMP2, BMP4 and BMP7 in a BMP-Smad activation assay, we demonstrated that ectopic expression of GPC3 (but not GPC1) can block activities of these BMPs in C3H10T1/2 MSCs, MC3T3E1 osteoblastic cells, and MLO-Y4 osteocytic cells. We also observed that BMP2 activity can also be inhibited in MC3T3 osteoblastic cells by treatment with GPC3 (but not GPC1) protein and can be enhanced by anti-GPC3 monoclonal antibody. We further observed that GPC3 protein suppressed BMP2-mediated osteogenesis of MC3T3E1 osteoblastic cells in vitro.

CONCLUSIONS

GPC3 has inverse expression pattern to BMP2 during osteogenesis of bone marrow stromal cells. GPC3 blocks functional activities of BMP2, BMP4 and BMP7 while GPC1 seems to be specific for BMP4 in osteogenic cells. BMP2 activity can also be modulated in osteogenic cells using recombinant GPC3 protein and monoclonal antibodies. GPC3 protein can reduce BMP2-mediated in vitro osteogenesis of MC3T3E1 osteoblastic cells. GPC1 and GPC3 are expressed in osteocytes, osteoblasts and bone marrow cells in vivo.

Thus, the inverse relationship in expression levels of BMP2, BMP4 and GPC3 during osteogenesis and the functional inhibition of BMP activities by GPC3 (but not GPC1) and the suppression of osteogenesis of osteoblastic cells by GPC3 implies an inhibitory role of GPC3 in modulating BMP activities during osteogenesis.

ACKNOWLEDGEMENTS

This work was funded in parts by project grants from National Health and Medical Research Council (NHMRC) of Australia.

REFERENCES

1. Filmus J, Capurro M, and Rast J (2008). *Genome Biology* **9**: 224.
2. Dwivedi PP, Grose RH, Filmus, J, Hi CST, Xian CJ, Anderson PJ and Powell BC (2013). *Bone* **55**, 367-376.

SESSION 2 – BIOMECHANICS 2

INTERVERTEBRAL DISC AND FACET JOINT CONTRIBUTIONS TO THE SIX AXIS MECHANICAL PROPERTIES OF THE HUMAN LUMBAR FUNCTIONAL SPINAL UNIT

[1]Isaac M Lawless, [2]Dana Sommerfeld, [1]Dhara B Amin, [1]Richard M Stanley, [3]Boyin Ding and [1]John J Costi

[1] Biomechanics & Implants Research Group, Medical Device Research Institute, School of Computer Science, Engineering and Mathematics, Flinders University, Adelaide, SA
[2] Institute of Biomechanics, TUHH Hamburg University of Technology, Germany
[3] School of Mechanical Engineering, The University of Adelaide, SA
Email: john.costi@flinders.edu.au

INTRODUCTION

The functional spinal unit (FSU) is a three joint multiplex comprised of an intervertebral disc (IVD) and two sagittally symmetrical diarthrodial synovial facets. The strength and flexibility enjoyed by the healthy spine is a result of the cumulative contribution of these joints to load bearing and flexibility at each spinal level. The pathological spine can experience deficits in mechanical behavior or pain as a result of injury or degeneration to one or more of the three joints of the FSU. Accordingly, current interventions tend to treat and replace the FSU component-wise. However, there remains limited literature on the complex three-dimensional (3D) mechanical properties of the joints, whose nominal function the interventions must reproduce in order to restore quality of life [1].

The aim of this study was to determine the component-wise contribution of the IVD and facet joints to the 3D mechanical properties of the FSU.

METHODS

Sixteen osseoligamentous human lumbar FSUs were tested in each of 12 directions at 0.1 Hz along the six anatomical degrees of freedom (DOF) while exposed to physiologic preload (0.5 MPa), hydration (protease-inhibited, phosphate-buffered saline bath) and temperature (37°C) conditions in a hexapod robot [2]. The testing suite was then repeated after a complete facetectomy, leaving only the IVD. The primary testing axis was driven in position control while the off-axis coupling was minimized in load control. Non-destructive cycle amplitudes were 1.1 MPa compression, 0.6 mm shear, 3° lateral bending, 5° flexion, 2° extension and 2° axial rotation.

The segments' complex non-linear mechanical properties were approximated by a moving average toe region stiffness, exhaustive search best-fit linear region stiffness, full cycle average stiffness, peak force and phase angle.

Bonferroni-adjusted paired t-tests were used to detect significant differences ($p<0.05$) between the intact FSU and IVD tests in each direction. Independent samples t-test for equality of means was used to assess directional symmetry.

RESULTS AND DISCUSSION

Left and right lateral shear, lateral bending and axial rotation demonstrated symmetry and were pooled for analysis.

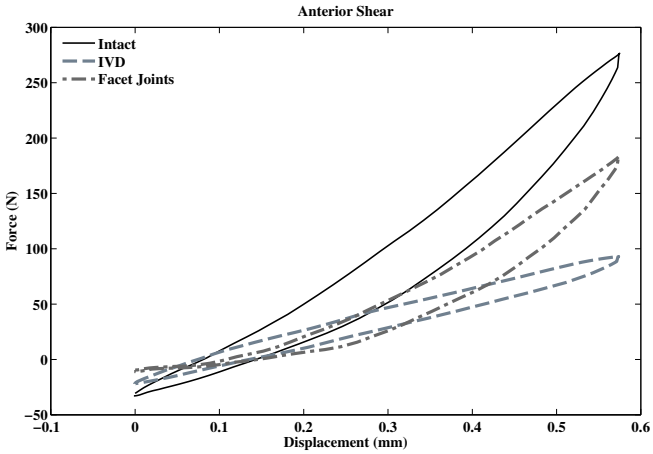

Figure 1: Contribution of the IVD and facet joints to FSU behaviour in anterior shear.

Significant differences were found between FSU and IVD properties in lateral shear ($p<0.001$ for all measures), axial rotation ($p<0.001$), extension ($p<0.021$), anterior shear ($p<0.002$ except phase angle $p=0.085$) and posterior shear ($p<0.005$ except phase angle $p=0.256$ and linear region stiffness $p=0.058$). There were no significant differences in compression ($p>0.099$), flexion ($p>0.093$) and lateral bending ($p>0.057$, phase angle ($p=0.008$) and peak force ($p=0.017$) significant), indicating minimal facet interaction in those directions over the explored range.

The contribution of the facet joints was highly direction dependent. Facet joints contribute the majority of FSU non-linear behaviour and more phase angle than intuition would suggest (Figure 1).

CONCLUSIONS

If highly efficacious implants are to be designed, we first need to understand the mechanical properties of the joints they are intended to replace. This work explores the contribution of the components of the lumbar FSU to its overall behaviour in asymmetric 6DOF.

REFERENCES

1. Costi JJ, Freeman BJ, Elliott DM, 2011. *Expert Rev Med Devices*. 8:357-76.
2. B. Ding, R.M. Stanley, B.S. Cazzolato, J.J. Costi, 2011. *Proc. IEEE Industrial Electronics Society*, 211–216.

THE EFFECT OF REVERSE DYNAMIZATION ON BONE HEALING

[1]Nicole Loechel, [1]Vaida Glatt, [1]Lidia Koval, [1]Roland Steck, [3]Ronny Bindl, [3]Anita Ignatius, [1,2]Michael Schuetz, [3]Lutz Claes and [1]Devakar Epari

[1]Institute of Health and Biomedical Innovation, Queensland University of Technology, Brisbane, QLD
[2]Trauma Service, Princess Alexandra Hospital, Brisbane, QLD
[3]Institute of Orthopaedic Research and Biomechanics, University Hospital of Ulm, Germany
email: n.loechel@qut.edu.au

INTRODUCTION

It has been well established that the healing of fractures is influenced by the mechanical environment. However, the most beneficial regimen of mechanical stimulation in different phases of healing is currently unknown. We hypothesize the healing of fractures in long bones can be accelerated by the imposition of an appropriate mechanical environment that is purposefully modulated as healing progresses. We postulate that it may be most beneficial to flexibly stabilize the fracture during the earlier stages of healing to promote larger callus formation, and then the fixator stiffness should be increased allowing callus mineralisation and bridging to occur. Thus, the aim of this study is to investigate the modulation of fixation from flexible to stiff, on the healing outcome.

METHODS

A custom-made external fixator was implanted on the right femur of rats using four threaded stainless steel pins [1]. An osteotomy of 1 mm was created in femurs between the two inner pins of the fixator. Three groups were investigated including two control groups, with either flexible or stiff fixation for the entire healing period of 5 weeks, and a Reverse Dynamisation (RD) group where flexible fixation was used for the first 3 weeks followed by stiff fixation for the final two weeks of bone healing. After five weeks bone healing was analysed using microcomputed tomography (µCT), histology and biomechanical testing.

RESULTS AND DISCUSSION

After 5 weeks, fractures stabilized with stiff fixation lead to superior flexural rigidity compared to flexible fixation, confirming findings of the previous studies performed with this model [1]. Moreover, the RD and the stiff groups resulted in significantly lower callus volume (129 mm^3 and 120 mm^3 respectively) compared to the flexible group (179 mm3). The evidence of this can be observed in the µCT and histological images (Figure 1) presenting with the higher amounts of un-mineralised tissue and cartilage (1.65 mm^2) within the osteotomy in the flexible group compared with the RD (0.64 mm^2) and stiff (0.27 mm^2) groups. This data was also confirmed by the biomechanical testing data with the RD and stiff groups having a significantly higher flexural rigidity compared to the flexible group indicating a superior healing outcome.

Contrary to our hypothesis, there was no significant difference between the stiff and the RD groups. An additional experiment using flexible fixator for 14 days to examine the pattern of bone healing was conducted. Histological images at this time point revealed a large amount of callus formation, composed of both cartilaginous tissue and woven bone, implying the modulation of fixator stiffness was conducted too late in the healing period in this study. Hence further investigation is required into the timing of this mechanical manipulation, particularly the effect on the early stages of healing, in order to comprehensively test our hypothesis and to further understand the mechanobiological mechanisms involved in the fracture healing process.

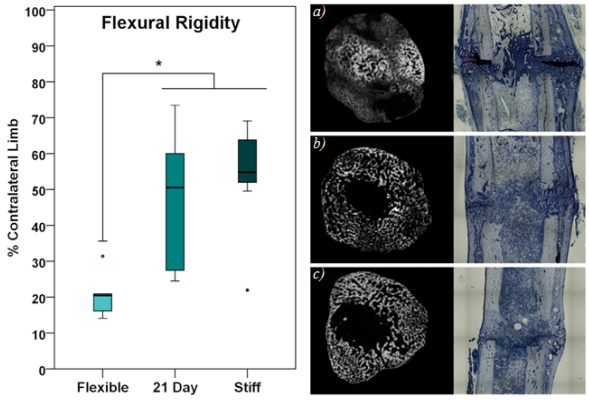

Figure 1: Flexural rigidity of the fracture callus, µCT and histological images of osteotomy at 35 days post-operatively: a) flexible fixation; b) Reverse Dynamization (3-weeks; and c) stiff fixation.

CONCLUSIONS

Performing reverse dynamization at 3 weeks produced a significantly improved healing outcome compared to the more flexible fixation. Clinically, this demonstrates the potential to improve the healing outcome through stabilization of unstable fractures, particularly for non-unions.

ACKNOWLEDGEMENTS

This study was funded by a AO Trauma Asia Pacific grant.

REFERENCES

1. Claes, L, et al., Journal of orthopaedic research. 27:22-27, 2009.

BIOMECHANICAL OUTCOMES OF A NOVEL SURGICAL ROTATOR CUFF TENDON REPAIR TECHNIQUE

[1]Jonathan Caldow, [2]Martin Richardson, [2]Subash Balakrishnan, [2]Tony Sobol, [1]Peter Lee, [1]David Ackland
[1]Department of Mechanical Engineering, University of Melbourne, VIC; [2]Epworth Healthcare, VIC
Email: dackland@unimelb.edu.au

INTRODUCTION

The ultimate tensile strength and stiffness of a repaired rotator cuff tendon have been widely used as indicators of the longevity of surgical repairs. More recently, tendon footprint contact area and contact pressure have been shown to be essential in facilitating biological healing at the tendon-bone interface [1]. Double-row rotator cuff tendon repairs have been shown to display superior ultimate tensile strength, stiffness, footprint contact area and contact pressure compared to conventional single-row repairs [1], but are more difficult, time-consuming and costly to perform. As a result, single-row repairs are receiving increasing attention. The aims of this study were twofold. Firstly, to measure the ultimate tensile strength, stiffness, footprint contact area and footprint contact pressure of a new single-row cruciate suture repair, and secondly, to compare these results to those of the Mason-Allen double-row and transosseous repair techniques.

METHODS

Sixty-four infraspinatus tendons were harvested from lamb shoulders obtained from a local abattoir. All soft tissue was dissected from the humerus and scapula. The infraspinatus and humerus from each shoulder were randomly assigned to the following four repair groups: (i) single-row Mason-Allen repair (ii) double-row repair with medial mattress stitches and lateral Mason-Allen stitches (iii) transosseous bone tunnel repair, and (iv) single-row cruciate suture repair, consisting of crossed stitches oriented 45 degrees to the tendon (Figure 1). Twenty-four shoulder specimens were assigned to footprint testing and were surgically repaired directly over high-sensitivity pressure-sensitive film (Fuji, Tokyo, Japan). Tendon tension was standardised by applying 10 N tendon loading using a free weight and pulley. The mean total pressed area (mm^2) and average contact pressure (MPa) were measured. The remaining thirty-six shoulder specimens were mounted to an Instron material testing system and displaced upward at a constant rate of 1 mm/s. The ultimate tensile strength (N) and stiffness (N/mm) of the repair was calculated from the peak and the gradient of the load-displacement curve, respectively.

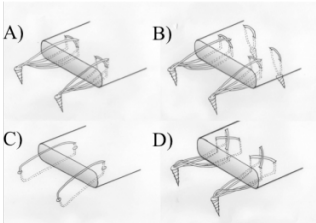

Figure 1. Rotator cuff repairs techniques A) Mason-Allen, B) double-row, C) transosseous D) cruciate suture repair

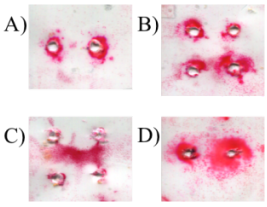

Figure 2. Representative tendon-bone contact pressure distributions A) Mason-Allen, B) double-row, C) transosseous D) cruciate suture repair

RESULTS AND DISCUSSION

The cruciate suture repair established greater footprint contact area compared to the Mason-Allen repair (mean difference = 100.5 mm^2, 95% confidence interval (CI) [37.1, 163.9] p=0.003) (Table 1). No significant difference in contact area was recorded between the double-row, transosseous and cruciate suture repairs ($p>0.05$). The footprint contact pressure for the cruciate suture repair of 0.78 MPa was similar to that of the Mason-Allen repair (0.74 MPa) and double-row repair (0.79 MPa) (Figure 2). The double-row repair recorded the largest ultimate tensile strength (187.3 N) and stiffness (16.4 N/mm) of all repairs. There was no significant difference between the cruciate suture and Mason-Allen repairs in ultimate tensile strength or stiffness ($p>0.05$). The cruciate suture repair demonstrated significantly greater repair stiffness to the transosseous repair (mean difference = 4.69 N/mm, 95% CI [1.19, 8.19], p=0.006).

Table 1. Average footprint contact area and pressure, ultimate tensile strength and stiffness measurements for Mason-Allen, double-row, transosseous and cruciate repairs.

	Cruciate suture	Mason-Allen	Double-row	Trans-osseous
Footprint contact area (mm^2)	252.5	152.0	293.3	271.7
Footprint contact pressure (MPa)	0.8	0.7	0.8	0.3
Ultimate tensile strength (N)	141.8	136.1	187.3	79.3
Stiffness (N/mm)	10.9	10.1	16.4	6.2

CONCLUSIONS

The new cruciate suture repair reported in this study recorded similar ultimate tensile strength and a larger footprint contact area and contact pressure to that of the Mason-Allen repair, indicating equal or improved tendon healing and longevity compared to the Mason-Allen repair. The cruciate suture repair, while only requiring a single-row of bone anchors, demonstrated comparative footprint contact area to that of a double-row repair. Therefore, the cruciate suture repair may represent a faster, easier and more cost effective alternative to conventional double-row repairs. Future studies ought to assess clinical outcomes of the 'footprint' repair relative to other commonly used repair techniques.

REFERENCES

A musculoskeletal model for the evaluation of shoulder muscle and joint function

[1]Wen Wu, [2]Karen Ginn, [3]Mark Halaki, [4]Adam Bryant, [5]David Lloyd, [6]Thor Besier, [1]Peter Lee, [1]David Ackland
[1]Melbourne School of Engineering, University of Melbourne, VIC; [2]Sydney Medical School, University of Sydney, NSW; [3]Faculty of Health Sciences, University of Sydney, NSW; [4]Melbourne School of Health Science, University of Melbourne, VIC; [5]Griffith Health Institute, Griffith University, QLD; [6]Auckland Bioengineering Institute, University of Auckland, New Zealand
Email: wenw1@student.unimelb.edu.au

INTRODUCTION

Elucidation of the upper-limb muscle forces that lead to joint motion is important in our understanding of upper-limb muscle and joint disease, injury prevention, prosthesis design, rehabilitation therapy and robotics. Since no non-invasive muscle force measurement strategies are available, computational simulations are widely used to infer muscle and joint function. The purpose of this study was to develop an open source musculoskeletal model that can be used to evaluate shoulder muscle and joint loading. This modelling framework is an extension of that reported previously [1].

METHODS

A musculoskeletal model based on previously reported bone geometries [1] was developed (Fig. 1). Eight degrees-of-freedom was used to describe motion of the thorax, clavicle, scapula and humerus. The model was actuated by 27 muscles representing the major axioscapular, axiohumeral and scapulohumeral muscle groups. Each muscle was modelled as a Hill-type muscle-tendon actuator. The architectural properties and muscle-tendon parameters of each muscle-tendon actuator were taken from the literature [2]. Muscle moment arms were matched to our previously reported measurements [3].

OpenSim was used to calculate joint torques from inverse dynamics and obtain muscle-tendon parameters and muscle moment arms. A Matlab optimizer was then used to decompose the net joint moments into muscle forces by minimizing the sum of squares of muscle activations. Constraints applied to the optimiser included (i) limits to each muscle's operation along its force–length/force-velocity curve (ii) A minimum muscle force of zero and maximum muscle force equal to peak isometric muscle force (iii) glenohumeral (GH) joint force direction restricted to pass through the glenoid, to avoid joint dislocation (iv) constraints on the scapulothoracic joint force to act at the centre of area of the anterior scapula surface. While the scapulothoracic contact force acts normal to the thorax and may contribute to scapula stability, it does not contribute to motion of the scapula within the scapula gliding plane. Simulations of coronal-plane abduction, elevating only against the weight of the arm, were performed using the musculoskeletal model. Muscle forces as well as GH joint reaction forces and scapulothoracic contact forces were subsequently calculated.

Table 1. GH joint force calculated with the musculoskeletal model and measured using an instrument implanted [4]

Abduction (degrees)	Calculated (%BW)				Measured (%BW)
	Anterior	Superior	Medial	Resultant	Resultant
30	29.4	-8.5	46.9	56.0	42.2
60	24.4	-17.3	74.5	80.2	67.3
90	12.3	-7.0	92.0	93.0	91.9

RESULTS AND DISCUSSION

The anterior and middle deltoid muscles were the dominant abductors, reaching their peak forces 44.5% and 30.78% of body weight respectively at close to 90° of abduction. The GH joint reaction force during abduction peaked at 90° of abduction (Table 1), while the scapulothoracic contact force was larger at 60º of abduction (Table 2).

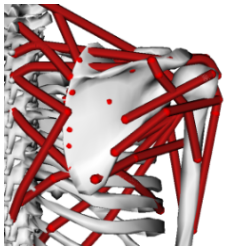

Figure 1. Posterior view of musculoskeletal shoulder model

Table 2. Scapulothoracic contact force during abduction

Abduction (degrees)	Force (%BW)
30	7.4
60	9.2
90	8.6

CONCLUSIONS

This study reports a musculoskeletal model of the shoulder complex. Preliminary GH joint force magnitudes are in reasonable agreement with instrumented implant data reported in the literature. Future work will include addition of the remaining muscles and joints of the upper limb, use of medical images to create the musculoskeletal models, parameter-optimization approaches to evaluate optimal fibre lengths and tendon slack lengths, and electromyography-informed methods to derive muscle excitations. This open-source musculoskeletal model will be made freely available to the biomechanics community.

REFERENCES

1. Holzbaur, K.R., W.M. Murray, and S.L. Delp, Annals of biomedical engineering, 2005. 33(6): p. 829-840.
2. Garner, B.A. and M.G. Pandy, Computer methods in biomechanics and biomedical engineering, 2001. 4(2): p. 93-126.
3. Ackland, D.C., et al., Journal of Anatomy, 2008. 213(4): p. 383-390.
4. Westerhoff, P., et al., Medical engineering & physics, 2009. 31(2): p. 207-213.

A NEW SOFTWARE PIPELINE FOR MICRO-FINITE-ELEMENT SIMULATIONS OF WHOLE-BONE MECHANICS

Saulo Martelli, Egon Perilli, Greg S. Ruthenbeck, Mark Taylor and Karen J Reynolds

School of Computer Science, Engineering and Mathematics, Medical Device Research Institute, Flinders University, Bedford Park, Australia
email: saulo.martelli@flinders.edu.au

INTRODUCTION

Knowledge of the tissue-level mechanics can improve our understanding of age-related bone changes and related fractures. Finite-element (FE) models based on micro-CT images allow estimating the mechanical behavior of cortical and trabecular compartments in entire bones at high resolution. However, generating, solving and analyzing FE models of 20-100 million elements, such as micro-FE models of entire human vertebrae [1], is computationally challenging and requires ad-hoc software and hardware solutions. In this paper we present a novel software pipeline for generating, solving and analyzing micro-FE models of entire human lumbar vertebral bodies, on a desktop computer.

METHODS

The software pipeline was developed using image datasets of five human vertebrae (L2, L3) generated with a micro-CT scanner at 17.4 µm isotropic pixel size (Skyscan 1076, Skyscan NV, Kontich, Belgium) [2]. Each dataset comprised a stack of up to 2352 axial cross-section images (corresponding to 40 mm length), 3936×3936 pixels each image (68 x 68 mm), stored in 8bit greylevel format (.bmp), containing the entire vertebra. Micro-FE models were generated on a 64GB RAM, 24 CPUs desktop computer and solved using a 256 GB RAM, 8 CPUs desktop computer under Windows© 7 operating system. Images were resampled to 69.6 µm/pixel (nearest neighbor interpolation, TConv v2.1, Skyscan). Grey-level images were binarized by segmenting bone as a solid (global threshold), followed by a 3D-sweep algorithm to remove isolated disconnected voxels (speckles) and keep only the largest object in 3D (vertebra) (CT Analyser v1.14, Skyscan). The mesh was generated using an in-house built software tool based on a Vertex Pooling algorithm [3]. This tool streams the binarized images from the hard-disk, and generates an indexed set of node positions and eight-node hexahedral elements for each solid voxel (bone). Regions are defined using bounding boxes. As voxels are processed, they are first sorted into the regions where a separate instance of the node reference counting system is used. Nodes and elements are stored in text files and processed using Matlab (The Mathworks Inc., USA) for generating the simulation input file (ABAQUS, Simulia, RI, USA), including user-defined element sets, node sets, material properties and load steps. The tool was first tested by generating a mesh of 484 M hexahedrons using a stack of 500 images, 984×984 pixels each, binarized as a full homogenous solid. Linear elastic simulations were run in parallel over 8 CPUs using ABAQUS/Explicit (Simulia, RI, USA). The mesh was assigned a homogenous Young modulus of 18 GPa. The inferior endplate of the vertebra was fully constrained, while to the superior endplate was imposed a displacement of 0.4 mm towards the inferior endplate (compression test). The running time required by each simulation was recorded.

RESULTS AND DISCUSSION

The test mesh (484 M elements) was successfully generated in 2.7 h. Vertebra FE models were composed of 20.2-49.9 M nodes, 11.5-28 M hexahedrons, generated in 0.5-1.1 h, requiring 1.3-4.7 GB of memory (RAM). The first model (20.2 M nodes) required 22 h and 91 GB of RAM to reach solution. Results were visualized using ABAQUS View (Fig. 1). As the simulations of the remaining models (23-49.9 M nodes) met the upper threshold for the solver, diverse solvers are currently under evaluation.

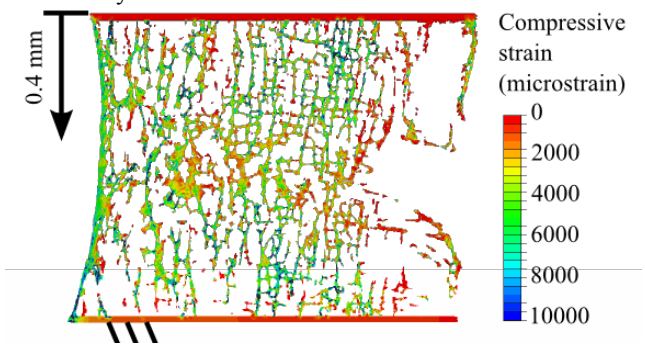

Figure 1: The compressive strain map over a sagittal cross-section of the vertebra model #3.

CONCLUSIONS

The test model of 484 M nodes was successfully generated in 2.7 h computation time on a desktop computer, while vertebra models with to 49.9 M elements were generated in less than 1.1 h. Hence, the presented pre-processing software is well suited for generating high-resolution (~ 70 µm) models of bones as big as entire human vertebral bodies and bigger. However, the FE solver could resolve models with up to 23 M nodes, which nonetheless was sufficient for the smaller vertebra model. Evaluation of different solvers is currently in progress, which may be capable of solving bigger FE models.

ACKNOWLEDGEMENTS

Australian Research Council (DE140101530).

REFERENCES

1. Fields et al. *J Bone Miner Res*. **24**:1523-30, 2009.
2. Perilli et al. *Bone*. 50:1416-25, 2012.
3. Ruthenbeck et al. Comp Meth BBE., Epub, 2013.

TIME-ELAPSED SCREW INSERTION INTO CANCELLOUS BONE

[1,2]Melissa Ryan, [1,2]Aaron Mohtar, [2]Tammy Cleek, [1,2]John Costi and [1,2]Karen Reynolds

[1]Biomechanics & Implants Research Group, Medical Device Research Institute, Flinders University, Adelaide, SA
[2]School of CSEM, Flinders University, Adelaide, SA
email: melissa.ryan@flinders.edu.au

INTRODUCTION

"Time-elapsed" or "image-guided failure" assessment of bone is a relatively new technique that uses sequential image acquisition to analyse trabecular bone mechanics under a given loading regime. To date, this procedure has been employed to analyse trabecular mechanics during uniaxial compression [1, 2], screw pull-out [3], and screw push-in tests [4]. Nazarian et al. (2004) validated the use of this method for the assessment of microstructural trabecular mechanics, demonstrating no difference in the macroscopic behaviour of cancellous bone specimens under continuous or step-wise loading conditions [2]. These methods have provided valuable insight into the failure mechanisms of bone under specific loading conditions. Work within our laboratory, however, has sought to better understand the interactions between bone and implant during screw placement. The purpose of this work was to devise a method to allow time-elapsed imaging during the tightening phase of screw insertion.

METHODS

A strong linear relationship exists between the plateau torque measured just prior to head contact $T_{plateau}$, and stripping torque (T_{max}) [5]. Based on this relationship a computer controlled device was developed that sits inside a microCT scanner. The device incorporates a torque transducer to measure applied torque, a load cell to measure compression under the head of the screw and an encoder to record rotation. The screw was tightened to head contact, based on this torque, T_{max} was predicted and the screw was then step-wise tightened stopping at 4 time points between head contact and predicted T_{max} to obtain micro-CT image data.

RESULTS AND DISCUSSION

Screw insertion was successfully completed, with the device predicting stripping torque with an error < 1%. The time-elapsed image data allowed visualization of the peri-implant trabeculae with respect to applied tightening torque for the first time. Image analysis revealed significant trabecular deformation, leading to screw stripping, occurs after 91% of T_{max}.

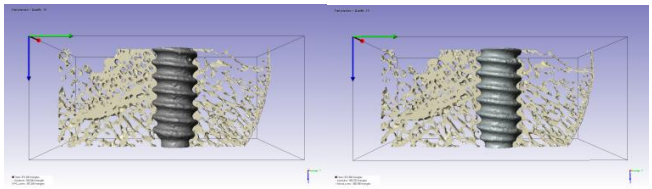

Figure 1: 3D rendering of micro-CT data obtained at head-contact (left) and post failure (right) of a cancellous lag screw inserted into an excised femoral head.

CONCLUSIONS

This study demonstrated the ability to predict stripping torque from torque attained at head contact, and to generate time-elapsed micro-CT image datasets based on step-wise screw insertion.

ACKNOWLEDGEMENTS

This study was funded by the NHMRC Grant ID 595933.

REFERENCES

1. Müller, R., S. Gerber, and W. Hayes, *Micro-compression: a novel technique for the nondestructive assessment of local bone failure.* Technology and Health Care, 1998. **6**: p. 433-444.
2. Nazarian, A. and R. Müller, *Time-lapsed microstructural imaging of bone failure behavior.* J Biomech, 2004. **37**(1): p. 55-65.
3. Gabet, Y., et al., *Endosseous implant anchorage is critically dependent on mechanostructural determinants of per-implant bone trabeculae.* Journal of bone and mineral research, 2010. **25**(3): p. 575-83.
4. Mueller, T., et al., *Time-lapsed imaging of implant fixation failure in human femoral heads.* Medical Engineering & Physics, 2013. **35**(5): p. 636-43.
5. Reynolds, K., et al., *Predicting cancellous bone failure during screw insertion.* Journal of biomechanics, 2013. **46**: p. 1207-1210.

;

EFFECTS OF ACCUMULATED FATIGUE DAMAGE ON THE FRACTURE RESISTANCE OF CORTICAL BONE

[1]Lloyd Fletcher, [1,2]John Codrington and [2,3]Ian Parkinson

[1]School of Mechanical Engineering, University of Adelaide, Adelaide, SA
[2]Bone and Joint Research Laboratory, SA Pathology and Hanson Institute, SA
[3]Discipline of Anatomy and Pathology, The University of Adelaide, SA
email: lloyd.fletcher@adelaide.edu.au

INTRODUCTION

Everyday loading of the skeletal system causes the accumulation of fatigue damage in bones. Bone has the ability to repair this damage, however, this ability to repair damage deteriorates with age or disease. The accumulation of fatigue damage is thought to contribute to fragility fractures in the elderly and stress fractures in the young [1]. Therefore this study aims to determine the effects of accumulated fatigue damage on the fracture resistance of cortical bone.

METHODS

Twenty un-notched rectangular beam specimens were machined from a single bovine femur parallel to the long axis of the bone (longitudinal). A further twenty un-notched beams were machined from another bovine femur perpendicular to the long axis of the bone (transverse). Ten specimens from each femur were allocated as control specimens while the remaining ten specimens were allocated as damaged specimens. The damaged specimens underwent fatigue loading at 2Hz in 3 point bending until 5% stiffness loss had occurred. The fatigue damage was then imaged using fluorescence microscopy. After fatigue loading all specimens were notched and fracture resistance tested using the unloading compliance method in accordance with ASTM E1820 [2]. The fracture resistance curve was calculated in terms of the J-integral. Following resistance curve testing the crack path toughening mechanisms for both groups were observed via fluorescent microscopy.

RESULTS AND DISCUSSION

The 95% confidence intervals for the fracture resistance curves of the longitudinal and transverse specimens are shown in Figure 1 (a) and (b) respectively. The fracture resistance curves were compared based on two parameters: the fracture initiation toughness (intercept of the resistance curve) and the growth toughness (slope of the resistance curve), shown in Table 1. There was no significant difference between the resistance curves of the control or damaged groups. Analysis of the fluorescent images of the fatigue damaged specimens showed that the fatigue damage concentrated on the outer edges of the specimen away from the crack path.

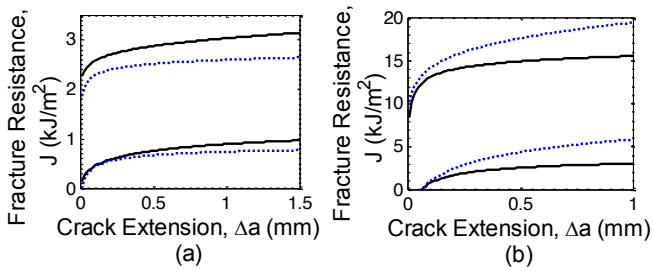

Figure 1: Confidence intervals for the fracture resistance curves of the longitudinal group (a) and transverse group (b), black solid lines denote control group and blue dashed lines denote the damaged group.

CONCLUSIONS

The results of this study show that the fracture initiation toughness and growth toughness of bone is unchanged when the fatigue damage is not in the vicinity of a propagating crack. A previous study by the authors using large scale longitudinal specimens has shown that when the fatigue damage is along the crack path a reduction in toughness is observed [3]. Future work will include the development of a method by which the fatigue damage can be concentrated ahead of the crack path for small scale transverse specimens.

REFERENCES

1. Burr D, et al., *Journal of Bone and Mineral Research*. **12**:6-15, 1997
2. ASTM Standard E1820, *Test method for the measurement of fracture toughness*, 2011
3. Fletcher L, et al., *Journal of Materials Science: Materials in Medicine*, doi: 10.1007/s10856-014-5213-5:,2014

Table 1: Fracture initiation toughness (J_0) and growth toughness (dJ/da) results for longitudinal and transverse specimens, all results presented as mean ± standard deviation. \

	Longitudinal, Control	Longitudinal, Damaged	Transverse, Control	Transverse, Damaged
J_0 (kJ/m²)	1.10±0.71	1.01±0.48	2.50±1.02	3.00±1.40
dJ/da ((kJ/m²)/mm)	1.47±1.39	1.96±1.10	18.91±11.59	20.95±11.05

MULTISCALE CORTICAL BONE REMODELLING: TOWARDS PREDICTING WHOLE BONE STRENGTH

[1]Xiaoming Wang, [2]Raj Das, [3]John Clement, [3]David Thomas, [4]Helen Davies, and [1]Justin Fernandez

[1]Auckland Bioengineering Institute, University of Auckland, New Zealand
[2]Mechanical Engineering, University of Auckland, New Zealand
[3]Melbourne Dental School, University of Melbourne, Australia
[4]Melbourne Veterinary School, University of Melbourne, Australia
email: j.fernandez@auckland.ac.nz

INTRODUCTION

The strength of bone is intimately linked to its hierarchical structure. In the neck of the femur, about 70% of the strength is contributed by the cortical bone and is where failure almost certainly occurs. Despite the crucial role of cortical bone in load-bearing in elder populations, there has been surprisingly little focus on 3D models of cortical bone remodelling at the micro-scale level. We present an efficient mechano-statistical model to link cortical micro bone architecture to whole bone strength.

Extensive studies of large-scale continuum models of bone and microstructural models of trabecular bone are present in the literature. However, there are limited 3D cortical bone models at the microscopic level, hence, the development of cortical bone microstructural patterns and their effect on load-bearing is not well understood. Here we present the traditional description of bone remodelling based on the ‘,mechanostat’, combined with a novel ‘fading memory’ effect, which accounts for historically changing loading schemes with peak load fluctuations. In addition and independently from the ‘mechanostat’, we model Haversian canal tunnelling, known as ‘the cutting cone’, concept.

METHODS

A whole femur digitised from the Visible Human was linked to Synchrotron imaging data of a 1mm^3 specimen of human cortical bone from the Melbourne Femur collection (Figure 1). This was segmented using a snake-evolution feature in the open-source software ITK-SNAP. The resulting STL geometry was voxel meshed in Hypermesh to generate a regular grid and regions classed as either bone or marrow. Elastic finite element stress simulations were solved using Abaqus and integrated with a python code to simulate remodelling based on the well-known ‘mechanostat’. The model accounts for adaption to loading history and the ‘cutting cone’ behaviour specific to cortical bone whereby osteoclasts remove bone and osteoblasts mineralise new bone producing Haversian canals that lie along the length of principally loaded directions.

RESULTS AND DISCUSSION

The bones were loaded by varying magnitude and location representing a variety of different scenarios that are experienced by the whole femur neck. The microstructural behaviours captured included the bones ability to adapt to recent loading history and reset the ‘mechanostat’; the creation of horizontal remodelling canals (Volkmann’s canals); the merging of pores to create ‘super osteons’; and the evolution of Haversian canals that represent patterns typically observed in cadaveric data. We also present a novel way of accounting for the complexity of computational simulation by creating a statistical model using partial least squares regression (PLSR) to describe the population of shapes that we predict. This is easily linked to the whole femur and hip for rapid estimation of remodelled material properties and fracture risk estimation due to changing micro cortical architecture.

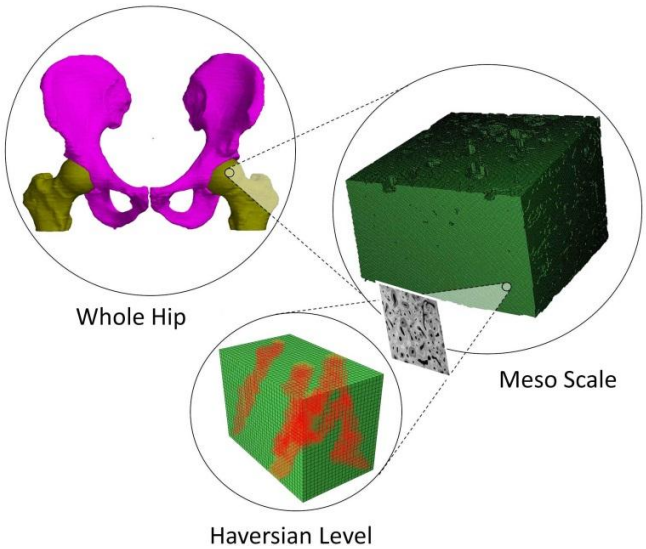

Figure 1: Multiscale pipeline showing whole hip linked to statistical model of micro cortical bone behaviour.

CONCLUSIONS

An efficient understanding of cortical bone architecture and its remodelling behaviour statistically linked to whole bone strength can rapidly help assist the prediction of fracture risk.

ACKNOWLEDGEMENTS

Funded by New Zealand’s Ministry of Business, Innovation and Employment (MBIE).

REFERENCES

1. Fernandez JW, et al., *Int j numer method biomed eng*. **29(1)**:129-43, 2013.

A NOVEL PROSTHETIC TOTAL JOINT REPLACEMENT SYSTEM FOR THE HUMAN TEMPOROMANDIBULAR JOINT

[1]David Ackland, [1]Russell Dow, [1]Adrian Moskaljuk, [1]Jason D'Souza, [1]Nick D'Arcy-Evans, [2]Chris Hart, [1]Peter Lee, [2]George Dimitroulis

[1]Department of Mechanical Engineering, University of Melbourne, VIC
[2]St Vincent's Hospital, Melbourne, VIC
Email: dackland@unimelb.edu.au

INTRODUCTION

Painful disorders involving the temporomandibular joint (TMJ), including osteoarthritis have a prevalence ranging from 16-59%[1]. TMJ replacement surgery is the established treatment for end-stage TMJ osteoarthritis; however, current TMJ prosthetic implant designs face a range of problems including fracture from metal fatigue; screw loosening; and difficulty in placement of the prosthesis to avoid the mandibular nerve. The aim of this study was to develop a musculoskeletal finite element of the TMJ based on the Visible Human Male (VHM) dataset, and to use this model to evaluate joint contact mechanics in the natural TMJ and in the TMJ after implantation of a novel TMJ prosthetic total replacement system.

METHODS

Axial images from the Visible Human Male dataset were digitally segmented and combined to reconstruct 3-D surfaces of the mandible, glenoid fossa and articular cartilage and discs. The major muscles of mastication – the masseter, temporalis (anterior and posterior), lateral and medial pterygoids – were also digitally reconstructed. Muscle lines of action, volumes and muscle fiber lengths were measured and used to calculate maximum isometric muscle force for each muscle. Using the measured muscle lines of action, and assuming ideal actuators, muscle forces during a normal chewing bite were computed by summing moments in three-dimensions about the TMJ joint centre. A static optimisation routine was used with a cost function chosen to minimise the sum of the squares of muscle activation subject to a bi-lateral bite force of 200N positioned at the second molar. TMJ contact forces were computed.

The calculated muscle forces were used as boundary conditions in a finite element model of the human jaw. The anatomy of the jaw included the three-dimensional surfaces of the mandible, glenoid fossa, articular cartilage and discs generated from the Visible Human Male dataset. A simulation of a normal chewing bite was performed and articular cartilage and disc contact stresses were calculated. A novel prosthetic TMJ system was designed and a virtual TMJ arthroplasty was performed on the left TMJ using the model. The condylar component was fixed with three screws (superior, mid and inferior), while the fossa component was rigidly fixed to the temporal bone. Muscle and joint forces were re-calculated, and a finite element model simulation performed to calculate implant stresses and strains during a chewing bite.

RESULTS AND DISCUSSION

The pre-operative joint reaction forces were 98.9N and 86.3N at the left and right TMJ, respectively. Pre-operatively, the maximum contact stress in the left and right condylar cartilage was 1.1MPa and 1.5MPa, respectively (Fig. 1). Post-operatively, the TMJ joint reaction force magnitudes on the left and the right TMJ were 79.1N and 78.3N, respectively.

At the TMJ joint prosthesis, the maximum contact stress at the condylar component and the fossa component was 85.0MPa and 166.1MPa, respectively (Fig. 2). The maximum stress and strain magnitudes in the condylar component were 279.9MPa and 2253.7×10^{-6}, respectively, occurring in the region of the screw hole closest to the implant condyle head. The maximum stress of the screw at this location was 338.2MPa.

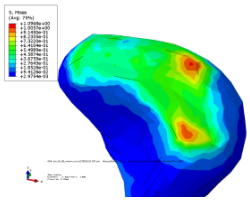

Fig. 1. Pre-operative contact-stress distribution on condylar cartilage

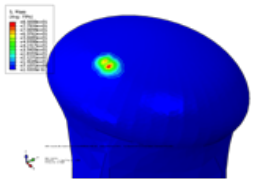

Fig. 2. Post-operative contact-stress distribution on condylar prosthesis

CONCLUSIONS

This study describes a new prosthetic TMJ, and provides estimates of muscle and joint-contact loads in the TMJ both before and after TMJ arthroplasty. While contact forces at the TMJ were of lower magnitude post-operatively, the contact stresses in the TMJ components were orders of magnitude higher than those in the pre-operative condylar cartilage. This finding indicates a potential mechanism for wear in the TMJ prosthesis. High stresses in the most superior screw-hole (closest to the condyle head) indicate risk of early screw loosening at this location.

REFERENCES

1. Carlson GE and LeResche L. (1995). *Temporomandibular Disorders and Related pain Conditions.* IASP Press, Seattle

EFFECT OF POTTING TECHNIQUE ON THE SIX DEGREE OF FREEDOM VISCOELASTIC PROPERTIES OF HUMAN LUMBAR SPINE SEGMENTS

[1]Dhara B Amin, [1]Isaac M Lawless, [2]Dana Sommerfeld, [1]Richard M Stanley, [3]Boyin Ding, and [1]John J Costi

[1] Biomechanics & Implants Research Group, Medical Device Research Institute, School of Computer Science, Engineering and Mathematics, Flinders University, Adelaide, SA
[2] Institute of Biomechanics, TUHH Hamburg University of Technology, Germany
[3] School of Mechanical Engineering, The University of Adelaide, SA
email: Dhara.Amin@flinders.edu.au

INTRODUCTION

Biomechanical testing requires rigid fixation of a specimen in a testing device and polymethyl methacrylate (PMMA) is perhaps the most popular fixation method for spine testing. The re-useability of low melting point fusible alloys such as Wood's Metal provides a more cost effective alternative to PMMA. However, a disadvantage of both mediums is that they heat the specimen while solidifying. The effect of potting medium on the mechanical properties of spinal disc segments under biomechanical testing remains unknown.

The first aim of this study was to compare the six degree of freedom (6DOF) viscoelastic properties of the disc when embedded in PMMA compared to Wood's Metal. The second aim was to compare the surface temperature of the disc when potted with PMMA and Wood's Metal.

METHODS

Six functional spinal units (FSUs) were dissected from human lumbar spines (Levels: L1-2 x 2, L3-4 x 1, L4-5 x 3, mean (SD) age: 88 (2.45) years, Thompson grade: grade 4 (N=2), grade 5 (N=4)). Each FSU was first embedded using PMMA and temperature readings of the external disc surface at anterior, right lateral, and left lateral positions were taken before and after potting. Each FSU was preloaded overnight (0.1MPa) in a saline bath. The FSU was then subjected to five cycles at 0.1 Hz for dynamic compression (1.1MPa), shear (±0.6mm), axial rotation (±2°), lateral bending (±3°), flexion (5°), and extension (2°) in the hexapod [1]. The sequence above was then repeated using Wood's Metal. Stiffness and phase angles were calculated for each DOF. Paired t-tests were performed between both potting groups for each DOF on the dependent measures of stiffness, phase angle, and region specific disc surface temperatures.

RESULTS

There were no significant differences between the stiffness values of PMMA and Wood's Metal for almost all 6 DOF tests ($p > 0.05$), apart for right lateral shear ($p=0.043$, Figure 1). There were no significant differences between the phase angles of the potting groups for all 6 DOF tests ($p > 0.05$). Significant differences were present between PMMA and Wood's Metal disc surface temperatures at the anterior position ($p=0.001$), with mean temperature values ranging from 18.3 to 19.1°C for PMMA and 20.9 to 25.7°C for Wood's Metal.

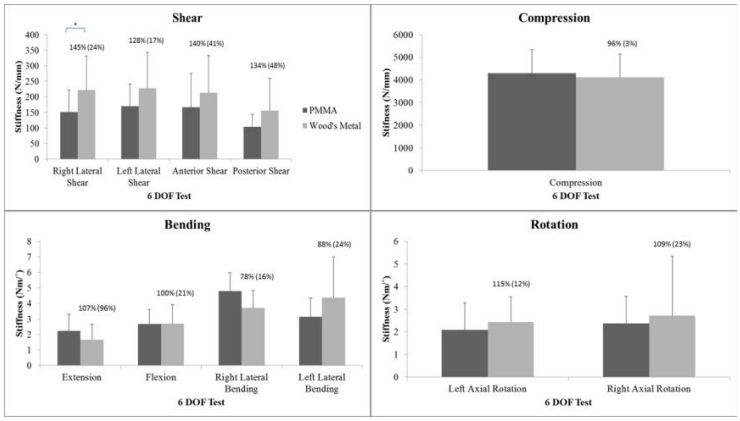

Figure 1: Mean (95% CI) stiffness values for all 6 DOF tests. The percentage (95% CI) normalised fractions are shown for each test and represent the Wood's Metal stiffness relative to the PMMA stiffness. * denotes significant differences between groups.

CONCLUSIONS

The mechanical properties of the disc did not significantly differ when potted in PMMA or Wood's Metal for the majority of loading directions apart for right lateral shear stiffness. However, we have found that with a small increase in sample size, there may be additional significant differences in stiffness between PMMA and Wood's metal in the shear translations and some rotational and bending DOFs. Surface disc temperatures were significantly different between PMMA and Wood's Metal for the anterior position. Comparing the magnitude of our mean normalised percentage differences to biological variation, disc injury, and degeneration studies, we found that Wood's Metal may eliminate approximately 20% of the variation in data compared to using PMMA. Wood's Metal is easier to remove than PMMA, is stiffer, linear elastic, cost effective and re-useable.

ACKNOWLEDGEMENTS

This project was supported by a scholarship from Whitaker International Program.

REFERENCES

1. Ding, B, et al., *37th Annual Conference on Industrial Electronics Society*, 2011

THE INFLUENCE OF THE PARASAGITTAL GROOVE ANGLE ON CARTILAGE STRESS AND DEGENERATION IN THE EQUINE METACARPOPHALANGEAL (FETLOCK) JOINT

[1]Helen Liley, [1]Justin Fernandez, [2]Helen Davies, [3]Elwyn Firth and [1]Thor Besier

[1]Auckland Bioengineering Institute, University of Auckland
[2]Melbourne Veterinary School, University of Melbourne
[3]Department of Sport and Exercise Science, University of Auckland
email: hlil007@aucklanduni.ac.nz

INTRODUCTION

The metacarpophalangeal (MCPJ), also known as the fetlock joint, is similar to the human knee, and is often used to evaluate human orthopaedic applications and cartilage pathology. Hence, it is useful for investigating equine and human musculoskeletal conditions. A recent study investigating the shape of the articulating surfaces of the MCJP highlighted that horses with a steeper parasagittal groove angle presented less bone lesions [1]. We hypothesise that this may be due to reduced shear stresses (characterised by a Von Mises stress) at the articular calcified cartilage – subchondral bone (ACC-SCB) interface near the lateral parasagittal groove, which is a common site for fracture initiation. [2]

METHODS

The right MCPJ of an adult Thoroughbred racehorse was imaged using both CT (to identify bone boundaries) and MRI (to identify the hyaline and calcified cartilage boundaries). Using this data, a finite element mesh was created in the software CMGUI (www.cmiss.org, Auckland Bioengineering Institute). A finite element solver (ABAQUS, Simulia) was used to simulate linear elastic loading between the third metacarpal and proximal phalanx to resolve contact and consequent Von Mises stress distribution throughout the articulating cartilage. The bones were defined as rigid bodies and the ligaments as tension-only connectors. The cartilage was modelled as a nearly incompressible isotropic linear elastic material [3]. Host mesh fitting was used to introduce different parasagittal angles (defined as B13 and B14 in figure 1), which define the sharpness of the sagittal ridge. For this presentation two extreme angles were used; B13 = 35.5° (shallow groove) and B13=42° (steep groove). A load of -1383 N (0.3% b/w [5]) was applied through the proximal phalanx, and the third metacarpal bone was fixed.

RESULTS AND DISCUSSION

Preliminary results show the Von Mises (VM) stress patterns through cartilage on the third metacarpal bone have a higher VM stress on the lateral side and a broader region of VM stress on the medial side at the ACC-SCB interface for B13 = 35.5°, including a higher Von Mises stress in the central ridge (figure 1). We hypothesize these are likely due to case B13 = 35.5° permitting more medial-lateral motion and hence more shear stress.

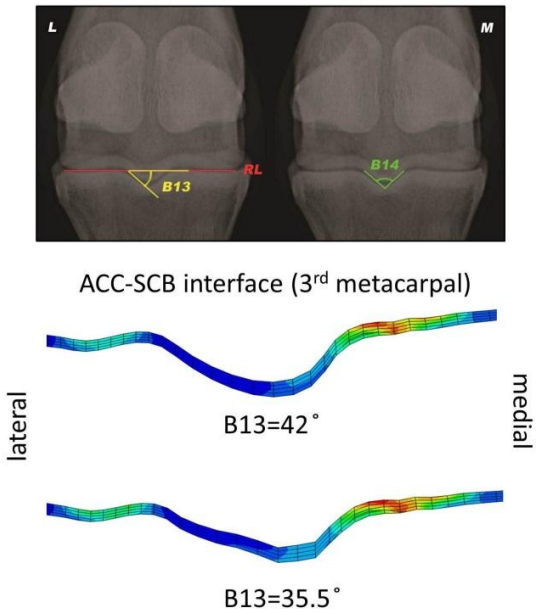

Figure 1: (Top) Radiograph showing the two angles (B13 and B14) that define the parasagittal groove in this study. Coronal slice through cartilage on the third metacarpal showing Von Mises stress for B13=42° (middle) and B13=35.5° (bottom). Red is 5 MPa.

CONCLUSIONS

Preliminary results show increased and broader regions of Von Mises stress at the ACC-SCB interface for a reduced parasagittal groove angle of 6.5° (B13=42° compared to 35.5°) and may explain why horses with shallower groove angles are more prone to bone lesions initiated by higher Von Mises stress at the ACC-SCB interface [4].

ACKNOWLEDGEMENTS

This work is supported by the NZ Equine Trust

REFERENCES

1. Alrtib, A.M, et al., *(in review)*
2. Stepnik, M.W. et al., *Veterinary Surgery*. **33**:2-10, 2004
3. Higginson, G.R. and Snaith, J.E., *Engineering in Medicine*. **8**: 11-14, 1979
4. Brama, P.A.J, et al., *Equine Veterinary Journal*. **33**:26-32, 2001.

KEYNOTE 5 – Dr Liza Raggatt

MACROPHAGES: A VIABLE THERAPEUTIC TARGET TO ENHANCE ENDOCHONDRAL FRACTURE REPAIR

Liza J Raggatt[1], Andy C Wu[1], Kylie A Alexander[2], Simranpreet Kaur[1], Susan M Millard[1], Michelle M Maugham[1], Roland Steck[3] Laura S Gregory[3], Martin E Wullschleger[4] and Allison R Pettit[1]

1. Mater Research Institute-UQ, Translational Research Institute, Woolloongabba, QLD, Australia. 2. Queensland Institute for Medical Research, Herston, QLD, Australia. 3. Institute of Health and Biomedical Innovation, Queensland University of Technology, Kelvin Grove, QLD, Australia 4. Queensland Health and The University of Queensland, Herston, QLD, Australia.

Macrophages (macs) have been indirectly implicated in the inflammatory phase of fracture repair, but their roles in later phases are unknown. It is likely that both, resident tissue and inflammatory macs, participate in fracture healing. Our discovery that bone tissues contain resident osteal macrophages (osteomacs) that exert pro-anabolic influence exposed a novel role for macrophages in bone biology. This included demonstration of a critical role for osteomacs in promoting intramembranous ossification during bone healing. Recruited inflammatory macs are polarized toward an appropriate activation pathway depending on the local environmental cues. M2 polarized macs have been shown to promote wound healing in soft tissue models.

Mac distribution and phenotype through the multiple stages of fracture repair were examined using an internally plated (MouseFix) femoral fracture model that heals via periosteal endochondral callus formation. An in vivo inducible mac depletion model (Mafia) was used to examine mac requirement during different healing phases. Callus formation was assessed via quantitative histology.

Inflammatory M2-like macs (F4/80^{+}Mac-2^{+}Arginase-1^{+}) were distributed throughout the fracture granulation tissue during the late inflammatory phase. Inflammatory macs persist in granulation tissue at the expanding callus fronts and were associated with soft callus vascular invasions. In the late anabolic and remodeling phases osteomacs (F4/80^{+}Mac-2^{neg}) predominated in the maturing hard callus. Local depletion of macs, initiated at the time of surgery, resulted in catastrophic failure of fracture healing, clinching the importance of mac contributions to the initiation of fracture healing. Delayed systemic mac depletion commencing at the transition to early anabolism resulted in a significant 3.3 fold reduction in callus associated macs and 50% reduction in soft callus area ($p=0.006$). A significant positive correlation was observed between residual callus size and efficiency of macrophage depletion ($r = 0.6$). Local administration of the mac-trophic cytokine CSF-1 (therapy initiated at transition to early anabolism) resulted in a 2 fold increased in soft callus formation ($p=0.03$), supporting that macs make substantive contributions to early anabolic processes during callus formation.

Overall, M2-like inflammatory macs are required for initiation and optimal early anabolic progression of fracture healing and are viable targets for development of novel anabolic fracture therapies.

SESSION 3 – IMAGING 2

NANO-CT IMAGING OF HUMAN TRABECULAR BONE USING A LABORATORY SYSTEM

[1]Egon Perilli, [1]Bryant C Roberts, [2]Sarah L Harmer, [2]Paul Kirkbride and [1]Karen J Reynolds

[1]Medical Device Research Institute, School of Computer Science, Engineering and Mathematics, Flinders University, Adelaide,
[2]School of Chemical and Physical Science, Flinders University, Adelaide, SA, Australia
email: egon.perilli@flinders.edu.au

INTRODUCTION

Nano-computed tomography (nano-CT) enables the investigation of bone structure at nano-meter level in 3D [1]. However, because of the small specimen dimensions in nano-CT, 500 μm or below, the specimen preparation is crucial [2].

As part of an ongoing study, we present a nano-CT examination of human trabecular bone using a laboratory system, with preparation details and 3D morphometric measurements performed on osteocyte lacunae.

METHODS

Five trabecular specimens were excised from the center of one human femoral head (fresh-frozen) of a male cadaver (donor age= 89 y). These were removed with a scalpel, obtaining specimens of about 100 μm diameter, 500 μm in length.

Then, specimens were prepared for scanning with a nano-CT system (Zeiss-XRadia Ultra XRM-L200, Carl Zeiss X-ray Microscopy Inc., Pleasanton, CA, US) located at University of South Australia (Ian Wark Research Institute, Mawson Lakes, SA). Under a microscope, specimens were glued (acrylic glue) onto the tip of a thin cylindrical pin (tip of 0.5 mm diameter graphite pencil), which enabled stable fitting into the specimen holder provided by the nano-CT manufacturer.

The nano-CT system was operated at an X-ray source voltage of 40 kV, current 30 mA, in modality "large field of view" (65 x 65 μm, length x width). Two scanning settings were used: (1) "Fast setting": 130 nm isotropic pixel size, rotation step 0.5° (binning 2, total scan time 1.5 hrs). (2) "Slow setting": 65 nm/pixel, rotation step 0.2° (binning 1, scan time 14 hrs).

Cross-section images were reconstructed (XM Reconstructor, Zeiss), exported as 8 bit greylevel images and analyzed (software CT Analyser, Bruker-Skyscan, Kontich, Belgium). Osteocyte lacunae morphology was quantified: lacuna volume, lacuna surface, structure model index (SMI) and the length of the main axes for the lacuna represented as an ellipsoid.

RESULTS AND DISCUSSION

Osteocyte lacunae were visible for both scanning settings, enabling morphometric quantification (Fig.1). The lacuna shown in Fig.1a had a volume of 243 μm^3, surface 449 μm^2, SMI= 3.2 (indicating a structure type more cylinder-like (SMI= 3) than sphere-like (SMI= 4) [3]), main axes lengths 20.5 μm, 6.1 μm, 5.0 μm. A 3D representation of that lacuna is shown in Fig.1b. A lacuna containing partial fillings was also visible, suggesting possible partial calcifications (Fig.1c).

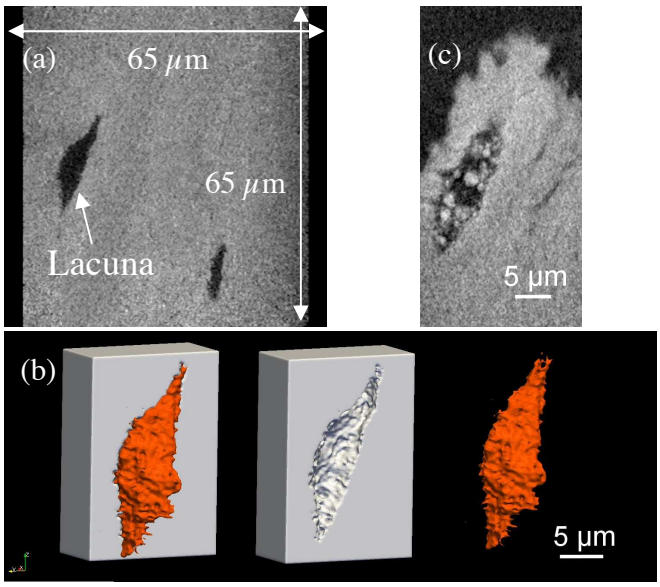

Figure 1: Nano-CT images of trabecular bone. (a) 2D cross-section image, at 130 nm / pixel ("fast setting"), mineralized tissue in light grey, voids in dark grey color. (b) 3D representation of the lacuna shown in (a), with bone in grey color and lacuna in red. (c) 2D cross-section image at 65 nm / pixel of a lacuna containing fillings (light grey), suggesting possible small calcifications.

CONCLUSIONS

We present preliminary results of a study on human bone, performed using a laboratory nano-CT system. Osteocyte lacunae were visualized and their morphology quantified in 2D and 3D at pixel sizes comparable or smaller than reported for similar studies [1] including at the synchrotron [2], although our specimen diameter was limited compared to those studies (0.1 vs. ~ 0.7 mm). A partial filling of an osteocyte lacuna was also visualized, suggesting possible small calcifications. The study is ongoing, with the aim of combining nano-CT with other characterization techniques.

ACKNOWLEDGEMENTS

Intrafaculty Collaborative Grant 2014, Faculty of Science and Engineering, Flinders University (Perilli E, Harmer SL, Kirkbride P)

REFERENCES

1. Van Hove RP, et al., *Bone*. **45**:321-329, 2009.
2. Pacureanu A, et al., *Med Phys*. **39**:2229-2238, 2012.
3. Perilli E, et al., *J Microsc*. **225**: 192-200, 2007.

THE RELIABILITY OF DEXA MEASUREMENTS OF BONE MINERAL DENSITY IN THE METATARSALS

[1,2]Joel Fuller, [1]Jane Archer, [1]Jonathan Buckley, [1]Margarita Tsiros and [2]Dominic Thewlis

[1]Nutrional Physiology Research Centre, University of South Australia, Adelaide, SA
[2]Biomechanics & Neuromotor Labs, University of South Australia, Adelaide, SA
email: joel.fuller@mymail.unisa.edu.au

INTRODUCTION

Measurement of bone mineral density (BMD) using dual-energy X-ray absorptiometry (DEXA) is common to assess bone health and fracture risk [1, 2]. Recently, DEXA has been used to measure BMD in the metatarsals [2], in an effort to explain the disproportionate second and third metatarsal stress fracture rates during running activities [3]. The purpose of this study was to assess the reliability of using DEXA to measure BMD in the metatarsals.

METHODS

BMD of the right foot was measured in 32 trained male distance runners aged 18-40 years using a DEXA scanner (Lunar Prodigy, General Electric Corporation, Madison, WI) with the foot in the plantar position. Separate regions of interest (ROI) were used to assess the BMD of each metatarsal shaft (1st-5th) for each participant. ROI analysis was then repeated one week later by the same investigator in a randomised order to determine intra-rater reliability and by a different investigator to determine inter-rater reliability. Test-retest reliability for DEXA scans was determined using repeat scans, undertaken on the same day, for 10 participants.

Rectangular ROIs were created for each metatarsal (Figure 1). For all metatarsals, the length of the rectangle was set so that only the diaphysis of each metatarsal was included in the ROI. In the case where there was no clear delineation between adjacent metatarsal shafts, the length of the rectangle was only extended to where the proximal end first met an adjacent metatarsal.

RESULTS AND DISCUSSION

Intra-rater reliability was consistently better than inter-rater and test-retest reliability. BMD assessment was consistently most reliable for the first metatarsal (CV=0.9-1.5%) (Table 1).

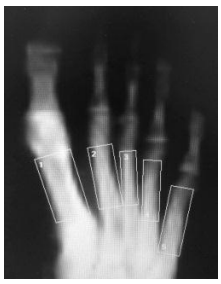

Figure 1: Example region of interest construction for assessment of bone mineral density in the metatarsals.

Reasonable reliability was achieved for the second and fifth metatarsals (CV=2.4-5.8%) (Table 1). Poor levels of reliability were demonstrated for the third and fourth metatarsals (CV=4.2-9.6%) (Table 1). Future research assessing BMD of the metatarsals should focus on measurement of the first, second and fifth metatarsals, which display the greatest levels of reliability. The poor levels of reliability achieved for the third metatarsal suggest that DEXA may not be an appropriate technique for investigating the reasons for disproportionate rates of running-related stress fractures in the third metatarsal [3].

CONCLUSIONS

A reliable method of measuring BMD was achieved for the first, second and fifth metatarsals. This method could be used in both clinical and research settings to assess bone health and fracture risk of these metatarsals.

REFERENCES

1. Kelsey JL, et al. *Med Sci Sports Exerc*. **39**:1457-63, 2007.
2. Sindel M, et al. *Anatomy*. **4**:39-44, 2010.
3. Gross TS, et al. Am J Sports Med. **17**:669-674, 1989.

Table 1: Intra- and inter-rater reliability for defining regions of interest and intra-rater reliability for test-rest DEXA scans.

Metatarsal	Intra-rater reliability ROI			Inter-rater reliability ROI			Test-retest scan reliability		
	Diff ($g \cdot cm^{-2}$)	CV	ICC	Diff ($g \cdot cm^{-2}$)	CV	ICC	Diff ($g \cdot cm^{-2}$)	CV	ICC
First	-0.001 ± 0.010	0.9%	>0.99	0.001 ± 0.010	1.2%	0.99	-0.010 ± 0.014	1.5%	0.98
Second	0.002 ± 0.017	2.4%	0.97	-0.001 ± 0.017	2.4%	0.97	0.006 ± 0.031	4.2%	0.90
Third	-0.001 ± 0.034	4.2%	0.92	-0.010 ± 0.039	4.8%	0.89	0.010 ± 0.058	8.2%	0.64
Fourth	-0.010 ± 0.066	9.1%	0.71	-0.028 ± 0.069*	9.6%	0.67	-0.003 ± 0.041	6.2%	0.80
Fifth	0.006 ± 0.022	3.3%	0.97	-0.010 ± 0.042	5.8%	0.90	-0.002 ± 0.027	4.2%	0.93

Note. Difference values are mean ± standard deviation. ROI, region of interest; Diff, difference for assessment #1 - #2; CV, coefficient of variation; ICC, intra-class correlation coefficient. *p<0.05.

IMPACT OF SUBCHONDRAL BONE PLATE INTEGRITY ON THE HOMEOSTASIS OF THE UNDERLYING SUBCHONDRAL TRABECULAR BONE IN LATE-STAGE OSTEOARTHRITIS

[1, 2]Guangyi Li, [1]Euphemie Landao-Bassonga, [1]Tak S Cheng, [1]Nathan J Pavlos, [2]Changqing Zhang, and [1]Ming H Zheng

[1] Centre for Orthopaedic Research, School of Surgery, The University of Western Australia, Perth, Australia
[2] Department of Orthopaedics, Shanghai Jiao Tong University Affiliated the Sixth People's Hospital, Shanghai, China
email: Leepotter2003@163.com

INTRODUCTION

Although osteoarthritis (OA) has long been considered as a primary disorder of cartilage, the contribution of subchondral bone to the pathogenesis of OA is arousing increasing interests. Subchondral bone, consisting of subchondral bone plate (SBP) and underlying subchondral trabecular bone (STB), has been widely reported to play a pivotal role in both the initiation and progression of OA. SBP, a thin dense mineralized lamella lying immediately underneath cartilage, has a significant mechanical and biochemical function in the joint homeostasis.

In early-stage OA, thinning and increased porosity of SBP has been described in several studies, together with the temporal bone loss in STB. These phenomena were testified to be strongly associated with cartilage degeneration. As the cartilage damage progresses, osteoblast activity is elevated, leading to an increase of SBP thickness, decrease of SBP porosity and sclerosis of STB. If the condition worsens and little or no cartilage remains, SBP will be exposed and the opposing joint surfaces may end up rubbing "bone upon bone". The direct hard tissue contact and grinding may eventually lead to the breach and damage of SBP, making the STB beneath denuded. However, little is known about the influence of SBP on the homeostasis of the underlying STB in late-stage OA when full-thickness loss of cartilage occurs.

This study was to investigate the impact of SBP integrity on the homeostasis of the underlying STB in late-stage OA when articular cartilage is eroded in full-thickness.

METHODS

Peri-articular bone cylinders were extracted in the load-bearing region of femoral heads from 110 patients with late-stage OA. After micro-CT scanning, the bone samples were categorized into two groups: 1) samples with partial-thickness abrasion of SBP, without exposure of STB; and 2) samples with full-thickness abrasion of SBP, with exposure of STB. Micro-CT and histology were performed to analyze the microarchitecture, bone remodeling and pathological changes of STB in all samples.

RESULTS AND DISCUSSION

In samples with full-thickness abrasion of SBP, STB was detected with a more sclerotic microarchitecture and more active bone remodeling, compared to the counterparts with partial-thickness abrasion of SBP. In samples with partially abrased SBP, most microarchitecture and bone remodeling parameters of STB did not correlate with thickness and porosity of SBP. However, in samples with full-thickness abrasion of SBP, the larger SBP defect area became, the more sclerotic in microarchitecture and more active in bone remodeling STB displayed. In samples with full-thickness abrasion of SBP, there were also higher occurrence of pathological lesions in STB, including bone cysts, bone marrow edema, fibrosis, and blood vessels with fibrinoid deposition and hyperplastic walls.

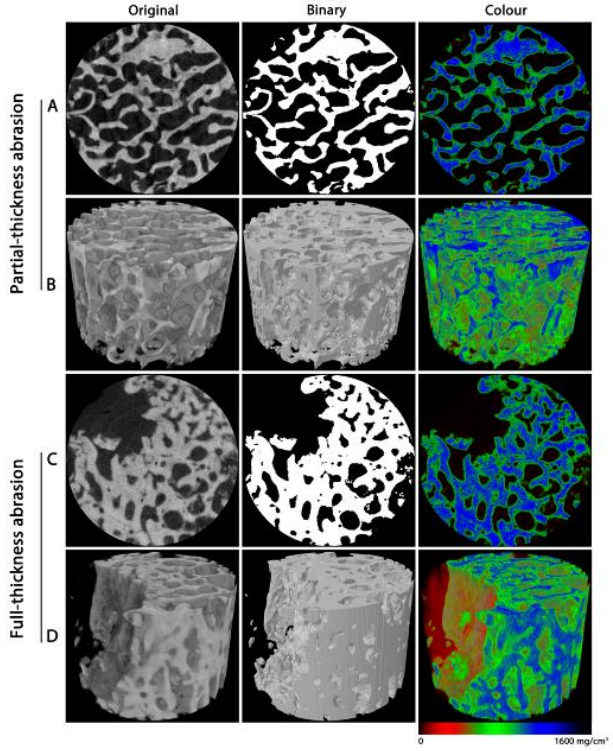

Figure 1: Representative original, binary and colour micro-CT images of the STB from the samples with partially abrased SBP or fully abrased SBP.

CONCLUSIONS

SBP plays a pivotal role in the maintenance of the underlying STB homeostasis, especially in late-stage OA when cartilage is completely eroded in thickness.

ACKNOWLEDGEMENTS

The authors would like to thank staff from Perth Bone & Tissue Bank for helping with patient recruitment and sample collection.

EARLY MIGRATION CHRACTERISTICS OF THE CL2 CEMENTLESS FEMORAL STEM AND CORAIL FEMORAL STEM: A RADIOSTEREOMETRIC ANALYSIS (RSA) STUDY

[1]Drew Grosser, [2]Graham Mercer, [2]Christopher J. Wilson, [3]Kjell G. Nilsson and [4]Jegan Krishnan

[1]The International Musculoskeletal Research Institute Inc., Repatriation General Hospital, Daw Park, SA, Flinders University, Bedford Park, SA, Australia
[2]Department of Orthopaedics, Repatriation General Hospital, Daw Park, SA, Australia
[3]Department of Orthopaedics, Umeå University Hospital, Umeå, Sweden
[4]The International Musculoskeletal Research Institute Inc., Department of Orthopaedic Surgery, Flinders Medical Centre, Bedford Park, SA, Australia
email: drew.grosser@imri.org.au

INTRODUCTION

Safety and efficacy of novel prostheses relies on the determination of early implant migration and subsequent risk of loosening. Radiostereometric Analysis (RSA) has been used to evaluate the clinical failure risks of femoral stems by reporting distal migration, a measure of stem subsidence, when examining early migration characteristics [1]. The migratory patterns of femoral stems, 24 months postoperatively, have provided a surrogate outcome measure to determine implant stabilisation and predict long-term performance and survivorship. RSA evaluated the early migration characteristics of the CL2 cementless femoral stem and compared the behaviour and pattern of migration with the Corail femoral stem.

METHODS

Twenty five patients undergoing primary total hip arthroplasty were implanted with the CL2 cementless femoral stem. The median age was 65 years (range, 43-75 years). During surgery tantalum markers were attached onto the distal tip and shoulder of the stem. Eight tantalum markers were inserted into the femur, four placed in each of the greater and lesser trochanter. RSA examinations were performed postoperatively at 4 to 5 days, 6, 12 and 24 months. The data from eleven patients who had complete RSA follow-up and the valid data from five patients who had incomplete RSA follow-up were used. RSA data were analysed to determine the movement of the femoral stem relative to the femur and were compared to the published data for the Corail femoral stem.

RESULTS AND DISCUSSION

At 24 months the magnitude of migration of the femoral stem translations for the y axis of movement was 0.32 mm (range, 0.00 to 2.04 mm) (Figure 1). Our data suggests that distal stem migration was confined to the first 6 months postoperatively with subsequent stabilisation exhibited between 6 and 24 months postoperatively. Mean subsidence/distal migration of the femoral stem was 0.22 mm at 6 months, 0.26 mm at 12 months and 0.20 mm at 24 months (Figure 2). In comparison with the Corail femoral stem [1] the CL2 cementless femoral stem demonstrates less stem subsidence when observing early migration characteristics with RSA.

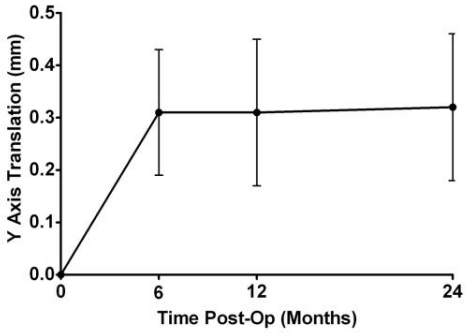

Figure 1: Mean absolute femoral stem translations for the y axis of movement after 6, 12 and 24 months postoperatively. The ranges show the standard error of the mean.

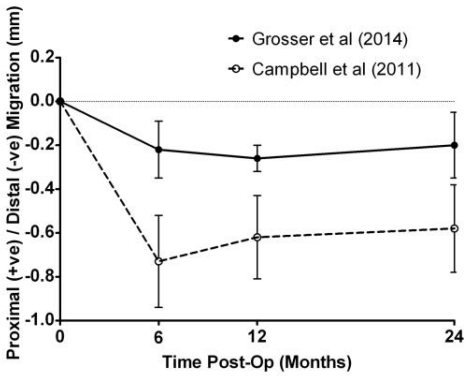

Figure 2: Comparison of mean femoral stem subsidence (mm) after 6, 12 and 24 months postoperatively. The ranges show the standard error of the mean.

CONCLUSIONS

Our study demonstrates a predictable migratory pattern for the CL2 cementless femoral stem with early migration characteristics that behave similarly to the Corail femoral stem.

REFERENCES

1. Campbell D, et al., *Int Orthop*. **35(4)**:483-488, 2011.

CONFLICT OF INTEREST DECLARATION

In the interests of transparency and to help reviewers assess any potential bias, ANZORS requires authors of original research papers to declare any competing commercial interests in relation to the submitted work. Referees are also asked to indicate any potential conflict they might have reviewing a particular paper.

If you have accepted any support such as funds or materials, tangible or intangible, concerned with the research by the commercial party such as companies or investors, choose YES below, and state the relation between you and the commercial party.

If you have not accepted any support such as funds or materials, choose NO.

Do you have a conflict of interest to declare? (DELETE TEXT as appropriate)

YES

If YES, please complete as appropriate:

1. The author(s) did receive payments or other benefits or a commitment or agreement to provide such benefits from a commercial entity.
   State the relation between you and the commercial entity:

   N/A

2. A commercial entity paid or directed, or agreed to pay or direct, any benefits to any research fund, foundation, educational institution, or other charitable or nonprofit organization with which the authors are affiliated or associated.

   The Department of Orthopaedics, Repatriation General Hospital (through its research arm, the International Musculoskeletal Research Institute Inc.) received payment from Austofix Surgical Pty Ltd to cover the costs of undertaking this research project.

   No member of the research team received a personal financial benefit from their involvement in this research project.

IMAGING FEMORAL PERIPROSTHETIC OSTEOLYSIS AROUND TOTAL HIP ARTHROPLASTIES USING A HUMAN CADAVER MODEL

Daniel Miles, Caroline Moran, Bogdan Solomon, Roumen Stamenkov,
Dennis Kosuge, Tim Cordier, Stuart Callary, Donald Howie.

Centre for Orthopaedic and Trauma Research, University of Adelaide,
Department of Orthopaedics and Trauma, Royal Adelaide Hospital, Adelaide, South Australia
email: Caroline.Moran@adelaide.edu.au

INTRODUCTION

Femoral periprosthetic osteolysis around Total Hip Arthroplasty can lead to aseptic loosening, periprosthetic fracture and complex revision surgery. The ability to measure osteolysis using a sensitive and accurate method may allow improved diagnosis, monitoring and predictions regarding the risk of progression and imminent catastrophic failures, as well as assist in pre-operative planning for revision surgery [1,2]. This study aimed to compare the use of plain radiographs (XR), computed tomography (CT) and Magnetic Resonance Imaging (MRI) for identifying and measuring simulated femoral periprosthetic bone lesions in a human cadaver model.

METHODS

Institutional ethics approval was obtained from the Royal Adelaide Hospital Ethics Committee. All specimens were prepared by an experienced orthopaedic surgeon (L.B.S.). Four cadaver femurs were imaged with AP and lateral XR views, CT and MRI at baseline (with no simulated defects) and then further 2 times, after the creation of increasingly large defects. A total of 77 lesions (mean volume 1.87cm^3, range 0.31 – 12.12cm^3) were created in Gruen Zones 1-7 to simulate femoral periprosthetic osteolysis. Each of the femurs was imaged individually with a cementless femoral component and then a cemented component, and also in a pair (bilateral cemented). A human cadaver pelvis from a previous in-vitro study [3] with bilateral acetabular components was used to position femurs in anatomical alignment during imaging.

The digital images were randomized and examined by 3 assessors experienced in clinical radiographic analysis. The presence and location of lesions were noted, and also measured for CT and MRI images. All assessors repeated their examinations approximately 2 months after their initial assessments.

Sensitivity was calculated as the proportion of actual positives correctly identified. Specificity was calculated as the proportion of negatives correctly identified. Accuracy of the volume measurements was calculated as the mean difference between the actual lesion volume physically measured in the specimen and the volume determined by the imaging technique. Statistical analysis was performed with SAS 9.3 software (SAS Institute Inc., Cary, NC, USA).

RESULTS AND DISCUSSION

The median sensitivity of bone lesion detection was 54% for XR and MRI, and 75% for CT. The difference between the maximum sensitivity achieved with each modality was not significant. Metal artefact on CT and MRI made it difficult to observe lesions in Gruen Zones 1 and 7 where the femoral component is thickest and resulted in weaker sensitivity for all three modalities. The median specificity was 95% for AP radiographs, 92% for CT and 95% for MRI. No significant difference was found between the three modalities regarding the specificity of bone lesion detection in any Zone. Plain radiographs do not allow volumetric measurement of bone lesions. The accuracy error of volumetric measurements was poorest in Zones 1 and 7 for both CT and MRI. Both modalities had comparable accuracy in the proximal region, however MRI was significantly more accurate in the distal region.

CONCLUSIONS

CT was found to have the highest sensitivity for bone lesion detection. Metal artefact limited the sensitivity of proximal lesion detection and accuracy of volumetric measurement for both CT and MRI. MRI was more accurate than CT for distal lesions. CT and MRI may both be useful for monitoring the progression of femoral periprosthetic osteolysis, predicting risk of progression and catastrophic failure as well as assisting in pre-operative planning for revision surgery

ACKNOWLEDGEMENTS

Authors wish to thank Suzanne Edwards, Discipline of Public Health, University of Adelaide for statistical advice and analyses.

REFERENCES

1. Howie et al., *Inflammopharmacology*, **6:**389, 2013.
2. Solomon et al., *J Arthoplasty*, **27:**913, 2010.
3. Stamenkov et al., *Clin Orthop Relat Res*, **412:**117, 2003.

THE UNIVERSITY of ADELAIDE
CENTRE FOR ORTHOPAEDIC AND TRAUMA RESEARCH

RADIOGRAPHIC ALIGNMENT ANALYSIS : INTEROBSERVER VARIABILITY POST TOTAL KNEE ARTHROPLASTY

[1]Anneka Stephens, [2]Christopher Wilson and [3]Meenu Shunmugam and [4]Jegan Krishnan

[1]International Musculoskeletal Research Institute, Adelaide, SA
[2]Repatriation General Hospital, Daw Park, SA
[3]Flinders Medical Centre, Bedford Park, SA
[4]Flinders University, Bedford Park, SA
email: Anneka.Stephens@imri.org.au

INTRODUCTION

Inter- and intra-observer variation has been noted in the analysis of radiographic examinations with regard to experience of surgeons, and the monitors used for conducting the evaluations. The aim of this study is to evaluate inter/intra observer variation in the measurement of mechanical alignment from long-leg radiographs.

METHODS

40 patients from the elective waiting list for TKA underwent long leg radiographs pre-operatively and 6 months post-operatively (total of 80 radiographs). The x-rays were analysed by 5 observers ranging in experience from medical student to head orthopaedic surgeon. Two observers re-analysed their results 6 months later to determine intraobserver correlation, and one observer re-measured the alignment on a different monitor. These measurements were all conducted blindly and none of the observers had access to the others' results.

RESULTS AND DISCUSSION

80 radiographs were analysed in total, 40 pre-op and 40 post-op. The mechanical alignment was analysed using Pearson's correlation (r = 0 no agreement, r = 1 perfect agreement) and revealed that experience as an orthopaedic surgeon has little effect on the measurement of mechanical alignment from long leg radiograph. The results for the different monitor analysis were also analysed using Pearson's correlation of long leg alignment. Monitor quality does seem to affect the correlation between alignment measurements when reviewing both intra and inter observer correlation on different computer monitors, but the effect displayed was shown to have no statistical significance. Bland-Altman plot of the results show little trend in the effect of deformity on the intraobserver analysis. The result illustrated the tendency for observers to measure alignment as are increasingly varus. Also demonstrated by the bland-altman plot is the tendancy of the medical student to over-estimate deformities.

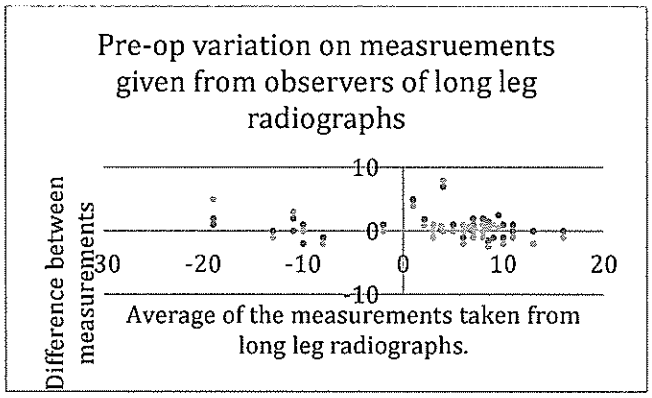

CONCLUSIONS

Surgical experience has little impact on the measurement of alignment on long leg radiographs. It seems that there is a tendency to overestimate the varus nature of the alignment measurement, and also with less experience and in the case of the medical student, the deformities seem to be overestimated. This observation demonstrates that measurement should be reviewed by a senior surgeon if the observer is very inexperienced.
Observers of higher levels of experience correlate well with the senior surgeons and their measurements are shown to be reliable when compared to that of the consultants.

ACKNOWLEDGEMENTS

Biomet Australia Pty Ltd

CONFLICT OF INTEREST DECLARATION

Do you have a conflict of interest to declare?

YES

If YES, please complete as appropriate:

1. A commercial entity paid or directed, or agreed to pay or direct, any benefits to any research fund, foundation, educational institution, or other charitable or nonprofit organization with which the authors are affiliated or associated.

SESSION 4 – BIOMECHANICS 3

Effect of ligament combination on menisci and cartilage loading following multiple ligament knee reconstruction

[1,2]Samuel Grasso, [1]Corey Scholes PhD, [2]Qing Li PhD, [1]Brett Fritsch FRACS

[1]Sydney Orthopaedic Research Institute, Sydney, NSW
[2]School of Aerospace, Mechanical and Mechatronic Engineering, The University of Sydney, Sydney, NSW
email: samuel.grasso@hotmail.com

INTRODUCTION

The knee is one of the most complex joints in the human body distinguished by its complex geometry and multi-body articulations. Optimal joint stability and compliance during functional activities are provided through anatomical structures such as the anterior cruciate ligament (ACL), posterior cruciate ligament (PCL), medial collateral ligament (MCL) and lateral collateral ligament (LCL), menisci, and articular cartilage.

Multiple ligament knee injuries (MLKI) occur when two or more of these ligaments are injured. Despite many investigations into knee biomechanics, the exact mechanical behaviour of the knee joint and its response to injury and treatment is still unknown. Clinical observations [1] have reported a higher incidence of knee osteoarthritis in individuals who had sustained a ligament injury, with one study concluding that individuals with a history of knee injury are 7.4 times more likely to develop osteoarthritis than those without [2].

The purpose of this investigation is to determine the location and magnitude of the stress on the menisci and cartilage, due to the loading of different reconstructed knee ligament combinations, their materials properties and physical dimensions after MLKI surgery.

METHODS

Two patients who underwent MLKI reconstruction (avg 52 ± 5 years old, 1.6 ± 0.6 m, 63 ± 2 Kg, 2 female) had both knees imaged with 3.0Tesla MRI approximately 10 years after surgery. Scans were manually segmented and 3D solid models of the femur, tibia, menisci, cartilage and the four ligaments were created (ScanIP, Simpleware)(Figure 1). The various ligament combinations were created by interchanging ligaments from both patients and placing them on the healthy knee of one of the patients. The ligaments were scaled to fit their anatomical position on the healthy knee under the guidance of a surgeon. The knee geometries were then converted into solid tetrahedral elements. Finally, meshed geometries were imported into ABAQUS FE package v6.10 (SIMULA, Waltham, MA) to generate the finite element models.

Table 1: Assigned material properties to FE knee structures

Structure	Density (g/cm^3)	Young's Modulus (Mpa)	Poisson's Ratio
[4] Bone	2	20,000	0.2
[3] Menisci	1.5	59	0.49
[4] Cartilage	1	15	0.475
[4] Ligaments	1	Hyper-elastic	-

The material properties assigned to each structure are summarised (Table 1). Constraints, interactions, and boundary conditions were chosen in a way to assure an unconstrained, stable response of the tibiofemoral articulations throughout range of motion. To optimise computational expense without

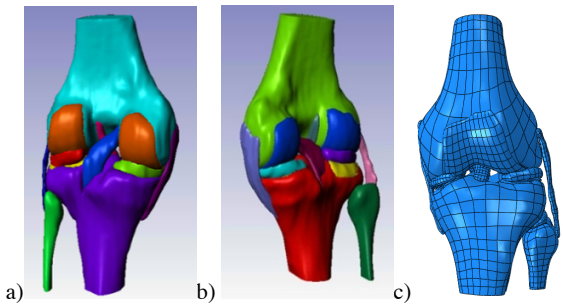

Figure 1: 3D Solid model a) reconstructed knee, b) healthy knee; c) Finite element model of the reconstructed knee.

conditions were chosen in a way to assure an unconstrained, stable response of the tibiofemoral articulations throughout the range of motion. To optimise computational expense without sacrificing model predictions, the distal femur, proximal tibia and proximal fibula were modelled as rigid bodies while the remaining structures were considered deformable. A frictionless surface-to-surface tangential contact with nonlinear finite sliding property was used to simulate articular surfaces [3,4]. A set of primary and secondary contact surfaces were defined for each contact pair [3,4].

RESULTS AND DISCUSSION

It will be lucid that the peak stress (σ=F/A) magnitude and location will be different on the menisci and cartilage due to the altered load (F) bearing from the different reconstructed ligament combinations. This is for the reason that the materials used to form the reconstructed ligaments have different materials properties and dimensions such as the Young's modulus ($E=\sigma/\varepsilon$), strain ($\varepsilon=l-l_0/l_0$) and cross-sectional area ($A=\pi r^2$). Stress is a measure of the internal force an object is experiencing per unit cross sectional area. The Young's modulus states how much a material will strain (ie., stretch or compress (l) from its original length (l_0)).

CONCLUSIONS

MLKI reconstruction surgery restores stability to the knee joint. However, optimal compliance during functional knee activities may be limited due to different material properties and dimensions reconstructed ligaments have.

ACKNOWLEDGEMENTS

This project has been funded by The Friends of the Mater Foundation and the Mater Medical Staff Association.

REFERENCES

1. Lohmander, L. S., et al., *Arthritis & Rheumatism,* **50(10)**, 3145-3152, 2004.
2. Wilder, F. V., et al., *Osteoarthritis and Cartilage*, **10(8)**, 611-616, 2002.
3. Bendjaballah, M. Z., et al., *Clin. Biomech*, **12(3)**, 139–148m, 1997.
4. Donahue, T. L., et al., *ASME J. Biomech. Eng.*, **124(3)**, 273–280, 2002.

SUBJECT-SPECIFIC KNEE KINEMATICS USING MRI INFORMED PARALLEL MECHANISM

[1]Simao Brito da Luz, [1]Luca Modenese, [1]Peter Mills, [1]Belinda Beck, [2]Nicola Sancisi and [1]David Lloyd

[1]Centre for Musculoskeletal Research, Griffith Health Institute, Griffith University, QLD
[2]DIEM, University of Bologna, Italy
Email: simao.britodaluz@griffithuni.edu.au

INTRODUCTION

Subject-specific neuromusculoskeletal (NMSK) computer simulation models can estimate muscle and joint articular forces, enabling the identification of the multiple factors causing joint disease or injury [1]. NMSK models include representations of joint kinematics, and common musculoskeletal simulation software, e.g. OpenSim [4], use simplified 2D sagittal plane knee models. These models are generic, and simply scaled for each subject using external markers from motion analysis. NMSK models with scaled generic knee kinematics produce less accurate estimates of measured knee articular forces compared to those with subject-specific kinematic models [2]. Methods are needed to readily create subject-specific joint kinematic models.

Passive tibia-femoral (TF) and patella-femoral (PF) kinematics measured in cadavers can be well predicted using 3D TF and PF models respectively [4,5]. These models integrate the cadaver's subject-specific bone and cartilage geometry, ligaments and tendon lengths and insertion points, to constrain the degrees of freedom (DOF) of the respective joints. Using the tibial-femoral (i.e. knee) flexion angle as input, the TF model estimates tibia's abduction-adduction and internal-external rotations as well as 3D displacements, relative to the femur [4]. The PF model estimates patella's 3D rotation and displacements relative to the femur also using knee flexion angle as input [4].

This study aimed to use MRI images of the *in vivo* knees to construct combined TF and PF subject-specific models for use in OpenSim. We also compared the resulting passive TF and PF kinematics with those from cadaveric studies.

METHODS

Both models were based on those described in [4,5], but modified to enable the geometry to be determined off the MRI images. Fourteen participants were scanned in a 3T MRI scanner with axial slices of the complete lower limb and sagittal slices of the hip, knee and ankle joints. Semi-automatic segmentation, alignment and smoothing of tissues of interest were performed, from which 3D volumetric surfaces were generated (Figure 1).

The segmented data were used to create anatomical geometry and bone coordinate frames according to the ISB standards. In this, spheres were fitted to the femoral and tibial condyles. Two spheres were also fitted to the femoral trochlea with their centers defining the PF hinge axis. Ligament attachment points were selected from regions where isometric fibers bundles exist.

For flexion angles from 0° to 90° the kinematics of the unknown 11 DOF from both TF and PF models were determined by minimizing the length change of ligaments and change in the distance between the spheres' centers, the latter having the effect of avoiding sphere inter-penetration and lift-off. Geometric optimization was performed with simulated annealing to avoid singularities and to best match the patterns of the cadaveric results.

Figure 1: 3D surface of femur, tibia and patella with respective cartilages with tibia and patella motion.

RESULTS AND DISCUSSION

Both TF and PF well approximated the cadaveric data. TF correlation values were 0.60± abd-adduction, 0.93 int-ext rotation, 0.93 ant-posterior, 0.97 prox-distal and -0.95 med-lateral displacements. PF correlation values were 0.99 flexion, 0.58 abd-adduction, 0.86 int-ext rotation, 0.91 ant-posterior, 0.76 prox-distal and 0.19 med-lateral displacements. The differences in participants bone and ligament morphology compared to cadavers may explain some of low correlations. Nevertheless, the overall good correlations indicate the models can be used to reproduce subject-specific knee kinematics.

CONCLUSIONS

TF and PF joints kinematics can be well estimated using 3D geometric models with parameters obtained from MRI. These can then be used in subject-specific NMSK models.

REFERENCES

1. Lloyd D.G, et al., *Routledge Handbook of Biomechanics and Human Movement Science*. 3-17,2008
2. Gerus P., et al., *Journal of Biomechanics*, **46**:2778-2786, 2013.
3. Delp,S.L.,.et al., *IEEE Transactions on Bio-Medical Engineering*, **54**:1940–1950, 2007.
4. Sancisi N, et al., *Journal of Mechanisms and Robotics*.**3**:1-7,2011
5. Ottoboni A, et al., *Journal of Engineering in Medicine*.**224**:1121-1132,2010

THE HOLDING STRENGTH OF CANCELLOUS SCREWS DEPENDS ON INSERTION TORQUE, BONE MICRO-ARCHITECTURE AND AREAL BONE MINERAL DENSITY

[1]Rosidah Ab-Lazid, [1]Egon Perilli, [1]Melissa Ryan, [1]John J Costi and [1]Karen J Reynolds

[1]Biomechanics & Implants Research Group, Medical Device Research Institute, School of Computer Science, Engineering and Mathematics, Flinders University, Adelaide, SA
email: abla0002@flinders.edu.au

INTRODUCTION

For cancellous bone screws, the respective roles of the applied insertion torque (T_{Insert}) and of the quality of the host bone (microarchitecture, areal bone mineral density aBMD), in contributing to the mechanical holding strength of the bone-screw construct ($F_{Pullout}$), are still unclear. During orthopaedic surgery screws are tightened, typically manually, until adequate compression is attained, depending on surgeons' manual feel [1]. This corresponds to a subjective insertion torque control, and can lead to variable levels of tightening, including screw stripping. The aim of this study was to determine, which among measurements of aBMD, bone microarchicture, and applied T_{Insert}, has the strongest correlation with $F_{Pullout}$ assessed experimentally.

METHODS

Forty-six femoral heads obtained from hip replacement surgery (donors' age mean (SD) = 78.2 (9.6) years; 17 females, 29 males) were utilised, over which microarchitecture and aBMD were evaluated using micro-computed tomography and dual X-ray absorptiometry [2].

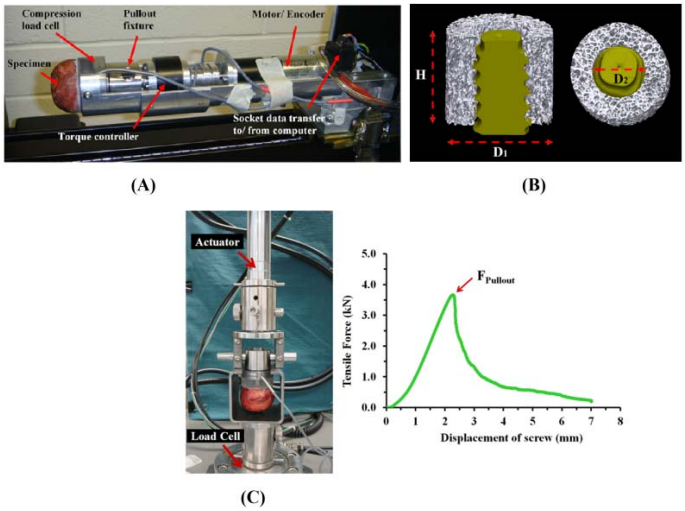

Figure 1: (A) Automated screw tightening by using the test rig. (B) 3D micro-CT images of the trabecular volume of interest surrounding the screw (H= 12 mm, D1=14 mm and D2 = 7.2 mm) over which microarchitectural parameters were evaluated. (C) Screw pullout test.

Using an automated micro-mechanical test device, a cancellous screw was inserted in the femoral heads at T_{Insert} set to 55% to 99% of the predicted stripping torque beyond screw head contact. Then, a screw pullout test was performed, to measure $F_{Pullout}$. Pearson's correlation coefficient (R) was used to evaluate the relationships between $F_{Pullout}$ and aBMD, the bone microarchitectural parameters (bone volume fraction (BV/TV), structure model index (SMI), trabecular thickness, number, separation) and T_{Insert}. Stepwise forward regression analysis was performed to evaluate whether the combination of aBMD, microarchitectural parameters and T_{Insert}, would improve the prediction of $F_{Pullout}$ beyond that with single parameters. In all tests, significance level was set to p=0.05.

RESULTS AND DISCUSSION

$F_{Pullout}$ exhibited the strongest correlation with T_{Insert} (R=0.88, p<0.001), followed by the microarchitectural parameters SMI (R=-0.81, p<0.001) and BV/TV (R=0.73, p<0.001), and by aBMD (R=0.66, p<0.001). Combinations of T_{Insert} with microarchitectural parameters and/or aBMD did not improve prediction of $F_{Pullout}$.

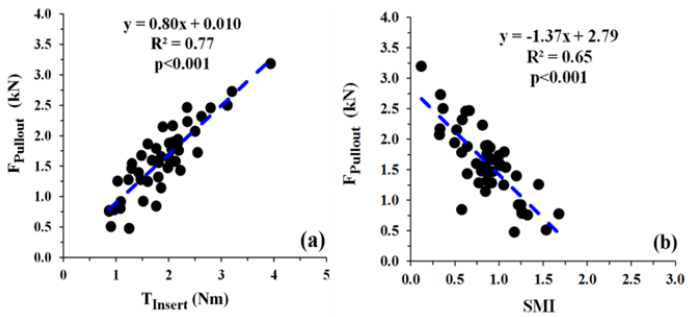

Figure 2: Scatter plots and best fit lines for (a) "$F_{Pullout}$ vs. T_{Insert}" and (b) "$F_{Pullout}$ vs. SMI (Structure Model Index)". SMI values range from 0 to 3, with SMI=0 indicating ideal plate-like structures, SMI=3 rod-like structures, values in-between a combination of the two.

CONCLUSIONS

These results indicate that, for cancellous screws, $F_{Pullout}$ depends most strongly on the applied T_{Insert}, followed by the microarchitecture and aBMD of the host bone. In cancellous bone, screw tightening increases the holding strength of the screw-bone construct.

ACKNOWLEDGEMENTS

This study is funded by the NHMRC Grant ID 595933.

REFERENCES

1. Siddiqui A, et al., Injury **36**(1):55-59, 2005
2. Ab-Lazid R, et al., *J. Biomech* **47**(2):347-353, 2014.

SIMPLE MEASURES OF PATIENT WEIGHT, BONE PROPERTIES AND GEOMETRY ARE PREDICTORS OF FEMORAL NECK STRAINS

Mark Taylor, Egon Perilli and Saulo Martelli
Medical Device Research Institute, School of Computer Science, Engineering and Mathematics, Flinders University, Bedford Park, South Australia, Australia
email: mark.taylor@flinders.edu.au

INTRODUCTION

Areal BMD measurements from DEXA are the standard tool for clinical assessment of patients at risk of femoral fractures, but they are poor predictors either in terms of sensitivity and specificity. Including 3D geometrical and BMD information, finite-element models generated from patients' CT scan have been shown to be more reliable [1]. However, FE modelling cannot be implemented in routine clinical practice because of the invasive nature of CT scans and generating FE models is time consuming, making it financial unviable.

Surrogate models can bridge the gap between FE models and the clinical application. Anatomical and physiological variation within the population of interest can be modelled. Therefore, surrogate models are well suited for exploring the relationships between FE-based bone strains vs 3D geometrical and BMD parameters collectable in the clinic. This study explores the development of a surrogate modelling approach to predict femoral neck strains, using previously developed population-based FE models.

METHODS

A population of 50, 100, 200, 500 and 1000 femurs was generated, by using a previously developed active appearance model (AAM) of the femur [2] and the latin hypercube sampling of the first 30 modes of the AAM. A further 100 synthetic femurs were generated, to later test the surrogate model. For each femur the following features were automatically measured from the FE model, using a custom matlab script: femur length, femoral head diameter, femoral neck max and min diameters, CCD angle, anteversion angle, femoral neck length, neck volume, neck bone mass, femoral neck cortical bone volume and the subject mass. Each femur was subjected to the peak forces associated with the stance phase of level gait, using a reduced muscle force set [3]. A region of interest was defined in the femoral neck, where the minimum, maximum and equivalent strain distributions were predicted.

Statistics: To estimate the strain in the femoral neck, a surrogate modelling approach was used, based on the subject's simple geometric information, bone volume and bone mass and body weight. Multivariate linear regression was performed to identify variables that were predictors of the mean and the 90th percentile strain values. Variables were selected based on a significance level of less than 0.05. Based on this analysis, a surrogate model was built and tested against FE predictions of the 100 unseen synthetic femurs.

RESULTS AND DISCUSSION

The main variables which determined the femoral neck strain were, in order of importance: subjects' body weight, femoral neck bone mass, femoral neck volume, and femoral neck length. Based on these four variables, the linear surrogate model was able to reliably predict the mean and 90th percentile equivalent strains (Fig. 1) with corresponding RMS errors of 1.64x10^{-4} (approx. 10% of the mean) and 3.95 x10^{-4} (approx. 10% of the mean). Similar predictive ability was seen for the minimum principal strain and the mean maximum principal strains (R^2 between 0.81 and 0.88). However, predictive ability of the surrogate model for the 90th percentile of maximum principal strains was lower (R^2 = 0.54 and RMSE = 3.95 x10^{-4}). Similar performance was achieved from the surrogate models based on a training set of just 50 femurs, as compared to 100 to 1000 femurs.

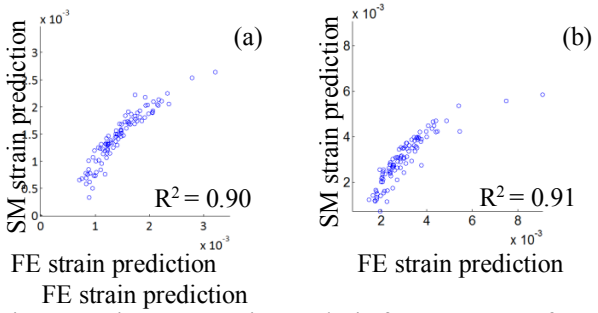

Figure 1: Linear regression analysis for 100 unseen femurs, of (a) the mean equivalent strain and (b) the 90th percentile equivalent strain, as predicted by finite element (FE) analysis (x axis) and the surrogate model (SM) (y axis).

CONCLUSIONS: A simple surrogate model, based on measures of a subjects' body mass, neck bone density and geometry can reliably predict the magnitude of femoral neck strains as as compared with predictions form CT based FE models (R^2=0.90). Such a model could be used to enhance the prediction of femoral neck fracture risk.

REFERENCES :

[1] Testi et al., Ann. Biomed. Eng., 2002, 30, 801-807.
[2] Bryan et al., J. Biomech., 2009, 42, 2171-2176.
[3] Heller et al., J. Biomech., 2005, 38, 1155-1163.

Three-dimensional frictional moment induced from head-cup bearings of hip joint implants

[1]Hamidreza Farhoudi, [1]Reza Oskouei, [2,3]Claire Jones and [1]Mark Taylor

[1]School of Computer Science, Engineering and Mathematics, Flinders University, SA, Australia
[2]School of Medicine & School of Mechanical Engineering, University of Adelaide, SA, Australia
[3]Adelaide Centre for Spinal Research, SA Pathology, SA, Australia
Email: reza.oskouei@flinders.edu.au

INTRODUCTION

Pseudotumors and metallosis have been associated with fretting and corrosion products generated at the taper junctions of modular total hip replacements (THR). The exact mechanisms leading to pseudotumors are poorly understood, but there is a higher incidence with large diameter heads and metal-on-metal articulations, suggesting that the mechanical environment plays an important role. In this study, an analytical method was developed to determine the frictional moment at the head-cup interface of THRs and the resulting torsional load at the modular head-neck interface. The analytical method was then used to investigate the frictional moments associated with walking gait.

METHODS

The head-cup frictional moment was determined by integrating the product of the differential friction force ($\mu_k.p.dA$; where μ_k is the coefficient of kinetic friction and p is the normal contact pressure according to Hertz contact theory), and its perpendicular distance to the rotation vector (lever arm D), over the contact area (A) (Equation 1, Figure 1a). The integral is calculated for each instant of activity, considering the body force (P) and the instantaneous axis of rotation (IAR). The IAR was determined via combined implementation of Euler Angle rotation, Fixed Angle rotation and Angle-Axis rotation methods. Analytical results were compared to the *in vitro* experimental results of Bishop [2] for a number of implant configurations; published graphs were quantized into 100 points per cycle and regressed against the corresponding frictional moment predicted by the analytical model. The method was used to evaluate walking gait with joint characteristics [3], body force during gait cycle [4] and joint kinematics [5] from published sources.

$$M_f = \oint_A D.\mu_k.p.dA \quad \text{(Equation 1)}$$

RESULTS AND DISCUSSION

The analytical method showed a good prediction of the *in vitro* frictional behavior of a metal-on-metal THR with head diameter 46 mm and friction coefficient 0.15 (Figure 1b) (R^2=0.996, RMSE=0.215, slope=1.140, intercept=-0.05).

The maximum head-cup frictional moment calculated for an 80 kg person for walking gait was 6.90 Nm which resulted in a 5.18 Nm torque at the head-neck interface. This considerable torque magnitude, along with its sharp change of direction, will induce torsional micromotion and contact shear stresses at the modular interface which may contribute to fretting wear and disruption of the passive layer on the metal surface. This may eventually cause enhanced fretting corrosion at the modular junction, which is recognized as one of the failure mechanisms in THRs.

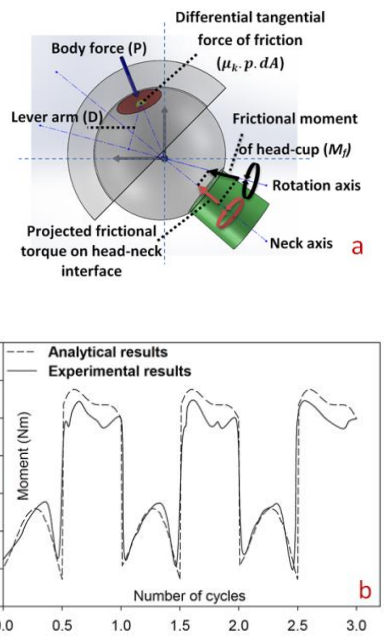

Figure 1: a) Frictional moment of head-cup and its projected torque at head-neck interface **b)** Experimental *in vitro* results and corresponding analytical results.

CONCLUSIONS:

An analytical method was developed to determine the frictional moment produced at the head-cup bearing and the projected torque at the head-neck interface of modular THRs, and the results compared favourably with experimental data. Knowledge of the *in vivo* torsional load acting at the head-neck interface may improve understanding of fretting corrosion at the head-neck junction of modular THRs.

REFERENCES

1. Bergmann G, et al., *Bio-Medi. Mat. Eng.* **20**:65-75, 2010.
2. Bishop NE, et al., *J. Orthop Res.* **31**:807-813, 2013.
3. Bishop NE, et al., *Med. Eng. Phys.* **30**:1057-1064, 2008.
4. Bergmann G, et al., *J. Biomech.* **34**:859-871, 2001.
5. Saikko V and Calonius O, *J. Biomech.* **35**:455-464, 2002.

MEASURING THE *IN-VIVO* RESPONSE OF MUSCLE AND SUBCUTANEOUS FAT TISSUES UNDER QUASI-STATIC SITTING LOADS USING HIGH-FIDELITY SUBJECT-SPECIFIC FE MODELS

[1]Rami M A Al-Dirini, [2]Matthew P Reed, [3,4]Dominic Thewlis,

[1]School of Engineering, University of South Australia, Adelaide - Australia; [2]University of Michigan Transportation Research Institute, The University of Michigan, MI-USA; [3]School of Health Sciences, University of South Australia, Adelaide – Australia; [4]Sansom Institute for Health Research, University of South Australia, Adelaide – Australia;
email: rami.al-dirini@mymail.unisa.edu.au

INTRODUCTION

Elevated strains in sub-dermal soft tissues is thought to contribute to tissue damage associated with prolonged sitting [1]. Current methods cannot measure the sub-dermal stresses and strains non-invasively. Alternately, subject-specific finite element (FE) models can provide valuable information about the sub-dermal stresses and strains as the human body interacts with seats and beds. Previous FE models of seated humans were based on gross assumptions about the geometry and material properties of the human body. This raises concerns about the fidelity of the stresses and strains measured from previous FE models [2]. The primary aim of this study was to develop and validate high fidelity three dimensional FE models of the buttock and thigh region specific for seated subjects. Such models can provide in-depth understanding of how the soft tissues respond to sitting loads.

METHODS

Six healthy males with different heights and body masses were scanned using a Positional MRI scanner (Fonar) [3]. The MRI scans were processed to generate six subject-specific 3D CAD models of the buttock and thigh. Each subject-specific CAD model (Figure 1) was imported into ANSYS workbench and meshed using only tetrahedral elements. Muscle and fat components were modelled as hyper-elastic material, while the bones and the seat surface were modelled as rigid bodies. Frictionless contact was assigned to all muscle-fat interfaces, and frictional contacts were assigned at all muscle-bone (μ_s=0.3) and fat-seat (μ_s=0.4) interfaces. A bonded contact was defined at the interface between the fat layer and the bony structures of the model. An axis-symmetric boundary condition about the sagittal plane through the mid-cross section of the sacrum was assumed to reduce solution time. 60% of the body weight was imposed on each model for 90ms of real-world time. Each model was validated by comparing FE predictions to MRI measurements of soft tissue deformation. Finally, the validated FE models were used to estimate the stresses/strains in muscle and fat tissues.

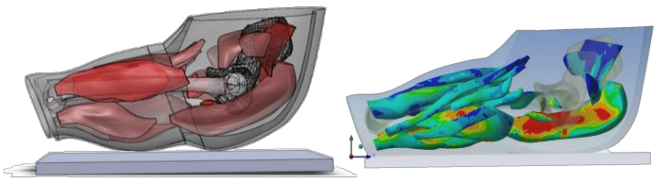

Figure 1: Undeformed subject-specific CAD model (right) and the compressive stress distribution after compression as predicted by the FE model (left)

RESULTS AND DISCUSSION

As expected, the highest stresses and strains were in soft tissues below the ischia for all subjects (Figure 1). The strains estimated using the FE models were highest in the gluteus maximus muscle for all subjects. The simulated stresses were higher in the subcutaneous fat layer than in muscles for all subjects. The means of the maximum strains and maximum stresses are summaries in Table 1. With further validation, detailed FE models of the type presented here may provide insight into mechanisms of tissue breakdown under sustained mechanical loading and provide an opportunity for quantitative evaluation of countermeasures.

CONCLUSIONS

This study presented the development and validation of high fidelity subject-specific, 3D FE models for seated humans. The models showed that muscles are under higher strains that fat tissues, while fat tissues are under higher stresses.

REFERENCES

1- Al-Dirini, R.M.A, et al., *ACAM 7*. **2012**: Adelaide.
2- Linder-Ganz, E., et al., *Journal of biomechanics*, ***2007***. 40(7): p. 1443-1454.
3- Lim, D., et al. *RESNA 29th International conference*, June. **2006**.

Table 1: The Mean of the maximum stresses and maximum strains in muscle and subcutaneous fat tissues predicted by the subject-specific FE models

	Compressive strain (%)	Shear strain (%)	von-Mises strain (%)	Compressive stress (kPa)	Shear stress (kPa)	von-Mises stress (kPa)
Muscle	**29**	**71**	**54**	**0.9**	**1.7**	**3.1**
Subcutaneous Fat	**18**	**54**	**35**	**6.3**	**6.8**	**11.3**

A three dimensional finite element model of the head–neck junction of a modular total hip arthroplasty

[1]Khosro Fallahnezhad, [1]Hamidreza Farhoudi, [1]Reza Oskouei, [1]Mark Taylor
[1]School of Computer Science, Engineering and Mathematics, Flinders University, SA, Australia
email: reza.oskouei@flinders.edu.eu

INTRODUCTION

There have been a number of attempts to simulate the mechanical environment of the head-neck junction in total hip replacement. The finite element (FE) method has been used to model the taper junction and these have been limited by major simplifications (e.g. two dimensional models) [1]. In this study a three dimensional FE model of an isolated femoral head–neck junction was developed using ABAQUS/CAE 6.13-1. The model simulates non-linear frictional contact between the taper and trunnion and elastic-plastic properties of mating materials. The developed approach was verified against experimental results of assembly force and pull off loads reported by Morlock et al. for different head-neck junctions [2].

METHODS

The accurate geometry of the taper junction was modeled and the assembly force was applied as a quasi-static load instead of impact force to reduce the solution time by using the mass scaling technique. Considering the assembling process as a press-fit, it can be concluded that when both the impact and quasi-static loads result in the same pull-off loads, they create same normal stresses (pressure). Therefore, in experimental results of assembly/pull off loads (Morlock et al. [1]), each impact force can be replaced with a quasi-static load with the same pull-off force. To this end, assembling the head-neck models was performed under several quasi static loads (1970, 2500, 3700 and 4000 N) corresponding to the reported experimental impact loads. Using a trial and error method, different pull-off loads were then applied to find the adequate load causing the head and neck to disassemble.

RESULTS AND DISCUSSION

Figure 1 shows the variation in maximum von Mises stress which occurs at the critical contacting region of the head and neck under an assembly load of 2500 N followed by three pull-off loads. The pull-off load of 1600 N released the stress and separated the head from the neck. As given in Table 1, the results were found in a good agreement with experimental tests with a maximum error of 10%. The von Mises stress at selected points on the neck under 2500 N assembly force are shown in Figure 2. It can be found that the highest stress at reaches 500 MPa after assembling process. This stress dramatically decreases for upper points located further away from the contacting edge of the head and neck.

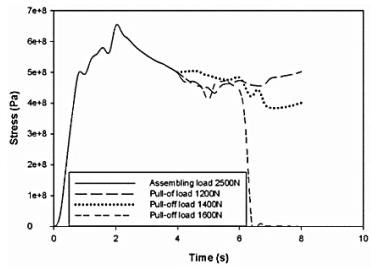

Figure 1: Maximum von Mises stress on the neck.

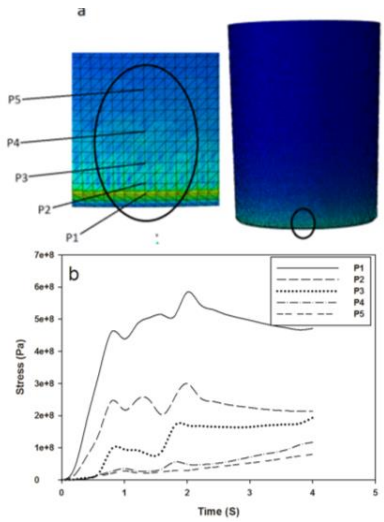

Figure 2: von Mises stress at selected points on neck.

CONCLUSIONS: A new three dimensional FE model was developed to simulate assembly force in taper junction of total hip replacement. A stress analysis showed the maximum stress at the contacting edge of the neck and bore of the head. This verified model can be used to explore the mechanical environment of the head-neck junction under in vivo loading at different physical activities.

REFERENCES

1. Zhang T, et al., *Tribology Internaional*.**65**:113-127, 2013.
2. Morlock M, et al., *Clinical Biomechanics*.**27**:77-83, 2012

Table 1: comparison of simulation results and experimental tests.

Assembly force (N)	1970	2500	3700	4000
Experimental Pull-off load (N)	1100	1400	2080	2250
Numerical pull-off load (N)	1200	1600	2300	2500

IN VITRO DEGRADATION OF MECHANICAL PROPERTIES OF PORCINE FEMORAL HEAD BONE FOR DEVELOPMENT OF AN *IN VITRO* OF AVASCULAR NECROSIS

[1]Mahsa Shahi Avadi, [2]James A Anderson, [1]John Fisher and [1]Sophie Williams

Institute of Medical and Biological Engineering, School of Mechanical Engineering, University of Leeds, Leeds, UK
[2]DePuy Synthes Joint Reconstruction, Leeds, UK
E-mail: mnmsa@leeds.ac.uk

INTRODUCTION

Avascular necrosis (AVN) of the femoral head develops following a lack of blood flow into the bone and leads to changes in bone architecture. Bone is weakened and can no longer resist applied loads and begins to collapse [1]. Various biological models of AVN have been developed in vitro [2], however none of these models demonstrate the mechanical failures observed in human AVN. The development of a physical disease model would be advantageous when developing mechanically based treatments.

The aim of this study was to assess methods that can be used to degrade mechanical properties of animal femoral heads in such a way that would replicate the mechanical properties of femoral heads in AVN. Brown et al. [3] demonstrated this to be 59% reduction in elastic modulus and 41% reduction in yield strength. These methods will be used in the future to create a mechanical model of AVN of the femoral head in vitro.

MATERIALS AND METHODS

Bone plugs were removed from the load bearing region of porcine femoral heads (24-26weeks old, 24-48 hours after slaughter) and frozen until use (max. 3 months). They were treated in the following solutions for the stated time frames, at room temperature with agitation.

Potassium hydroxide (KOH) 1M: 14, 7, 3 and 1 days
Ethylenediaminetetraacetic acid (EDTA) 12.5%: 28, 14 and 7 days
Hydrochloric acid (HCl) 1M: 48, 24, 18 and 6 hours

Computed tomography scans of the samples were obtained prior and after treatment to measure and compare bone mineral density (BMD). Compression testing carried out on treated plug samples provided yield strength and elastic modulus. Data were compared to untreated control bone plugs.

RESULTS AND DISCUSSION

Samples that were soaked in KOH for 14 days were dissolved in the solution; therefore no further measurements were obtained. Samples soaked in KOH for 7 days were CT scanned, however they were not tested in compression due to severe swelling in KOH which caused the samples to lose their mechanical integrity.

Significant reductions in bone mineral density were seen in all groups that were treated with EDTA and HCl, though only samples treated in KOH for 7 days demonstrated a significant reduction (Figure 1). Conversely KOH samples soaked for shorter times demonstrated a slight increase in BMD, which may be due to absorption of potassium into the bone.

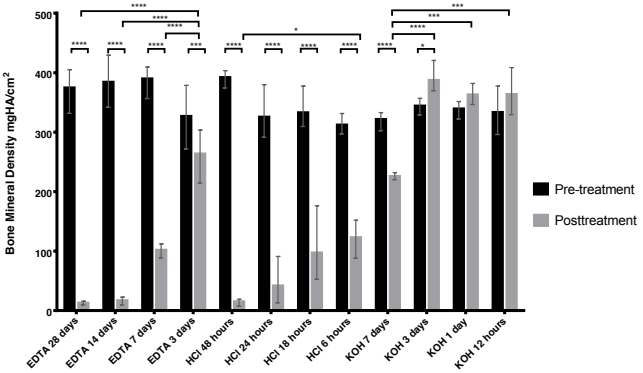

Figure 1 - Change in BMD of porcine bone plugs before and after treatment. ANOVA tests showed P value <0.001 where 3 and 4 asterisks are shown, presenting extremely significant differences. 1 asterisk is p value of 0.01 to 0.05, showing significant differences.

Elastic modulus and yield stress values were significantly lower in all cases compared to control untreated samples. A reduction of 47% elastic modulus and 46% yield stress was observed in samples treated in EDTA for 3 days, which is similar to the findings presented by Brown et al. [3].

CONCLUSIONS

HCl was most effective in reducing mechanical properties of bone in shorter time and may be more suitable in in vitro model development of avascular necrosis on whole femoral heads. Further work is required to establish optimum concentrations and treatment time for the final model.

REFERENCES

[1] Mont & Hungerford, *JBJS Am*. **77** (1995) 459.
[2] Jones & Allen, Clin. Rev. *Bone Miner*. *Metab*. **9** (2011) 63.
[3] Brown, et al., *CRRS*. (1981) 240.

Table 1- Elastic modulus and yield stress values obtained following treatment of samples vs control samples

Treatment	EDTA				HCl				KOH			Control
No. of days	28	14	7	3	2	1	0.75	0.25	3	1	0.5	
Elastic modulus (MPa)	1.12	5.53	22.45	89.44	3.86	8.53	26.62	25.05	8.17	33.84	33.54	168.90
Yield Stress (MPa)	0.00	0.01	0.03	8.20	0.05	0.02	0.02	0.01	0.74	3.36	4.13	15.34

CONFLICT OF INTEREST DECLARATION

In the interests of transparency and to help reviewers assess any potential bias, ANZORS requires authors of original research papers to declare any competing commercial interests in relation to the submitted work. Referees are also asked to indicate any potential conflict they might have reviewing a particular paper.

If you have accepted any support such as funds or materials, tangible or intangible, concerned with the research by the commercial party such as companies or investors, choose YES below, and state the relation between you and the commercial party.

If you have not accepted any support such as funds or materials, choose NO.

Do you have a conflict of interest to declare? (DELETE TEXT as appropriate)

YES

Mahsa Shahi Avadi is supported by EPSRC (UK) studentship (Industry partner: DePuy Synthes Joint Reconstruction, UK)
James A Anderson is an employee of DePuy Synthes Joint Reconstruction

LOWER LIMB MUSCLES FUNCTION AS WE AGE: IMPLICATION FOR SARCOPENIA

[1,2]Hossein Mokhtarzadeh, [1,2]David Scott, [6]Graeme Jones, Elizabeth Skinner[2,4] , Tim Wrigley[3], Rana Hinman[3], Kim Bennell[3], Peter Pivonka[1,2], Adam Bryant[3], Peter Ebeling[2,5]

[1]NorthWest Academic Centre, University of Melbourne, VIC, Australia
[2]Australian Institute of Musculoskeletal Science, VIC, Australia
[3]Centre for Health, Exercise & Sports Medicine, University of Melbourne
[4]Western Health Physiotherapy Department, Melbourne, Australia
[5]School of Clinical Sciences, Faculty of Medicine, Nursing and Health Sciences, Monash University
[6]Menzies Research Institute, University of Tasmania, Hobart, Australia
email: mhossein@unimelb.edu.au

INTRODUCTION

Sarcopenia is the age-related decline in muscle mass and function [1]. Improved muscle function during daily activities such as walking may play a major role in stabilizing the lower limbs to avoid falls in the elderly. In people aged 50-70 years, this study aims to explore the following hypotheses (H). Significant age-related changes in induced acceleration of center of mass as measured by musculoskeletal modeling will be observed at early stance where it may correlate to falls compared to mid and late stance. (H1). Changes with age observed in H1 will demonstrate similar patterns to age-related muscle strength changes characteristic of sarcopenia (H2). Also, we will compare our results with lower-limb muscle strength changes across the same range of ages from a population-based study (Tasmanian Older Adult Cohort study; H2)

METHODS

We developed subject-specific musculoskeletal models for 34 healthy participants aged between 51-78 years old. OpenSim (open source software to simulate movement developed in Stanford) was used to develop these models. Participants performed self-selected pace walking barefoot. Vicon system collected the joint motions by tracking plug-and-gait marker sets on the anatomical land marks. Ground reaction forces were collected using AMTI force plates. Following importation the motion and GRF data, the OpenSim generic model was scaled to match with anthropometric measurements. Muscle force prediction then enabled us to find the contribution of each muscle to induced acceleration of center of mass during walking in OpenSim. The association of age with lower-limb muscle strength (knee and hip extensors) from a population-based study (1069 participants from the Tasmanian Older Adult Cohort study) was compared with our calculated muscle forces.

RESULTS AND DISCUSSION

The results of muscle function during stance phase of gait are presented. A representative graph for gastrocnemius, as observed in other muscles, during stance phase showed no significant changes with respect to ageing. However, muscle strength test for the same age group for the knee (r=-0.21;P<0.001) and hip extensors (r=-0.17;P<0.001) revealed weak but significant declines with age. Musculoskeletal modeling suggests muscle forces during the stance phase of self-selected gait do not change during ageing, whereas maximal lower limb strength decreases with age; therefore, other high demanding gait activities such as stair climbing or maximal walking speed should be investigated for sarcopenia diagnosis.

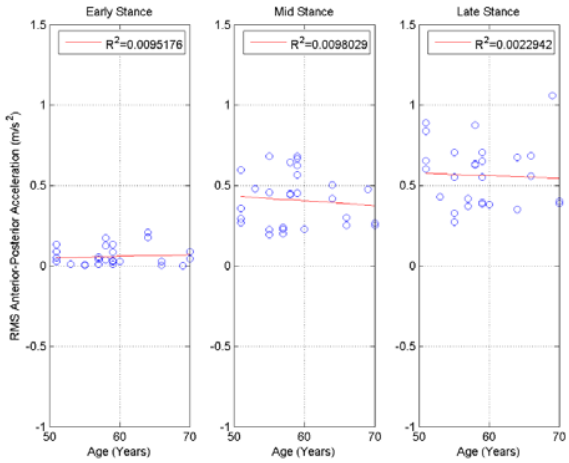

Figure 1: RMS values for A/P induced acceleration of gastrocnemius at three different time points during gait.

CONCLUSIONS

Muscle forces during self-selected gait do not demonstrate age-related declines characteristic of sarcopenia. Future studies should focus on high demanding activities with the same approach to find the underlying effect of individual muscle functions during daily activities.

ACKNOWLEDGEMENTS

Authors would like to thank AIMSS Seed Funding 2013 and Mr. Laurence Fok and Mr. Mario Andres Munoz for their invaluable contributions to the modelling.

REFERENCES

1. Cruz-Jentoft, et al., *Age and Ageing* 2010

FEASIBILITY OF USING KINECT 2 DEPTH MAP TO DETERMINE THORACIC KYPHOSIS ANGLE

[1,2]Gino Coates, [1,2]Alessandro Timmi, [1,2]Peter Pivonka, [3,4]Adam Leigh Bryant and [1,2]Hossein Mokhtarzadeh,

[1]North West Academic Centre, The University of Melbourne, VIC, Australia
[2]Australian Institute of Musculoskeletal Science, VIC, Australia
[3]Department of Physiotherapy, Faculty of Medicine, Dentistry and Health Sciences, The University of Melbourne, VIC, Australia
[4]Centre for Health, Exercise & Sports Medicine, The University of Melbourne, VIC, Australia
email: gcoates@student.unimelb.edu.au

INTRODUCTION

Thoracic Kyphosis (TK) is the technical term describing the curvature of the spine in the sagittal plane. Excessive TK is related to many diseases such as Osteoarthritis, Scheuermann's disease and cystic fibrosis (CF) and has been linked to incidences of back pain in patients with CF [1].

The Modified Cobb Angle measures the angle between intersecting lines drawn parallel to the endplates of limit vertebrae on radiographic images [2] and is the current gold standard for assessing TK. While satisfying results have been achieved using this technique there are a variety of drawbacks, including measurement errors due to manual handling, intra/inter-observer variability, and frequent exposure of patients to X-rays for longitudinal assessment. A number of non-radiological alternatives to measure spinal curvature have been developed. For example, the Flexicurve is a flexible ruler pressed against the spine and transferred to paper to calculate the kyphosis index/angle. However, this device may not retain its shape once removed from the spine and pressure applied during measurement may change the patients posture [3].

Microsoft Kinect is a low cost, portable device with the capability to produce 3D depth maps. A previous study has used a first generation device to assess spinal curvature [4], but used depth surface reconstruction due to the low fidelity depth map. The soon to be released Kinect for Windows v2 (Kinect 2) includes improved specifications and a higher fidelity depth map based on Time of flight technology, making the need for depth map reconstruction obsolete and allowing for real-time calculation of spinal curvature. This study assesses the feasibility of using the Kinect 2 depth maps as a non-radiological means to estimate TK angle (TKA)

METHODS

Using a pre-release alpha version of Kinect 2, a 3D depth map of the patients back was captured. Using an approach similar to [5], landmarks were manually selected in the depth map corresponding to the C7, T1, T12 and L1 vertebrae. Linear interpolation produced six evenly spaced points between the T1 and T12 vertebrae and depth values were retrieved for both manually selected and interpolated positions. A cubic spline was used to connect the depth values at the selected positions and to estimate thoracic spinal curvature. Tangents to the curve at points T1, T12 were determined and the intersection of perpendicular lines to these tangents was used to calculate TKA.

RESULTS AND DISCUSSION

The application developed as part of this study can calculate kyphosis angle in real-time (Figure 1). Resolution of the Kinect 2 depth map is sufficient to estimate spinal curvature without depth map reconstruction. Identification of the appropriate spinous processes is still difficult in the depth map however and may be aided with visual markers placed on the subject in a future version of the software.

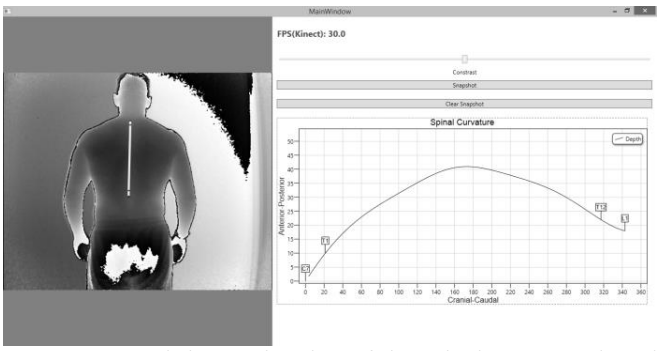

Figure 1: Real-time estimation of the spinal curvature based on selected landmarks in the Kinect 2 depth map

CONCLUSIONS

Kinect 2 can be used as a low cost, portable, non-radiological device to assess spinal curvature. Availability of such a device, in combination with ad-hoc developed software, would allow more frequent assessment of spinal curvature in sufferers of disease related to excessive kyphosis. In future works, the software will be validated for accuracy and reliability against existing radiological and non-radiological techniques.

REFERENCES

1. Tattersall R and Walshaw MJ, *J. R. Soc. Med.*, **96 Suppl 4**, 18–22, 2003.
2. Greendale G a et al., *Osteoporos. Int.*, **22**, 1897–905, 2011.
3. Caine MP et al., *Int. J. Rehabil. Res.*, **19**, 271–278, 1996.
4. Reyes M et al., *Comput. Ind.*, **64**, 1316–1325, 2013.
5. De Oliveira TS et al., *Rehabil. Res. Pract.*, **2012**, 186156, 2012.

QUADRICEP AND HAMSTRING FORCE RATIO IN THE TRANSVERSE PLANE: IMPLICATIONS FOR ACL INJURY

[1,2]Ruwindi Setunge, [1,2]Hossein Mokhtarzadeh, [3]Luke Perraton, [1,2]Peter Pivonka and [3,4]Adam Bryant.
[1]NorthWest Academic Centre, University of Melbourne, VIC, Australia
[2]Australian Institute of Musculoskeletal Science, VIC, Australia
[3]Centre for Health, Exercise & Sports Medicine, University of Melbourne
Email: rsetunge@student.unimelb.edu.au

INTRODUCTION

Anterior Cruciate Ligament (ACL) injuries are debilitating amongst professional athletes, often requiring a reconstruction. ACL tears commonly occur following dynamic landing tasks, where excessive forces load the ACL. However the function of muscle forces produced at the knee joint are still not well understood. The force ratio of the agonist and antagonistic quadriceps and hamstring muscles (Q/H) can be used to predict the force generated by muscle co-contraction at the knee. To date, biomechanical assessment of reconstructed individuals (ACLR), with single bundle reconstructions are shown to have increased transverse plane internal tibial rotation (ITR) compared to controls during dynamic tasks [1]. So we speculate if the Q/H ratios, medially and laterally, in the transverse plane could be an indicator of recovery and re-injury in ACLR individuals. The aim of this study is to compute the lateral and medial Q/H ratios and compare them between ACLR and control groups during a dynamic hop task. It is hypothesised that ACLR subjects will not restore the medial and lateral QH ratios following injury compared to control subjects at foot-strike, peak GRF and peak knee flexion.

METHOD

8 subjects were recruited, 4 ACLR and 4 healthy control. ACLR subjects had reconstructions using an STGT graft between 11-24 months prior to testing. Informed consent was obtained, complying with the University of Melbourne's Human Ethics standards. Both control and ACLR subjects performed a single-legged hop landing onto three force plates embedded in the ground, utilised to collect the GRF of the landing foot. Each subject repeated this for 5 trials. For each trial, marker data of each subject was collected by motion capture analysis (Vicon MX, Oxford Metrics, UK). Biomechanical models of each subject were then developed using the OpenSim software, an open-source 3D musculoskeletal modelling software [2,3]. Muscle forces and joint angles were calculated based on inverse kinematics and the static optimisation method in the OpenSim software for each subject. Matlab (Mathworks Inc) software packages were then utilised to export data from OpenSim, to perform an independent t-test between the ACLR and control groups.

RESULTS AND DISCUSSION

The lateral Q/H ratio of the ACLR vs Control is represented in the Figure 1 below. Interestingly we observe that at max knee flexion the lateral Q/H ratio in ACLR is significantly lower than Control p=0.0003. However in the lateral q/h ratio no significance difference between ACLR and Control subjects were seen at foot-strike or peak GRF. There was also no significance seen between the medial Q/H ratios in ACLR vs Control subjects.

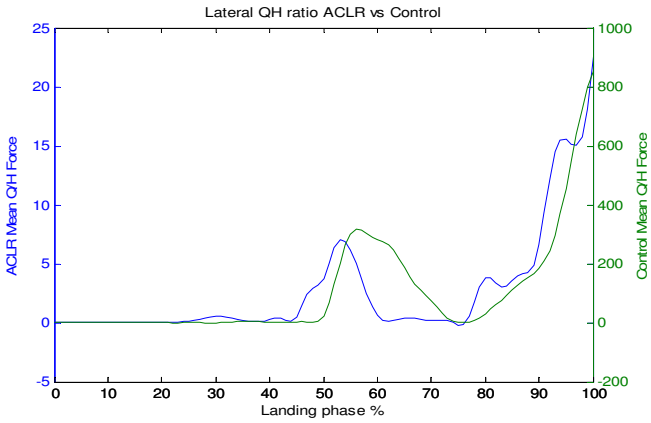

Figure 1: ACLR vs Control Lateral Q/H ratio.

CONCLUSIONS

The findings of this study support the hypothesis that the lateral Q/H co-contraction ratio in the ACLR subjects at max knee flexion was significantly different to that of Control subjects. Although there was no significance seen in the medial Q/H, the lateral Q/H force variation between ACLR and Control highlight that force deficits in muscles spanning the knee joint may be linked with ACL recovery and re-injury.

REFERENCES

1. Stergiou et al. Sports Medicine. 37:601-613, 2007.
2. Delp, S. L., et al.,*IEEE Transactions* 54:1940-1950,2007.
3. Mokhtarzadeh H,*WCB 2010*, Singapore, 171-173, 2010.

Table 1: Mean and (Sd) lateral Q/H ratio

	ACLR	Control	P value
Foot-strike: Lateral Q/H ratio	1254.8 (376.5)	827.9(125.2)	0.1
Peak Grf: Lateral Q/H ratio	0.1(0.2)	0.08(0.06)	0.8
Max Knee Flexion: Lateral Q/H ratio	22.6(25.4)	855.7(222.2)	0.0*

IN VITRO TESTING OF 4- AND 5- STRAND CONSTRUCTS FOR ACL RECONSTRUCTION

Broadhead M, Singla A, Sideris A, Broe D, Bertollo N, Walsh WR

Surgical and Orthopaedic Research Laboratories, Prince of Wales Hospital Clinical School,
University of New South Wales, Sydney, NSW

Email: w.walsh@unsw.edu.au

INTRODUCTION

When employing suspensory fixation in Anterior Cruciate Ligament Reconstruction, 4-strand hamstring grafts have been shown to have higher stability rates than 2-stranded repairs. This study was conducted to test the hypothesis that 5-stranded hamstrings graft suspensory fixation repairs have superior strength to a 4-stranded construct in an idealised in-vitro setting.

METHODS

Four- and 5-stranded suspensory fixation (EndoButton, Smith and Nephew) constructs (n=8 per group) prepared with freshly-harvested ovine flexor tendons were tested in uniaxial tension using an MTS machine. Constructs were prepared by whip-stitching free ends of the tendon grafts with #2 Ethibond to facilitate pre-tensioning and enhance fixation in cryogrips during testing. Five-stranded constructs were prepared by suturing the doubled-over fifth strand to the Endobutton as described by Brown *et al*. Constructs were fixed to the testing machine, preconditioned, stress-relaxed and destructively tested ($20mm.min^{-1}$). Stress-relaxation, stiffness and ultimate load of the constructs were compared using a one-way ANOVA.

RESULTS AND DISCUSSION

No differences in either stress-relaxation ($p=0.592$), initial stiffness ($p=0.301$), secondary stiffness ($p=0.796$) or ultimate load ($p=0.462$) between the 4- and 5-stranded constructs was detected. Inconsistent failure patterns for both constructs were observed and which included failure of the Endobutton, failure of the graft, or a combination of these two mechanisms.

CONCLUSIONS

Our in vitro results suggests that the fifth strand may not contribute mechanically to a 5-stranded repair, which is mechanically equivalent to a gold-standard 4-strand. The potential biological benefit from religamentisation and bony integration perspectives to having more autologous tissue in the intra-articular space and bony tunnels remains unknown.

CLINICAL ASSESSMENT OF KNEE KINEMATIC PARAMETERS USING THE KNEEKG SYSTEM

Sideris A, Hamze A, Broe D, Bertollo N & Walsh WR

Surgical and Orthopaedic Research Laboratories, Prince of Wales Hospital Clinical School,
University of New South Wales, Sydney, NSW

Email: w.walsh@unsw.edu.au

INTRODUCTION

Quantification of knee kinematics is a useful tool in the assessment of patients for operative planning and measuring outcomes of surgical intervention. The recent introduction of the KneeKG motion tracking system provides an opportunity to quickly, easily and routinely monitor patients clinically. This study assessed the intra and inter-observer reproducibility in asymptomatic subjects using this system and changes in knee kinematics following ACL reconstruction surgery.

METHODS

Knee motion was quantified using the KneeKG (Emovi Inc, Canada) with subjects walking on a treadmill. The KneeKG system is composed of passive motion sensors fixed on validated harnesses, an infrared camera and computer with the analysis software. Following application of the trackers, a calibration procedure was performed to identify joint centres and define segment coordinate systems. After a treadmill habituation (1-2 min), trials were conducted at three speeds (2, 3 and $4 km.h^{-1}$) over 45 sec. Averaged clinical rotations and translations as a function of gait cycle were output and analysed using a two-way ANOVA, where differences considered significant for $p<0.05$. ACL deficient patients with planned surgical intervention were assessed pre-operatively and at 6 weeks and the changes analysed.

RESULTS AND DISCUSSION

The KneeKG was successfully applied to subjects in this study, with a full analysis typically requiring less than 30 minutes to complete per case. We found the system to have a moderately steep learning curve, with a reduction in intra-observer variability observed following application and observation in approximately 15 subjects. In the hands of different observers motion patterns were reproducible and the system robust. In ACL deficient patients, differences were noted between pre and post-operative kinematics.

CONCLUSIONS

This study has demonstrated the robustness and reproducibility of the KneeKG system, with its stand-alone nature making it amenable to quick, easy and routine monitoring of patients in a clinical setting. This was demonstrated in patients who had had ACL tears by monitoring pre and post-operative knee kinematics.

Australian & New Zealand Orthopaedic Research Society

ANZORS 20th Annual Scientific Meeting

List of Registered Delegates

(at the time of printing, surname ordered alphabetically)

Surname	First Name	Institute	E-mail
Abrahams	John	Royal Adelaide Hospital	john.abrahams@student.adelaide.edu.au
Al-Dirini	Rami	University of South Australia	alyrm001@mymail.unisa.edu.au
Algate	Kent	The University of Adelaide	kent.algate@adelaide.edu.au
Amin	Dhara	Flinders University	dhara.amin@flinders.edu.au
Arnold	John	University of South Australia	john.arnold@mymail.unisa.edu.au
Bartnikowski	Michal	Queensland University Technology	m.bartnikowski@qut.edu.au
Bramwell	Donald	IMRI	
Brito da Luz	Simao	Griffith University	simao.britodaluz@griffithuni.edu.au
Buenzli	Pascal	Monash University	pascal.buenzli@monash.edu
Callary	Stuart	Royal Adelaide Hospital	Stuart.Callary@health.sa.gov.au
Chen	Song	Australian National University	song.chen@anu.edu.au
Chen	Yongjuan	University of Sydney	yong.chen@sydney.edu.au
Clifton	Thomas	Royal Adelaide Hospital	tclifton85@gmail.com
Coates	Gino	The University of Melbourne	gcoates@student.unimelb.edu.au
Cory	Xian	University of South Australia	cory.xian@unisa.edu.au
Costi	John	Flinders University	john.costi@flinders.edu.au
Costi	Kerry	Royal Adelaide Hospital	kerry.costi@health.sa.gov.au
Crotti	Tania	The University of Adelaide	tania.crotti@adelaide.edu.au
Dan	Barker	Zimmer	Daniel.Barker@zimmer.com
David	Ackland	University of Melbourne	dackland@unimelb.edu.au
Derrick-Roberts	Ainslie	SA Pathology	ainslie.derrickroberts@adelaide.edu.au
Dharmapatni	Kencana	The University of Adelaide	a.dharmapatni@adelaide.edu.au
Dwivedi	Prem	University of South Australia	prem.dwivedi@unisa.edu.au
Ewing	Katie	University of Melbourne	ewingk@unimelb.edu.au
Fallahnezhad	Khosro	Flinders University	Khosro.Fallahnezhad@flinders.edu.au
Farhoudi	Hamidreza	Flinders University	hamidreza.farhoudi@flinders.edu.au
Fernandez	Justin	The University of Auckland	j.fernandez@auckland.ac.nz
Findlay	David	The University of Adelaide	david.findlay@adelaide.edu.au
Fletcher	Lloyd	The University of Adelaide	lloyd.fletcher@adelaide.edu.au
Fountain	Stephanie	Queensland University of Technology	stephanie.fountain@qut.edu.au
Fuller	Joel	University of South Australia	joelfull_03@hotmail.com
Gao	Ryan	The University of Auckland	ygao921@gmail.com
Glatt	Vaida	Queensland University of Technology	vaida.glatt@qut.edu.au

Grasso	Samuel	Sydney Orthopaedic Research Institute	samuel.grasso@hotmail.com
Haynes	David	The University of Adelaide	david.haynes@adelaide.edu.au
Hua	Martin	University of Sydney	mhua8891@uni.sydney.edu.au
Hunter	David	University of Sydney	david.hunter@sydney.edu.au
Jadhav	Gaurav Vijay	The University of Western Australia	gaurav.jadhav@research.uwa.edu.au
Jones	Claire	The University of Adelaide	claire.jones2@health.sa.gov.au
Kang	Laurant		
Kuek	Vincent	The University of Western Australia	20256286@student.uwa.edu.au
Lam	Cheuk Ho	Monash University	cheuk.lam@icloud.com
Lazid	Rosidah	Flinders University	abla0002@flinders.edu.au
Lerebours	Chloe	Monash University	chloe.lerebours@monash.edu
Levinger	Pazit	Victoria University	Pazit.levinger@vc.edu.au
Li	Guangyi	The University of Western Australia	Leepotter2003@163.com
Liley	Helen	University of Auckland	hlil007@aucklanduni.ac.nz
Lim	Bay Sie	The University of Western Australia	20594496@student.uwa.edu.au
Liza	Raggat	University of Queensland	liza-jane.raggatt@mater.uq.edu.au
Loechel	Nicole	Queensland University of Technology	n.loechel@qut.edu.au
Lonbani	Zohreh	Queensland University of Technology	z.baranilonbani@gut.edu.au
Lu	ZuFu	University of Sydney	zufu.lu@sydney.edu.au
Lynch	Joe	Australian National University	joe.lynch@act.gov.au
Martin	Brianna	Flinders University	brianna.martin@flinders.edu.au
McCarl	Benjamin	Flinders University	mcca0336@flinders.edu.au
McDonald	Ben	Flinders Medical Centre	benjamin.j.mcdonald@gmail.com
Moran	Caroline	Royal Adelaide Hospital	caroline.moran@health.sa.gov.au
Morgan	Rowan	IMRI	rowan.morgan@flinders.edu.au
Munro	Jacob	The University of Auckland	jacob.munro@auckland.ac.nz
Muratovic	Dzenita	The Univeristy of Adelaide	dzenita.muratovic@healt.sa.gov.au
Murison	Emma	The University of Adelaide	tania.crotti@adelaide.edu.au
Musson	David	The University of Auckland	d.musson@auckland.ac.nz
Ng	Benjamin	The University of Western Australia	20217728@student.uwa.edu.au
No	Young Jung	University of Sydney	yono7153@uni.sydney.edu.au
O'Rourke	Dermot	Flinders University	dermot.orourke@flinders.edu.au
Ormsby	Renee	The University of Adelaide	renee.ormsby@adelaide.edu.au
Oskouei	Reza	Flinders University	reza.oskouei@flinders.edu.au
Pavlos	Nathan	The University of Western Australia	nathan.pavlos@uwa.edu.au
Perilli	Egon	Flinders University	egon.perilli@flinders.edu.au
Perriman	Diana	Australian National University	diana.perriman@act.gov.au
Pivonka	Peter	The University of Melbourne	peter.pivonka@unimelb.edu.au
Prideaux	Matthew	University of Adelaide	matt.prideaux@adelaide.edu.au
Reilly	Keryn	The University of Auckland	k.reilly@auckland.ac.nz
Reinke	Daniel	University of Adelaide	daniel.reinke@adelaide.edu.au
Roberts	Bryant	Flinders University	bryant.roberts@flinders.edu.au
Robinson	Dale	University of Melbourne	daleleerobinson@gmail.com
Roohani-Esfahani	Seyed-Iman	University of Sydney	
Ryan	Melissa	Flinders University	melissa.ryan@flinders.edu.au
Saad	Sylvia	The University of Adelaide	sylvia.saad@student.adelaide.edu.au

Sarah	Hemming	The Univeristy of Adelaide	sarah.hemming@adelaide.edu.au
Saulo	Martelli	University of Melbourne	saulo.martelli@unimelb.edu.au
Schutz	Christine	The University of Adelaide	cschutz@woc.com.au
Setunge	Ruwindi	University of Melbourne	ruwindi.setunge@gmail.com
Shahi Avadi	Mahsa	University of Leeds	mnmsa@leeds.ac.uk
Sideris	Anders	Prince of Wales Hospital	anders.sideris@uon.edu.au
Soira	Tamang	Flinders University	sweratamang@gmail.com
Solomon	Bogdan	Royal Adelaide Hospital	bogdan.solomon@health.sa.gov.au
Stamenkov	Roumen	Royal Adelaide Hospital	Roumen.Stamenkov@health.sa.gov.au
Steck	Roland	Queensland University of Technology	r.steck@qut.edu.au
Stephens	Sebastien	Griffith University	srj_stephens@hotmail.com
Su	Yu-Wen	University of South Australia	yu-wen.su@unisa.edu.au
Theodore	Willy	Flinders University	willy@optimizedortho.com
Theodoulou	Annika	IMRI	annika.theodoulou@imri.org.au
Thewlis	Dominic	University of South Australia	dominic.thewlis@unisa.edu.au
Walter	Jonathan	The University of Melbourne	walterj@unimelb.edu.au
Watts	Amy	IMRI	amy.watts@imri.org.au
Wei	Gu	University of Melbourne	w.gu12@student.unimelb.edu.au
Wilson	Christopher		
Xiang	Zhu	The University of Western Australia	Crawlxiang@hotmail.com
Xu	Jiake	The University of Western Australia	jaike.xu@uwa.edu.au
Yan	Mengzhen	University of New South Wales	mengzhen.yan@student.unsw.edu.au
Yeung	Kelvin	The University of Hong Kong	wkkyeung@hku.hk
YingChing	Tiong (Esther)	Flinders University	tiong.esther@gmail.com
Zawawi	Muhamad	The University of Adelaide	muhamad.zawawi@adelaide.edu.au
Zhou	Fiona	University of South Australia	fiona.zhou@unisa.edu.au
Zotti	Mario	Royal Adelaide Hospital	mariozotti@gmail.com